Preliminary Report of the Hakuho Maru Cruise KH 90-1

June 25-July 28, 1990

Geological and Geophysical Investigation
of
Japan Trench and Izu-Ogasawara Region

Ocean Research Institute
University of Tokyo
1991

Preliminary Report
of
the Hakuho Maru Cruise KH 90-1

June 25-July 28, 1990

Geological and Geophysical Investigation
of
Japan Trench and Izu-Ogasawara Region

by
The Scientific Members of the Expedition
Edited by
Kazuo KOBAYASHI

PREFACE

Cruise KH 90-1 of the Research Vessel Hakuho Maru of the Ocean Research Institute, University of Tokyo is divided into two Legs according to their target areas of survey. In Leg 1 (between June 25, 1990 sailing out from Tokyo and July 10, 1990 arriving at a port of call in Yokosuka) the vessel went to the central Japan Trench to investigate detailed topography of the trench walls along total 43 parallel EW tracks by means of the multi-narrow beam echo sounder *Seabeam*. Good acoustic condition of the Hakuho Maru enabled us to complete the work even in some rough weather.

This area is situated immediately south of Box 1 in the northernmost Japan Trench (41°17.5'N ~ 39°40'N) which was surveyed by the French research vessel *Jean Charcot* in 1984 under the aegis of the French-Japanese cooperative scientific program, *KAIKO* Project. By combining two projects nearly 2/3 of Japan Trench which has axial length of about 600 km was completely surveyed. A cruising speed of 16 knots was quite good for efficient survey. Trench walls between 6,000 and 6,500 m in depths are candidate targets of dives of newly launched Japanese manned research submersible *Shinkai 6500*. Our bathymetric data together with the *KAIKO* results in digital magnetic tapes will provide useful guide maps for divings as well as for further tectonic consideration.

Along one 300 km long EW profile from 146°00'E (on the crest of the outer swell) to 142°20'E (upper continental slope) at latitude of 38°45'N multi-channel seismic profiling was made. On the crest of the outer swell a small mound which appears to be a mud volcano (diapir) was recognized and described in this report. Normal faulting structure of the seaward wall of the trench is particularly eminent in the profiler data. Bathymetric map indicates that the faults in some places continue toward the landward toe and affect topography of the toe slopes as well as the trench axis. Landslide morphology is clearly recognized in the landward slope particularly in the area surveyed in this cruise.

On the way to and from this target area a chain of seamounts east off the Joban district, northeastern Honshu, Japan was surveyed in detail. Several seamounts including Daini-Kashima, Daisan-Kashima, Daiyon-Kashima, Hitachi, Iwaki and Bosei (Mizunagidori) seamounts are aligned on a nearly straight line trending N52°E, although a few (*e.g.*, Daigo-Kashima and Futaba) seamounts are situated slightly off the straight line. Location of some seamounts shown in currently available bathymetric charts was proved to be

shifted toward the line. Topography of these seamounts surveyed by Seabeam indicated their elongated shape parallel to the trend of the seamount chain.

Magnetic total force and three-components were measured throughout these surveys. The 3.5 kHz subbottom profiler was operated in these periods. Precise measurement of gravity was done by the new gravity meter on board the Hakuho Maru. In addition a line was surveyed by a deep-towed proton magnetometer. It was still in reconnaissance stage but some interesting results were obtained as described in this report.

A deep-sea monitoring system (DESMOS) composed of a deep-towed TV and still cameras together with CTD and hydrocast devices was first used for scientific operation in this leg. It was very successful and yielded much important information on the sea bottom features on the trench walls. It was proved that the SSBL (Super-short Base-Line) transponder attached to the towed system and received by the transducer at the ship's hull-bottom is very powerful to locate the sensor precisely. Detailed visual observation of above-mentioned mud volcano east off the Japan Trench was attempted by this technique.

In Leg 2 of this cruise (between July 15 from Yokosuka and July 28, 1990 to Tokyo) a surface-towed oceanfloor imaging system, so called *IZANAGI*, was operated on the Hakuho Maru in an area around the northern Izu-Bonin arc-trench region. Its use simultaneous with Seabeam was tested and proved to be possible but cause some problems. A few multichannel seismic reflection lines were taken crossing the trench-arc-backarc system of the Izu-Bonin. Electric conductivity was measured by means of Ocean Bottom Electrometer (OBE) deployed on the ocean bottom in the Izu-Bonin region. An Inverted Echo Sounder (IES) measurement was also done in the same area.

Chief scientist of the entire cruise (Kazuo KOBAYASHI) would like to acknowledge Drs. Asahiko TAIRA and Kiyoshi SUYEHIRO who served as acting directors of the Leg 2 after Kobayashi disembarked at Yokosuka. We are very grateful to officers and crew of the R. V. Hakuho Maru for their skillful shipboard work and collaboration to various kinds of ship's operations. Thanks are given to fishermen on the fishing boats among which we were able to survey the trench walls safely owing to their kind cooperative information on their fishing schedule.

March 1991

Kazuo KOBAYASHI
Chief Scientist of the Cruise

CONTENTS

1. SCIENTISTS ABOARD THE R. V. HAKUHO MARU CRUISE KH 90-1

KOBAYASHI, Kazuo[A] [Chief Scientist]	Ocean Research Institute, University of Tokyo
ABE, Shintaro[D]	Department of Earth Sciences, Chiba University
AMISHIKI, Toshiyuki[D]	Department of Earth Sciences, Chiba University
DJAJADIHARDJA, Yusufu S.[B]	Ocean Research Institute, University of Tokyo
FUJII, Ikuko[D]	Ocean Research Institute, University of Tokyo
FUJIMOTO, Hiromi[A]	Ocean Research Institute, University of Tokyo
FUJIWARA, Toshiya[A]	Ocean Research Institute, University of Tokyo
FUKUDA, Yoichi[E]	Ocean Research Institute, University of Tokyo
FURUTA, Toshio[A]	OKI Electric Industry Co., Ltd.
IGARASHI, Chiaki[F]	Ocean Research Institute, University of Tokyo
IINO, Hideaki[B]	Dept. of Earth & Planetary Sci., Kyushu Univ.
IKARI, Hideo[B]	University of Electro-Communications
ISEZAKI, Nobuhiro [A]	Department of Earth Sciences, Kobe University
ISHIZAKI, Hiroshi[A]	Ocean Cable Co., Ltd.
KASHIHARA, Koji[B]	Department of Earth Sciences, Kobe University
KITO, Tsuyoshi[D]	Dept. of Earth & Planetary Sci., Kyushu Univ.
KOIZUMI, Kin-ichiro[A]	Ocean Research Institute, University of Tokyo
MASARU, Desiderius, C.P.[A]	Ocean Research Institute, University of Tokyo
MATSUMOTO, Takeshi[A]	Japan Marine Science and Technology Center
MATSUOKA, Hiromi[D]	Ocean Research Institute, University of Tokyo
MIZOHATA, Shigeharu[D]	Department of Earth Sciences, Kobe University
MURAYAMA, Masafumi[D]	Ocean Research Institute, University of Tokyo
NAKA, Jiro[D]	Japan Marine Science and Technology Center
NAKANISHI, Masao[A]	Ocean Research Institute, University of Tokyo
NAMBU, Hiroki[A]	Department of Earth Sciences, Chiba University
NG, Raymond[D]	Seafloor Surveys International, Inc.
OGAWA, Yujiro[A]	Dept. of Earth & Planetary Sci., Kyushu Univ.
OHTA, Suguru[A]	Ocean Research Institute, University of Tokyo
OKADA, Makoto[B]	Ocean Research Institute, University of Tokyo
OHKOUCHI, Naohiko[D]	Ocean Research Institute, University of Tokyo
OSHIDA, Atsushi[B]	Ocean Research Institute, University of Tokyo
OTSUKA, Kiyoshi[D]	Japan Marine Science and Technology Center
SEKI, Satoshi[A]	Tsurumi Seiki Co., Ltd.
SHANE, Hugh[D]	Seafloor Surveys International, Inc.
SHINOHARA, Masanao[D]	Department of Earth Sciences , Chiba University
SUYEHIRO, Kiyoshi[F**]	Ocean Research Institute, University of Tokyo
TAIRA, Asahiko[E*]	Ocean Research Institute, University of Tokyo
TAKAHASHI, Narumi[D]	Drpartment of Earth Sciences, Chiba University
TAKATSUGI, Kaori[A]	Department of Earth Sciences, Kobe University
TAKEUCHI, Tomoyoshi[E]	University of Electro-Communications
TAMAKI, Kensaku[A]	Ocean Research Institute, University of Tokyo
TANAKA, Takeo[A]	Japan Marine Science and Technology Center
TOH, Hiroaki[D]	Ocean Research Institute, University of Tokyo

(continued from the previous page)

TOKUYAMA, Hidekazu[C]	Ocean Research Institute, University of Tokyo
TSUKIOKA, Satoshi[B]	University of Electro-Communications
UEKI, Toshiaki[E]	Ocean Research Institute, University of Tokyo
WATANABE, Masaharu[A]	Ocean Research Institute, University of Tokyo
YAMAMOTO, Fujio[D]	Ocean Research Institute, University of Tokyo
YANG, Chul Soo[D]	Ocean Research Institute, University of Tokyo
YORIMITSU, Kazuo[E]	Image and Measurement, Inc.

A from June 25 (Tokyo) to July 10 (Yokosuka) only
B from June 25 (Tokyo) to July 27 (Yokohama) only
C from July 14 (Yokosuka) to July 28 (Tokyo) only
D from July 14 (Yokosuka) to July 27 (Yokohama) only
E from July 14 (Yokosuka) to July 20 (Hachijojima) only
F from June 25 (Tokyo) to July 28 (Tokyo)

* acting Chief Scientist: from July 14 to July 20
** acting Chief Scientist: from July 20 to July 28

2. Index Maps of Cruise KH 90-1 Leg 1

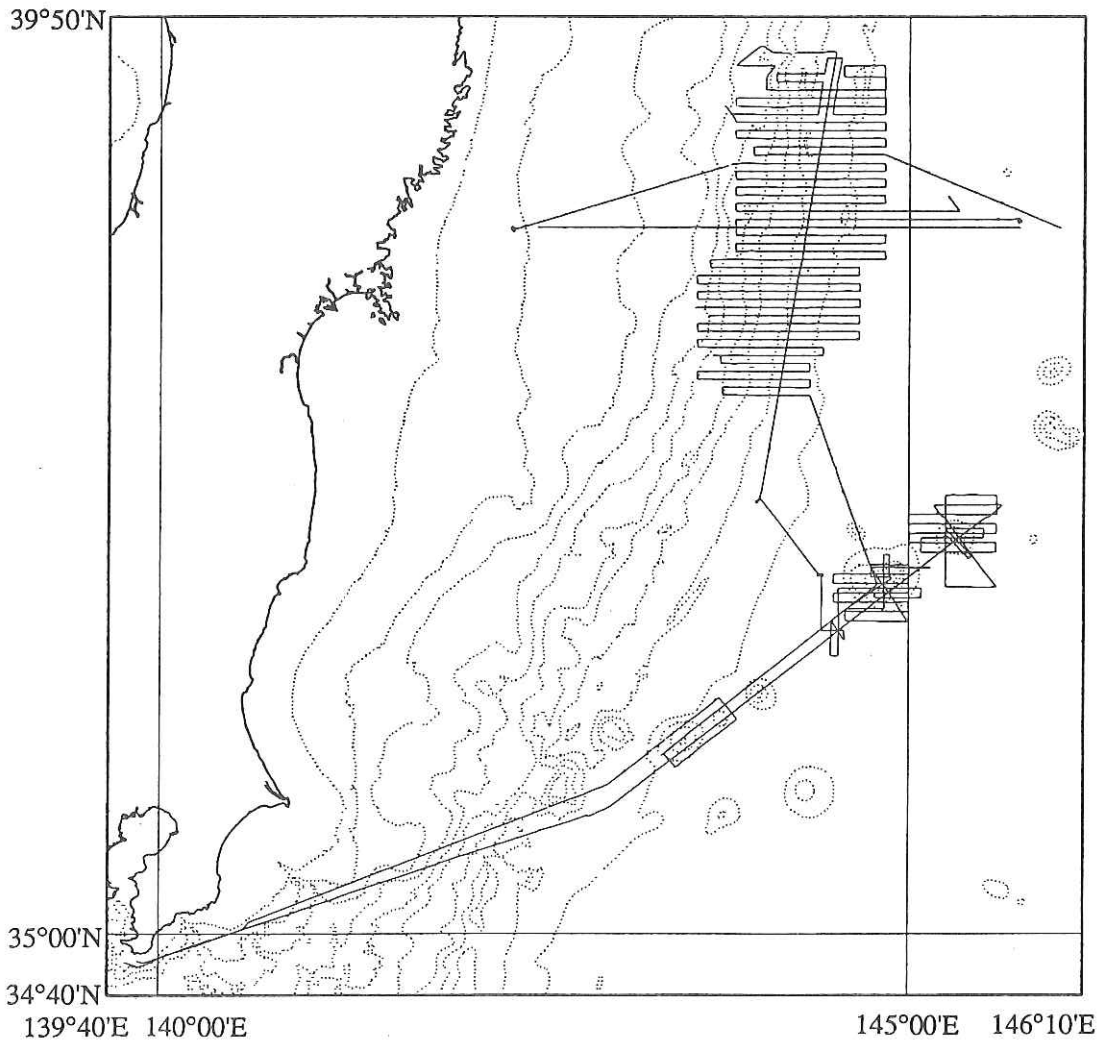

Fig. 2-1. Ship's tracks for the entire cruise KH 90-1, Leg 1
Contour interval: 1,000 m except for a 200 m contour next to the coast line.

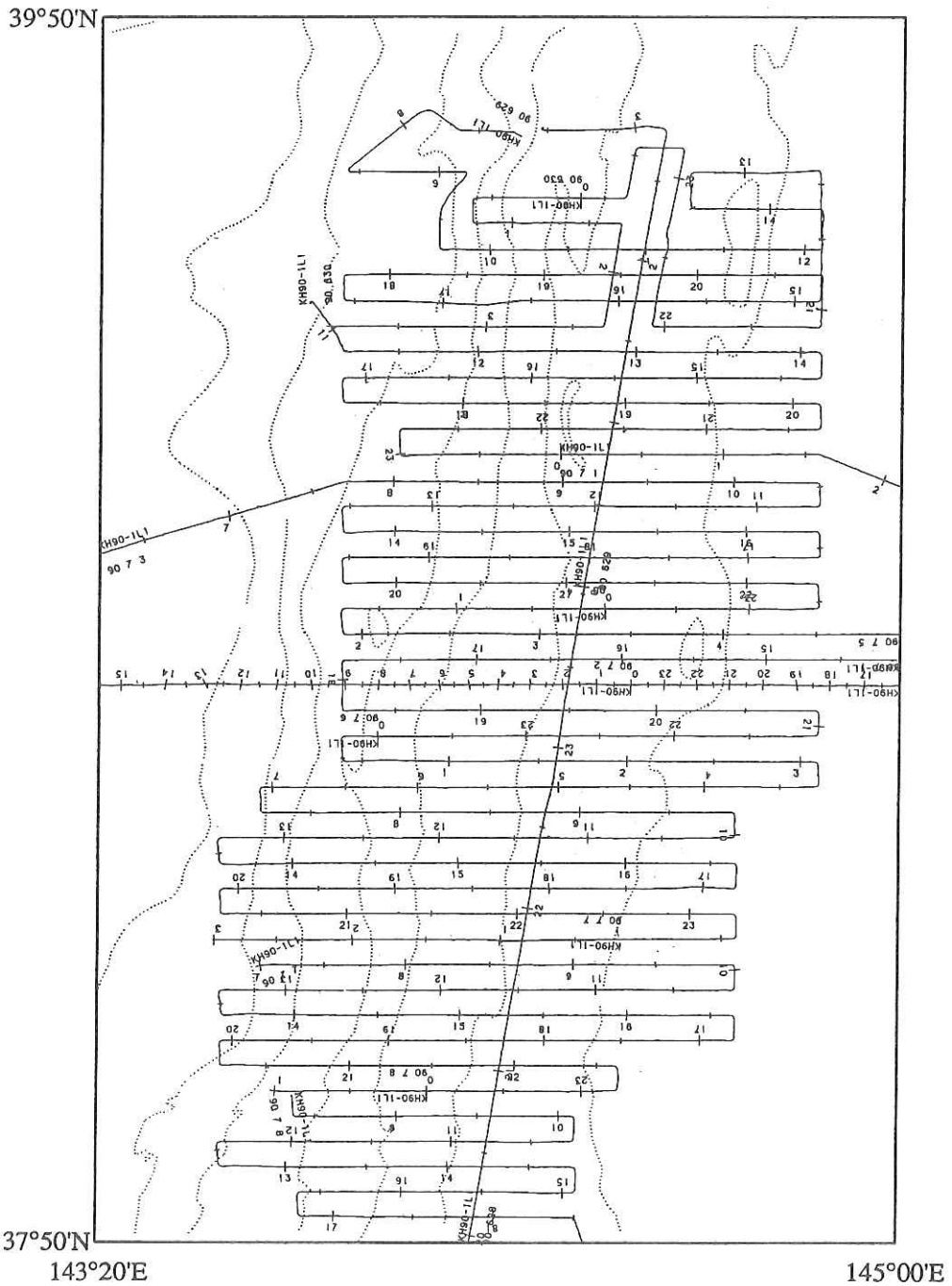

Fig. 2-2. Ship's Tracks for Japan Trench Survey
Contour interval: 1,000 m.

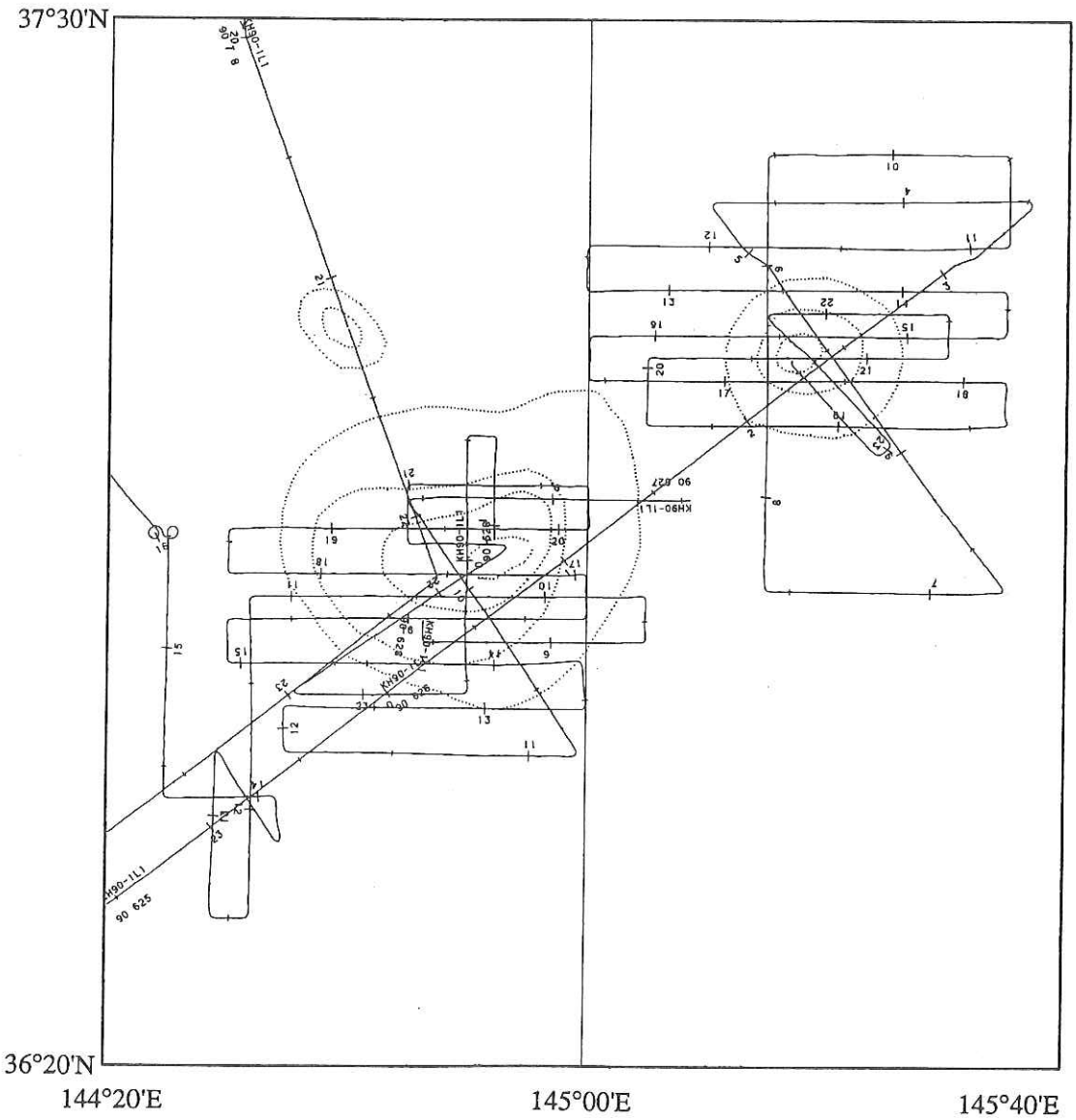

Fig. 2-3. Ship's Tracks for Seamount Survey
Contour interval: 1,000 m.

3. Index Maps of Cruise KH 90-1 Leg 2

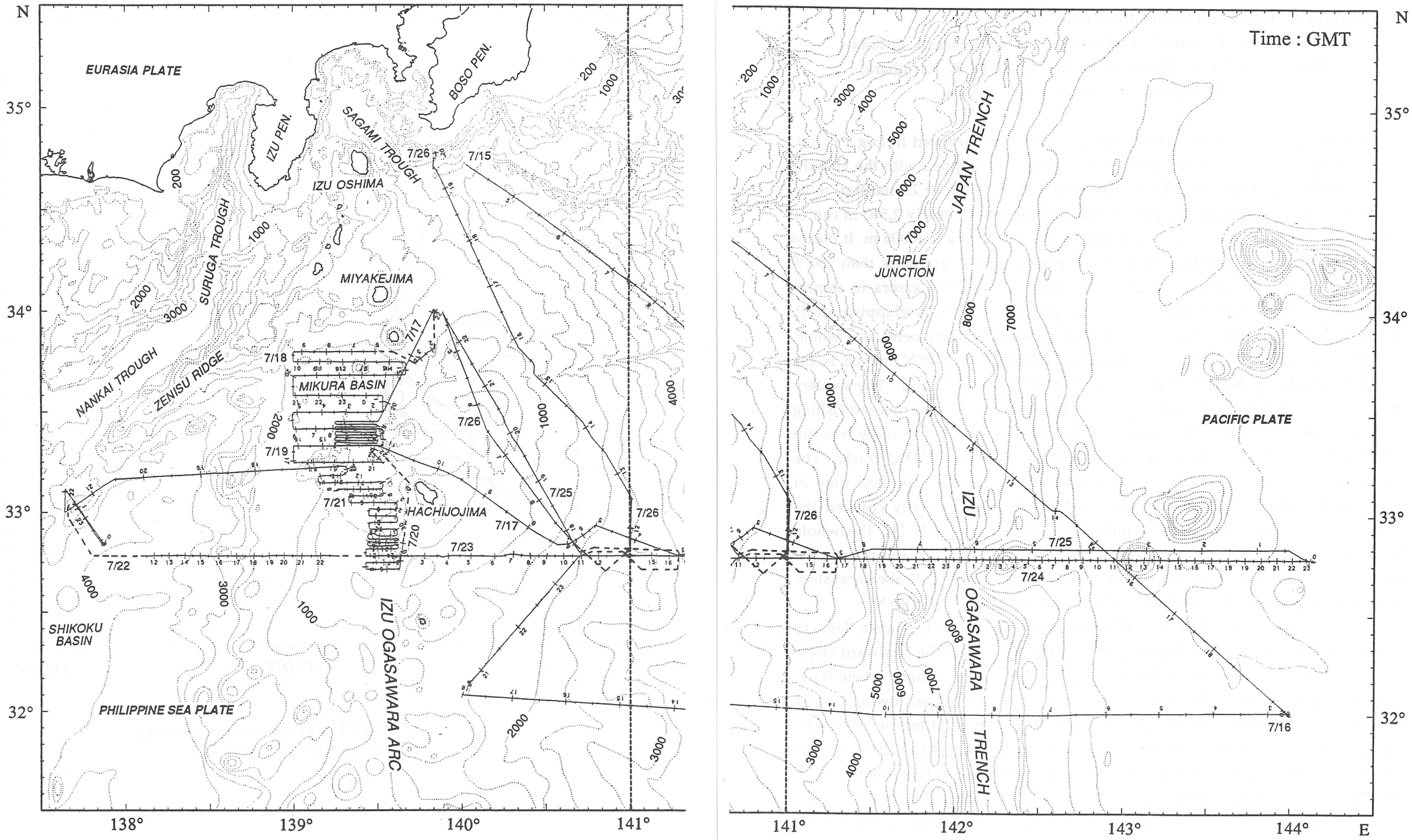

Fig. 3-1. Ship's tracks for the entire cruise KH 90-1, Leg 2 (continued to the next page)

4. Bathymetry of the North-Central Japan Trench by Seabeam

4. 1 Outline of Survey and Main Objectives

K. Kobayashi, K. Tamaki, H. Fujimoto, M. Nakanishi, A. Oshida,
D. C. P. Masalu, Y. Ogawa, H. Iino, T. Tsukioka, K. Kashihara,
T. Matsumoto, T. Tanaka and T. Furuta

Bathymetry of the north-central Japan Trench was surveyed in Leg 1 of this cruise by means of a swath mapping system Seabeam equipped with the Hakuho Maru. Most of the survey tracks are EW with spacing of about 2.5 nautical miles (4,500 m). As the Seabeam has precise swath width of 43°, nearly 2,500 m can be covered by one limb of one track at water depths amounting to 6,000 m. It means that swath depths obtained by tracks in the present survey are more than 100 % coverage. Considering wide angles may cause appreciable errors in depths owing to undetectable variations in velocity profiles, slightly overlapping swath mapping in the present survey provide good accuracy of bathymetry as a whole.

The northernmost track is situated at a latitude of 39°40'N, which is the southern margin of the survey area in the KAIKO Project [1, 2, 3]. The western half of the second northernmost track was abandoned owing to moored fishing nets at night. However, full coverage of the trench by Seabeam survey was not interfered, since it is almost overlapped with a southern KAIKO track. The southern border of the present survey forced according to a limited time of cruise is at latitude of 37°52.5'N. As the KAIKO survey already covered the Daiichi-Kashima Seamount area south of the latitude 36°10'N [4], the whole Japan Trench of nearly 600 km in length from the Erimo Seamount to the Daiichi-Kashima Seamount has mostly been surveyed by the Seabeam system except for its 200 km long southern portion between 37°52.5' ~ 36°10'N.

As this survey aims at obtaining topographic features of the Japan Trench, each survey track ended at a depth approximately 5,000 m in the landward slope and at the top of the steepest wall on the east of the trench. Length of one track is thus roughly 100 km. A few tracks were surveyed part by part owing to two reasons; (1) Deep-sea monitoring work is planned in daytime at relatively shallow sites, (2) Fishing boats were at work only at midnight in the northern portion of surveyed area and we chose survey time there in daytime to avoid conflict with their fishing nets. As survey lines are numbered (0 to 60) in order of time, several tracks are composed of more than two lines with discontinuous numbers (Fig. 4-1). The new data cover an area of nearly 20,000 km^2. Only one

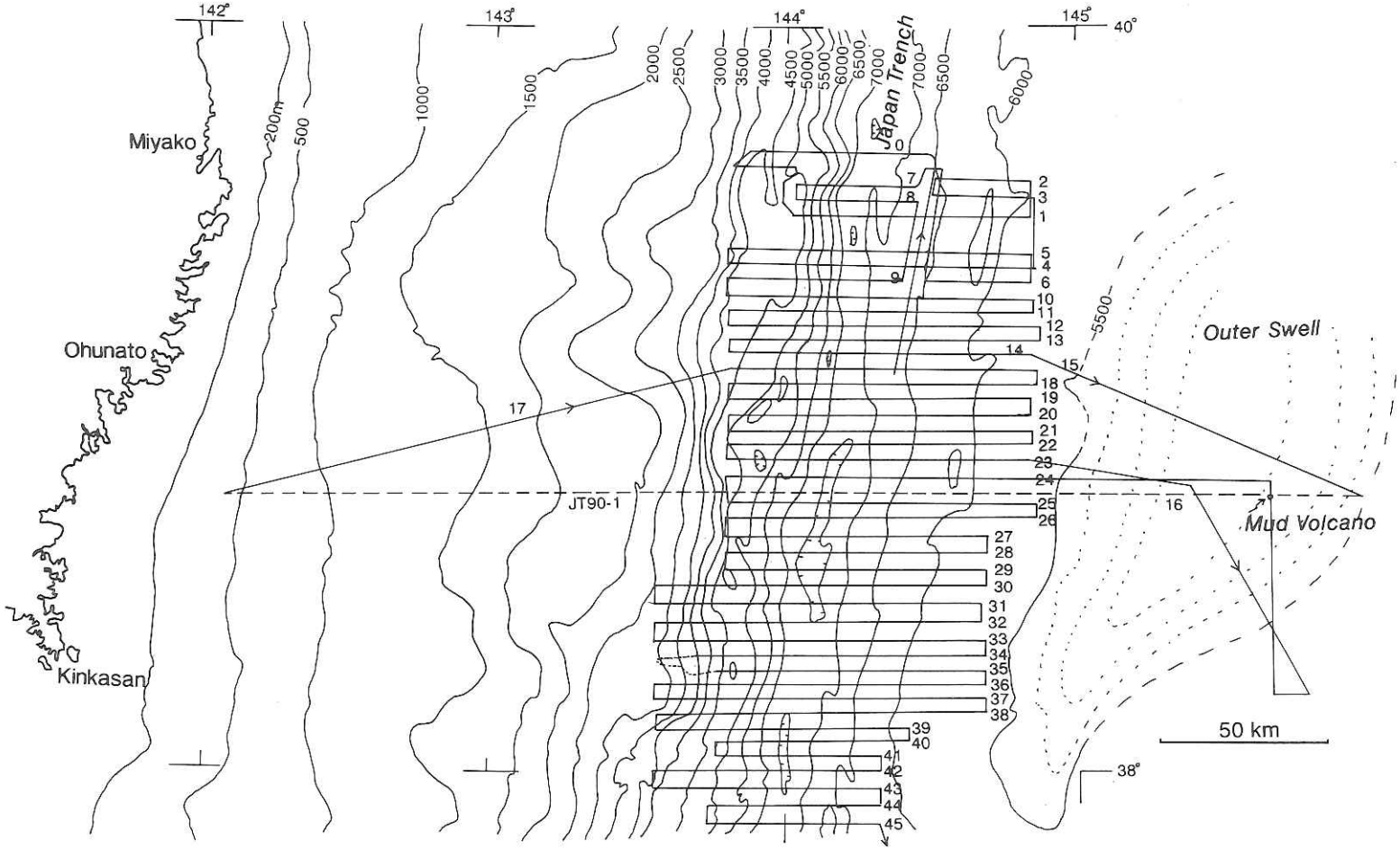

Fig.4-1. Index map of surveyed area, showing the SeaBeam and 3.5 kHz profiling Lines 0 to 45, including the multichannel line, JT90-1 (=Line 16).

profile is extremely long (nearly 300 km) from 146°00'E (the crest of the trench outer swell) to 142°20'E (the upper continental slope, D = 500 m) at a latitude of 38°40'N. Multichannel seismic profiling was done along this transect at a speed of 5 knots as described in Chapter 10 of this report.

Seabeam bathymetry was successfully done simultaneously with water gun shots along this line. Two oblique profiles between the edge of survey box at a latitude of 39°05' ~ 39°07.5'N and each end of this line were also surveyed by Seabeam. On the way to the northern margin of the box from 37°20'N: 140°00'E a track of Seabeam was taken along the upper ocean wall of the trench at an approximate depth of 6,400 m. A number of cross points indicate that water depths given by Seabeam are consistent regardless the heading of the ship, confirming the overall reliability of the bathymetric maps.

Principal objectives of this survey are as follows;

(1) Define more precisely trends of normal faults occurring at the seaward slope of the trench.
(2) Examine detailed features; thrust faults, deep-sea terraces and landslides onthe landward slope of the trench.
(3) Confirm morphology of the trench bottom which seems to be affected by the subducting seaward topography.
(4) Investigate the tectonic effect of bending of the axis of the Japan Trench which trends roughly NS in the north of 38°N, whereas it is in a direction of N30°E south of it; the Japan Trench is convex toward the ocean at a latitude of 38°N.

4. 2 Results of Bathymetric Measurement

K. Kobayashi, K. Tamaki, H. Fujimoto, M. Nakanishi, J. Oshida,
D. C.P. Masalu, Y. Ogawa, H. Iino, T. Tsukioka, K. Kashihara,
T. Matsumoto, T. Tanaka and T. Furuta

Bathymetric maps with scale of 1/100,000 and contour interval of 40 m were prepared on-line real time basis in the Seabeam lab on board the Hakuho Maru while the ship was running at a cruising speed of 16 knots. The data were post-processed by the computer in Lab no. 8 of the ship and by a computer in Nakano main campus of the Ocean Research Institute. A map for the whole surveyed area of Japan Trench with scale of 1/350,000 and contour interval of 50 m was reproduced and attached in a back pocket of this report. Bathymetry was colored by computer with the same size and also attached in a back pocket.

A three-dimensional view (so called whale's-eye view) of the whole trench region was drawn with colors. It is inserted in the back pocket.

All of these maps clearly show that the seaward wall of the trench is characterized by a great number of normal faults forming horsts and grabens. Majority of the faults are nearly parallel to the trend of the trench axis, whereas an appreciable number of faults are oblique to the axis. These oblique faults are classified into three according to their trends; (1) normal faults trending parallel to N65°E, (2) faults trending N45°E and (3) those trending N30°W. A group of faults (2) and (3) form zigzag alignment on the generally westerly dipping trench wall, which marks a great contrast to the northern box surveyed by the KAIKO Project [1].

4. 3 Tectonic Implications of the Topographic Features of Japan Trench

Y. Ogawa, K. Kobayashi, K. Tamaki, H. Fujimoto, J. Oshida
T. Tanaka, T. Matsumoto and H. Iino

Description of the Seabeam topography

Trench oceanward slope

The Pacific plate is going to subduct to WNW at a rate of about 9 cm/yr. The average dipping angle of the oceanward slope is around 2.3° but becomes much steeper when approaching the landward region. Representative dip of the slope is taken from the Lines 14 and 15 as indicated in Fig. 4-2. After a significance bulge at the Outer Swell, the dip in the upper slope is still 0.3°, but in the middle it becomes 1.2°, and in the lower 2.6°. In the lowest slope it attains 5.1° or larger.

Many normal faults incised the seaward slope, and very systematic horst and graben structures are developed. It is well shown on the whale's-eye views of in the northern part (Fig. 4-3). According to these figures, in the north the north-south trending faults are remarkable. Each plain on the horst and graben dips to the trenchward, increasing the angle nearer to the trench, though they are very low angle from 0.2° to 1.2° (See the 3.5 kHz chapter). This suggests that the mode of down-going slab is like a belt conveyor rather than an escalator (Fig. 4-4). The local slope angle at the side of the horst and graben structure is read from the Seabeam maps as in Fig. 4-2. Angle 9° to 20° are common, but very locally 36° is recognized, and 9° to 20° is common. Though there are several exceptions, the dip angle of the slope is steeper on the trench-facing rather than the ocean-facing. This also supports the belt conveyor model.

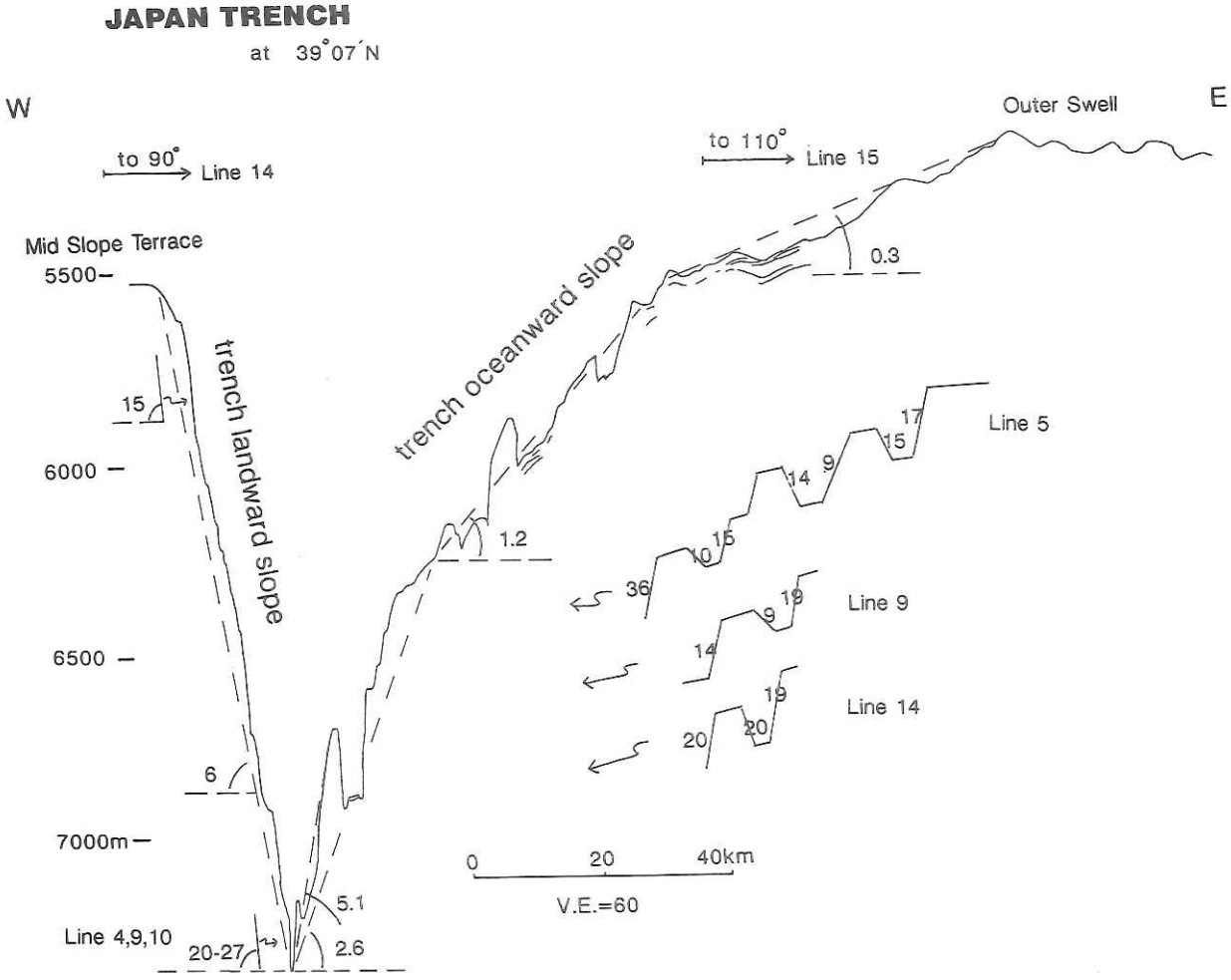

Fig.4-2. Representative profiles crossing the central Japan trench; Lines 14 and 15 based on the 3.5 kHz profile. Three examples of schematic topography are included in the right-handed bottom. Numericals indicate the slope angle.

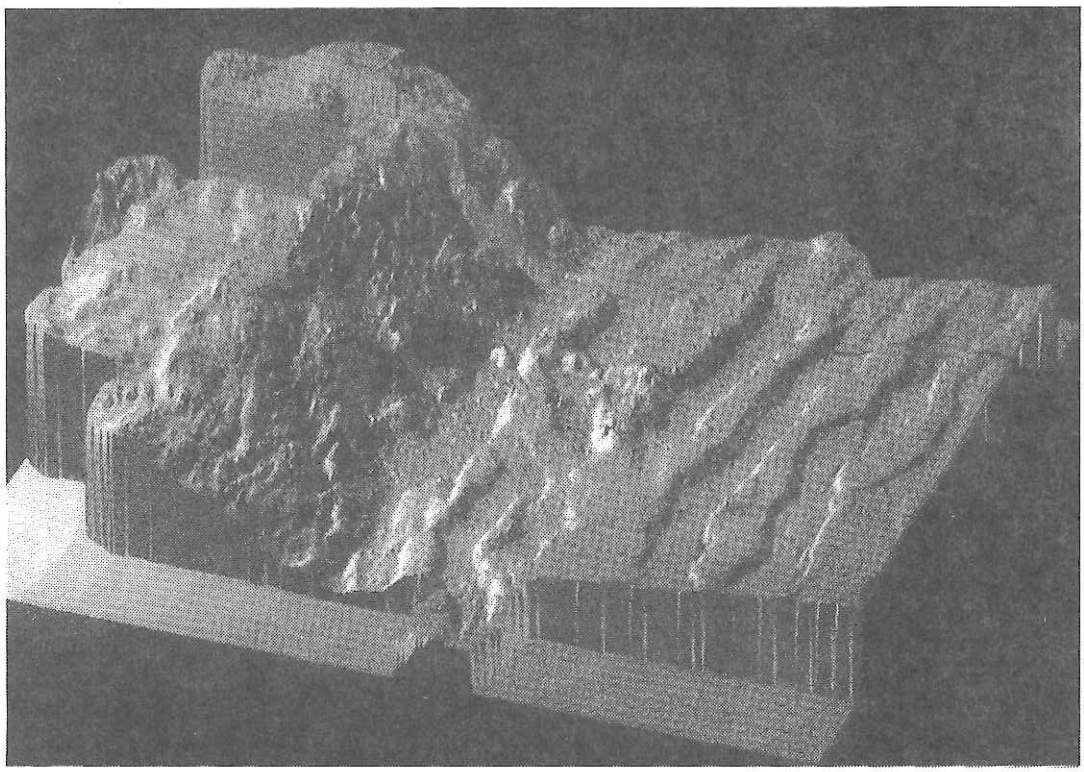

Fig. 4-3. Digitally processed whale's-eye view of the central Japan trench based on the Seabeam data (4.3). Looking down from SE, vertical exaggeration=1:12. A; the northern part, B; the middle part of the surveyed area, both the same scale with 93 km wide (E-W) and 65 km long (N-S). C; detailed view in the northern part, the width about 20 km and height of the steep cliff attains about 1 km.

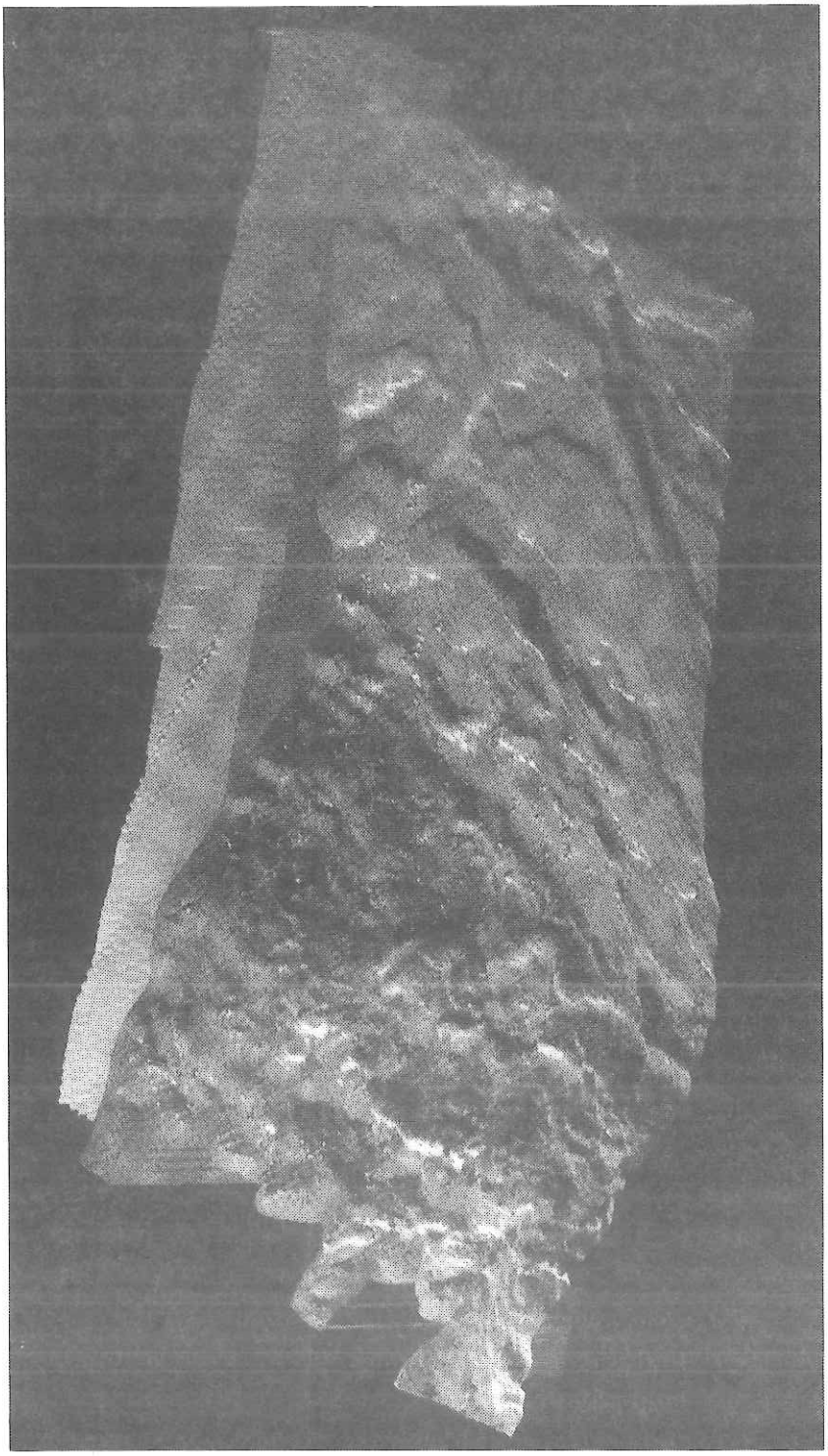

Fig. 4-3 (B).

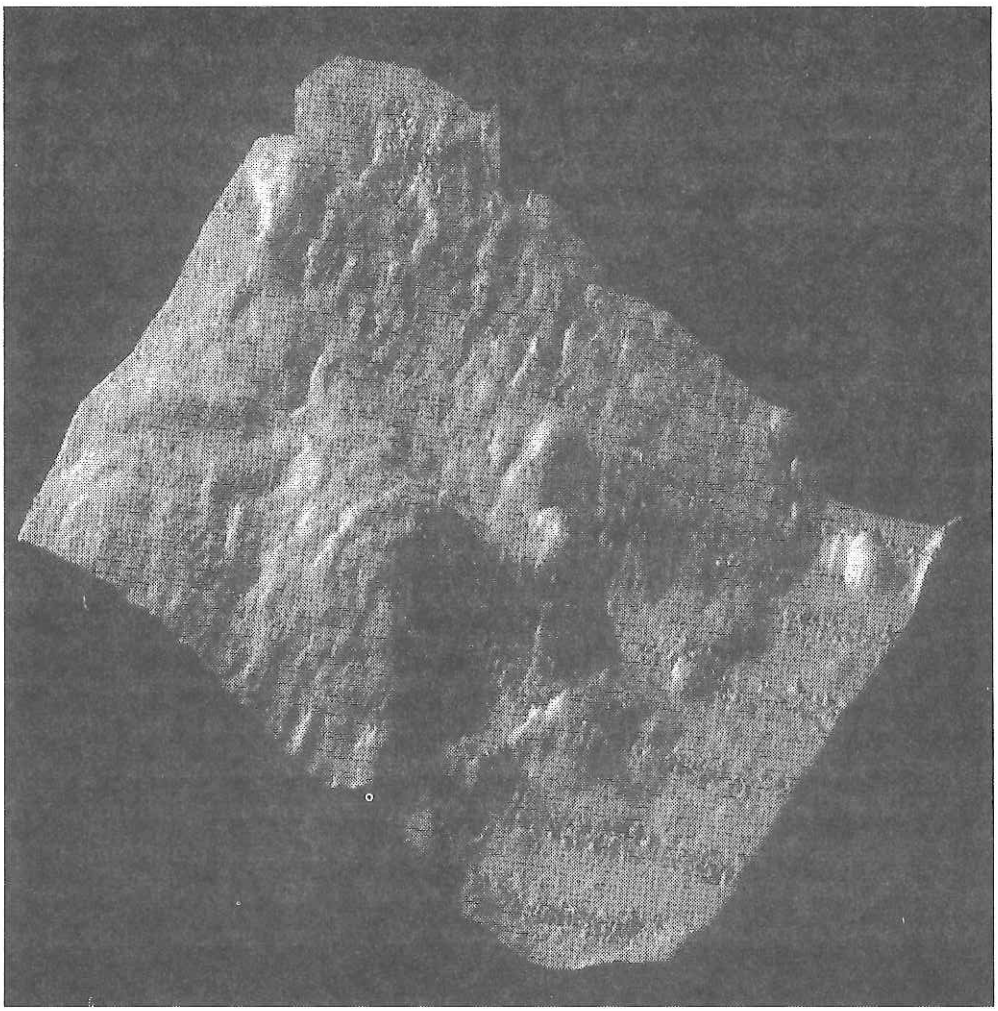

Fig. 4-3 (C).

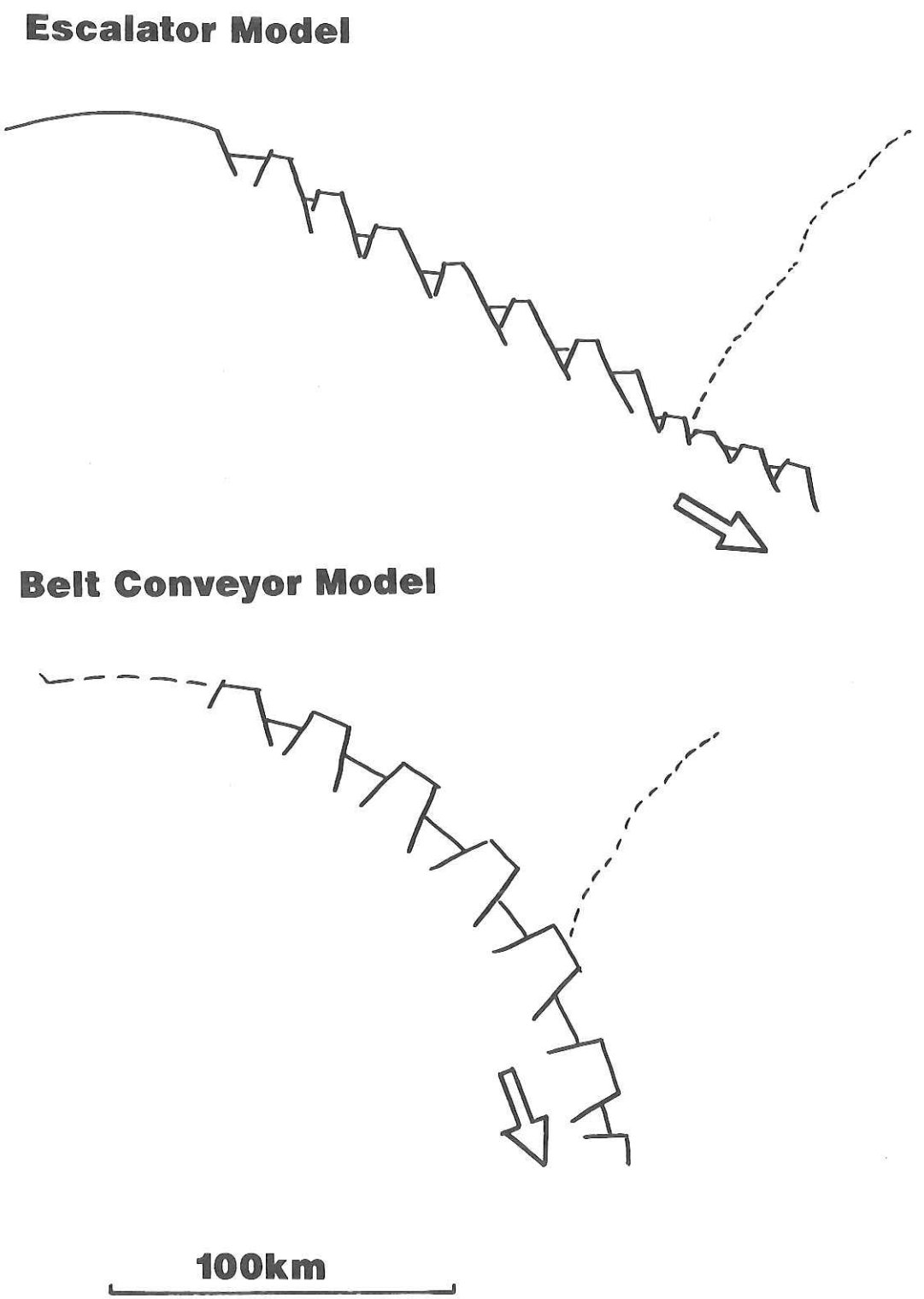

Fig. 4-4. Escalator model vs. belt conveyor model. Vertically exaggerated.

The fault direction becomes much more complicated to the south (Fig. 4-3). In the middle part of the surveyed area, around the lines from 17 to 29, three directions of the scarp are recognized, one is north-south, roughly parallel to the trench direction, the second is N20°E to N40°E, mostly parallel to the Kuril trench direction. This is not exactly the same as the trend of the magnetic lineations in the Pacific plate as shown in Nakanishi *et al.* [6]. The other direction is N20°W to N30°W, which is almost perpendicular to the magnetic lineations and must be correlated to the old transform fault as mentioned later.

At some places the faults with NE trend seem to cut and dislocate those with N-S and N-W trends, whereas at another place *vice versa*. It is not exactly known how these three components are explained, but it can be safely said that all of them are quite young, younger than a time when the plate began to come down to the subduction zone. It must be characterizing the fracturing and faulting on the down-going slab, between the directions of two trenches, the Japan trench, the Kuril trench and old magnetic lineations.

According to recent magnetic study by Nakanishi *et al.* [6], magnetic anomaly lineations around the present area trend N67°E. There are rather few fault scarps of this trend, rather there are quite a few examples of the trend perpendicular to this. The latter may correspond to the ridge-ridge transform faults, and they may be reactivated due to the bending related to the down-going plate subduction. On the other hand, the faults exactly parallel to the trench direction might be due to direct consequence of extension of the bending of the oceanic plate. The Sanriku Earthquake occurred in 1933, M=8.3 associated with large Tsunami may have originated from one of the gigantic normal faults in this trench oceanward slope in the northern part of the surveyed area.

Trench floor

The Japan Trench trends almost north to south in the north-central zone. In further north it is northeastward, and in further south it trends southwestward. Depth of the trench floor ranges about 7,200 to 7,500 m with the deepest part at 38°40'N, *ca* 7,540 m deep. The trench floor is only 5 to 10 km wide in the northern part. In further south the trench has no flat wide bottom, indicating very low sedimentation. Just north of 39°27'N, there is a small seamount or knoll standing in the trench floor. NE and NW trending ridges or horsts of the ocean plate commonly extend to the trench floor, indicating that the original topography in the oceanic side remains even in the trench floor. This means that little sedimentation occurs in the trench axis.

The trench axis has a zigzag pattern particularly in the central and southern part of the surveyed area. This may be an extension of the original seaward topography in the trench axis and , in some places, even toward the landward toe.

The 3.5 kHz subbottom profile along 38°45'N shows almost flat 100 m thick acoustically transparent sediment in the floor. Trench sediments seem to be relatively thicker in the northern part, but it is still very thin in the KAIKO area north of the present box [2, 3]. Slump bodies are well recognized along the landward border of the trench. It will be mentioned in the next section.

Trench landward slope

Trench landward slope is variable in its topography from north to south, but it is generally divided into three; the lower, middle and upper slopes. The lower slope has an average slope angle of about 6° to 9° and water depths from 5,000 to 7,200 m. Very steep cliffs or slopes with angles greater than 20° are developed forming three to four steps, particularly in the lowest trench slope (Fig. 4-2). In the upper part of the lower trench slope sometimes 15° slope is seen. Above the lower slope, almost flat, less than 1° dipping slopes are seen. This corresponds to so-called "Mid Slope Terrace" of Cadet *et al.* [1], who surveyed the zone just north of the present area under the French-Japanese KAIKO Project, Phase 1, Leg 3. In the KAIKO area the terrace is of 4,400-4,500 m deep, while in the present area the depth varies from place to place. In the northern part, it is about 5,000 m deep, in the middle part, 5,400 m (Fig. 4-3) and in the southern part, 3,500 m. In the middle and southern parts, very rough and hammocky topography is seen (Fig. 4-2). The Mid Slope Terrace may be characteristic topography developed in the northern part of the Japan trench, and seems to diminish southward.

Above the Mid-Slope Terraces, only Line 16 in the present survey recorded topography shallower than that (Fig. 4-5). In that transect the middle slope is characterized by a slope gentler than the lower slope but still rather steep with about 7° dip. It continues until a depth of 2,000 m, and above it much gently (1.4°) dipping upper slope is developed until the shelf edge.

Tectonic erosion and non-accretion at the toe of the trench landward slope : an interpretation

The lower slope is characterized by steep cliffs, associated with sliding or slumping masses accumulated below them. This is well recognized by the

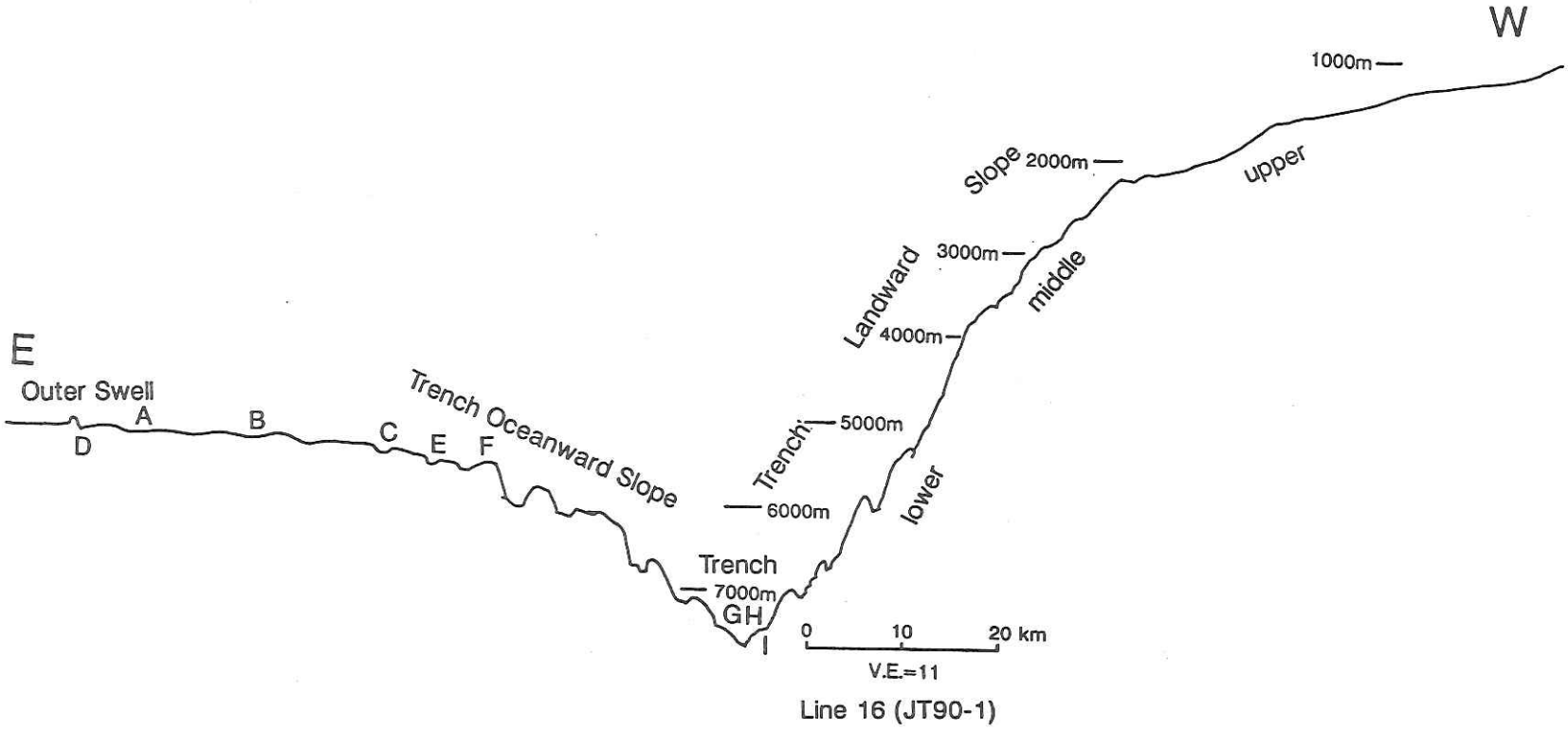

Fig. 4-5 Long profile based on 3.5 kHz profiler from the outer swell to the trench landward slope through the trench oceanward slope and the trench axis along the Line 16 (=JT90-1).

existence of small round basins (or depressions) and swells (or knolls) (Fig. 4-6). This is also clearly shown in very nicely processed whale's-eye view diagrams in the northern part of the area, particularly along the Lines 4, 5, 9 and 10 (Fig. 4-3). This feature is very similar to the examples of sliding or slumping onland, and typical listric normal fault-like scarps are observed. The problem is whether the sliding or slumping was due to normal faulting or thrusting, and where the plate boundary between the North American and Pacific runs. This question is related to why and how no accretionary prisms are developed in the Japan Trench [1, 5].

As for the listric topography, it seems that the sliding or slumping is due to gravity-driven normal fault-type sliding. At the exact plate boundary on the foot of the slope, as far as we see or "watch" the Seabeam maps, there are scarcely existent sharp boundaries on the very foot of the landward slope. In contrast rather many slide deposits, slumped masses or hills are overlapping at the trench landward edge. It is well shown along the Lines 9 , 17, 23, 25, 26 and 27, and discussed again in the 3.5 kHz chapter (Chapt. 12). It is interpretatively illustrated in Fig. 4-7.

Comparing with general features of the accretionary prisms like those in the Nankai trough where thrusting is common, topography is quite alike here. Probably it is natural to think the lowermost part of the landward slope of the Japan Trench is normally faulted or land slided, and the slided or slumped masses overlapped the plate boundary to the Pacific plate side, then they are incorporated to the downgoing slab to be subducted. Therefore the landward rock might not increase but eroded to loose its volume. This is because no accretionary prism there. Still there is a question how the landward slope has become upheaved. This may be due to the horizontal compression from the Pacific side, or the old accretionary prism remained beneath the sediment cover of the slope makes the resistance against the erosion to be still steep of the slope.

Interpretation of 3.5 kHz subbottom profile along 38°45'N (Line 16)

A transect of 24-multichannel seismic profiler with 4-set water guns was obtained from July 1st to 3rd, 1990, together with two proton gradiometers survey, gravity measurement, Seabeam mapping and 3.5 kHz subbottom profiling along an E-W line from 146°00'E to 142°30'E at a latitude of 38°45'N (Line 16) in the middle of the surveyed area (Fig. 4-1). The multichannel line is called JT90-1. The ship speed was kept at 5 knots. The line began at the east of

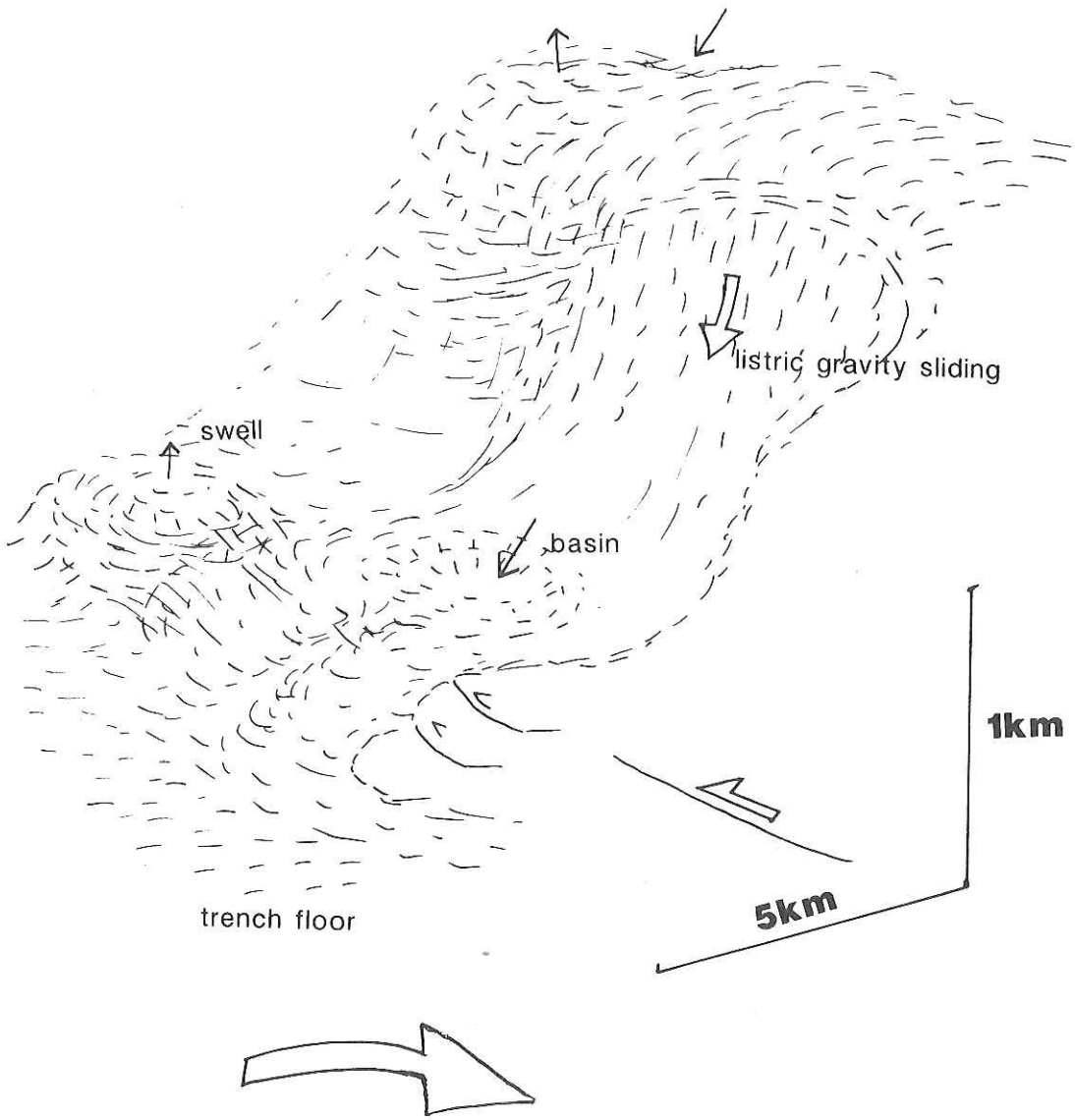

Fig.4-6. Schematic illustration of the foot of the trench landward slope around Lines 4, 5 and 9.

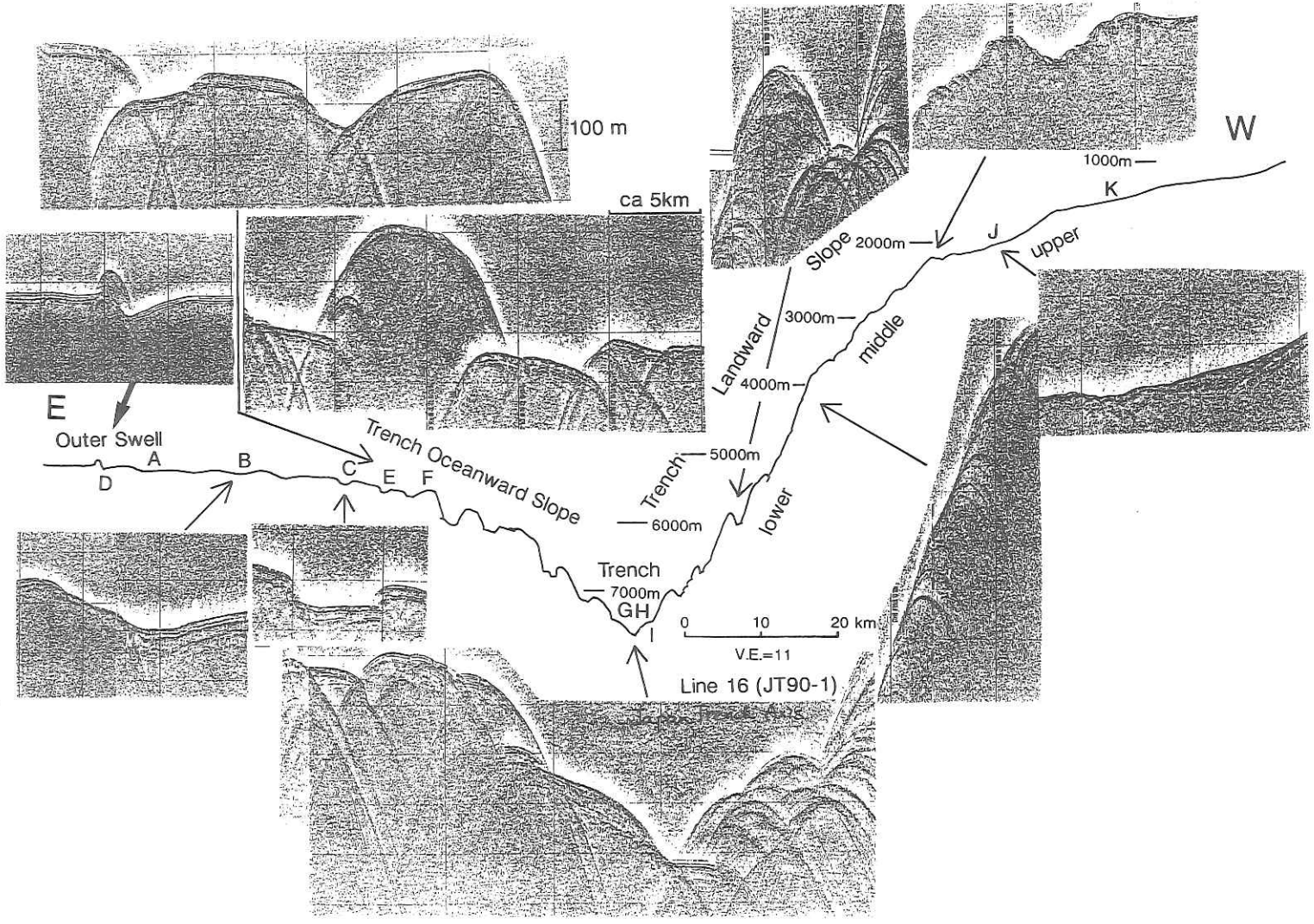

Fig. 4-7. Representative 3.5 kHz subbottom profiles along Line 16.

the outer swell, came down the trench seaward slope, crossing the trench axis, then came up the trench landward slope until the depth of 1,000 m (Fig. 4-1).

As for the 3.5 kHz profiling, profiles in the 1,000-m range were continuously taken in detail (at the easternmost portion a 2,000-m range profile was obtained). The followings are our interpretation mainly based on the 3.5 kHz subbottom profiles and Seabeam maps (Fig. 4-7).

Outer swell

The top of the trench outer swell is nearly 5,200 m deep with a relative height of about 400 m from the abyssal plain. The top is situated at 146°E on this line. It has swells of a small cycle with 50 m relief (A in Fig. 4-7), although no remarkable faults are recognized except for some examples around a mud volcano described in the next chapter. Most of the small swells are covered by sediment drape with minor faults merely dislocating the sea bottom surface (B in Fig. 4-7). The outer swell topography sharply changes to that of the trench oceanward slope on its west.

A conjugate set of normal faults form a graben with 40 m high scarps (C in Fig. 4-7). These horsts and grabens may be either on the fracture zones trending N20°W [6] or N-S. The sediment covers are 50 m thick acoustically transparent layer with several reflective interlayers. Such a sedimentary structure is equivalent all over the trench oceanward slope. The transparent layer seems to be diatomaceous clay or mud of pelagic or hemipelagic origin and the reflective interlayers might be ash layers blown from the Tohoku Nihon (Northeast Japan) volcanic arc [7]. The origin of these ash layers have not yet been identified but will be an important task in future (T. Furuta, personal communication, 1990).

From the single channel seismic profile of the KAIKO Project, Phase 1, Leg 3 [2, 3], about 0.44 second (two-way travel time) or roughly 400 m thick transparent layer (the upper half is relatively reflective) is known to overly more reflective, presumably chert or cherty sediment above the oceanic layer 2 of the Pacific plate. The above-mentioned tephra-rich sediments atop the Pacific plate seem to be deposited quite recently when the Pacific plate approached the Japanese Islands [9].

A mud volcano was found at 145°44.2'E (D in Fig. 4-7). It is situated just on a fault of 30 m down-dip dislocation. The fault may trend northeastward, judging from elongation of the mud volcano. It is about 1 x 3 km in diameter and 150 m high. The mud is not acoustically transparent, probably due to

desiccation of the muddy materials after the "eruption". This mud volcano is described in detail in a separate chapter (6) of this report.

Trench oceanward slope

The swell is transformed to a steep down-slope topography at a water depth of about 5,500 m. Normal faults appear suddenly, and six sets of horsts and grabens are observed down to the trench (E to G in Fig. 4-7). Relief of the fault scarp is variable; the maximum reaches a height of about 500 m. Among these scarps the trench-facing slope has higher scarps than the sea-facing ones as mentioned previously. This favors the down-dip normal faults of the descending oceanic slab trenchward. The top envelope of the horsts make an upward concave curve, the average dip of the trench oceanward slope being about 3.2° in general. It is gentler (about 1.7°) in the upper portion and becomes steeper (about 6.2°) in the lower slope. Assuming the average dip of 3.2°, the curvilinear radius is calculated to be about 700 km. Calculating from the Seabeam maps, it is known that the steepest seaward dipping wall is about 11° to 14°, while that landward dipping is about 13° to 17° along this line. Much steeper local slopes are recognized along other lines as described previously (Fig. 4-2).

The top surface of the horst and the floor of the graben, all but one exception, incline trenchward, and the dip angle increases from 0.3° to 1.2° through 0.7° down to the trench floor. These values are far less than the general slope dip, suggesting the very top is covered by much more horizontally deposited recent sediments. However, the steeper trenchward slope still supports the model of *belt conveyor* rather than of *escalator* (Fig. 4-4) [8]. As a simple case the escalator model yields the same dip inclination of the fault scarps of the horst and graben either of the ocean-facing or trench-facing, while the belt conveyor model could provide the steeper slopes of the tench-facing scarps. However, the dip of the slope does not always show the original dip of the fault plane, but buried by debris on the cliff, we have to pay attention for this discussion. This problem should be resolved by the future dives.

One exception of the inclination of the slope is seen at the beginning of the trench oceanward slope (F in Fig. 4-7). This oceanward inclination of the top of the horst can be explained by slumping of the block with backward rotation. Sediment cover of the trench seaward slope is almost the same as that in the outer swell area. The sediment layers are disturbed around the fault scarp, sometimes the drag by the fault movement, sometimes submarine sliding on

the fault scarp. Above all the relatively steep dipping surface just east of the trench axis (G in Fig. 4-7) is underlain by rather thick cover, nearly 100 m. The lower part appears to dip more steeply trenchward. This may suggest that the layer has been depositing during the downwarping of the trench oceanward slope including sliding.

Trench floor

The trench floor at 144°08'E is about 1.8 km wide and about 7,500 m deep. It is almost flat, but very slightly inclines by less than 0.1°. To say critically it is relatively steeper near the toe of the foot of the landward slope. The acoustically transparent sediments about 100 m thick with several reflective interlayers is recognized from the profile. The 3.5 kHz appearances of the trench sediments are very similar to those on the trench oceanward slope. If this is true, no additional supply of sediments have ever come to the trench axis after the sediments were deposited and dipped landward. Possibly rate of sedimentation here is very low.

Tench landward slope

At the very foot of the trench landward slope small swell (knolls) and basins (depression) are recognized in the Seabeam maps. Just back of them a sharp steep cliffs are developed. Such swells and basins are shown by many parabolic expressions in the the 3.5 kHz profile (H in Fig. 4-7). These features are probably due to the submarine slumping, a sharp listric sliding plane and slid mass which make small swells forward by the backward rotation as shown in Fig. 4-8. The plate boundary between the Pacific and the North American may be delineated along the foot of the sliding plane, but not well recognized in the profile. The slumped mass might come underneath the upper plates as to cause sediment subduction. If this phenomenon continuously occurs, the upper plate, the trench landward slope might be eroded downward and be subducted. Subduction erosion or tectonic erosion may take place by such a mechanism (Fig. 4-8).

A very sharp upslope, in average 7.3° dipping, begins with a strange image of duplicated parabolic patterns. Such an image is known to be duplication of "ghosts" by side echo of the cliffs. In the Seabeam maps, many round swells and basins of several km in diameter and several tens to several hundreds m deep are recognized, lying side by side. These swells and basins may have originated from submarine slumping. The sharp cliffs might be due to thrusting. No

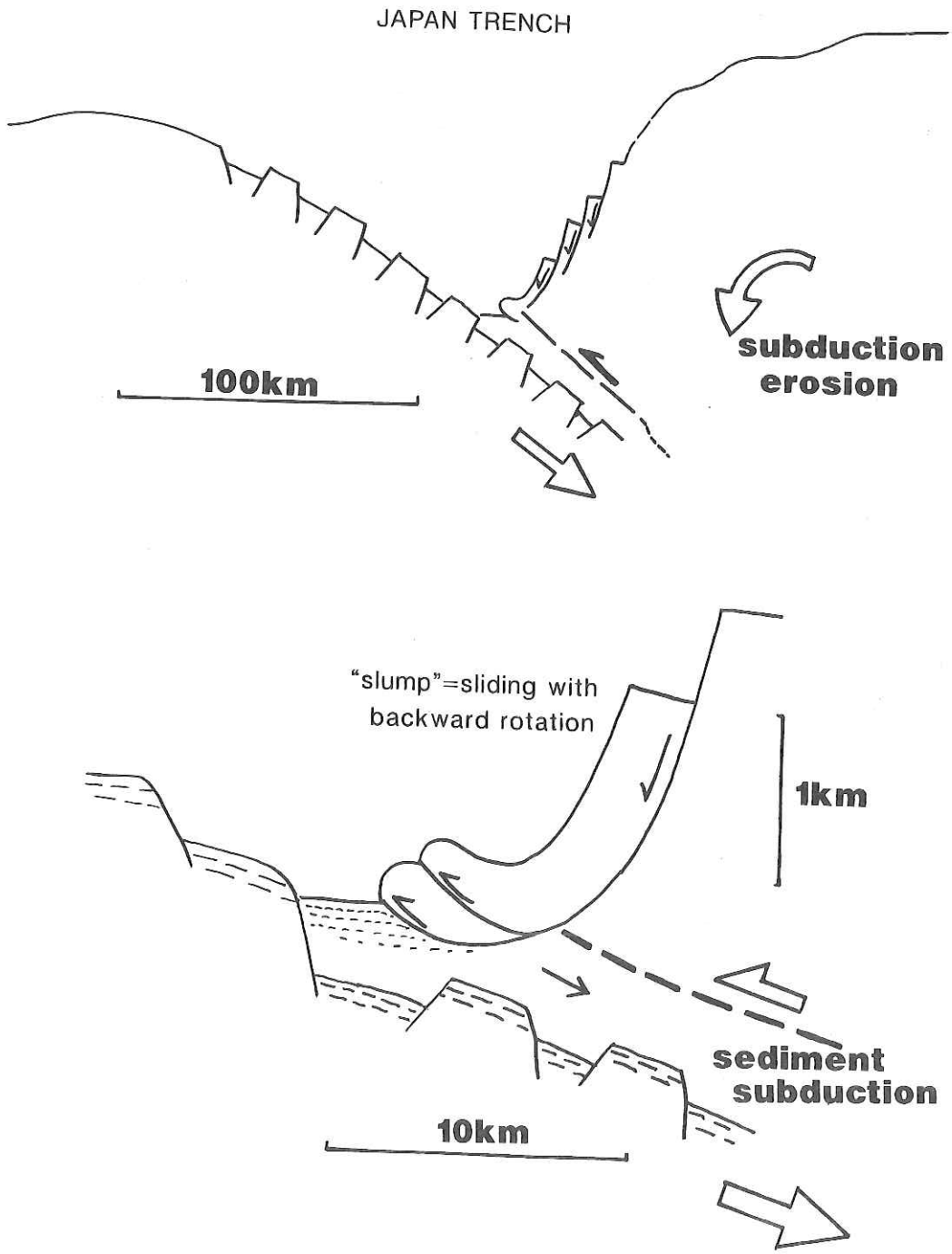

Fig. 4-8. Schematic illustration showing a large scale subduction erosion (tectonic erosion) ocurring in the trench landward slope. Its detailed diagram shows sediments subduction of the trench deposits and slumped mass in below. Bold dashed line denotes plausible subduction plate boundary between the overlying North American plate and underlying Pacific plate.

sediment-bearing ponds are observed in the profile, suggesting these cliffs are not formed by thrusting unlike accretionary prisms as in the Nankai Trough landward slope.

The bottom surface is solid or otherwise paved by coarse sediments. The latter case is not plausibly and a hard *rock*, possibly the Tertiary sedimentary rocks seem to be exposed. The cliff locally dips at 9.7°. No systematic horst and graben are seen in contrast to the trench oceanward slope. These steep cliffs roughly trend north-south. The steep slope continues up to about 3,500 m in depth. This is the lower trench landward slope. There is no distinct "Mid Slope Terrace" along this line or around this area unlike in the northern part as described previously.

From depths of 3,500 m to 2,200 m, relatively gentle slope of about 3° is existent. This is the middle slope (Fig. 4-7). Then a gentle slope of 2.5° begins. It is an upper slope. Several tens of meters thick not highly transparent sediments are observed in the small slope basins, otherwise no sediments are recognized. Submarine sliding is recognized at two positions (J and K in Fig. 4-7). Profiling was finished at a depth of about 1,000 m. Above it a shelf edge may have been developed at 150 m deep bottom.

Further study

If we discuss the Seabeam topography together with the 24-multichannel seismic profile carried out at the same time on this line, we have been able to consider tectonics much more in detail. This area is one of the best targets for the near future divings by "Shinkai 6500", a new submersible of JAMSTEC. There are several steep cliffs and slopes both on the trench oceanward and landward slopes. On the former the layer 2, the oceanic crust composed of basaltic rocks is most probably exposed occasionally with thin cover of pelagic sediments. Real features of faulting of the down-going slab would be observed there.

On the landward slope, many steep cliffs and slopes are dislocated either by normal or reverse faults. Looking at the deep-towed TV used in this cruise, many deep sea animals were observed but not *Calyptogena* which is an indicator of methane seepage. It was observed at the KAIKO phase II at trench landward slopes [10, 11] and hoped to be seen by the future dives. Some of the cliffs in this area may have originated from reverse faults.

Many other topics and problems to be solved are in this area, and this line 16 (JT90-1) is the best surveyed line during this cruise, so that further discussion for future planning must be hopefully done on this line.

References for Chapter 4

[1] J.P. Cadet, K. Kobayashi, J. Aubouin, J. Boulegue, J. Dubois, R. von Huene, L.Jolivet, T. Kanazawa, J. Kasahara, K. Koizumi, S. Lallemand, Y. Nakamura, G. Pautot, K. Suyehiro, S. Tani, H. Tokuyama and T. Yamazaki, The Japan Trench and its junction with the Kuril Trench: cruise results of the Kaiko I, Leg 3, *Earth & Planet. Sci. Lett.*, **83**, 267-284, 1987.

[2] KAIKO I Research Group, *Detailed Topography of Trenches and Troughs around Japan,* Univ. of Tokyo Press, 1986.

[3] KAIKO I Research Group, *Topography and Structure of Trenches around Japan--Data Atlas of Franco-Japanese KAIKO Project, Phase I*--Ocean Res. Inst., Univ. of Tokyo, IFREMER & CNRS, 305pp., 1986.

[4] K. Kobayashi, J.P. Cadet, J. Aubouin, J. Boulegue, J. Dubois, R. von Huene, L.Jolivet, T. Kanazawa, J. Kasahara, K. Koizumi, S. Lallemand, Y. Nakamura, G. Pautot, K. Suyehiro, S. Tani, H. Tokuyama and T. Yamazaki, Normal Faulting of the Daiichi-Kashima Seamount in the Japan Trench revealed by the Kaiko I Cruise, Leg 3, *Earth & Planet. Sci. Lett.*, **83**, 257-266, 1987.

[5] R. von Huene and R. Culotta, Tectonic erosion at the front of the Japan Trench convergent margin. *Tectonophysics*, **160**, 75-90. 1989.

[6] M. Nakanishi , K. Tamaki and K. Kobayashi, Mesozoic magnetic anomaly lineations and seafloor spreading history of the northwestern Pacific,*J.Geophys.Res.*,**94**, 15437-15462,1989.

[7] Scientific Party of DSDP Legs 56/57, Intitial Reports of DSDP, **56-57**, Part 1 & 2, 1980.

[8] J. Kasahara and K. Kobayashi, Consideration of some characteristic tectonic features surrounding trenches (in Japanese), *Chikyuu extra*, **3**, 45-50, 1991.

[9] K. Fujioka, Synthesis of Neogene explosive volcanism of the Tohoku Arc, deduced from the marine tephra drilled around the Japan Trench region, Deep Sea Drilling Project Legs 56, 57 and 87B, in H. Kagami, D.E. Karig, W.T. Coulbourn (eds.), *Intitial Reports of DSDP,* **87**, 703-723, 1985.

[10] J.P. Cadet, K. Kobayashi, S. Lallemand, L. Jolivet, J. Aubouin, J. Boulegue, J. Dubois, H. Hotta, T. Ishii, K. Konishi, N. Niitsuna and H. Shimamura, Deep

scientific dives in the Japan and Kuril Trenches, *Earth & Planet. Sci. Lett.*, **83**, 313-328, 1987.

[11] G. Pautot, K. Nakamura, P. Huchon, J. Angelier, J. Bourgois, K. Fujioka, T. Kanazawa, Y. Nakamura, Y. Ogawa, M. Seguret and A. Tekeuchi, Deep-sea submersible survey in the Suruga, Sagami and Japan Trenches: preliminary results of the 1985 Kaiko cruise, Leg 2, *Earth & Planet. Sci. Lett.*, **83**, 300-312, 1987.

5. Topography of the Joban Seamount Chain

5. 1 Bathymetric Mapping of the Joban Seamount Chain

D.C.P. Masalu, A. Oshida, M. Nakanishi,
K. Tamaki, K. Kobayashi and Y. Ogawa

Introduction

The Seabeam system of the Hakuho Maru (see Fujimoto *et al.* [1] for its description and functioning) was used for bathymetric survey of a chain of seamounts located in the northwestern Pacific basin east off the southern portion of the Japan Trench. A name, the Joban Seamount Chain was proposed by the scientific party onboard Leg 1 of KH 90-1 cruise. Total of six seamounts on the chain were surveyed. These are, from NE to SW, Mizunagidori (Bosei), Iwaki, Hitachi, Daiyon-Kashima, Daisan-Kashima and Daini-Kashima Seamounts. Topography of the Daiyon-Kashima Seamount was surveyed only along two tracks on the way to and from the survey area and, therefore, will not be described so much as the others. A small seamount found nearby the chain was named Futaba and also treated here.

One seamount called Daiichi Kashima Seamount situated in the axis of the southern Japan Trench was investigated in the KAIKO Project [2, 3] using the Seabeam of *Jean Charcot* and the present survey will provide much further information, if data are combined with the KAIKO results.

Outline of Survey and Data

Location of the whole area surveyed on the Joban Seamount chain is shown in Fig. 5-1. The ship's tracks for this survey are shown in Figs 2-2 & 5-2 and the Seabeam bathymetric map obtained from this survey is represented in Fig. 5-3. The northern three seamounts were most intensively surveyed at the beginning of this cruise. The southern two were surveyed in the last part of leg 1 of this cruise after surveying the Japan Trench. The Joban seamount chain, although already known to be existing (*e.g.*, chart 6312 of the Hydrographic Department of Maritime Safety Agency of Japan [4, 5]), was not yet surveyed to this extent using a Seabeam system.

The seamount chain was surveyed to map their topography in some detail by using a Seabeam system and to collect other geophysical data which, when used together with the detailed Seabeam topography, could yield a wider range of our geological and geophysical knowledge of this seamount chain. It is hoped

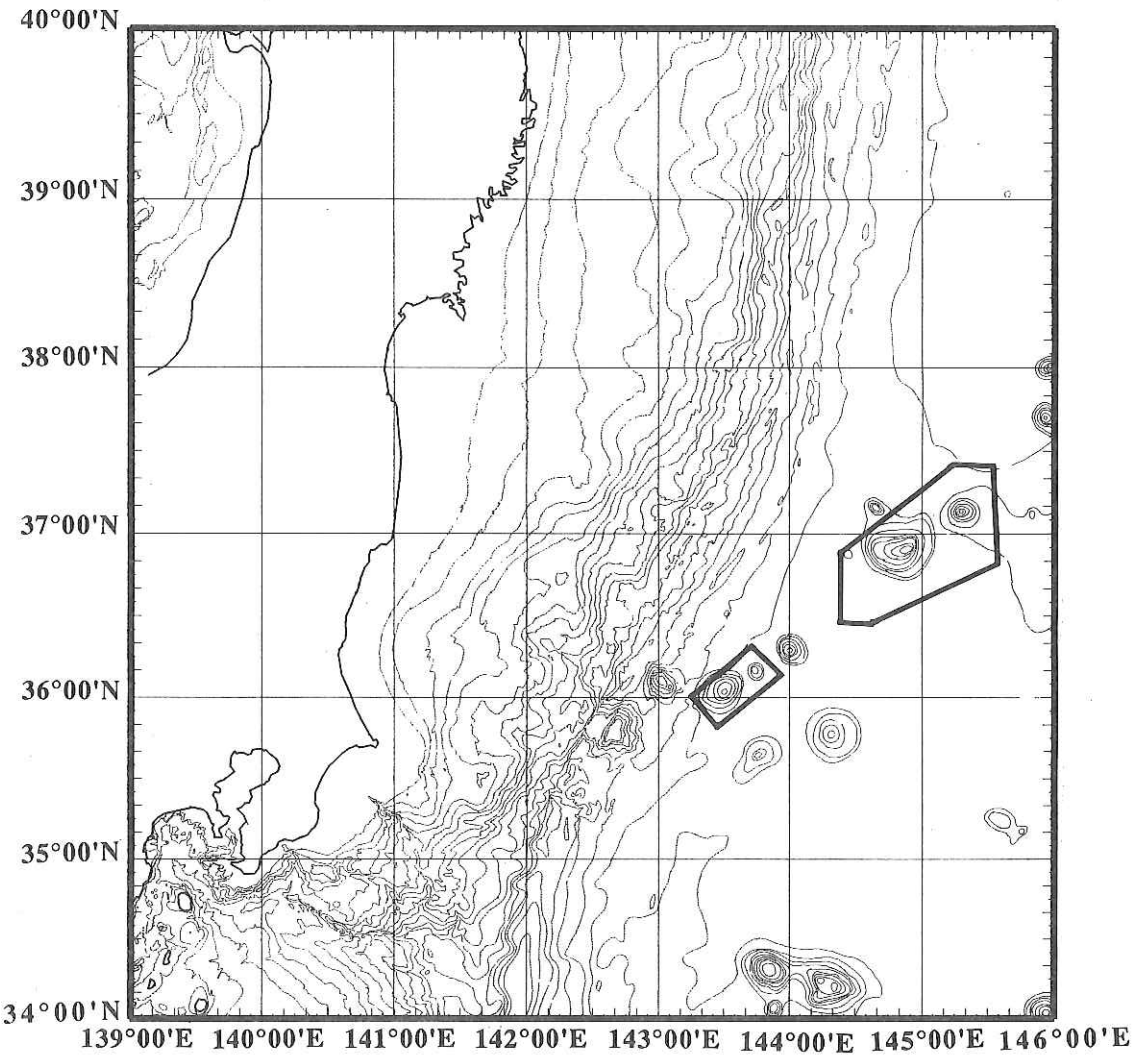

Fig. 5-1 Location map of the whole area surveyed (boxed) on the Joban Seamount chain during leg 1 of KH 90-1 cruise.

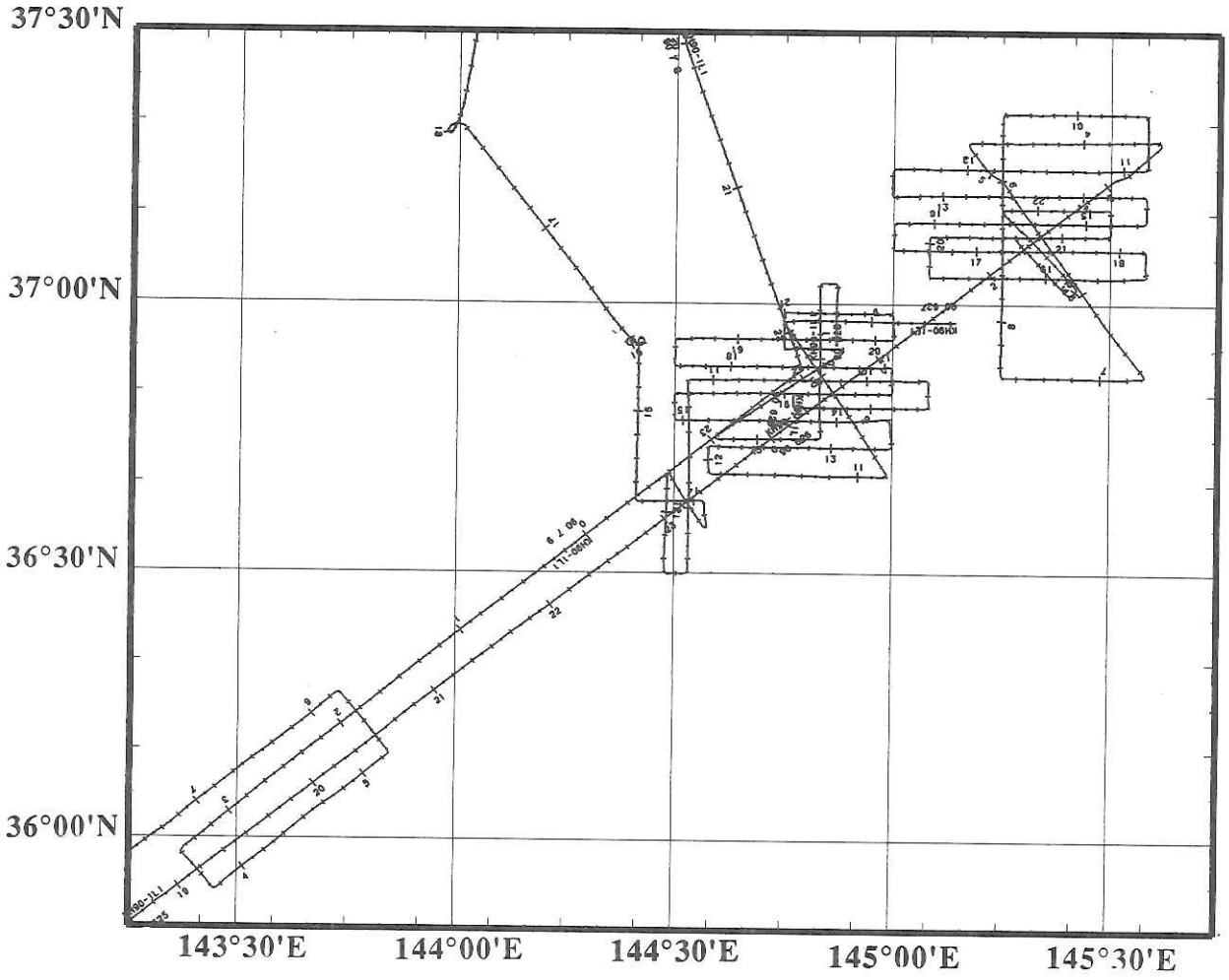

Fig. 5-2 Ship's tracks for comprehensive survey of the Joban Seamount chain during leg 1 of KH 90-1 cruise.

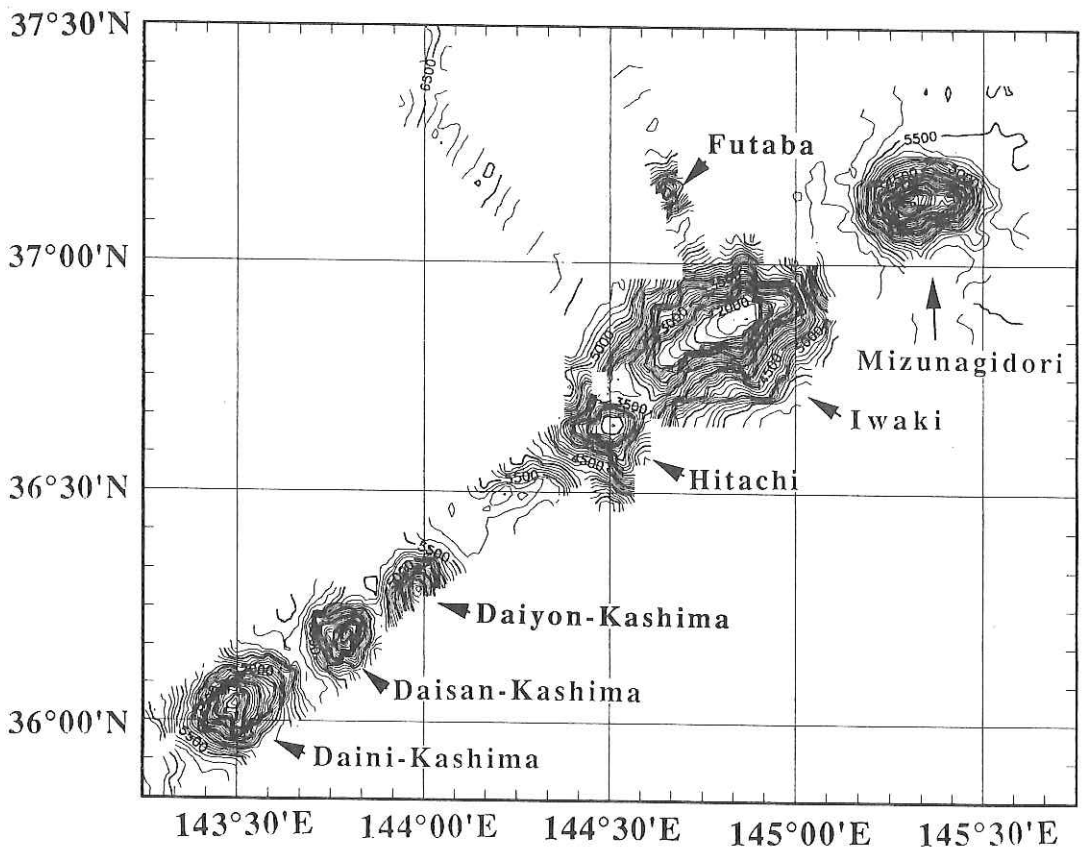

Fig. 5-3 Seabeam bathymetric map of the Joban Seamount chain based on the survey of leg 1 of KH 90-1 cruise. Contour interval is 100 m.

that further study may lead to sound understanding of the origin of the seamounts forming this chain.

A Brief Description of the Seamounts Surveyed

Seamounts surveyed during leg 1 of this cruise are summarized in Table 5-1 and briefly described below.

Table 5-1. Main Characteristics of Seamounts on the Joban Seamount Chain.

Seamount	Location	Crestal Depth (m)	Height (m)	Morphological Remarks
Bosei	37°08'N 145°17.5'E	2,200	3,400	Sharp ridge, trending N60°E, oblate shape in W-E direction
Iwaki	36°52'N 144°49'E	1,680	4,000	Guyot, flat top inclines W, oblate shape in N60°E direction
Hitachi	36°39.5'N 144°29.5'E	2,360	3,300	Small conical guyot
Daiyon-Kashima	36°20'N 143°48'E	3,600	2,100	Conical seamount
Daisan-Kashima	36°11'N 143°47'E	3,100	2,600	Conical seamount
Daini-Kashima	36°0303'N 143°29'E	2,800	2,900	Conical seamount
Futaba	36°54.9'N 144°46.5'E	2,310	1,400	Small conical shape

Mizunagidori (Bosei) Seamount

This seamount, also called the Bosei Seamount (*e.g.* chart number 1009 of the Hydrographic Department, Maritime Safety Agency of Japan), is situated on the northeastern end of the seamounts chain surveyed in this cruise. It has crestal depth of 2,200 m rising by about 3,600 m above the 5,800 m deep abyssal plain. This seamount has an oblate shape like a ridge oriented in an E-W direction. A moat with depths ranging between 5,800 and 5,900 m surrounds this seamount on the southwestern side. Several ridges on its slope, although not very distinct, run in a few different directions, forming a star-fish shape of this seamount. The crestal ridge runs in the E-W direction. Its top is sharp and narrow. This is not a guyot. The flank depth is 5,400 m on the eastern side of the seamount, 5,700 m on the western side, 5,400 m on the northern side and

5,600 m on the southern side. This indicates that the oceanfloor on which this seamount is situated as well as the seamount itself is inclined southwestward.

Iwaki Seamount

This seamount is located 40 km SW from the Bosei Seamount. It has a flat top of 1,680 to 1,700 m in depth and was classified as a guyot by the scientific party onboard leg 1 of this cruise. Its flat or nearly flat top plain is very elongated. The 2,000 m contour line has a SW width of 21 km, whereas an NW width is only 9 km. The flat top plain is also asymmetrical; the steep slope below the flat top surface begins at 1,800 m deep at the north, at 1,900 m deep at the east and south, whereas at 2,400 m at the west-southwest (Fig. 5-3). The shallowest part of its crest is located on the northeastern side. This might be a reef which was developed on a dominant wind side to stand against wind.

Its flank is also elongated, 56 km wide from SW to NE, 35 km wide from NW to SE. Depths of the flank, the end of the slope of the seamount, vary place to place, 5,000 m at the north, 5,700 m at the east, 5,600 m at the south and 3,500 m at the west. It indicates that this seamount has a long flank to the north, but a very sharp cliff at the west. As a whole the seamount is elongated along the trend of the Joban Seamount chain, N60°E. This may reveal a mechanism of the formation of the seamount itself and the seamount chain. It may be due to a fissure eruption of magma through the fracture of the oceanic plate like an example of the present Samoa.

A gentle slope spreads from a flat top, down in the southwest direction. This, together with the flank depth variation, suggests that the oceanfloor on which this seamount is situated as well as the seamount itself are inclined south-westward in the same manner as the Bosei Seamount. Correct position and detailed shape of this seamount was obtained by the present survey and the bathymetric charts should be revised.

Hitachi Seamount

This is a seamount newly found by this cruise. It is located just 10 km SW of the flank of the Iwaki Seamount. It is very close to the Iwaki seamount to the extent that they were thought to be of a body or formed as a flank knoll. The two seamounts share the same contours deeper than 3,500 m. The Hitachi Seamount has a flat top with an average depth of 2,500 m. A gentle slope exists on its top with depths from 2,400 m to 2,800 m. It has ridges which run in southeast and west directions. It has a gently dipping flank on its northern side.

It is followed by a steep cliff at its southwest. All these evidences suggest that this seamount is inclined southwestward. These three seamounts are just on the outer swell of the Pacific plate descending to the Japan trench. However, it is still unknown why they are not inclined westward toward the trench axis.

Daisan-Kashima Seamount

This is a conical seamount having a top of 3,100 m in depth. It has a steep cliff on its southeast side which separates two prominent ridges on the same side. A cliff and a ridge are also located on this northwestern side. From the 4,000 m depth to the top, this seamount is oblate in shape and is elongated along the trend of the Joban Seamount chain. The northern flank of this seamount has a depth of 5,400 m and the southern flank has a depth of 5,800 m. The eastern flank has a depth of 5,300 m and the western flank is 5,800 m deep. A gentle slope spreads from the 3,500 m contour to 5,000 m contour. Another gentle slope spreads from 3,000 m to 3,500 m contours in the northeast direction. The flank depths indicate that the oceanfloor on which this seamount is situated as well as the seamount itself are inclined southwestward. This is further indicated by the presence of the gentle slope along the northeast and northwest sides of this seamount.

Daini-Kashima Seamount

This seamount has a top 2,800 m deep. Two prominent ridges run in the southeast and southwest directions. A prominent cliff separates these two ridges. Another cliff exists at the northern side of the seamount. The flank depth of this seamount are as follows; on the northern and southern sides 5,800 m. On the eastern side it is 5,100 m and on the western side it is 5,900 m. This indicates that the oceanfloor on this area as well as the seamount are inclined westward.

Futaba Seamount

This seamount is located on the northwest of the Iwaki Seamount. The top of the Futaba seamount is 3,700 m deep and it rises by about 1,400 m from the 5,100 m deep abyssal plain. It is situated not just on the Daini-Kashima---Bosei line but on the Daiichi-Kashima---Katori seamount line. It seems plausible that there exist another chain parallel to the Joban seamount chain. The two might have the same or related origin.

Preliminary interpretation

The Joban seamount chain trends along a N53°E trend which is quite different from N68°E of the magnetic anomaly lineations M14 and 13 [6] in this area. This fact rules out possibility of formation of this seamount chain along a spreading center. A most plausible explanation of the origin of this seamount chain is the 'hotspot'. None of the seamounts forming this chain has been dated. Hence it is difficult to test validity of the hotspot hypothesis. Magnetic analysis (see Masalu *et al.*, Chapt. 9 of this report) may hopefully provide a clue to this question.

Another key to mechanism of the Joban Seamount chain may result from size, shape and elongation of the Iwaki Seamount and its correlation in depth contours to those of adjacent Hitachi Seamount. It seems to imply a fissure eruption of magma through a fracture of the oceanic plate in the same manner as the formation of the present Samoan islands [7].

The seamount bodies and surrounding oceanfloor are slightly inclined southwestward with an exception of the Daini-Kashima inclined westward. This appears to be contradictory to the N30°E trend of nearby trench. This southwestward inclination seems to indicate that down-buckling of the Pacific plate is going southwestward. Westward tilting of the Daini-Kashima may be accounted for by the fact that this seamount is very close to the Japan trench compared to the other seamounts on the Joban chain, since influence of the trench dynamics is proportionally great there enough to govern its inclination.

5. 2 Topography and Nomenclature of the Joban Seamount Chain

Y. Ogawa, K. Kobayashi and D. Masalu

In the bathymetric chart of No.6312 (Tohoku Nippon) of the Hydrographic Department, Maritime Safety Agency of Japan, it is described that to the southeast off the coast of Ibaraki Prefecture, five seamounts are existent east off the Japan Trench at latitudes of 35°40'N ~ 37°10'N. They are, from southwest to northeast, the Daiichi-Kashima Seamount, Katori Seamount, Daini-Kashima Seamount, Daisan-Kashima Seamount and Daiyon-Kashima Seamount (Fig. 5-4). We confirmed that these seamounts form a chain trending to N53°E. The Daigo-Kashima Seamount is isolated to the southeast from this line. This chain extends further to the northeast from the Iwaki Seamount and Bosei Seamount. The name of the latter is after the chart No. 1009. A name "Mizunagidori" was first proposed by Tomoda [8] when he surveyed it in 1969, although later

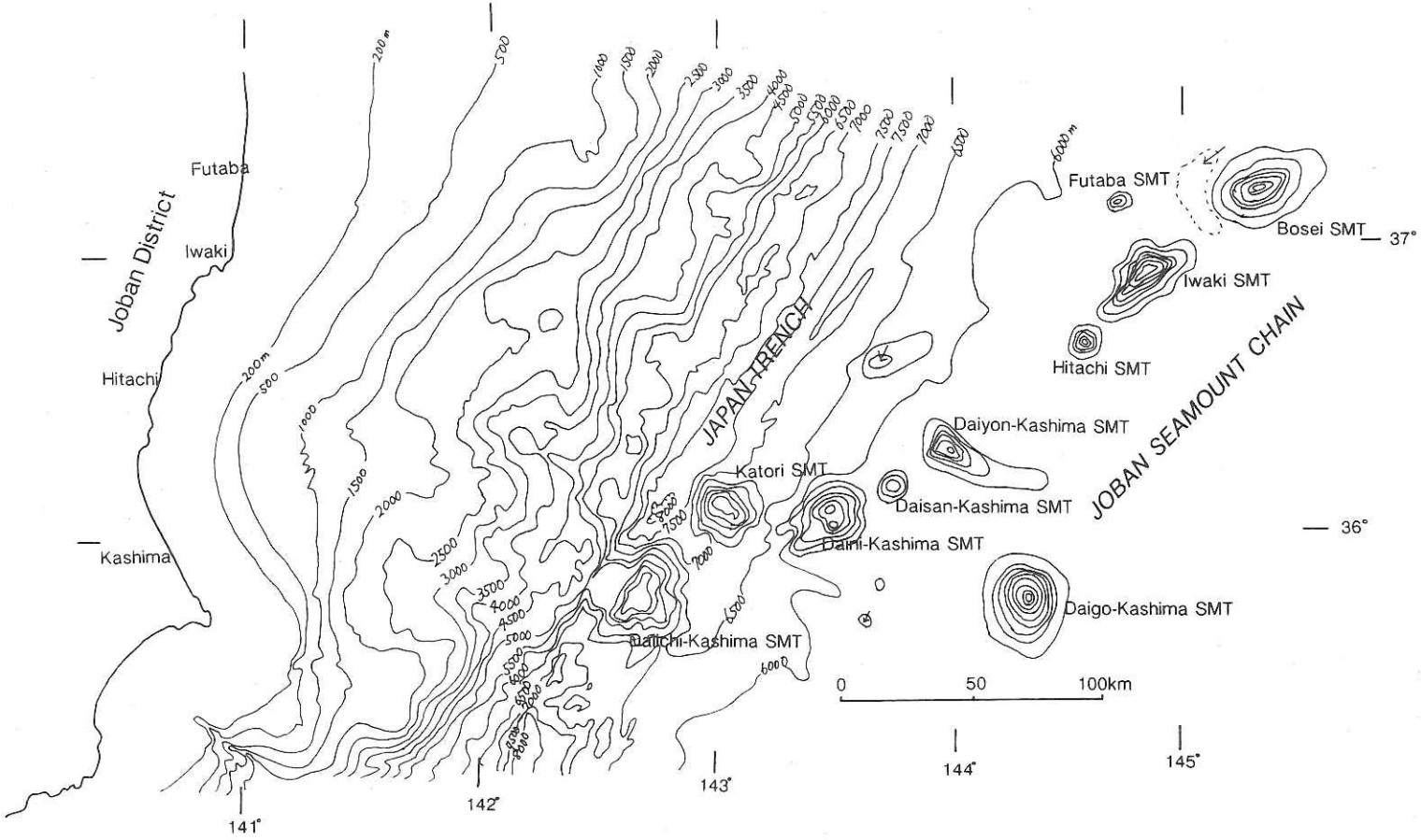

Fig. 5-4. Index map showing the "Joban" Seamount Chain. Bathymetry adopted from topographic map of No. 6312 published by the Hydrographic Department, Maritime Safety Agency. Two newly found seoumounts were added. Local names onland from which the seamounts were named are also shown.

detailed work by Murauchi and others using the Bosei-Maru proposed this name which has been adopted by the Ocean Topography Nomenclature Committee.

Among these seven seamounts, the former two may be on the other line, running *en echelon* to the other ones. We found that the Iwaki Seamount is not situated at the position as shown in the map No. 6312 but slightly SE of it and just on the line of the chain. We propose here that this seamount chain of N53°E direction, from the Daiichi-Kashima to the Bosei, the "Joban" Seamont Chain, after the old local territory name nearest from the area (Fig. 5-5).

During the cruise of the R. V. Hakuho Maru, KH-90-1, we first surveyed three seamounts on this line. They are the Bosei, Iwaki and a new one, named here "Hitachi". The name of this seamount, found at the SW side of the Iwaki Seamount, was suggested by the scientific party onboard leg 1 of this cruise. It is after the nearest city in the east coast of the northeastern Honshu, Japan, *i.e.* the "HITACHI" city.

In the Hydrographic Department maps, the Iwaki Seamount is shown to have two peaks. However during the initial survey of this seamount, only one peak was confirmed to exist. After surveying the Japan Trench, it was decided to confirm possible presence of a topographic high connected to the Iwaki at the site as shown in the Hydrographic Department maps. We found existence of the peak, although it does not seem to be a part of the Iwaki seamount. It seems to be an independent seamount and was named "Futaba" by the scientific party onboard leg 1 of this cruise, after the geological town in Fukushima Prefecture which yielded a Dinosaur remain "Futaba-Suzuki-Ryu".

References for Chapter 5

[1] H. Fujimoto, T. Furuta, A. Oshida, M. Nakanishi and K. Kobayashi , Bathymetric Mapping using the Seabeam System, In J. Segawa (ed.), *Preliminary Report of the Hakuho Maru Cruise KH-89-1* Ocean Research Institute, University of Tokyo, 1990.

[2] J.P. Cadet, K. Kobayashi, S. Lallemand, L. Jolivet, J. Aubouin, J. Boulegue, J. Dubois, H. Hotta, T. Ishii, K. Konishi, N. Niitsuna and H. Shimamura, Deep scientific dives in the Japan and Kuril Trenches, *Earth & Planet. Sci. Lett.*, **83**, 313-328, 1987.

[3] G. Pautot, K.Nakamura, P. Huchon, J. Angelier, J. Bourgois, K. Fujioka, T. Kanazawa, Y. Nakamura, Y. Ogawa, M. Seguret and A. Tekeuchi, Deep-sea submersible

survey in the Suruga, Sagami and Japan Trenches: preliminary results of the 1985 Kaiko cruise, Leg 2, *Earth & Planet. Sci. Lett.*, **83**, 300-312, 1987.

[4] Chart No. 6312 (Tohoku Nippon), Hydrographic Department, Maritime Safety Agency of Japan

[5] Chart No. 1009 (Tohoku Nippon), Hydrographic Department, Maritime Safety Agency of Japan

[7] J.H. Natland, The progression of volcanism in the Samoan linear volcanic chain, *Amer. J. of Sci.*, **280**-A, 708-735, 1980.

[8] Y. Tomoda, *Reference Book for Gravity, Magnetic and Bathymetric Data of the PacificOcean and adjacent Seas*, 1963-71. Univ. of Tokyo Press, 158pp., 1974.

[6] M. Nakanishi, K. Tamaki and K. Kobayashi, Mesozoic magnetic anomaly lineation and seafloor spreading history of the northwestern Pacific.*J. Geophys. Res.*, **94**, 15437-15462,. 1990

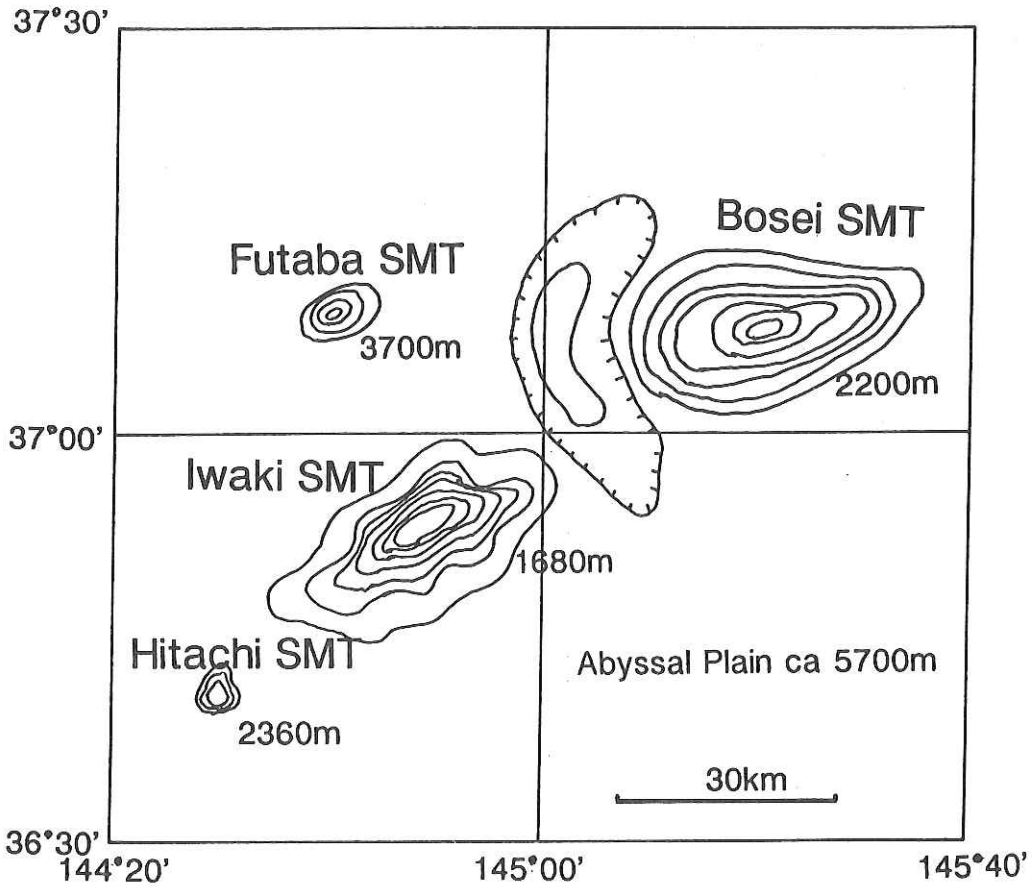

Fig. 5-5. Location of newly surveyed seamounts with depths of the summits. Contours are only schematical. See Fig. 5-3 for detailed Seabeam maps.

6. Mud Volcano on the Outer Swell east off the Japan Trench

Y. Ogawa, K. Kobayashi and S. Ohta

A small mound was found by Seabeam survey associated with the 3.5 kHz subbottom profiling on top of the outer swell east off the Japan Trench during the R. V. Hakuho Maru cruise, KH 90-1, June to July, 1990. If this mound is a mud volcano as we considered, this is its first discovery at an outer swell area.

It is situated at 38°45' N, 145°42.2' E, and 5,220m deep. It is about 130 m high with 3 km NE-SW and 1 km NW-SE in diameter (Figs. 6-1, 6-2 and 6-3). The shape of the mound is oblate elongated to SW-NE on a horizontal plane. Judging from the 3.5 kHz profile (Fig. 6-3), it has a gentle parabolic cross section without a concave basin as a crater or vent on top. It is lying just on a fault, trending from SW to NE. The ocean floor has a more than 100 m thick transparent layer with several thin reflecting stripes, probably ash layers.

The fault dislocates these top layers about 100 meters, west side down, probably in a sense of a normal fault. Moats are recorded both in the Seabeam map and 3.5 kHz profile on both the west and east sides in the order of 40 m and 10 m depth respectively. Considerable upward drag of the surrounding layers is remarkable around the mound (Fig. 6-4), definitely suggesting the injection by diapirism which dragged the surrounding layers.

During the deep-towed camera work, the 3.5 kHz profiling recorded the mound. The profile indicates relatively reflectable mass is below the surface as an injective mass. A much smaller injective body, which did not yet penetrate the top layer is also recorded to the west side of the mound describe here (shown by a small arrow in Fig. 6-4).

Judging from the observation mentioned above, this mound is definitely characterized by lines of evidence for mud volcano. Particularly its three dimensional shape, cross section and existence of drag of the surrounding layers indicate this mound was due to the injection. The injected material might be mud, although we did not sample the rocks inside nor on the mound. Possibly the materials did not flow over the vent, but rather the injected material might have been cooled or desiccated to make itself remain a diapiric body. Even in such a case from the shape it can be called a volcano.

Surface of the mound as observed by the deep-towed camera has a gentle slope composed of materials which look and seem to be semi-consolidated mudstone covered by thin mud of gray in color. Many benthic animals, such as sea cucumbers, sea anemonea *etc.* were observed. Some gastrapods were found

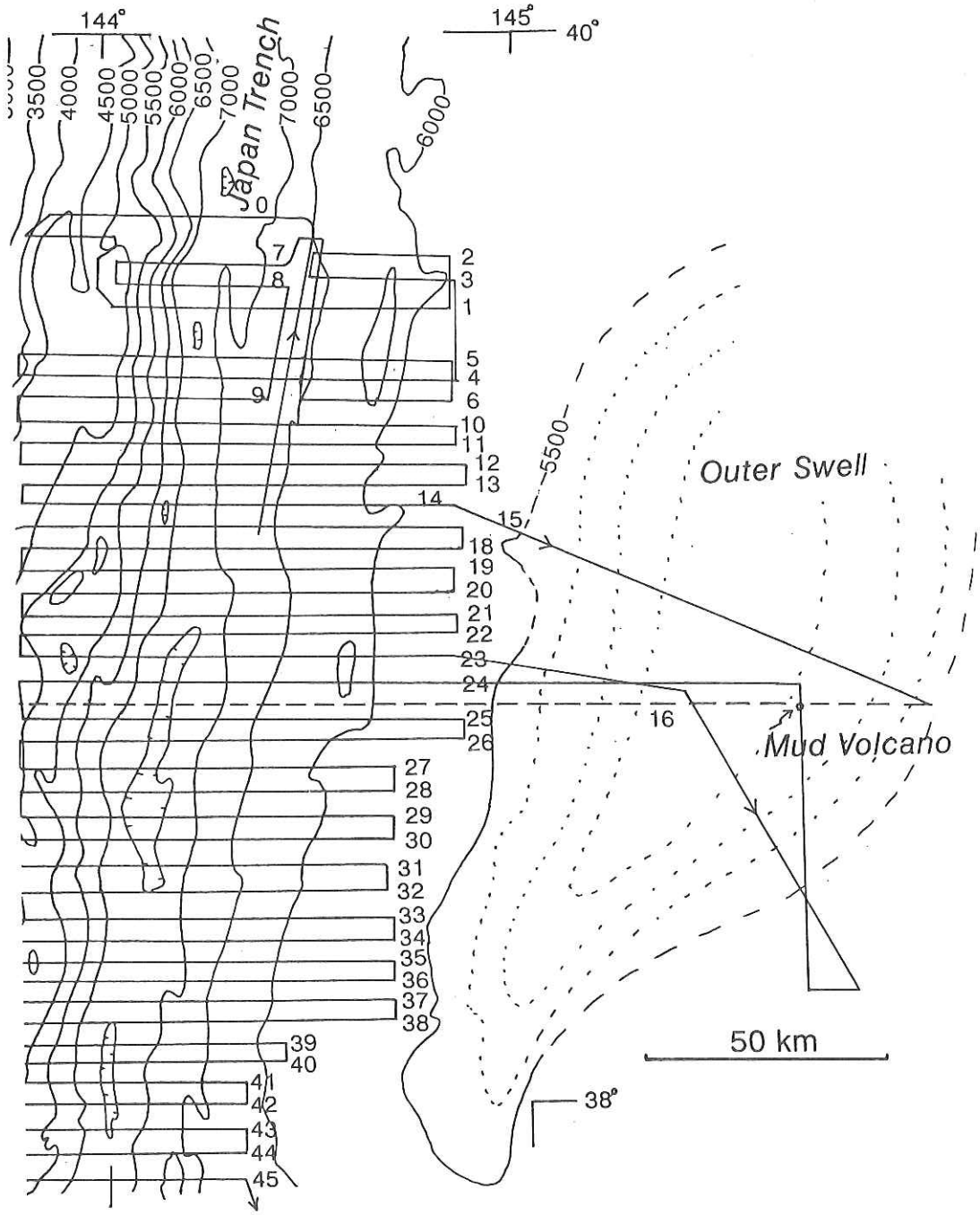

Fig. 6-1. Index map of location of the mud volcano.

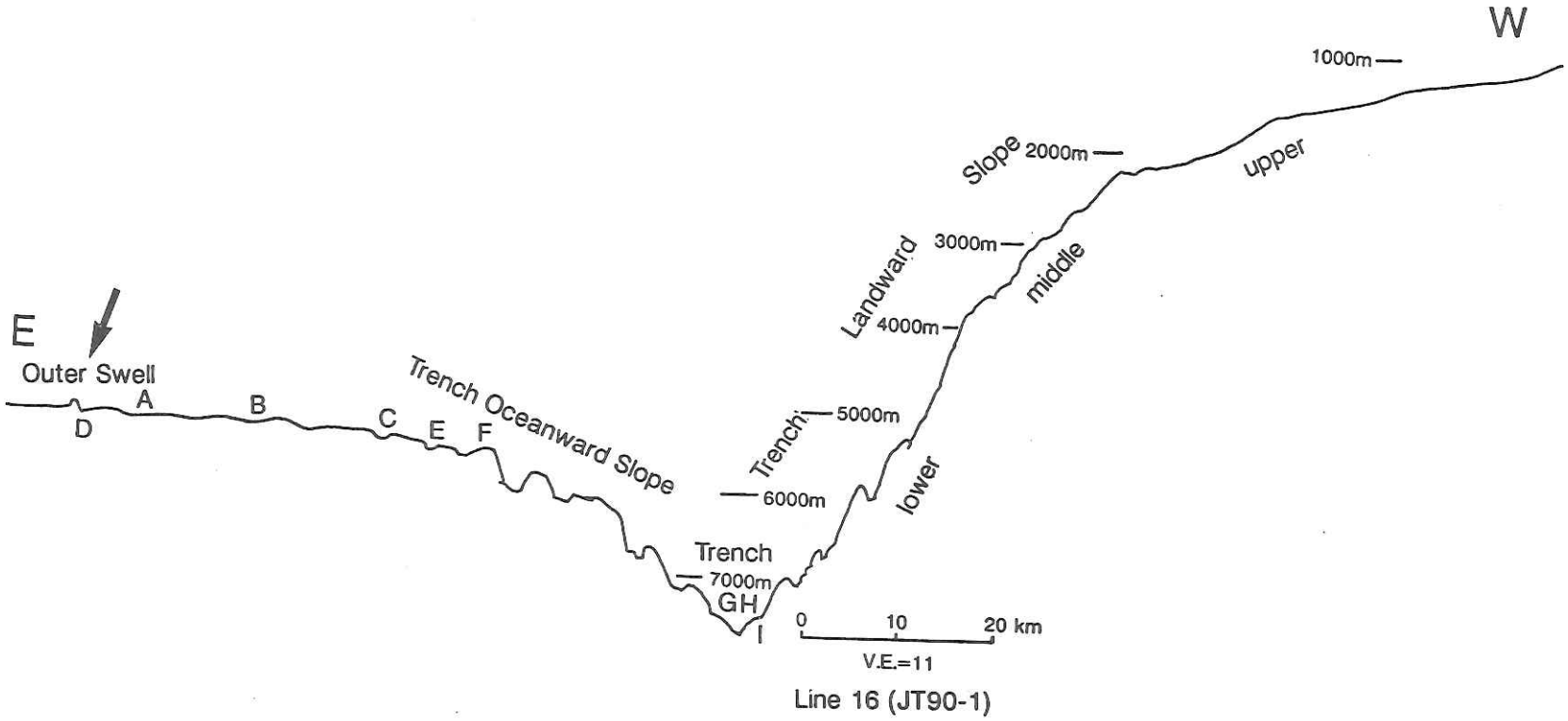

Fig. 6-2. Location of the mud volcano indicated by arrow at D.

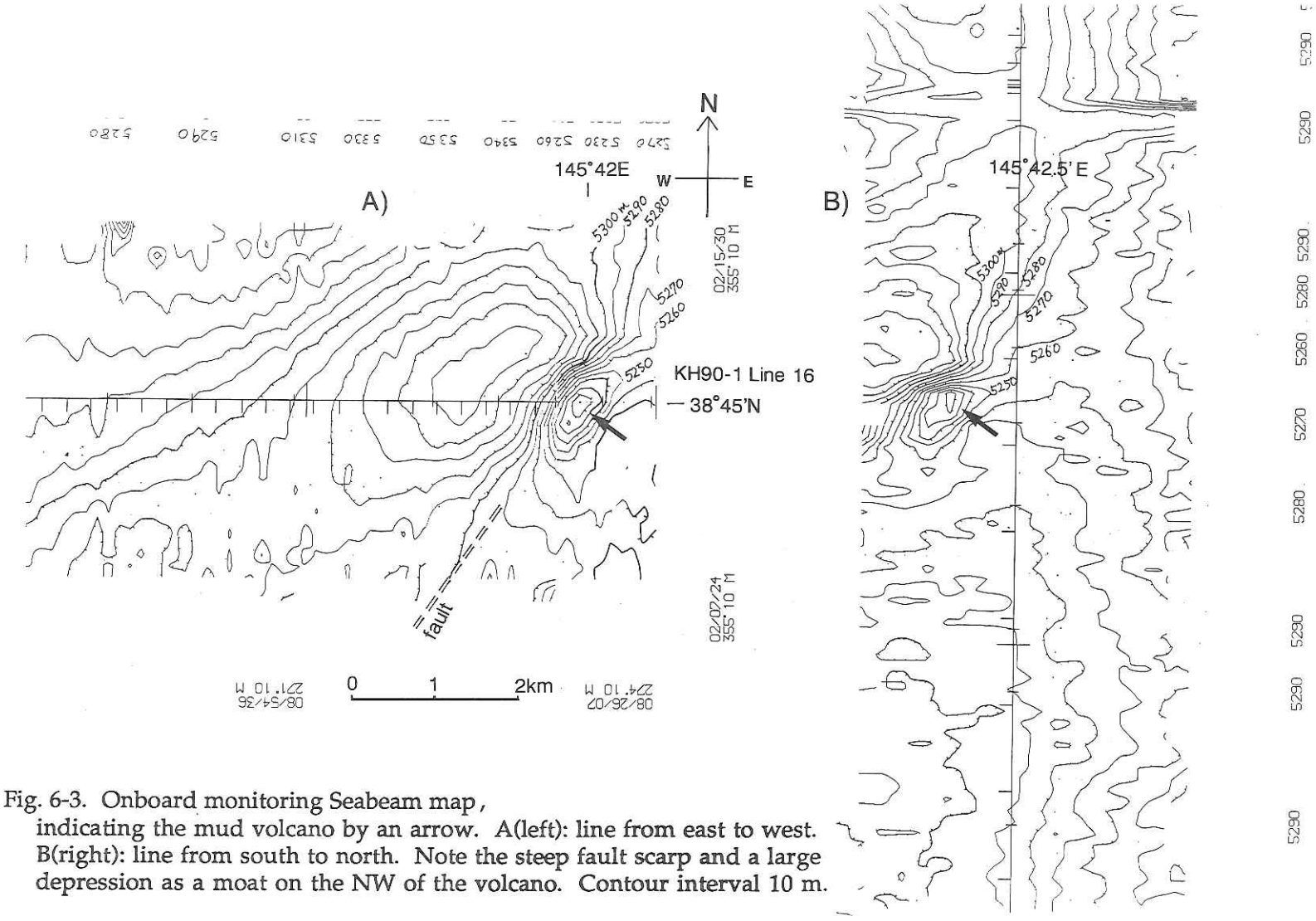

Fig. 6-3. Onboard monitoring Seabeam map, indicating the mud volcano by an arrow. A(left): line from east to west. B(right): line from south to north. Note the steep fault scarp and a large depression as a moat on the NW of the volcano. Contour interval 10 m.

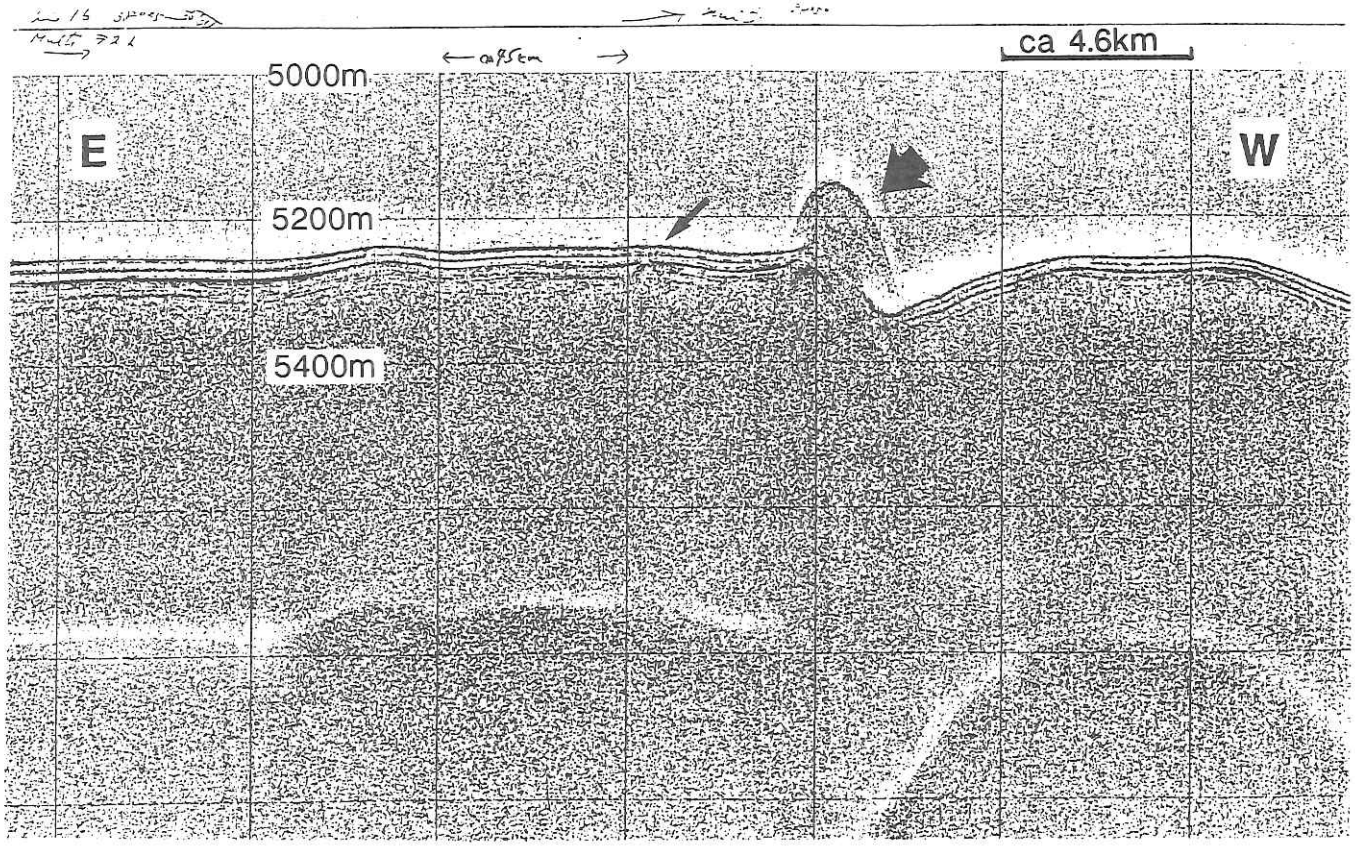

Fig. 6-4. A 3.5 kHz profile on the Line 16, KH 90-1 cruise.

but bivalves were not found. Near the top of the mound, the floor has become rather rough with small to large (centimeter to several tens of centimeters in diameter) blocks of semi-consolidated mudstone. They might have been from the injective body. Some of them were blacky on the surface, probably due to Mn-hydroxide coating. No seepage of fluids, no *Calytogena* individuals nor communities are existent, indicating that no venting occurs at present; *i.e.*,this mud volcano is no longer active. It may be several thousands to several tens of thousands years old, but still rather young because the fault is cutting the top layer of the sediments which must be quite recently deposited.

Two possible origins for this mud volcano might be considered. One idea is that this erupted due to the shock of faulting. This fault may be a normal one characterizing the extension of the superficial part of the buckling or bending layer of the plate at the outer swell. The shock by faulting might have made the sediments liquefied due to its thixythotropic characters and then the liquefied and pressurized mud intruded and erupted. Such a case was commonly observed onland at the time of an earthquake as sand or mud injection. In Smatra many mud volcanoes are fault controlled on a line [1].

The other idea is the mud "magma" with considerable pressure was prepared due to the collapse of the structure of the sediments during compaction in a certain depth, and the faulting might have given the stress release to erupt the magma to the floor. This is also a common geological phenomenon observed in Barbados [2].

Which idea is more preferable? As far as concerned on the 3.5 kHz profile, probably the latter case may well explain the situation, for the magma candidate is now waiting for the next eruption as indicated by a small arrow in Fig.6-4. However, the former idea is not totally denied, because the self-overpressured sediments is only known in a area of very high sedimentation rate such as muddy accretionary prism areas like Barbados [2, 3]. According to the results of DSDP Leg 56, Site 436, about 100 km north of this site on the same outer swell area, the top layer is composed mostly of transparent vitric diatomaceous mud or ooze about 300 m thick.

The uppermost 90 m thick layer is of Quaternary to late Pliocene age, and the sedimentation rate is about 70 mm/1000 yrs [5] This value is considerably high as for the pelagic or hemipelagic realm. This is even faster than the fast model of sedimentation rate at Barbados [4]. Using a fast rate of 20 mm/1000 yrs, they calculated that pore fluid pressure reaches the lithostatic pressure at a depth of about 1.3 km at a certain stage (Fig. 3 of Shi and Wang [4]). We do not know for

the off-Japan trench case, the much faster sedimentation rate could make the high pore pressure much easier. Therefore, it is highly possible to produce the high pore pressure within the superficial sediments without any fault shock. It is likely that the both two ideas may stand for the mud volcano eruption. It is further possible that the mud magma waiting for the stress release, further generated due to the shock by the faulting, and finally erupted along the fault. The fault may have been just on the partly liquefied zone, because the area was fairly week.

References

[1] A.J. Barber, S. Tjokrosapoetro and T.R. Charlton, Mud volcanoes, shale diapirs, wrench faults and melanges in accretionary complex, eastern Indonesia. *Amer. Assoc. Petroleum Geol., Bull.*, **70**, 1729-1741, 1986.

[2] K. Brown and G. Westbrook, Mud diapirism and subcretion in the Barbados Ridge accretionary complex: the role of fluids in accretionary process. *Tectonics*, **7** 613-640, ,1988. .

[3] Y. Shi and C.Y. Wang, High pore pressure generation in sediments in front of the Barbados ridge complex. *Geophys. Res. Lett.*, **12**, 773-776, 1985.

[4] Y. Shi and C. Y. Wang, Generation of high pore pressure in accretionary prisms: inferences from the Barbados Subduction Complex. *J. Geophys. Res.*, **93**, 8893-8910, 1988.

[5] Shipboard Scientific Party,*Initial Rep.DSDP, 56-57,* Govern.Printing Office,Washington, DC, 1980.

7. Geomagnetic Total Force Anomalies

7. 1 Measurement of Geomagnetic Total Force

M. Nakanishi , A. Oshida, D. C. P. Masalu and K. Tamaki

Geomagnetic total force was measured by a proton precession magnetometer during this cruise. The system for measurement consists of a magnetometer unit and a data processing unit. Fig. 7-1 is a block diagram of the system for the geomagnetic total force measurement. The magnetometer unit consists of a console, a sensor and a cable with a length of 250 m. The data processing system was a set of a micro-computer made up of a CPU (NEC PC9801VM21), a color display and a printer. The data processing system is controlled by the navigation data from the integrated navigation system MAGNAVOX SERIES 5000. The navigation data are received from node which is installed in the laboratory using the RS232-C serial interface. The system of the network and the contents of the navigation data are described in detail by Nakanishi *et al.* [1].
The followings are the methods of measurement.

1. The main unit (electronic part) sends an exciting signal to the sensor with 30 sec interval.
2. The main unit of the magnetometer converts period of the proton's precessional motion around the geomagnetic field to frequency.
3. The data of frequency are converted from analogue signals to digital signals in the main unit and then transmitted to the micro-computer through the bit-parallel interface.
4. The micro-computer receives the data of frequency from the main unit with 30 sec interval and the navigation data including date (day, hour, minute, second), latitude, longitude, ship's speed against seafloor, ship's direction against seafloor and water depth from the navigation system with one sec interval.
5. The micro-computer calculates the geomagnetic total force from the data of frequency and display it with navigation data on the color display.
6. The data of geomagnetic total force with navigation data are logged in a floppy disk and printed out with one min. interval.

Magnetic anomalies are calculated using reference field of IGRF 1985 [2].
Magnetic anomaly profiles along all the tracks are shown in Fig. 7-2.

References

[1] M. Nakanishi, H. Fujimoto and T. Furuta, Real-time data processing and distribution system of the Hakuho-Maru, *Jour. Japan Soc. Mar. Sur. Tech.*, 2, 1-10, 1990 (in Japanese with English Abstract).

[2] IAGA DIVISION I, WORKING GROUP 1, International Geomagnetic Reference Field 1985, *J. Geomag. Geoelectr.*, **37**, 1157-1163, 1985.

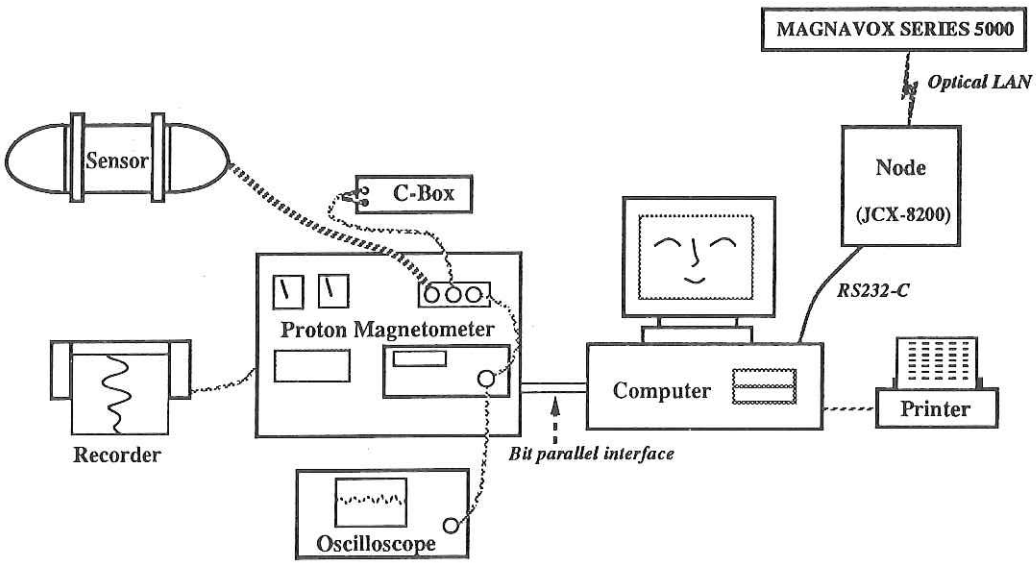

Fig. 7-1 Block diagram of measurement of the geomagnetic total force.

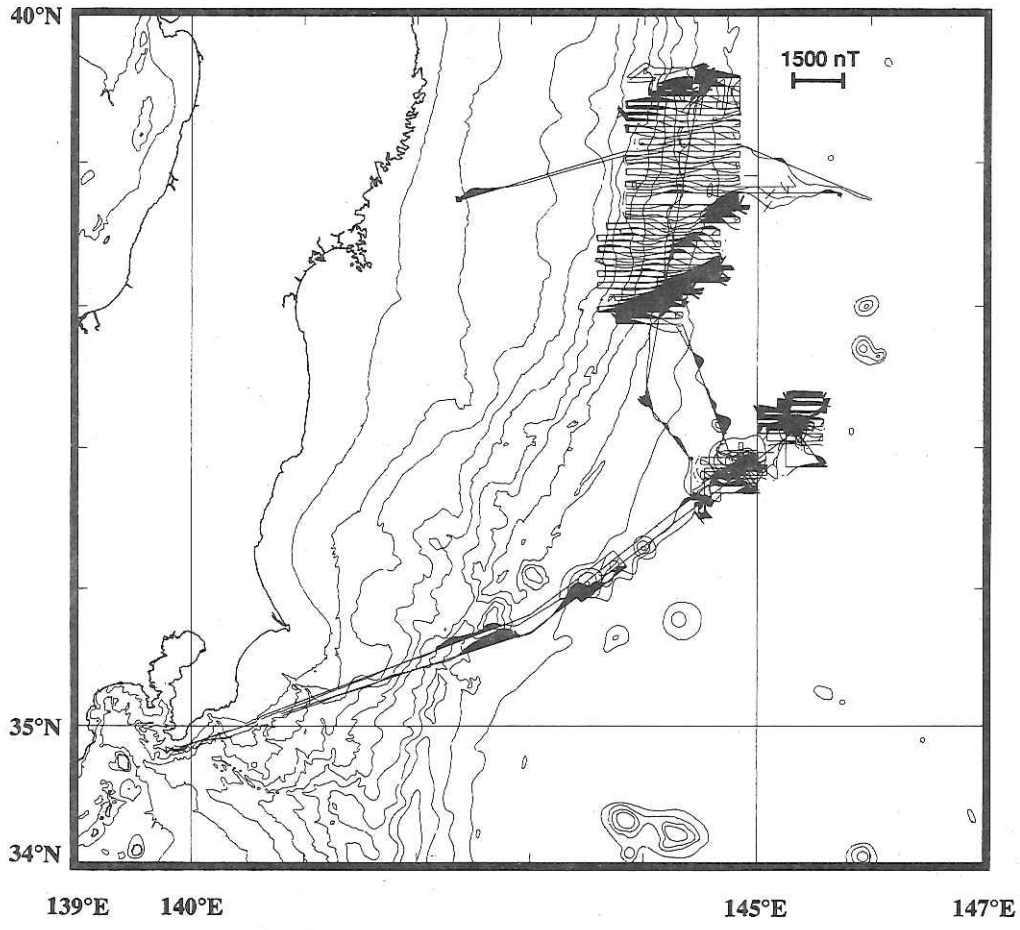

Fig. 7-2 All the magnetic anomaly profiles along tracks (reference field IGRF 1985) obtained in Leg 1 of this cruise. Portions of positive anomalies on the profiles are shaded. The GEBCO (General Bathymetric Chart of the Oceans) bathymetric contours are shown for reference. Its contour interval is 1,000 m.

7.2 Magnetic Anomalies in the Japan Trench

M. Nakanishi, A. Oshida, D. C. P. Masalu and K. Tamaki

The Japan Trench is well-known because there are magnetic anomaly lineations on the landward side [1, 2]. The pattern of magnetic anomalies south of 39°N is not so order as that north of 39°N [1]. Nakanishi *et al.* [2] identified an unknown event between lineations M10N and M11 in south of 39°N (see Fig. 8 in [2]). They also indicated that the strike of lineation M11 changes near the Japan Trench (see Plate 1 in [2]). We carried out measurement of the geomagnetic total force to expose the pattern of the magnetic anomalies south of 39°N.

Fig. 7-3 shows result of the survey. Six magnetic lineations were identified in the surveyed area. All the lineations were identified across the Japan Trench. Figure 2 shows a profile across the surveyed area and the result of identification of lineations. The model profile were calculated on basis of the geomagnetic time scale by Kent and Gradstein [3]. The age range of identified lineations is 133-130 Ma. Our result of the survey confirm existence of the unknown event identified by Nakanishi *et al.* [2] and the change of the strike of lineations M10N and M11. The strike of lineations M10 ~ M10B is N70°E. That of lineation M10N changes from N50°E to N60°E across the trench axis. The strike of lineation M11 is N55°E. Amplitude of anomalies M10 and M11 is about 400 nT. That of anomalies M10A and M10B is less than 300 nT. That of anomaly of an unknown event is 500 nT. That of anomaly M10N decreases from 600 nT to less than 50 nT as the distance from east to west across the trench axis.

Lineation of the unknown event has the same strike (N70°E) as adjacent ones. A chart of the Seabeam indicates that there are no topographic elevations with strike the same as those of the magnetic lineations. Therefore, the lineation of the unknown event is certainly not due to topographic elevations.

Detailed survey by Seabeam in the Japan Trench revealed three major strikes of topographic features; N-S. N40°E, and N40°W (see Ogawa *et al.*, Chapt. 4. 3 in this report). The strike of the lineations M10N (N50°E ~ N60°E) and M11 (N55°E) are not the same as any strikes of topographic features on the seafloor under the lineations. There is a topographic elevation on the seafloor under the lineation M10N, but its strike is N40°E. A similar bending in lineations was identified in the Gorda plate [4]. Stoddard [5] suggested that the bending lineations were due to a rift propagation associated with a non-rigid deformation of the Gorda plate. Different strike of lineations M10N and M11

may be caused by a rift propagation.

References

[1] S. Oshima, Characteristic features of geomagnetic anomaly distribution around Japan, *Rep. Hydrogr. Dep. Jpn.*, **22**, 41-73, 1987. (in Japanese with English abstract).

[2] M. Nakanishi, K. Tamaki and K. Kobayashi, Mesozoic magnetic anomaly lineations and seafloor spreading history of the northwestern Pacific, *J. Geophys. Res.*, **94**, 15437-15462, 1989.

[3] D. V. Kent and F. M. Gradstein, A Cretaceous and Jurassic geochronology, *Geol. Soc. Am. Bull.*, **96**, 1419-1427, 1985.

[4] A. D. Raff and R. G. Mason, Magnetic survey off the west coast of North America, 40°N latitude to 50°N latitude, *Geol. Soc. Am. Bull.*, **72**, 1267-1270, 1961.

[5] P. R. Stoddard, A kinematic model for the evolution of the Gorda plate, *J. Geophys. Res.*, **92**, 11524-11532, 1987.

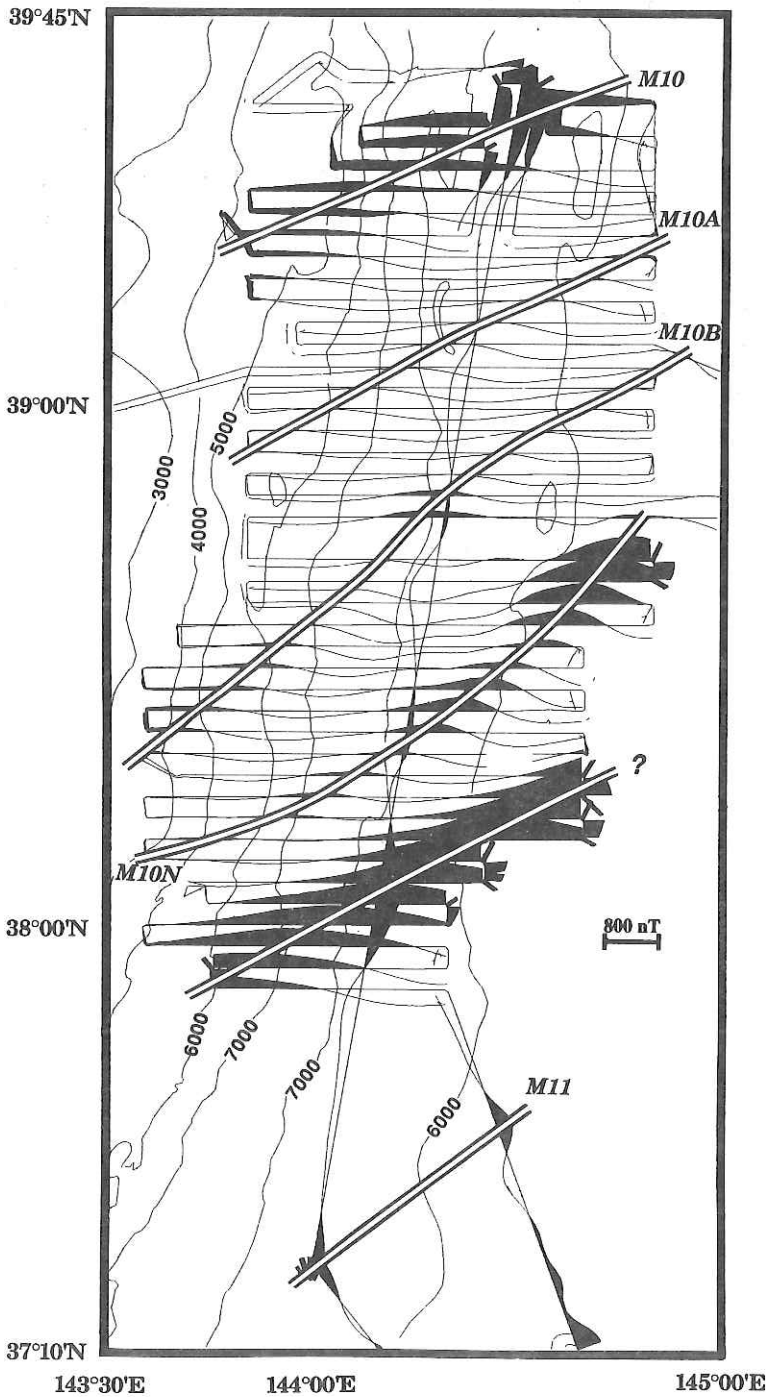

Fig. 7-3 Magnetic anomaly profiles along ship's tracks (reference field IGRF 1985) in the detailed surveyed area. Portions of positive anomalies on the profiles are painted black. The GEBCO (General Bathymetric Chart of the Oceans) bathymetric contours are shown for reference. Its contour interval is 1000 m.

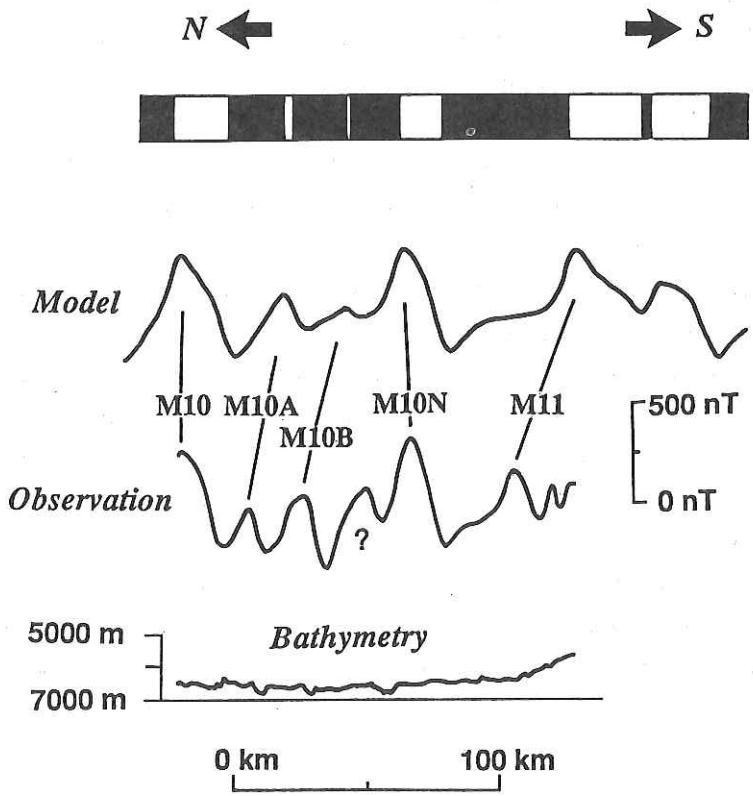

Fig. 7-4. Correlation of magnetic anomaly lineations. The upper profile is synthesized on basis of the geomagnetic time scale of Kent and Gradstein [3].

7. 3 Trials of the Marine Magnetic Gradiometer

A. Oshida, K. Tamaki, M. Nakanishi, D. C. P. Masalu,
M. Watanabe and K. Kobayashi

Trials

A tentative trial of the marine magnetic gradiometer was carried out in each two legs of this cruise. The both trials were done with the multi-channel seismic surveys, with a ship speed of 5 knots. The first trial was done at the Japan Trench and the second one at the south of Hachijojima Island, Izu-Ogasawara Arc (Fig. 7-5). The second trial was truncated on the way, because the poor data were being recorded. The interval of measurements was every 3 seconds or more shorter.

The slave (forward) and master (trailing) sensors, set longitudinally, were towed about 550 m and 700 m behind the winch respectively, so the distance between two sensors was 150 m. Although the total length of the trailing cable was 800 m, the remainder of 100 m was kept on the winch. This large distance from the ship to the sensors, six or seven times of the ship length (100 m), enabled to reduce the magnetic effect of the ship magnetization biased on measured magnetic field.

The system used in these trials is a EG & G Geometrics Model G-811G Proton Gradiometer (Fig. 7-6). The marine towing system of it has been always settled at the No. 8 winch on board of the Hakuhomaru. The console is only shipped at each time.

The sensor used in this system is mounted a preamplifier to boost the signal so that electrical noise does not degrade the performance of the system and it is enabled to use a long towing cable which has a few electrical resistivity increasing with a length. The catalog specification for the accuracy of absolute total field measurement about the sensor is ±0.5 nT or less. This system also has a capability of monitoring measured a depth and temperature of the sensor with an automatic tuning function.

Gradiometer

Marine magnetic gradiometer is an equipment to get a time variation free earth's magnetic field. A marine tow system of gradiometer was composed of the two proton magnetometer sensors aligned longitudinally with a distance of 150 m, and a towing cable (Fig. 7-6). The principles underlying marine gradiometer are simple. The time variations of the earth's magnetic field, *i.e.*

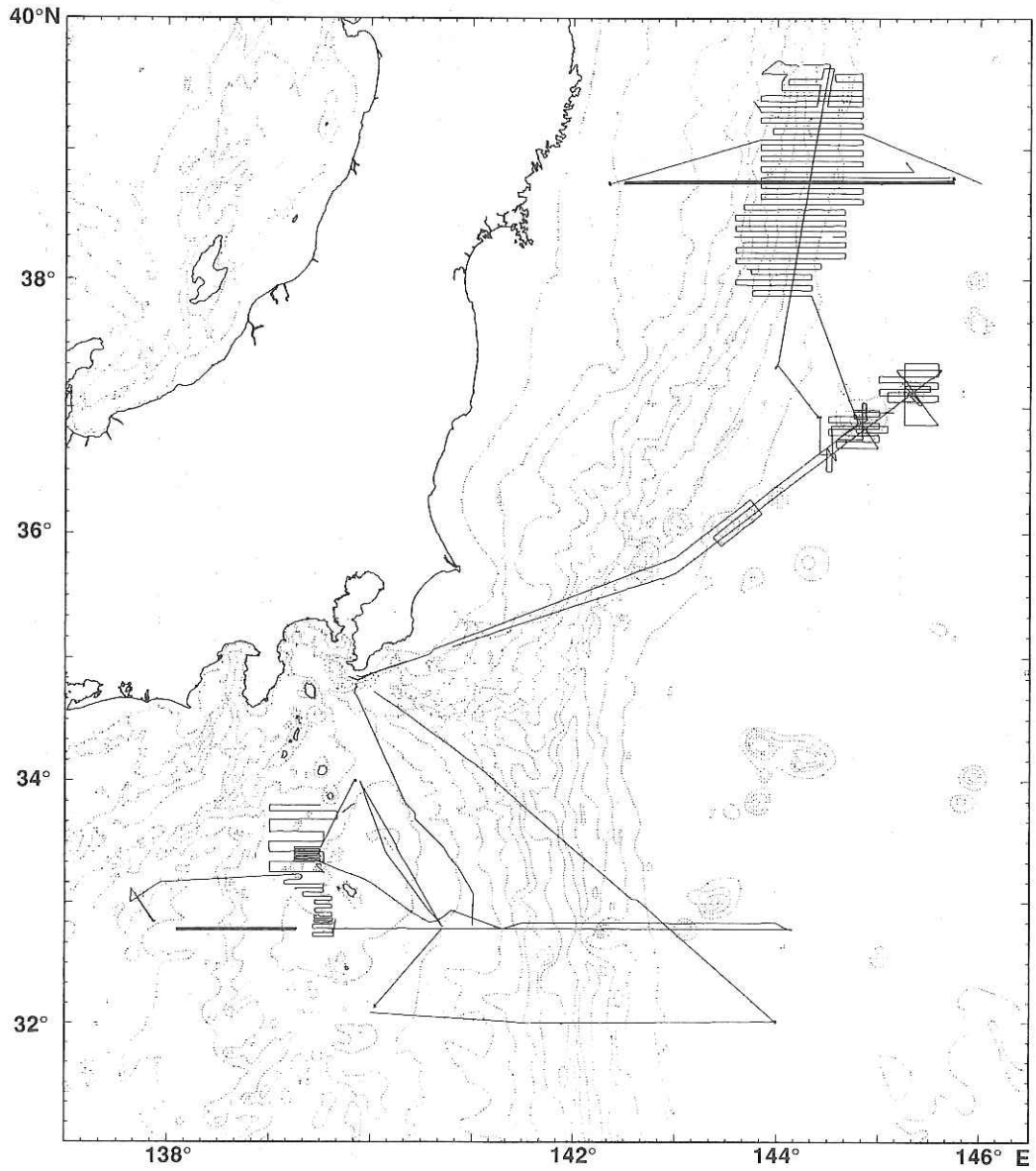

Fig. 7-5 Location of the gradiometer tracks. Thick line shows a gradiometer track.

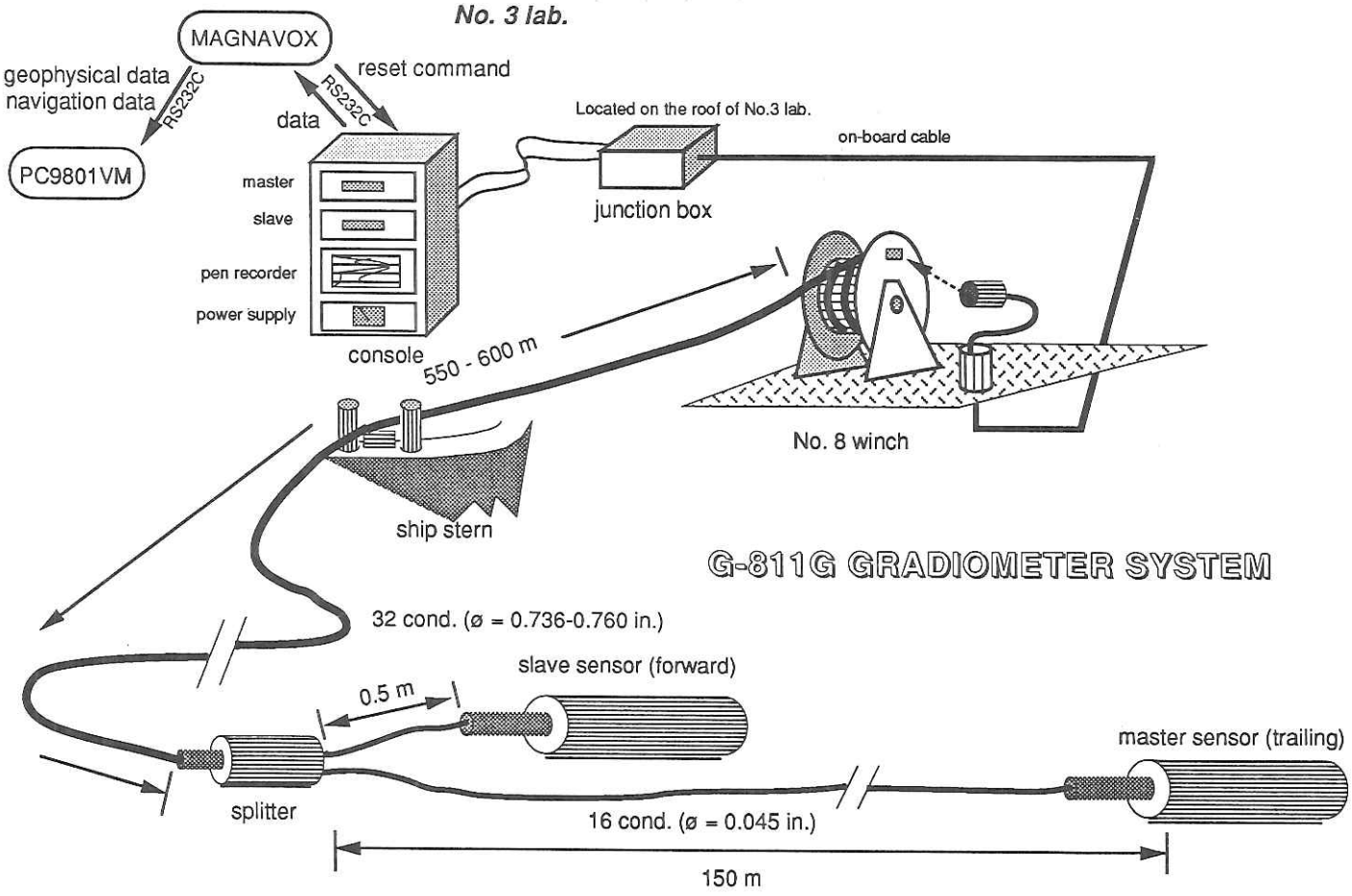

Fig. 7-6 Scheme of the gradiometer system of the Hakuhomaru.

daily variation and magnetic storm, have a long wave length in the space, so it could be considered that the values of the earth's field measured by the two sensors at a time include a same bias caused by the time variation.

Difference between the values at the two sensors is, therefore, essentially free of the effects of time variations in the earth's field. By dividing the difference by the distance between two sensors (150 m), the actual geological gradient between the sensors could be estimated. The signal reconstruction is proceeded by using a simple numerical integration algorithm based on the trapezoid rule as follows,

$$r(x_i) = r(x_{i-1}) + \frac{(x_i - x_{i-1})}{d} \frac{(s(x_{i-1}) + s(x_i))}{2} \qquad (i = 1, 2, 3, ...),$$

where

x_i ; a position at the i-th reading measured from origin of the survey line,
$r(x_0)$; geomagnetic field at the origin of the survey line,
$r(x_i)$; reconstructed field at the i-th reading,
d ; a distance between the sensors (150 m), and
$s(x_i)$; a difference of the earth's magnetic field between two sensors at the i-th reading.

Some measurement errors, system noise, heading errors, geometrical effects and swell noise, are expected, but the considerations about them are omitted at this time. The value of $r(x_0)$ may originally include a time variation component.

Results

We get the results of measurement as the expressions of magnetic total field at the master sensor and the difference between the sensors. The differences are used for the reconstruction of the magnetic field and the first reading of the master sensor $r(x_0)$ is only used as the initial constant of the integration. Therefore the shape of the reconstructed curve is susceptibly underlain by the differences. The differences obtained in the trial of leg 1 (the middle of Fig. 7-7) have the margin of error of 12 nT. This value is larger than that of a normal operation of the single proton magnetometer. The cause of it is not still analyzed.

In the bottom graph of Fig. 7-7, the both trace of the total magnetic field obtained by the master sensor and reconstructed are drawn. All the peaks and

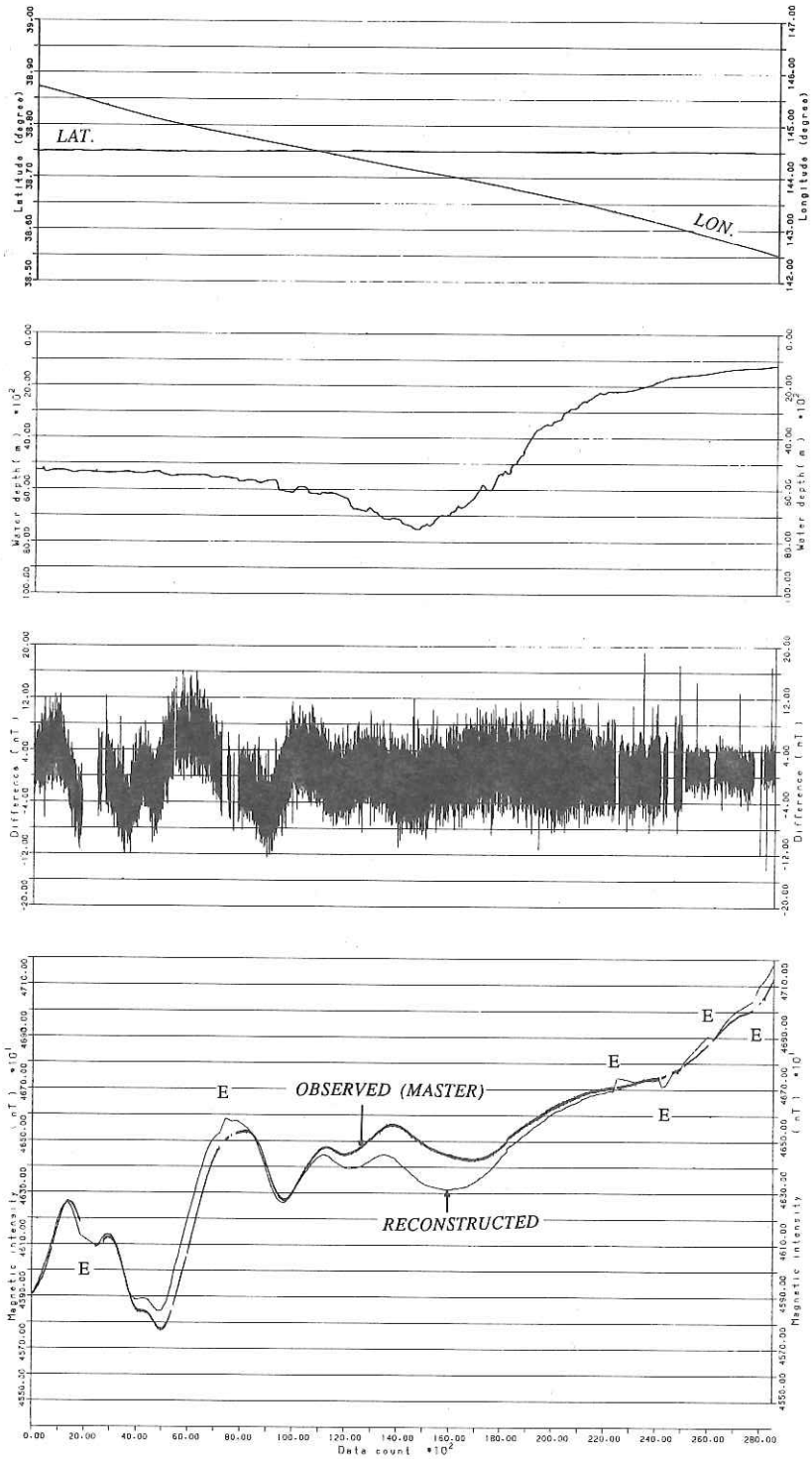

Fig. 7-7 Result of the reconstruction of the earth's field. E shows the error caused by the lack of data.

troughs between two traces are corresponded, but the positions (in the both axes of data count and magnetic total force) of each pare are slightly shifted. If these shift are not the error derived from poor data, they are showing the time variations during this time which have relatively a longer wave length than geological anomalies. The lacks of data during a series of the operations cause the errors on the reconstructed profiles ('E's of Fig. 7-7). This kind of error is apt to be arisen by a breakdown of the tandem operation of two magnetometers.

7. 4 Deep-towing Measurement of Geomagnetic Total Force

K. Tamaki, A. Oshida and M. Nakanishi

Total force of geomagnetic field was measured by a deep-towed proton precession magnetometer system in the northwestern Pacific Basin at the east of the Japan Trench during the first leg of KH90-1 cruise. Magnetic anomaly lineations of the Mesozoic are well identified in the basin [1]. The strike of the magnetic anomaly lineations is NEE and anomalies M5 to M15 are observed at the east of the Japan Trench. The trend of transect of the current deep-towing measurements was determined to cross the lineations by high angle (Fig. 7-8). The objective of the measurement was to obtain near sea-bottom record of the intensity of geomagnetic total force and to investigate the possibility of the existence additional small event between anomaly M10N and M11 [2].

The system used for the current measurement is a deep-two proton magnetometer system ORI-DTP I. The detailed description of the system are presented by [3] and [4]. The current survey was the 7th trial since the development of the system and called DTP-7. The condition and operation log during the survey were summarized in the Tables 7-1 and 7-2. ORI-DTP I is a self-contained deep-tow proton magnetometer system. The system is towed behind the ship by a wire without any electric connection and is workable at the water depth of 6,000 m at maximum. Total geomagnetic force and the water depth of pressure housing were measured every 60 seconds. The surface tow proton magnetometer of Geometrics G811 was also towed to obtain geomagnetic total force at sea surface concurrently. The G811 magnetometer sensor has real-time depth monitoring capability. The depth of the G811 sensor was in the range from 109 m to 195 m during the survey. The results of the measurements by surface towed magnetometer were shown in Fig. 7-9.

Towing ship speed was maintained at 2.5 kts system log speed (absolute ship speed against the sea floor). Bottom of the survey area was generally smooth with about 5,300 m water depth showing some variation from 5,279 to 5,363 m while towing the system. Length of towing wire reached 8,000 m, whereas the deep-towed system attained the depth of 3,667 m at maximum below sea surface. Stable and constant towing depth was about 3,600 m (Figs. 7-10 and 7-11), which is 1,700 m above the sea floor. The SSBL (Super Short Baseline) acoustic positioning system installed to the towed system is capable of sensing slant range and towing depth of the towed system to the vessel in real time. Transmitted information, however, was scarce during the deep-towed survey

probably because of high inclination of the wire (48°) and its large slant range (8,000 m).

Measurements of geomagnetic force by deep-tow system were unfortunately terminated after five hours of operation because of the rapid exhaust of battery caused by the extreme low temperature condition in the deep sea. The towing depth of 3,600 m attained this time was the deepest towing depth ever reached by the current system so that we encountered an unexpected problem about the life of the battery under the deep-sea low temperature condition. While we currently use normal alkaline batteries, we are trying to overcome this problem by increasing the voltage of batteries.

The profile of total geomagnetic force obtained by deep-towing is shown in Fig. 7-12 with the comparison between surface towed and deep-towed geomagnetic data. In the deep-towed geomagnetic profile, a positive anomaly with an amplitude of 600-300 nT is observed at GMT time of 10:10. In the surface tow profile, however, the anomaly only exhibits a bench without showing any peak. The results demonstrate that the amplitudes of wiggle of deep-tow geomagnetic profile as well as its resolution were unequivocally enhanced over than the surface towed one. Although the current survey was not completed by battery trouble and the original objective was not achieved, the advantage of the deep-tow measurements of geomagnetic total force was well confirmed by the currents results.

Through the past seven experiments of our deep-tow proton magnetometer system, we now can assign a couple of main targets to be achieved in near future for the improvement of the current system. One of them is an improvement of the operation duration by increasing the voltage of the battery as mentioned above. The second one is an improvement of towing methods. This time we attached 500 kg of weights and attained the maximum tow depth. This was the first time for us to have attached extra weights to the system. In future we plan to attach 1,000 kg of weights. In this case specially designed weighing system is necessary for the safe and smooth handling of the system on board. Our currently anticipated goal is to achieve the towing depth of 5,000 m with a ship speed of 2.5 kts. For this achievement we need to increase the length of the wire during towing the system as well from the current 8,000 m to 10,000-12,000 m. As deploying the wire is taking time, we plan to increase speed of wire deployment from the current 1 m/sec to 2 m/sec. As the high speed of wire deployment causes jamming of the tow system, we have to increase the ship speed during deployment. The profile of towing depth shown in Fig. 7-11

displays rather rapid shallowing of the system with an extent of 350 m just after ceasing deployment of the wire. After the shallowing the depth again goes deep and reaches a stable tow-depth. It took 3 hours for the system to reach a stable towing condition. To reduce or eliminate this duration we plan to control ship speed to decrease gradually for maintaining the tow-depth of the system undisturbed.

References

[1] M. Nakanishi, , K. Tamaki, and K. Kobayashi, Mesozoic magnetic anomaly lineations and seafloor spreading history of the northwestern Pacific, *J. Geophys. Res.*, **94**, 15437-15462, 1989.

[2] J. E. T. Channell and K. Tamaki, Additional geomagnetic reversals recorded in early Cretaceous magnetostratigraphic and marine magnetic anomaly data, *EOS Trans. AGU*, **70**, 1065, 1989.

[4] K. Sayanagi, A. Oshida, and M. Nakanishi, Magnetic measurements by means of a deep-towed proton magnetometer, in S. Segawa (ed), *Preliminary Report of The Hakuho Maru Cruise KH-89-1*, 44-49, Ocean Res. Inst., Univ. Tokyo, 1990.

[3] K. Sayanagi and K. Tamaki, Distributions of amplitudes of marine magnetic anomalies and crustal magnetizations in the Pacific, Atlantic, and Indian Oceans, *EOS Trans. AGU*, **71**, 866, 1990.

Table 7-1 Condition and summary of survey DTP-7.

Deep Tow Proton Site Notes (Ocean Research Insitute)

Site No.: DTP-7 **Date:** 90.07.04 **Results:** Halfly success

Vessel: Hakuho-maru **Cruise ID:** KH90-1 **Sea state:** Good

Area: West of Japan Trench between M10N/M11 **WaterDepth:** 5279-5363 m

Positions: 38°50'N, 145°20'E - 38°15.43', 145°45.75'E

Operators: K. Tamaki, A. Oshida, M. Nakanishi

Max WireOut: 8000m **WireOut Speed:** 1 m/sec **Wireout Ship's speed:** 3.5 kts

Max Tow Depth: 3667 m **Constant Tow Depth:** 3350 m (By ship's system speed only)

System: ORI-DTP I **Meas. Interval:** 60 sec **Tow Ship's speed:** 2.5 kts

Configuration: G856(alkali batt. 1.6Vx8,auto mode,auto tune,Display on), Depth meter(alkali batt. 13.95V), Pressure Vessel(stainless steel,80kg,6000m),Silicagel, Proton sensor (kerosene,fin,15m cable,6000m), Parashoot,2 tons swivel,OKI transponder -SSBL(50m above Vessel), two 250kg weights, with 300 m G811 surface tow, with No.1 winch

Objective: Figuring out minor events between M10N and M11

Comments: SSBL did not work after wire out of 6000m. But only twice aith wire out fo 8000m we received signal and the deoth was 2765 m, then we slowed down to 1.5 kts (EM log) and 2.5 kts (system ship speed).

Summary: Unfortunately G856 stopped measurements before towing is stabilized. But we confirmed 200 nT surface tow amplitudes were exaggerated to 600 nT. The analyses of this data may be a bit confusing because of unstabilized sensor depth. Also we attained maximum towing depth of 3400 m constant by addition of 0.5 ton weight with 2.5 kts.

Table 7-2 Log of the survey DTP-7.

Site No.: DTP-7

Time	WD(m) Depth	WireOut Incll/Dec	ShipSp EM/Sys	Course Gyro/Sys	Lat Lon	Remarks
7:00						Start of wire out
(GMT)						surface proton depth: 109 m
8:06	5320	2738	2.6	161.2	38°50.53'	slant range 3124 m
		48°/?	3.5	134.9	149°19.65'	sensorr depth 1460 m
8:42						2278/4742
9:00	5295	5880	2.3	169°	38°48.04	
		48°/2°	3.2	148°	145°21.47'	
9:36	5363	8000		143		Stop wire out.
		48/2		169		Have been lost the position of SSBL.
10:15	5355	8000	3.8	163	38°44.07'	
			2.5	151	145°24.47'	
10:40						Slant 8092 Dpeth 2765 Bering167.1
10:50	5349					Start of speed down
10:55		8000	1.0		38°41.94'	speed down complete, wire tension
			2.5		145°26.07'	4.2ton Surface proton depth 188m
11:30	5368	8000	1.1	167	38°40.54'	Wire tension 4.22ton
		48/2	2.6	171	145°27.08'	Surface tow proton 185 m
12:30	5350	8000	1.2	153	38°38.01'	Wire tension 4.22ton
		48/2°	1.4	167	145°28.98'	Surface tow proton 195 m
13:00	5339	8000	1.4	127	38°36.81'	
		48/2°	2.9	167	145°28.98'	
13:30	5338	8000	1.7	137	38°35.58'	
		48/2°	1.6	162	145°30.64'	
14:00	5337	8000	1.9	150	38°34.24'	
		48/2°	1.6	161	145°31.60'	
14:30	5332	8000	1.1	152	38°32.9	
		48/2°	1.5	156	145°32.5	
15:00	5330	8000	1.8	139	38°31.61'	
		48/2°	1.4	157	145°33.68'	
15:30	5332	8000	1.8	156	38°30.24'	Tension=4.22t
		48/2°	3.6	148	145°34.61'	
16:00	5327	8000	1.7	154	38°28.84'	Course=system course
		48/2°	3.1	172	145°35.67'	Gyro/HB=heading OK?
16:30	5321	8000	1.7	153	38°27.47'	
		48/2°	3.5	136	145°36.79'	
17:00	5293	8000	1.3	155	38°26.11'	Tension=4.22t
		48/2°	2.8	146	145°37.72'	
17:30	5309	8000	1.1	149	38°24.75'	Tension=4.22t
		48/2°	2.6	154	145°38.73'	
18:02	5299	8000	1.4	150	38°23.34'	Tension=4.22t
		48/2°	2.7	156	145°39.81'	
18:30	5308	8000	1.5	146	22.11	Water speed 1.2
		48/2	2.8	141	40.62	Water direction 148
19:00	5290		1.7		20.78	
			3.5		41.68	
19:40	5300		1.7	142	18.89	811G Depth 135m
			3.0	146	43.09	
20:05	5312	8000	1.2	145	17.85'	Water speed 1.3kts
			2.7	155	43.99'	Water direct 153°
20:40	5287	8000	1.6	149	16.34'	WS 1.5kts WD 145 811G Dep 148m
			3.1	143	45.14'	
21:00	5279	8000			15.43'	G811 Proton pull in
					45.75'	Wire pulling in
22:00	5272	4635	-0.9	205	13.35'	Tension 2.86ton
			0.2	162	47.00'	
22:30	5326	2846	1.4	236	12.55'	Tension 2.52ton
			2.0	228	46.36'	
23:00	5301	1052	1.8	258	38°11.86'	Tension 1.26ton
			2.0	254	145°45.25'	
23:28						DTP at sea surface

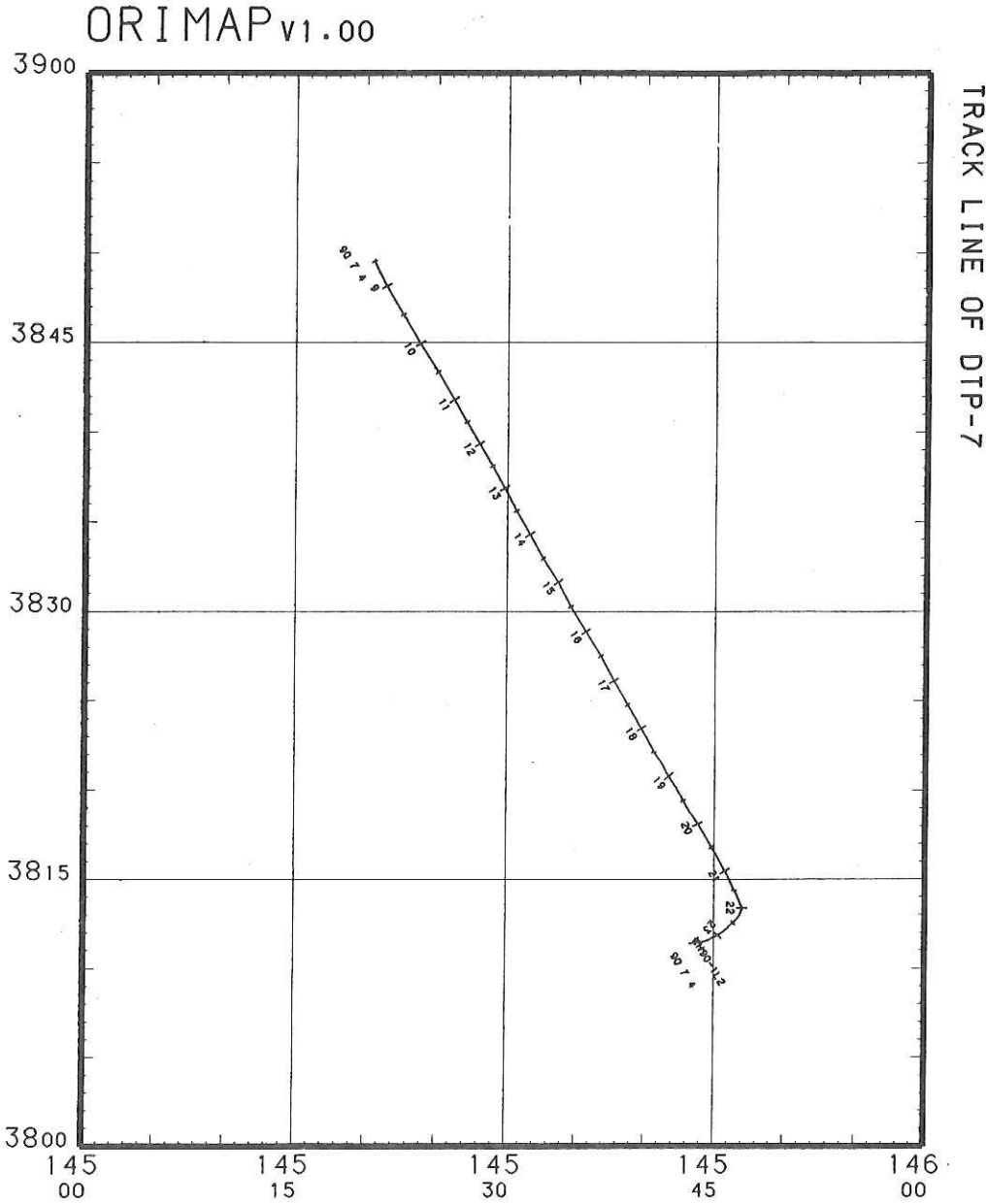

Fig. 7-8 Track line of deep tow survey.

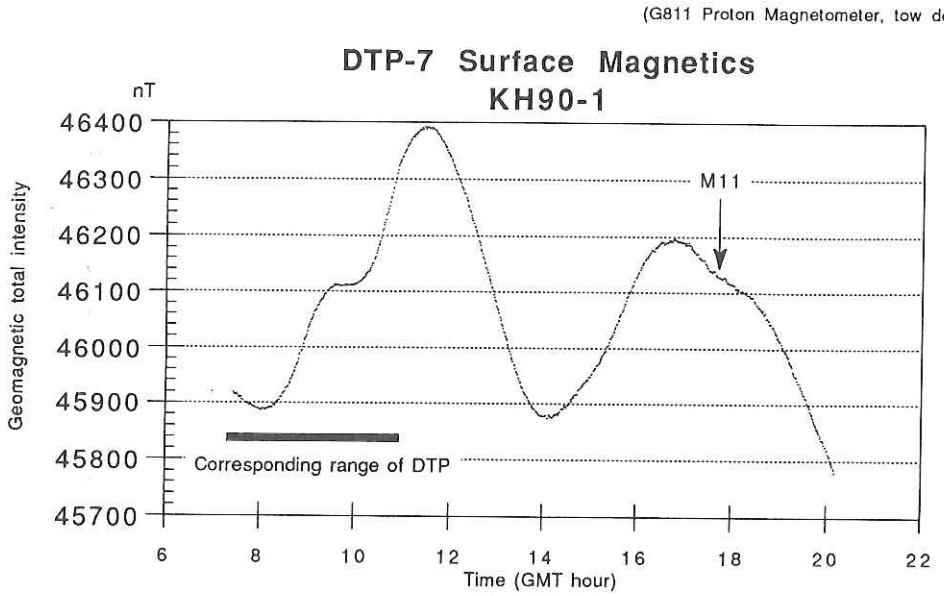

Fig. 7-9 Profile of geomagnetic total intensity near sea surface.

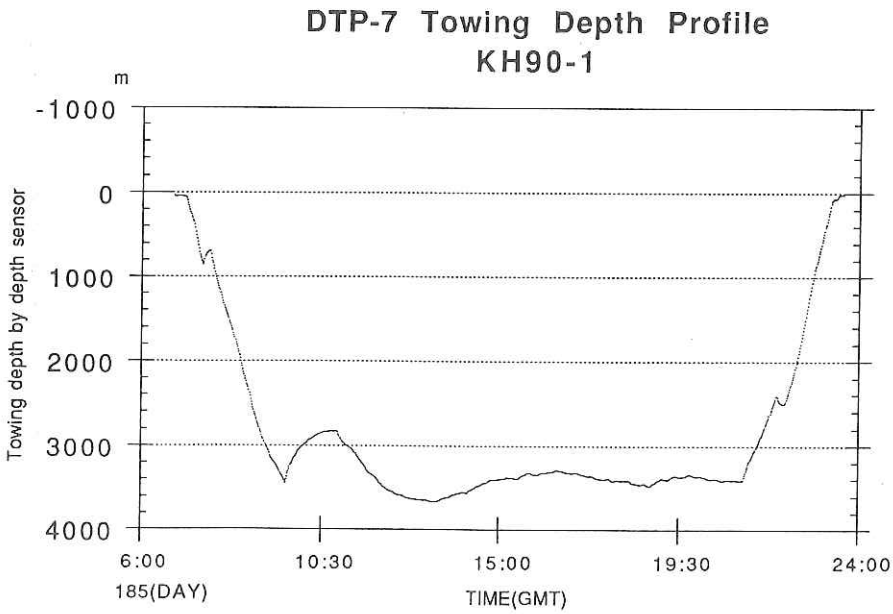

Fig. 7-10 Towing depth profile of DTP-7.

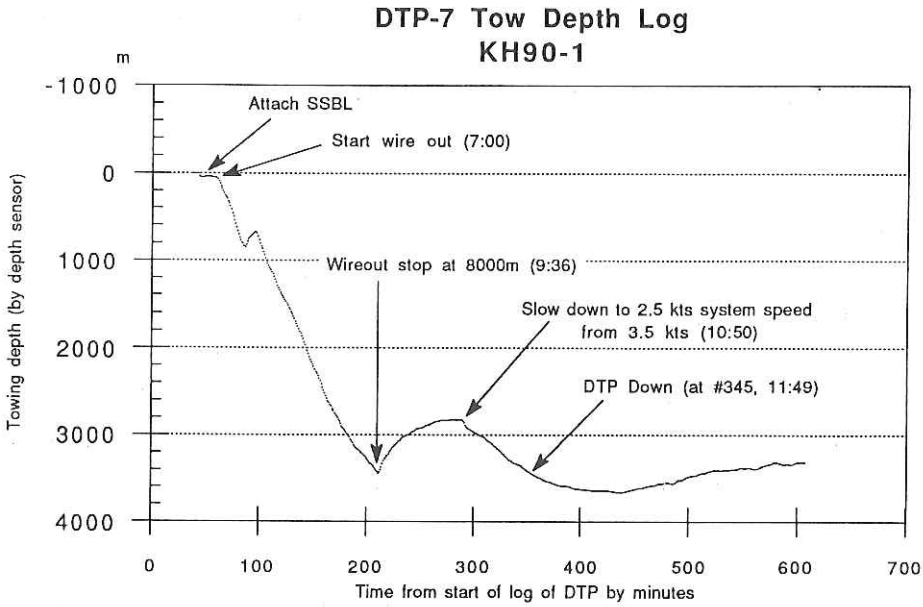

Fig. 7-11 Description of depth profile of DTP-7.

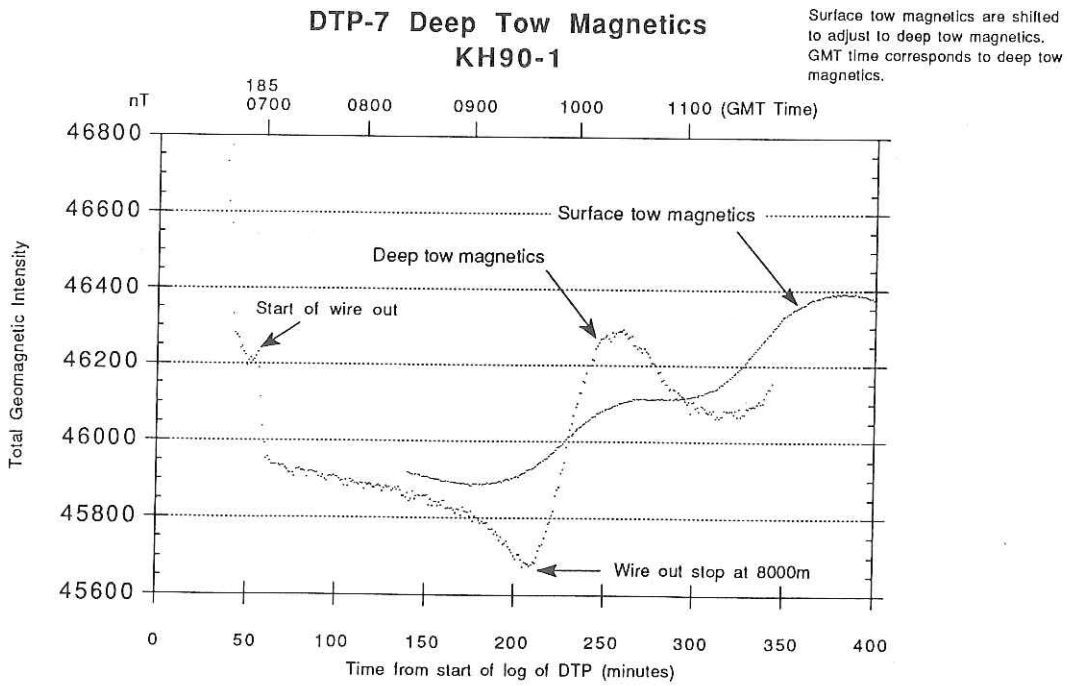

Fig. 7-12 Profile of geomagnetic total intensity obtained by deep tow system in comparison with that by near sea surface tow system .

8. Three-Component Geomagnetic Anomalies Over the Japan Trench

N. Isezaki, K. Kashihara, S. Mizohata and K. Takatsugi

Introduction

STCM (Shipboard Three-Component Magnetometer, [1]) has been used for measuring geomagnetic three-components on board a ship by Japanese institutions, for instance, National Institute of Polar Research (NIPR), Geological Survey of Japan, and Universities. We have got the new phase of interpreting the STCM data obtained by the icebreaker Shirase (NIPR) and R. V. Hakuho-Maru (Ocean Research Institute, University of Tokyo), because the gyrocompass equipped with these two vessels, measuring the yaw, pitch and roll angles of a ship, has very high quality and the analyzed three-components of geomagnetic field using these angles have much better quality than those so far obtained. It has been well known that an error in the yaw angle measured by a gyrocompass affects much the results of analysis of the STCM data (e.g. Seama and Isezaki [2]). In this paper we will report the three-component anomalies of geomagnetic field which show clear features of the magnetic anomaly lineations over the Japan Trench.

STCM

The three flux-gate sensors were set on the roof of the steering bridge and a PC (NEC PC9801) controlled all signals from the north to south as shown Fig. 8-1. These 6 segments are coincident with those of the eastern boundary of the trench shown by the dotted lines implying that the subducting Pacific Plate, or at least its surface suffers some tectonic deformations in the trench region.

Figs. 8-2, 8-3 and 8-4 show X (northward), Y (eastward) and Z (downward) component anomalies of geomagnetic field, respectively. As the previous studies revealed (*e.g.* [3, 4]) , there are Mesozoic geomagnetic anomaly lineations, M10 to M10N in this area and they can easily be identified and traced all in the trench area as seen in these figures. We can, however, find some deformations of lineations. Especially at the boundary of the segment 2 and 3 (see Fig. 8-1), all three component anomaly lineations are greatly disturbed. In Fig. 8-4, we can see that Z component positive anomaly lineation (P3) is cut in two parts by this boundary and the amplitude of P3 becomes large to the north of the boundary.

The same feature can be seen in X and Y component anomaly lineations (Figs. 8-2 and 8-3). Amplitude of P4 is the greatest also at this boundary and

decreases gradually towards the trench axis. It can be seen, however, the amplitude at the boundary of the segment 3 and 4 becomes peculiarly small and P4 cannot be traced beyond the segment 5 and 6 although any other lineations can be traced all in this tench region. The same feature is found on P2 whose amplitude is the smallest on the boundary of the segment 1 and 2.

These features mentioned above suggest that the upper part of the subducting Pacific Plate, probably including the whole oceanic crust taking, the dimension of deformation of geomagnetic anomaly lineations into account, do not have so uniform structure, but locally deformed and segmented structure which reflect the sea bottom topography.

Further studies

To know causes of such local segmentation of the Pacific Plate, we will work further with the detailed analysis of the STCM data as mentioned below,

1. determination of detail distribution of horizontal strike of geomagnetic anomaly lineations, namely strike of the source body producing the geomagnetic anomaly lineations, from which we can know the detail boundary distribution of segments of the plate,
2. determination of undulations of the source body of geomagnetic anomaly lineations, which should correspond to undulations of the plate. The swells of the seafloor located seaside of the trench produced probably by bending of the plate, and the inclined plate located landside of the trench reflect undulations and inclination of the magnetic source body which could be obtained from the STCM data.

Table 8-1. Date and position of "8 shape rotations" conducted during, this cruise.

No.	Day	Month	Year	Latitude	Longitude
1.	29	June	1990	36°55.8 N	141°24.1 E
2.	3	July	1990	38°44.4 N	142°20.8 E
3.	5	July	1990	38°47.7 N	145°43.9 E
4.	1	July	1990	32°00.8 N	143°59.2 E
5.	17	July	1990	32°08.7 N	140°51.3 E
7.	22	July	1990	32°50.3 N	137°52.3 E

References

[1] N. Isezaki, A new shipboard three component magnetometer, *Geophysics*, **51**,1992-1998,1986

[2] N. Seama and N. Isezaki, Seafloor magnetization in the northeastern part of the Japan Basin, *Tectonophys.*, **181**, 285-297,1990

[3] T.W.C. Hilde, N. Isezaki and J.M.Wageman, Mesozoic seafloor spreading in the North Pacific, *AGU Geophys. Monogr.* Ser., **19**, 205-226, 1976

[4] N. Nakanishi, K.Tamaki and K. Kobayashi, Mesozoic magnetic anomaly lineations and sea-floor spreading history of the Northwestern Pacific, *J.Geophys.Res.*, **94**, 15437-15462, 1989

[5] IAGA Division I Working Group I, International Geomagnetic reference field revision 1987, *J. Geomag. Geoelectr.*, **39**, 773-779, 1987

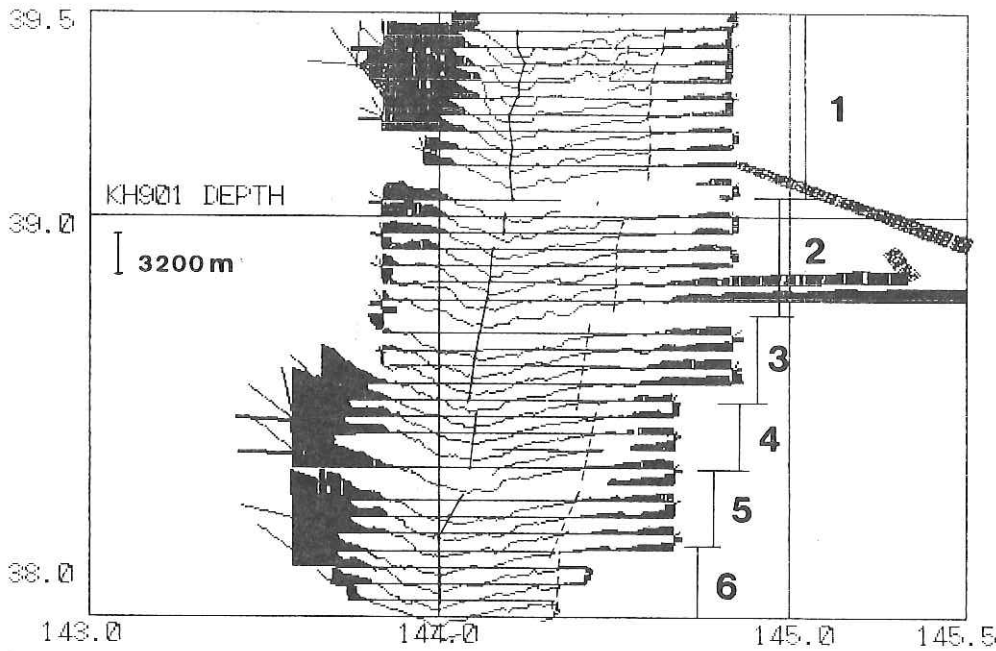

Fig. 8-1. Bathymetric profiles along ship tracks. The ship track corresponds to the level of 6000m depth and the black part of profiles indicates the sea depth shallower than 6000m. Solid lines show positions of the deepest sea bottoms (the trench axis) and broken lines show the eastern edge of the Japan Trench area. This area is divided 6 blocks numbered 1 to 6 from north to south.

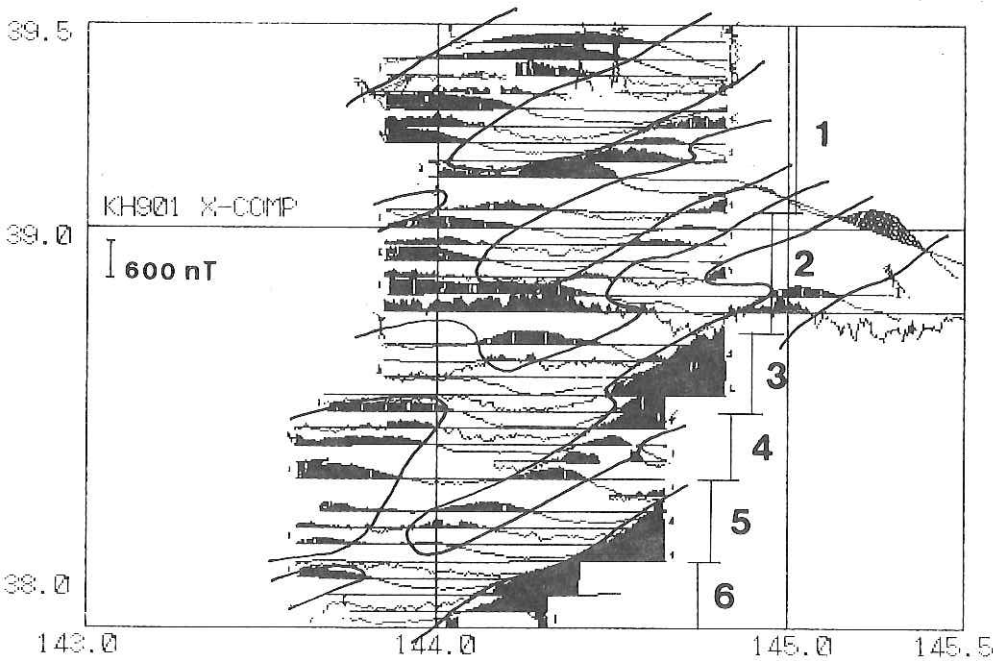

Fig. 8-2. X (north) component anomaly profiles of geomagnetic field referred to the IGRF85 field [5] along ship tracks. Black indicates the positive anomalies.

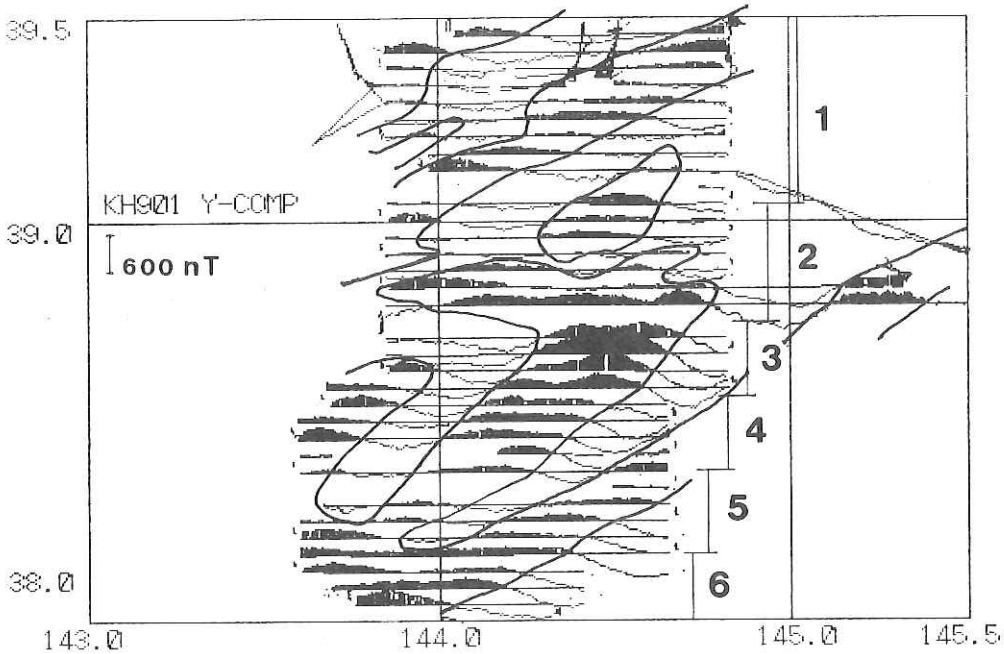

Fig. 8-3. Y (east) component anomaly profiles of geomagnetic field referred to the IGRF85 field [5] along ship tracks. Black indicate the positive anomalies.

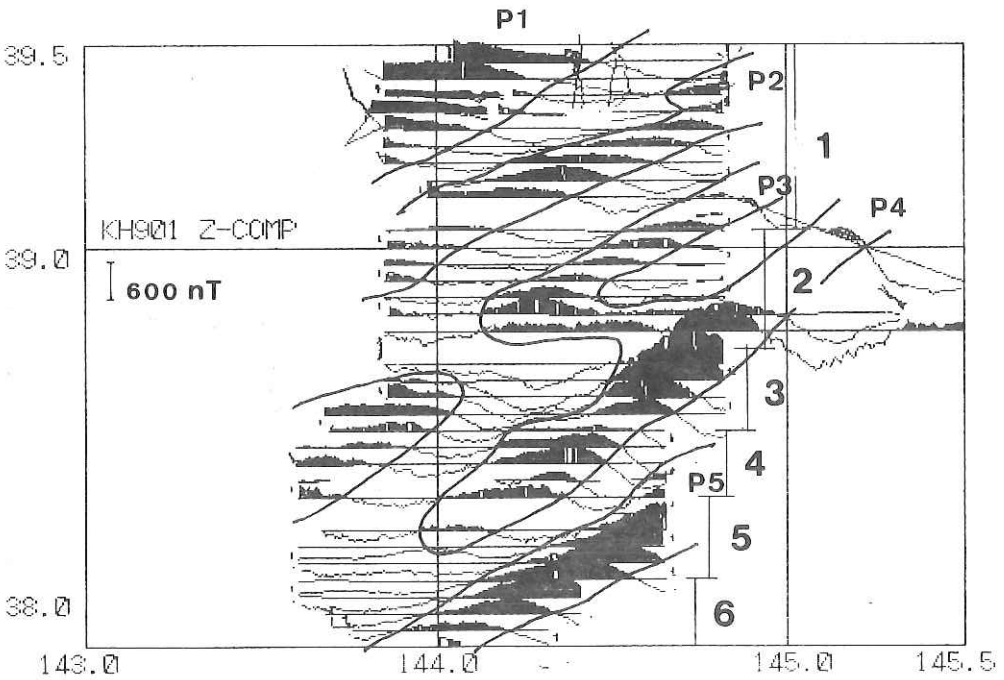

Fig. 8-4. Z (vertical) component anomaly profiles of geomagnetic field referred to the IGRI85 field [5] along ship tracks. Black indicate the positive anomalies which are numbered P1 to P5 from north to south.

9. Magnetic Anomalies of the Joban Seamount Chain

D. C. P. Masalu, , M. Nakanishi, A. Oshida, K. Tamaki and K. Kobayashi

Introduction

Along with the Seabeam survey (Masalu *et al.*, in Chapt. 5-1 of this report) geomagnetic total force was measured in the region of the Joban Seamount Chain. The purpose of this measurement is to eventually use magnetic anomaly data together with Seabeam bathymetry to deduce the magnetic properties such as paleomagnetic direction and intensity of the seamounts in this chain. This is expected to lead to the proper understanding of the origin of the seamounts forming this chain and to give some more light on the tectonics of the Pacific plate.

Measured Geomagnetic Total Force

Geomagnetic total force measured on this seamount chain is between 44,300 nT and 45,950 nT. The contour map for geomagnetic total force measured in this seamount chain is shown in Fig. 9-1. Magnetic anomalies were computed with reference to the IGRF 1985 (IAGA WORKING GROUP 1 [1]). Magnetic anomaly contour map was plotted as shown in Fig. 9-2. In addition to the linear anomalies which are correlatable to the seafloor spreading, magnetic anomalies related to the seamount topography are clearly recognized. They are particularly remarkable around the crests of the Iwaki, Hitachi, Daisan-Kashima and Daini-Kashima Seamounts. These anomalies range between --940 nT and +570 nT.

Brief Overview and Preliminary Interpretation of the Results

From the magnetic anomaly contour map (Fig. 9-2), we can straightforwardly conclude that all the seamounts surveyed are normally magnetized except the northeasternmost Mizunagidori (Bosei) Seamount (shown by the northernmost asterisk) [2]. Intensity of magnetization calculated from the observed anomalies varies with each seamount.

The magnetization of the Mizunagidori seamount is very obscure from this map. Two possibities can be deduced from this observation; the first possibility is that the Mizunagidori seamount is weakly magnetized compared to magnetization of other adjacent seamounts and the surrounding oceanfloor. The second possibility is that the seamount body is alternatively magnetized with the normal and reversed polarities to substantially reduce magnitude of

apparent anomalies. The second possibility seems to be more plausible, since the seamount is situated in a zone of linear anomalies.

In order to explore actual mode of magnetization of the seamount body itself, the effect of magnetic lineations caused by the surrounding ocean floor must be removed. It is hoped that the detailed analysis of these data will decipher some more light on the tectonics of the Pacific plate as well as on the origin of the seamounts forming the Joban seamount chain.

References

[1] IAGA WORKING GROUP 1, International Geomagnetic Reference Field 1985, *J. Geomag. Geoelectr.*, **37**, 1157-1163, 1985.

[2] Y. Tomoda, *Reference Book for Gravity, Magnetic and Bathymetric Data of the Pacific Ocean and adjacent Seas*, 1963-71. Univ. of Tokyo Press, 158pp., 1974.

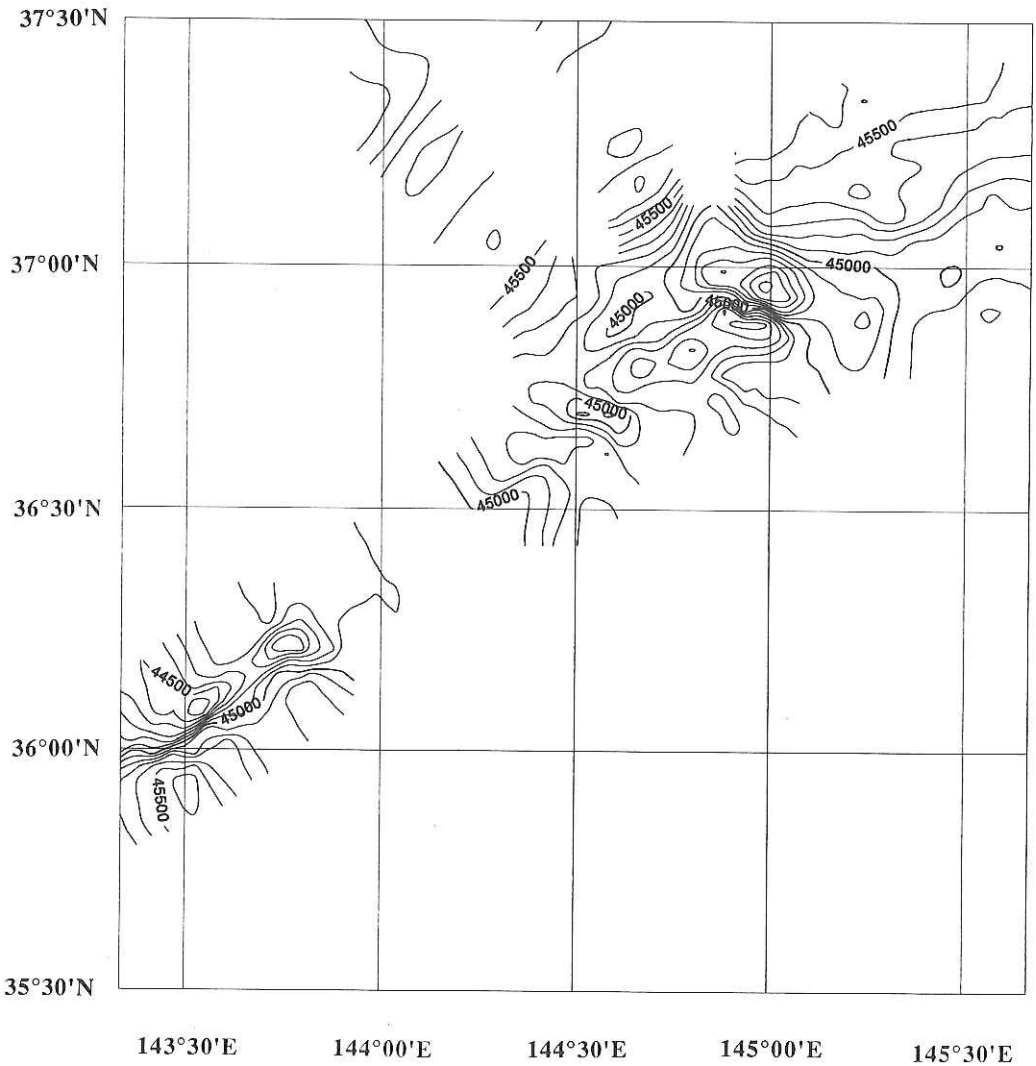

Fig. 9-1 Contours of geomagnetic total forces measured on the Joban Seamount chain during leg 1 of the cruise KH 90-1. Contour interval is 100 nT.

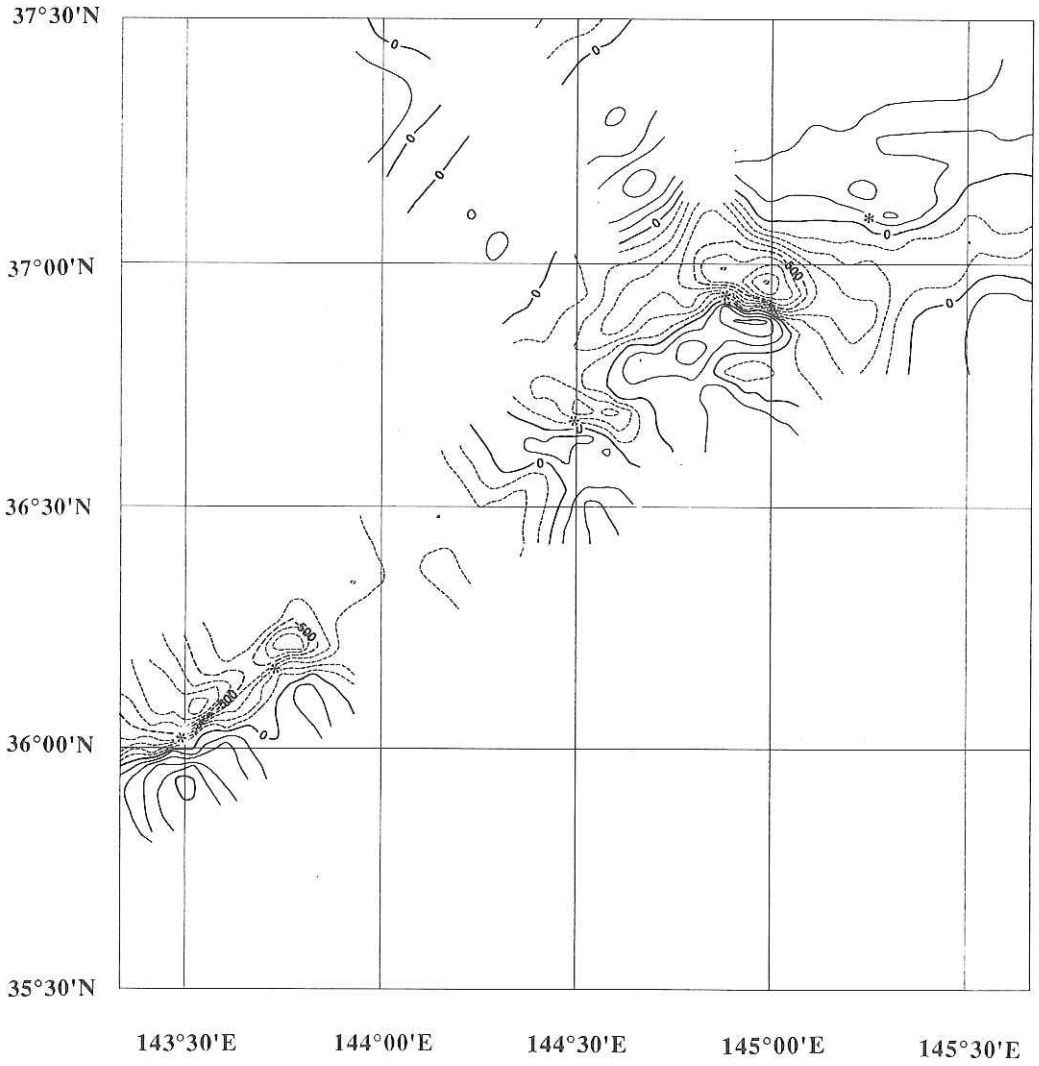

Fig. 9-2 Contours of magnetic anomalies computed from the geomagnetic total forces measured on the Joban Seamount chain during leg 1 of the cruise KH 90-1. Contour interval is 100 nT. Asterisks indicate positions of the peaks of seamounts.

10. Multi-channel Seismic Reflection by the R. V. Hakuho Maru KH 90-1 Cruise

10. 1 Multi-channel Seismic Reflection Survey System

K. Suyehiro, H. Tokuyama, and A. Taira

Introduction

We describe here our newly acquired marine 24-ch seismic reflection survey system (Fig. 10-1). While the system was designed to best operate on R. V. Hakuho-Maru, it is transportable to other ships. The system was first put into operation on KH-89-II test cruise of the new R. V. Hakuho-Maru in 1989. After some modification of the system based on the experience on the test cruise, KH-90-1 cruise marked its second operation.

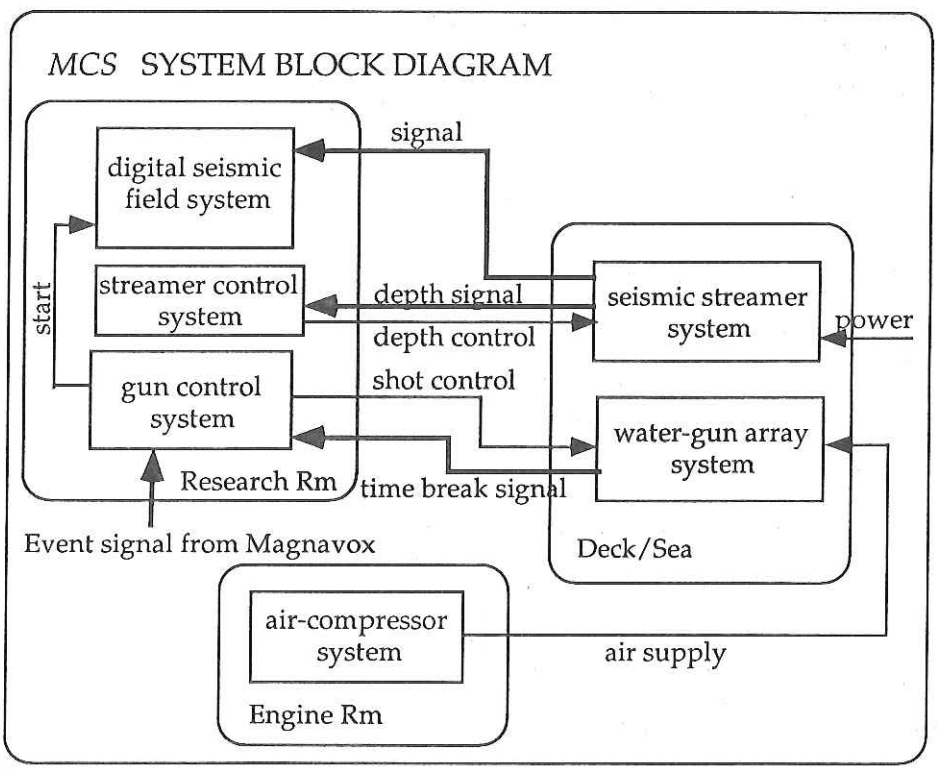

Fig. 10-1 Schematic view of the MCS system.

Though the system still requires further modifications for stable operations, it has proven to produce good quality, high resolution and deep penetration image of the crust beneath oceans.

Seismic Reflection Survey System

Components

Fig. 10-1 shows the schematic view of the MCS system. Specifications of each component are given in Table 10-1. Seismic signal is generated by an implosion-type source, namely a linear 5-watergun array towed behind the ship. The use of waterguns are intended for high resolution crustal image. Airguns can be used instead if deeper penetration is the main objective simply by exchanging guns, since both types operate pneumatically with the same air hoses and cables. Compressed air is supplied by two compressor systems permanently installed on the ship.

TABLE 10-1 System Specifications

Air Compressors (Engine Room)
Two LMF 200E-VGd 2310W17 compound compressors (screw type + piston-type): Each-capacity 20 m^3/min, electric motor, working pressure 17 bar
Watergun array system (Aft Deck)
Winch: Kitagawa Kogyo Co. Ltd. HZW-6-2C-TO Hydraulic-type, dual 2.3 x 2.3 x 2.9 m
Towing assembly
Watergun: Seismic Systems Inc.P400 model 02 420mm ϕmax x 1310 mm, 170 kg,400in^3
Seismic streamer system (Aft Deck)
Winch: AMG T-Streamer Winch 2.9 x 2.7 x 2.7 m, hydraulic
Streamer AMG 37/43
Hydrophone element: HC 202E, 24volts/bar, 100 m depth max.
Each channel: 48 hydrophones, 50 m length
Syntron cable leveller RCL-2 (3 units)
Deck Cable 100 m
Navigation system (Bridge): Magnavox Series 5000 Survey System GPS/NNSS/LORAN-C
Event control system : relay closure pulse width 0.01 s minimum
mode 1: distance events occur after a given distance parallel to survey line
mode 2: total distance events occur after a given distance
mode 3: time events at specified time interval
Streamer depth control system (Reasearch Room):
Syntron Command Console CC-801
AMG 4-ch. Depth Indicator
Watergun shot control system (Research Room)
Input/Output, Inc., Auto Sync I-WG
Field data acquisition system (Research Room)
Texas Instruments DFS-V

A 24-channel seismic streamer with 50 m length per channel receives the returned seismic signal. The streamer is equipped with three depth controllers which can be remotely monitored and controlled.

The real time multiplexed data are fed into the data acquisition system (TI, DFS-V) and the data are eventually stored onto digital magnetic tapes at 6250 bpi. Up to 60 channels' data can be handled.

Onboard data processing is currently not available because of the special data tape format which cannot be read by the on board tape drives.

Navigation

Reflection waveforms are usually stacked for the geometry of shot-receiver pairs that share a common mid point (CMP). The seismic signal generation is made at the same spatial interval as the streamer's channel separation. So, there will be 12 shot-receiver pairs or seismic traces that can be used for CMP stacking.

The R. V. Hakuho Maru is equipped with a navigation system which can transmit TTL level pulses *via* the shipboard network system (Event Mode) in a user specified mode to control the source geometry. There are three modes; (1) Constant time interval, (2) Distance along the line, and (3) Actual distance. Mode (2) is best suited for CMP stacking and is used. Table 10-2 describes the operation and data format of the Event Mode of the navigation system during a seismic survey. This information is especially important in case the shot time is needed for independent receivers such as an OBS.

Watergun Array System

A winch with dual drums for a chain and an umbilical cable is used to tow the gun array. Guns are suspended from the chain. Balloons are attached to the chain to control the gun depth. Fig. 10-2 shows how the towing system looks on board and off board.

The umbilical cable consists of a stress member, air hoses, and electric cables to provide electrical and pneumatic power to each gun. The towing system is installed on the R. V. Hakuho Maru only on seismic cruises. The gun array linearly holds up to five guns with about 4 m spacing (Fig. 10-2). The spacing is to achieve non-interaction among guns. Each gun has a near-field hydrophone attached to capture the actual shottime to be fed back to the gun controller system to simultaneously shoot the guns.

Table 10-2 Event Mode Data Format on Magnetic Tape

1 physical block on tape: 4097 byte/block (4096-byte data + 1-byte (LF))
1 physical record: 4096-byte (36-byte physical header + 4060-byte data)
Data: consists of logical records
1 Logical record: variable length (32-byte logical header + variable length data)
Physical record header:
(I: 2-byte integer; I4: 4-byte integer; R: 4-byte real; R8: 8-byte real; A: ASCII)

word count	
1	1 (I4): Physical record number
2	3 (I): Starting Word of the first complete logical record in this physical block
3	4 (I4): First complete logical record number
4	6 (I4): Last logical record number
5	8 (I): Year when logged onto tape
6	9 (I): Julian day when logged onto tape
7	10 (I): Hour when logged onto tape
8	11 (I): Minute when logged onto tape
9	12 (I): Second when logged onto tape
10	13 (I): Flag word
11	14 (I): Physical record header length (=18)

Logical record header

word count	
1	1 (I4): Logical record number
2	3 (I): Logical record type (=2600 for Event Data)
3	4 (I): Size of logical record (=typically 900)
4	5 (I): Year when written to buffer
5	6 (I): Julian day when written to buffer
6	7 (I): Hour when written to buffer
7	8 (I): Minute when written to buffer
8	9 (I): Second when written to buffer
9	10 (R8): Time since system start

Event Data record excerpt

word count
17 (I): Year of Event
18 (I): Julian day of Event
19 (I): Hour of Event
20 (I): Minute of Event
21 (I): Second of Event
22 (R8): Fraction of second of Event
26 (R8): Time stamp
30 (I): Event mode (2 is total distance mode)
31 (R8): Distance in m between events in mode 1 or 2
32 (R8): Time in s between events in mode 3
39 (R8): Elapsed time since previous event (s)
43 (I4): Event number
45 (I4): Total event number
47 (I4): Spare
49 (R8): Latitude
53 (R8): Longitude
57 (R8): Parametric latitude
61 (R8): Smoothed latitude
65 (R8): Smoothed longitude

R: Mantissa sign (Bit 15 of Word 1), Mantissa 23 bits (Bit 14 of Word 1 to Bit 8 of Word 2)
Exponent 7 bits (Bit 7 to 1 of Word 2), Exponent sign (Bit 0 of Word 2)
R8: Mantissa sign (Bit 15 of Word 1), Mantissa 55 bits (Bit 14 of Word 1 to Bit 8 of Word 4)
Exponent 7 bits (Bit 7 to 1 of Word 4), Exponent sign (Bit 0 of Word 4)

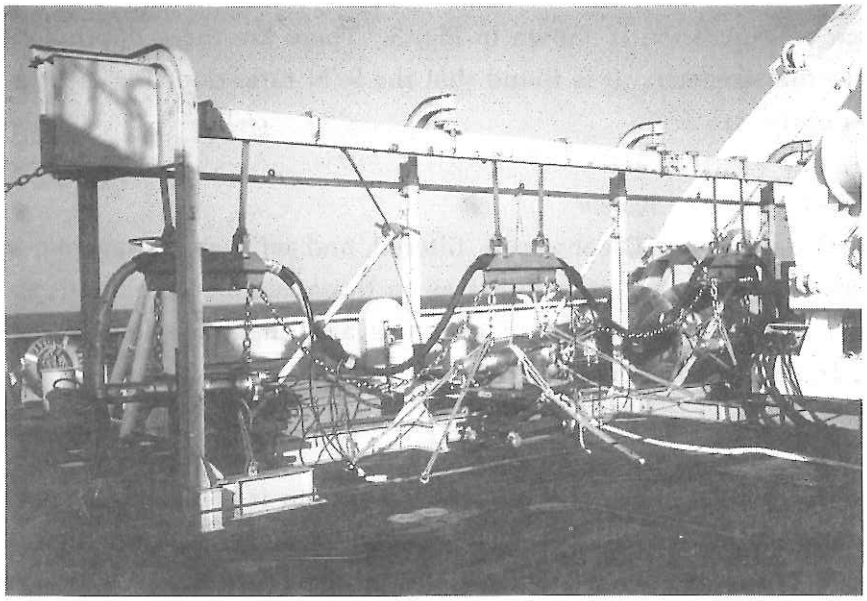

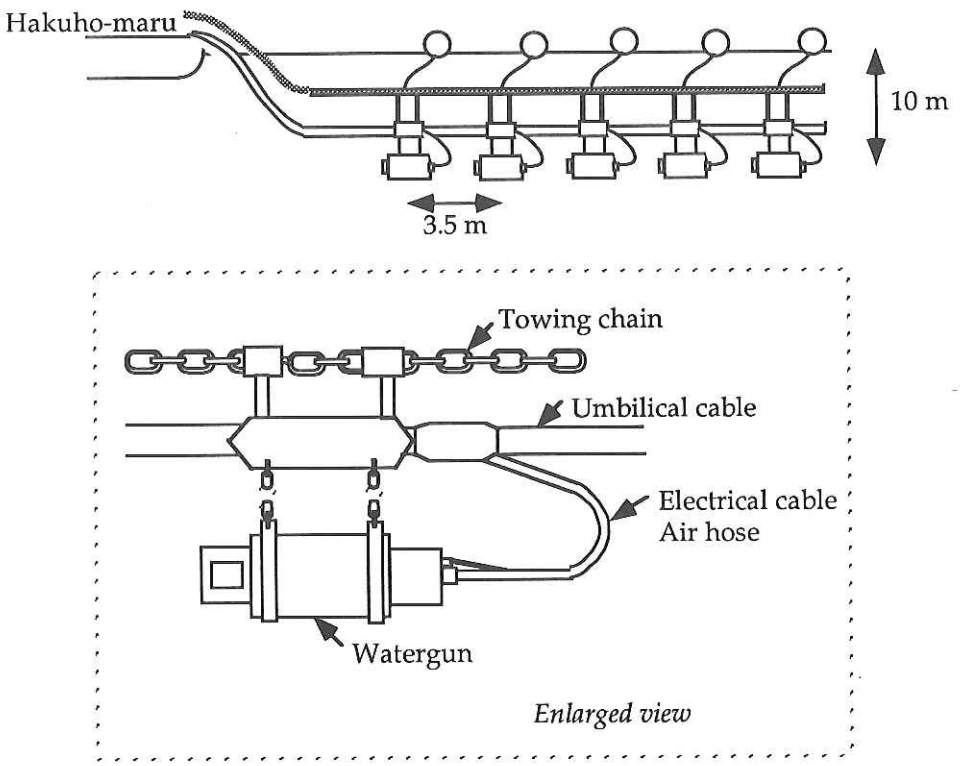

Fig. 10-2 Watergun-array towing system on deck (photo) and schematic view in water.

Hydrophone Streamer System

Present configuration is shown in Fig. 3. There are three depth controllers attached to the streamer. It is found that the S/N ratio depends greatly on the streamer depth.

Field Data Acquisition System

The raw data are A/D converted, filtered, and written to magnetic tapes in SEG-B format. There are constraints as to the available combinations of the sampling rate and the number of channels and the trace length. With 28 channels, 1ms sampling is required.

Concluding Remarks

Our new 24-ch seismic reflection survey system is a major advance of our seismic data acquisition system. The source volume has more than doubly increased. Watergun over airgun gives higher resolution. The receiver channels increased by double.

A number of improvements are necessary in the near future. As the R. V. Hakuho Maru is equipped with an advanced multi-computer network system, we should be able to immediately start processing the seismic data on board, which is not currently possible. The number of seismic channels can be increased to 48 channels simply by adding more active hydrophone sections. Also, a more stable towing of guns is necessary so that the umbilical cable is not damaged.

Thus acquired seismic data can be processed by main frame or mini computers once the field tapes are demultiplexed. Demultiplexing is currently available on a super mini computer at ORI.

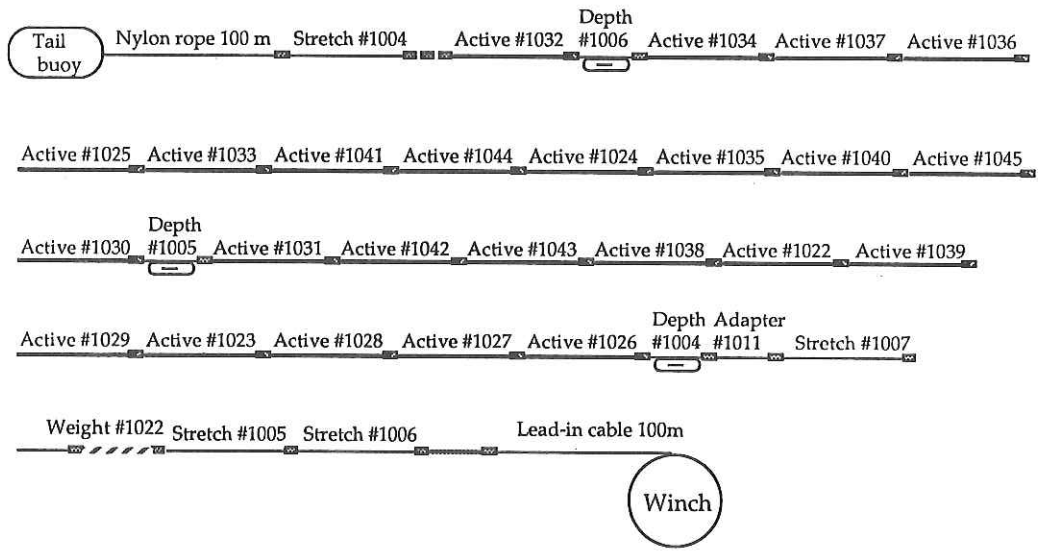

Fig. 10-3 Configuration of seismic streamer.

10. 2 Multi-channel Seismic Reflection Profiling

K. Suyehiro, C. Igarashi, Y. S. Djajadihardja,
M. Okada, H. Nambu, and F. Yamamoto

Introduction

The cruise marked the second opportunity to carry out the seismic reflection profiling with the newly acquired system of ORI (Suyehiro *et al.*, **10. 1**). Two profiles were shot during this cruise. One was shot east to west across the Japan Trench at about 38°45'N on Leg 1 (Fig. 10-4). The other was a long profile extending over 500 km, which was shot west to east across the Izu-Bonin Trench at about 32°47'N (Fig. 10-5).

Within the available time window, we have tried to transect two plate subduction zones with as much coverage as possible. Such data are, in fact, rare. The obtained data will be processed by the new seismic data processing system at ORI and seismic migrations and geological interpretations will be made. Furthermore, these data will be linked with the seismic refraction data to obtain a clearer view of the crust.

Japan Trench Profile (JT90)

Table 10-3 is the log record excerpts with operational parameters. Fig. 10-6 is the near trace monitor record of the whole profile. The record is the output from channel 1 (nearest the source). A bandpass filter (20-100 Hz) and a gain function for geometrical spreading compensation (traveltime squared) have been applied.

Horst and graben type feature is found to develop near the trench. The extent of these faults can be identified in SeaBeam maps also obtained on this cruise (Chapt. 4 of this report). These faults are seen to subduct.

Izu-Bonin Trench Profile (IB90)

Table 10-4 is the log record excerpts with operational parameters. Fig. 10-7 is the near trace monitor record for shots #4529 -#7999 with the same parameters as the Japan Trench record. Unlike the Japan Trench profile, there are no sediments at the trench. The subduction is not obvious with little processing of the data.

Concluding Remarks

We obtained two long profile records over the Japan Trench and the Izu Bonin Trench by shooting an array of four waterguns into a 24-channel seismic hydrophone streamer.

Not much can be said from unprocessed near trace records alone, on top of previous studies done in the area (see Table 10-5 for compilation). Our survey employed an array of waterguns in the hope of obtaining more details than previous images. Also, the profile lengths were taken as long as possible to capture all the deformations taking place in subduction zones. These details will be unveiled after extensive processing of the data.

TABLE 10-3. Records of Seismic Profiling LEG 1 July 1 17:08 ~ July 3 09:00

[Time used in this record only is JST = GMT + 9]

System startup (weather: fine, calm) July 01, 1990

14:15	ship slow down
14:40	load waterguns (Nos. 1, 2, 3, 5)
15:15	complete loading
15:26	start gun deployment
15:45	guns deployed
15:55	manual shot test
16:00	start hydrophone streamer deployment
16:41	end deployment, connect cable
17:08	DFS-V system start

Recording parameters
Number of channels: 28
Sampling rate: 1 ms
Trace record length: 6 s (partly 10 s)

Shooting parameters
Shot interval: 50 m (mode 1)
Number of waterguns: 4

July		Profile				
Date	time	shot	latitude	longitude	depth	
01	20:00	543	38° 44.96' N	145° 27.44' E	5,320 m	
01	22:00	903	38° 45.02' N	145° 15.27' E	5,340 m	
02	00:00	1227	38° 44.95' N	145° 04.59' E	5,413 m	
02	04:00	1796	38° 44.98' N	144° 47.43' E	5,668 m	
02	08:00	2296	38° 45.04' N	144° 30.94' E	6,151 m	
02	12:00	2859	38° 45.07' N	144° 13.83' E	7,126 m	
02	16:00	3340	38° 45.01' N	143° 58.61' E	6,671 m	
02	20:00	3876	38° 45.05' N	143° 41.79' E	3,789 m	
03	00:00	4472	38° 44.94' N	143° 22.66' E	2,200 m	
03	04:00	5127	38° 45.05' N	143° 00.78' E	1,596 m	
03	08:00	5807	38° 44.99' N	142° 37.78' E	1,276 m	
03	09:00	6004	38° 44.96' N	142° 30.95' E	1,200 m	LAST SHOT

* All figures are preliminary.

System retrieval

Jul. 3	09:13	start streamer windup
	09:20	start gun retrieval
	09:32	guns retrieved

TABLE 10-4. Records of Seismic Profiling LEG 2 July 22 22:19 ~ July 25 07:00
[Time used in this record only is JST = GMT + 9]

System startup (weather fine, calm) July 22, 1990

17:30	Two compressors started
18:14	Guns #2, 3, 4, 5 ready for operation

Recording parameters:
Number of channels: 28
Sampling rate: 1 ms
Trace record length: 6 s (partly 10 s)

Shooting parameters
Shot interval: 50 m (mode 1)
Number of waterguns: 4

July Date	time	Profile shot	latitude	longitude	depth	
22	20:00	029	32° 46.99' N	138° 04.70' E	3,804 m	
23	00:00	718	32° 47.04' N	138° 26.60' E	3,453 m	
23	04:00	1490	32° 47.05' N	138° 51.28' E	1,826 m	
23	08:00	2266	32° 46.97' N	139° 16.51' E	816 m	
23	12:00	3182	32° 46.95' N	139° 46.98' E	534 m	
23	16:00	4145	32° 47.47' N	140° 18.61' E	1,226 m	
23	20:00	4901	32° 46.99' N	140° 42.75' E	2,048 m	
24	00:00	5681	32° 47.11' N	141° 07.96' E	2,431 m	
24	04:00	6475	32° 46.96' N	141° 33.72' E	5,260 m	
24	08:00	7194	32° 47.00' N	141° 56.78' E	7,080 m	
24	12:00	7849	32° 46.99' N	142° 17.12' E	5,277 m	
24	16:00	8456	32° 46.99' N	142° 35.84' E	6,482 m	
24	20:00	9120	32° 46.98' N	142° 56.71' E	5,619 m	
25	00:00	9846	32° 47.03' N	143° 19.82' E	5,542 m	
25	04:00	0596	32° 46.96' N	143° 43.90' E	5,434 m	
25	07:00	1125	32° 46.99' N	144° 00.75' E	591 m	LAST SHOT

* All figures are preliminary.

Table 10-5 Previous Seismic Reflection Surveys in the Area

Japan Trench

Profile	Approx. Position	Type	Reference
P-849	(39°40'N,143°04'E)~(39°40'N,145°30'E)	MCS	Beck *et al.*, 1976
GH76-2	whole Japan Trench area JT90 is between L15 and L16	120-in^3:1-ch	Tamaki *et al.*,1977; Honza, 1980
JNOC-1	(40°39'N,142°48'E)~(40°39'N,144°40'E)	1490-in^3:48-ch	Matsuzawa *et al.*,1980
JNOC-2	(39°45'N,143°52'E)~(39°45'N,144°30'E)	1490-in^3:48-ch	Matsuzawa *et al.*,1980
JNOC-A~C	off Sanriku N-S	1490-in^3:48-ch	Matsuzawa *et al.*,1980
ORI78-3	(40°29'N,143°48'E)~(40°27'N,144°42'E)	1490-in^3:48-ch	Nasu *et al.*, 1980
ORI78-4	(40°07'N,143°49'E)~(40°05'N,144°42'E)	1490-in^3:48-ch	Nasu *et al.*, 1980
Kaiyo	off Joban	2000-in^3:48-ch	Sakurai *et al.*, 1981
ORI80-1~4 (KH80-1)	off Hachinohe	300-in^3:12-ch	Kagami *et al.*, 1980
GH80-3	Kashima Seamount. area	150-in^3:1-ch	Okamura *et al.*, 1984
ORI81-5~11 (KH81-3)	off Hachinohe	300-in^3:12-ch	Tokuyama *et al.*, 1982
KT83-16	off Kashima	1100-in^3: 6-ch	KAIKO II Res Group, 1987
M1	Kashima Seamount. area	?:12-ch	Oshima *et al.*, 1985
Kaiko 84-3	off Kashima, off Sanriku	80-in^3:1-ch	Cadet *et al.*, 1987; Kobayashi *et al.*,1987

Izu Bonin Trench (30°N ~ 35°N)

Profile	Approx. Position	Type	Reference
GH74-3	(29°32'N,143°45'E)~(31°25'N,137°12'E)	120-in^3:1-ch	Okuda *et al.*, 1976
GH74-3	(32°45'N,140°12'E)~(33°51'N,137°51'E)	120-in^3:1-ch	Okuda *et al.*, 1976
GH74-3	(29°32'N,143°45'E)~(31°25'N,137°12'E)	120-in^3:1-ch	Okuda *et al.*, 1976
GH79-4	30°0'N~33°0'N	300-in^3:1-ch	Tamaki *et al.*, 1981
GH80-3	33°30'N~34°46'N	300-in^3:1-ch	Tanahashi *et al.*,1984
Kaiko 84-2	TTT junction	80-in^3:1-ch	Renard *et al.*, 1987
FM3505/3507	30°30'N-32°30'N	3,065-in^3:120-ch	Taylor *et al.*, 1990
Geco Delta	TTT junction	4,830-in^3:120-ch	Iwabuchi *et al.*, 1990
IB89	TTT junction	2,000-in^3:24-ch	KH89-Test II

References

Beck, R. H., P. Lehner, P. Diebold, G. Bakker, and H. Doust, 1975, New geophysical data on key problems of global tectonics, *Proc. 9th World Pet. Congr.*, **5**, 3-32.

Cadet, J-P, K. Kobayashi, J. Auboin, J. Boulegue, C. Deplus, J. Dubois, R. von Huene, L. Jolivet, T. Kanazawa, J. Kasahara, K. Koizumi, S. Lallemand, Y. Nakamura, G. Pautot, K. Suyehiro, S. Tani, H. Tokuyama, and T. Yamazaki, 1987, The Japan Trench and its juncture with the Kurile Trench: cruise results of the Kaiko project, Leg 3, *Earth & Planet. Sci . Lett*, **83**, 267-284.

Honza, E., 1980, Pre-site survey of the Japan Trench transect, Deep Sea Drilling Project, in *Init. Rep. DSDP*, U. S. Government Printing Office, Wash., D. C., **56/57**, 449-458.

Iwabuchi, Y., A. Asada, and Y. Kato, 1990, Multi-channel seismic reflection survey around the plate triple junction off Boso Peninsula, *J. Jpn Soc. Mar. Surveys 7 Tech.*, **2**, 29-38.

Kagami, H., H. Tokuyama, K. Fujioka, C. Igarashi, and N. Nasu, 1980, Preliminary report on multichannel seismic profiling across Japan Trench off Sanriku, northeast Japan, In *Recent Seafloor Surveys*, Hydrogr. Dept., 49-59 (in Japanese).

KAIKO II Research Group, 1987, *6000 meters deep: A trip to the Japanese Trenches* . 106pp, Univ. of Tokyo Press/IFREMER/CNRS.

Kobayashi, K., J-P Cadet, J. Auboin, J. Boulegue, C. Deplus, J. Dubois, R. von Huene, L. Jolivet, T. Kanazawa, J. Kasahara, K. Koizumi, S. Lallemand, Y. Nakamura, G. Pautot, K. Suyehiro, S. Tani, H. Tokuyama, and T. Yamazaki, 1987, Normal faulting of the Daiichi-Kashima seamount in the Japan Trench revealed by the Kaiko I cruise, Leg 3, *Earth & Planet. Sci . Lett*, **83**, 257-266.

Matsuzawa, A., T. Tamano, Y. Aoki, and T. Ikawa, 1980, Structure of the Japan Trench subduction zone from multichannel seismic reflection records, *Mar. Geol.*, **35**, 171-182.

Nasu, N., R. von Huene, Y. Ishikawa, M. Langseth, T. Bruns, and E. Honza, 1980, Interpretation of multichannel seismic reflection data, Legs 56 and 57, Japan Trench transect, in *Init. Rep. DSDP*, U. S. Government Printing Office, Wash., D. C., **56/57**, 489-503.

Okamura, Y., K. Nakamura, M. Tanahashi, and Y. Okuda, 1984, Continuous seismic reflection profiling survey of Kashima No. 1 seamount and adjacent area, In T. Miyazaki and E.Honza (eds), *Geological Investigation of theJunction Area of the Tohoku and Ogasawara Arcs*, Geol. Survey of Jpn, 103-108.

Okuda, Y., M. Kimura, and E. Honza, 1976, Geological structure of the Izu-Ogasawara Arc and Trench, In E. Inoue (ed), *Izu-Ogasawara (Bonin) Arc and Trench Investigations*, Geol. Survey of Jpn, 29-45.

Oshima, S., T. Ogino, T. Katsura, K. Ikeda, M. Uchida, M. Nagano, M. Hayashida, K. Muneda, S. Kasuga, and S. Tani, 1985, Subduction of Daiiti-Kasima seamount into the landward slope of the Japan Trench, *Rep. of Hydrogr. Res.*, **20**, 25-46.

Renard, V., K. Nakamura, J. Angelier, J. Azema, J. Bourgois, C. Deplus, K. Fujioka, Y. Hamano, P. Huchon, H. Kinoshita, P. Labaume, Y. Ogawa, T. Seno, A. Takeuchi, M. Tanahashi, A. Uchiyama, and J-L Vigneresse, 1987, Trench triple junction off Central Japan-preliminary results of French-Japanese 1984 Kaiko cruise Leg 2, *Earth & Planet. Sci. Lett,* **83**, 243-256.

Sakurai, M., A. Mogi, J. Chujo, and T. Miyazaki, 1981, Multichannel seismic reflection profiling off Joban district, northeast-Japan, *Rept. of Hydrogr. Res.*, **16**, 1-24 (in Japanese).

Tamaki, K., Y. Inouchi, F. Murakami, and E. Honza, 1977, Continuous seismic reflection profiling survey, In E. Honza (ed), *Geological Investigation of Japan and Southern Kurile Trench and slope areas GH 76-2 Cruise April-June 1976*, Geol. Survey of Jpn, 50-72.

Tamaki, K., M. Tanahashi, Y. Okuda, and E. Honza, 1981, Seismic reflection profiling in the Ogasawara (Bonin) Arc and the northern Mariana Arc, In E.Honza, E. Inoue & T. Ishihara (eds.),*Geological Investigation of the Ogasawara (Bonin) and Northern Mariana Arcs,* Geol. Survey of Jpn, 83-91.

Tanahashi, M., Y. Okuda, Y. Okamura, and K. Nakamura, 1984, Continuous seismic profiling survey at the junction of the Tohoku and the Ogasawara Arcs in GH80-3 cruise, In T. Miyazaki and E. Honza (eds.), *Geological Investigation of theJunction Area of the Tohoku and Ogasawara Arcs*, Geol. Survey of Jpn, 109-111.

Taylor, B., G. Moore, A. Klaus, M. Systrom, P. Cooper, and M. MacKay, 1990, Multi-channel seismic survey of the central Izu-Bonin Arc, *Proc. ODP, Init. Repts.*, College Station, TX (Ocean Drilling Program), **126**, 51-60.

Tokuyama, H., H. Kagami, K. Y. Sae, C. Igarashi, and N. Nasu, 1982, The recent results from the multi-channel seismic profiling across the Japan Trench and Nankai Trough, In *Recent Seafloor Surveys*, Hydrogr. Dept., 73-80 (in Japanese).

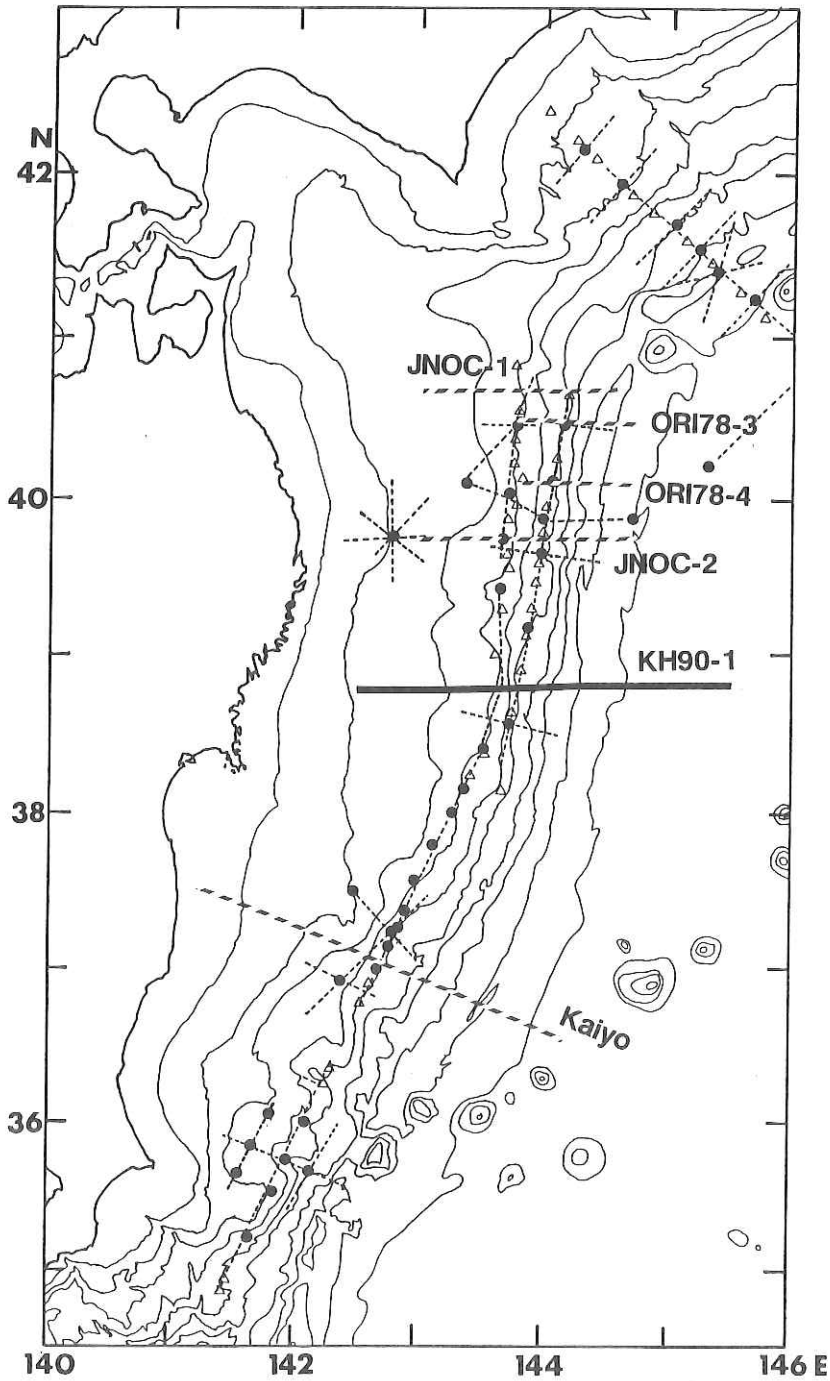

Fig. 10-4 Map of Japan Trench area. Profile 1 is shown by thick line. Broken lines are airgun-OBS refraction survey lines, where various symbols denote OBS arrays deployed temporarily. Other MCS profiles are also shown by thick broken lines.

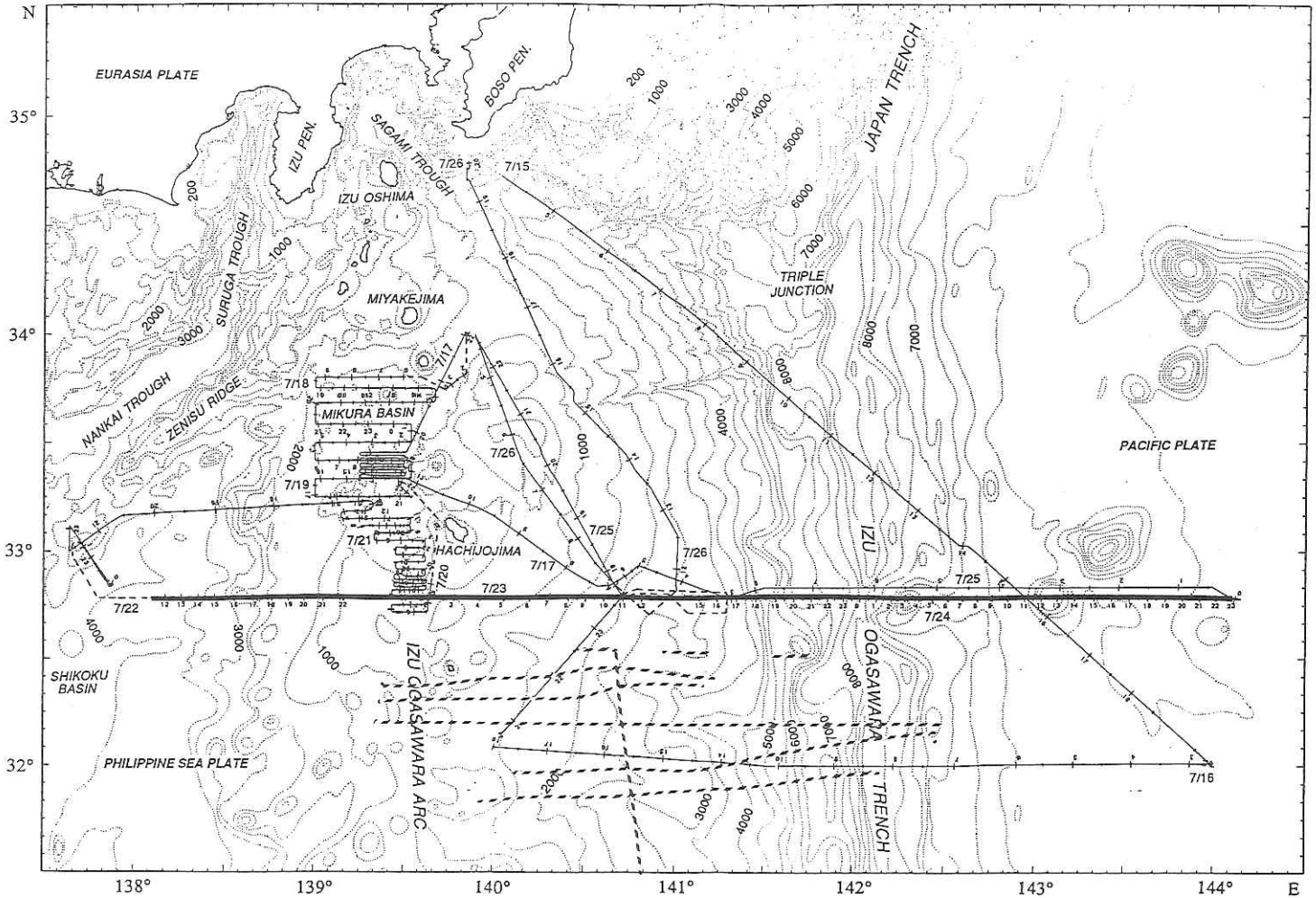

Fig. 10-5 Map of KH 90-1 Leg 2 area. Profile 1 is shown by thick line. Other profiles (FM3505/3507: See Table 10-5) are also shown by broken lines.

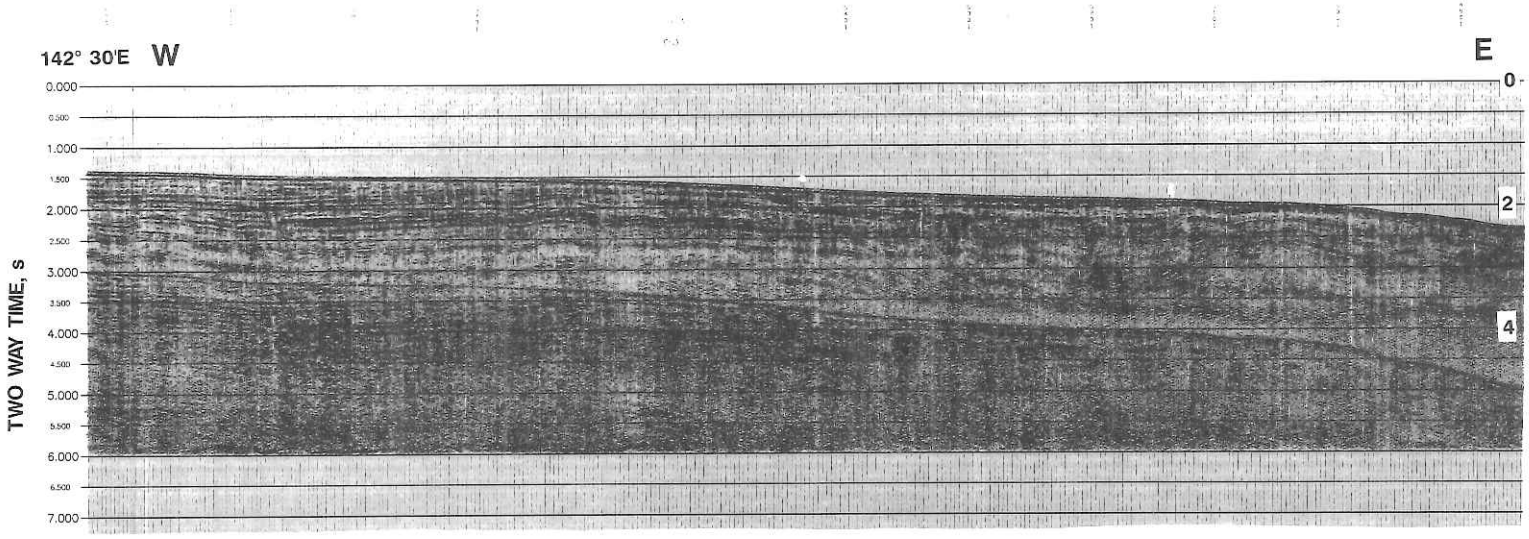

Fig. 10-6-1 Filtered near-trace records of Profile 1 across Japan Trench. The westernmost section.

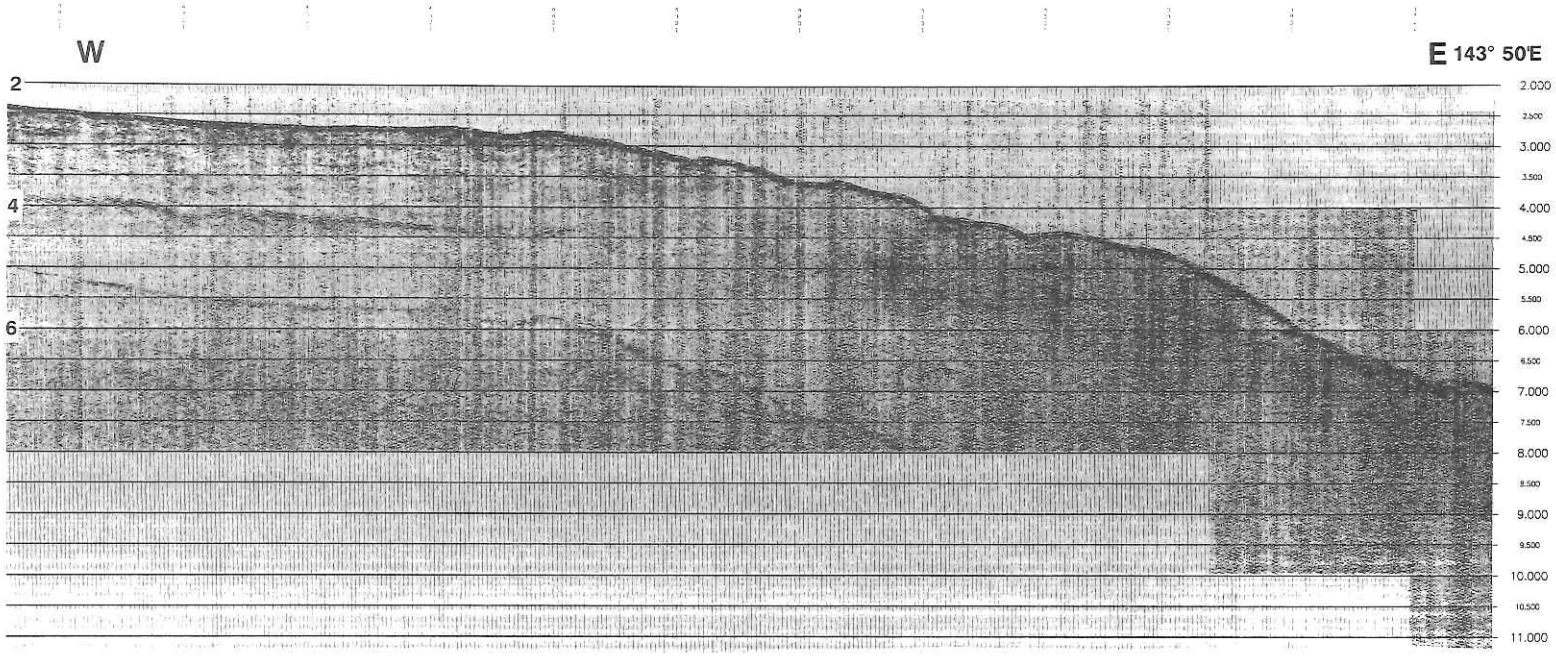

Fig. 10-6-2 Filtered near-trace records of Profile 1 across Japan Trench.

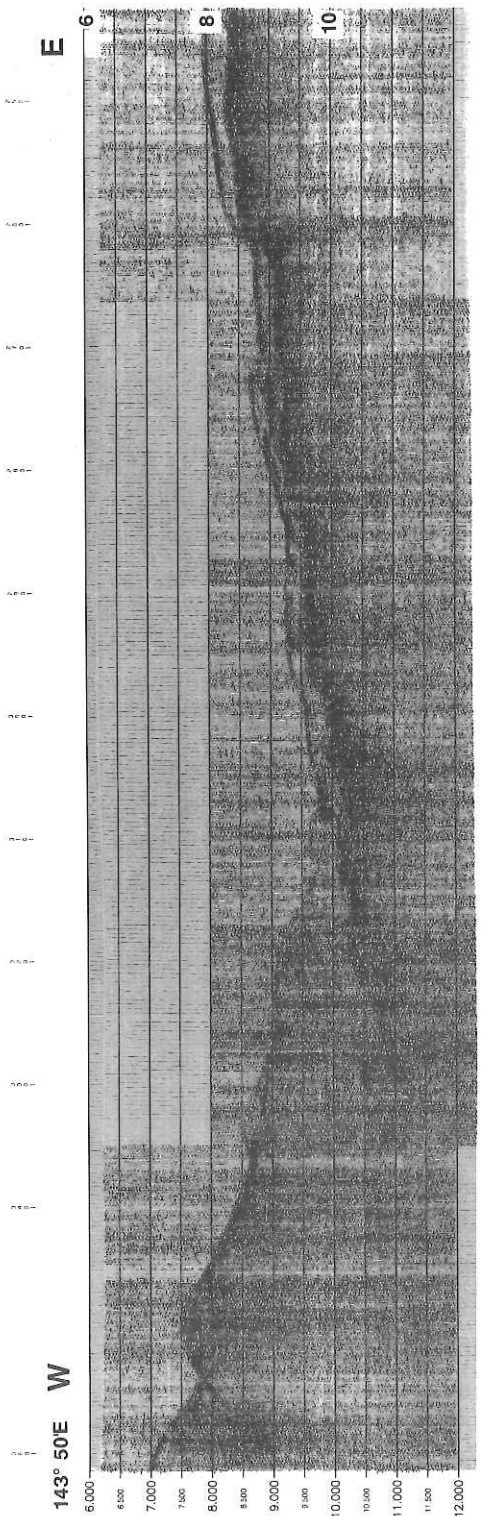

Fig. 10-6-3 Filtered near-trace records of Profile 1 across Japan Trench.

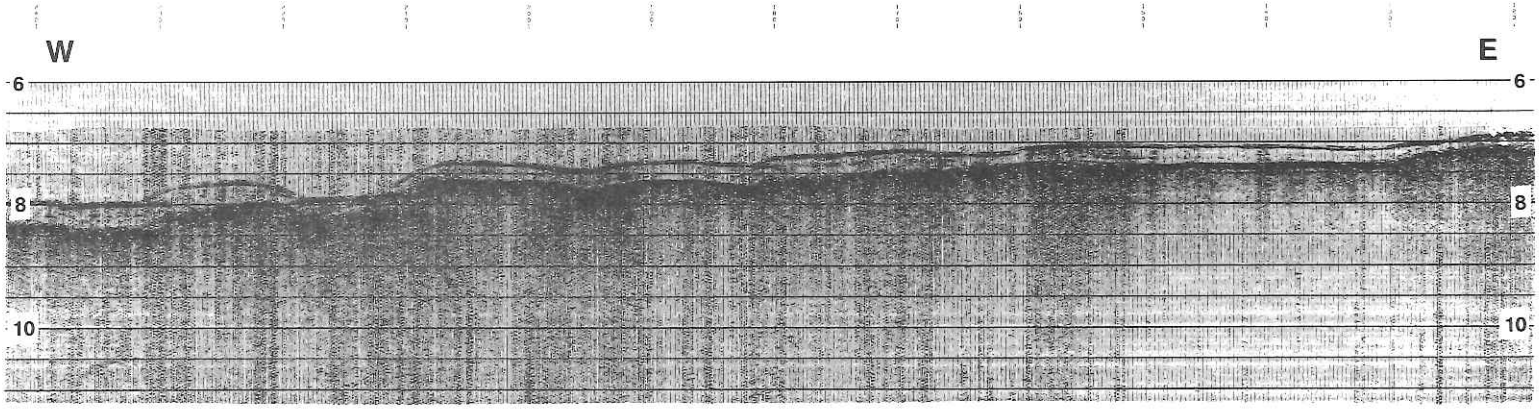

Fig. 10-6-4 Filtered near-trace records of Profile 1 across Japan Trench.

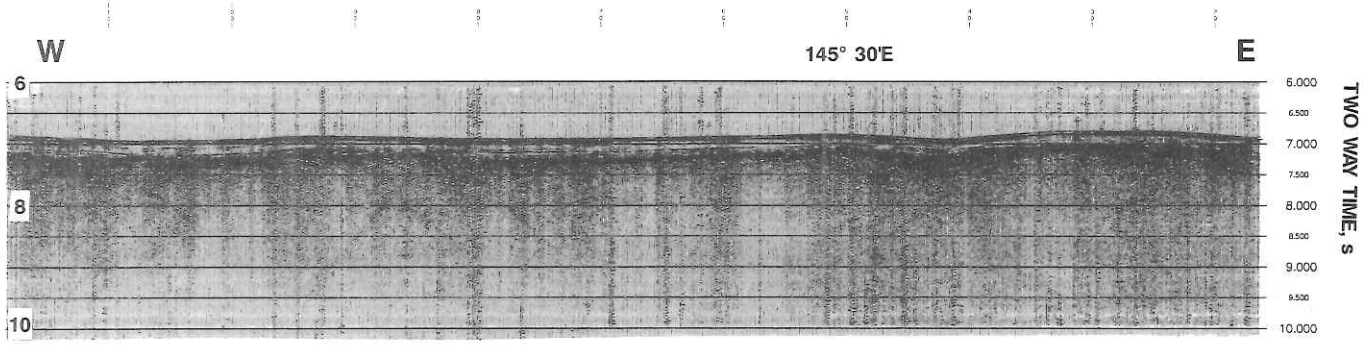

Fig. 10-6-5 Filtered near-trace records of Profile 1 across Japan Trench.
The easternmost section.

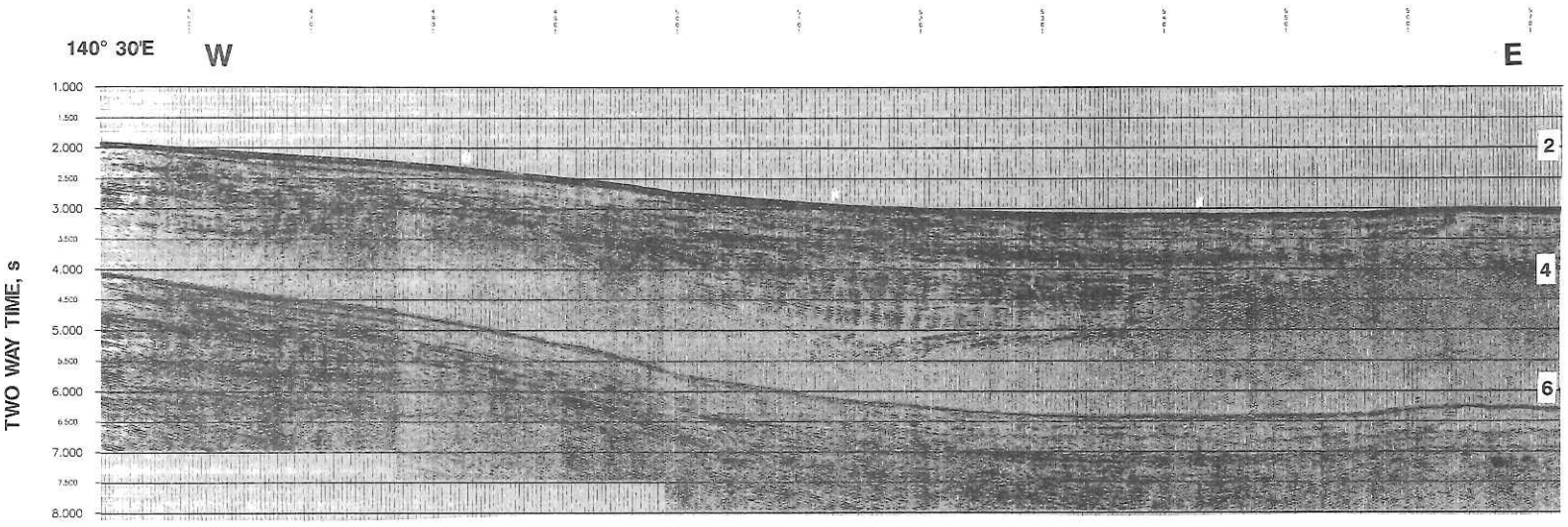

Fig. 10-7-1 Filtered near-trace record of Profile 2 (part) across Izu-Bonin Trench. The westernmost section.

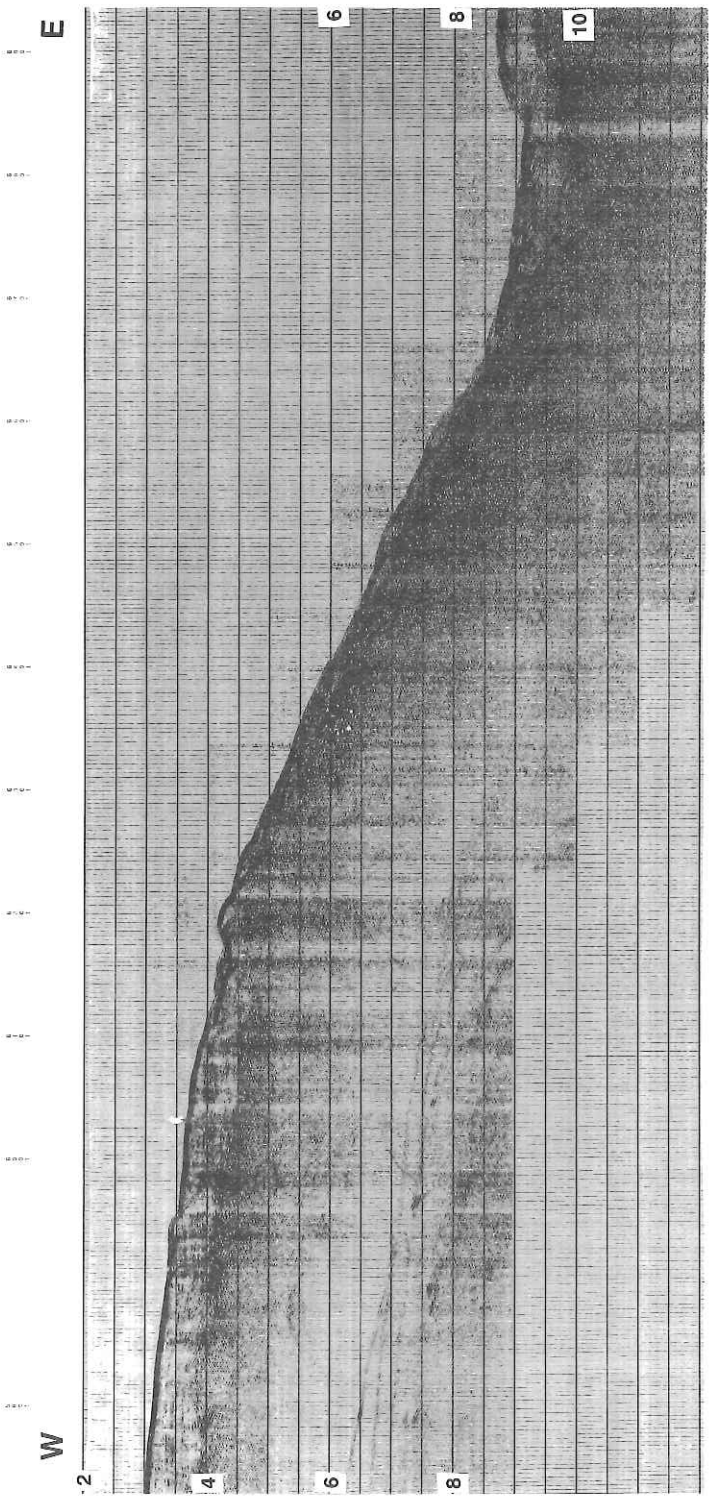

Fig. 10-7-2 Filtered near-trace recordof Profile 2 (part) across Izu-Bonin Trench.

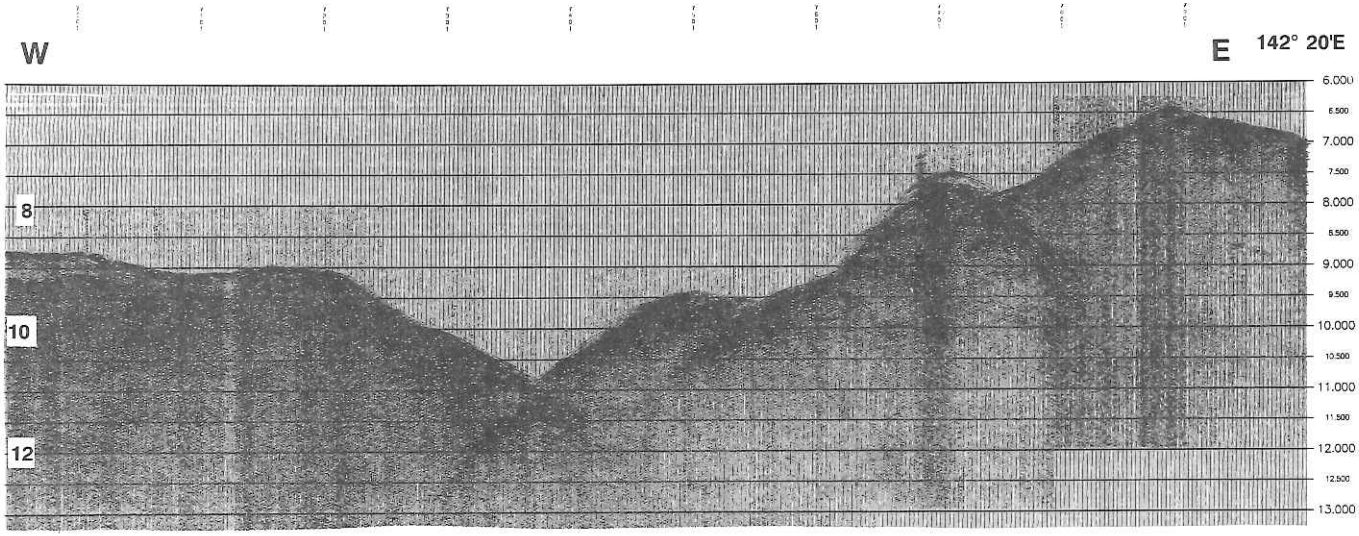

Fig. 10-7-3 Filtered near-trace recordof Profile 2 (part) across Izu-Bonin Trench. The easternmost section.

11. Deep-Sea Multi-monitoring System (DESMOS) Operation and Bottom Observations along the Japan Trench

S. Ohta, M. Watanabe, H. Ishizaki and S. Seki

A sophisticated deep-tow type bottom surveying system named "DESMOS" (deep-sea multi-monitoring system) was developed and put in use for exploration and pin-point observations of the crestal regions of the Iwaki and Bosei (Mizunagidori) Seamounts, and the landward and seaward slopes of the Japan Trench off Sanriku, northeastern Honshu, Japan during the R. V. Hakuho Maru Cruise KH-90-1.

Specifications and Operations of the System

The underwater vehicle of the DESMOS is composed of a stereo-pair of color TVs, a pair of stereo still cameras (up to 1,700 frames using 35mm, 100-foot long ASA400 strip films), CTD (Sea-Bird Electronics, Inc.: Model SBE 9/11, modified by Tsurumi Seiki Co. Ltd.), 6-bottle rosette water sampler (Niskin-type; 1.5 liter each) and a releasing clamp beside auxiliary instruments such as an acoustic altimeter, an inclinometer, an acoustic transponder and a pendulum suspended from the frame of the vehicle. Images illuminated by four 300 watt halogen lamps and measurement signals are transmitted to the shipboard console *via* 6,000 m long, 14.4 mm ϕ composite armored cable (consisting of 6 optical fibers, 4 signal wires and 6 power chords).

Taking photographs, water sampling and releasing of any kinds of instruments (such as miniature dredge) are controlled by the operators based on the real-time information displayed on shipboard monitors. Vertical and horizontal CTD profiles were monitored on CRT, X-Y plotter and printer. Horizontal mode of the CTD profile is specially designed for the quick discrimination of thermal anomalies on analog graphics. Video images and essential LAN data are displayed on two monitor TVs and recorded on S-VHS cassettes together with voice comments of the observers. The vehicle is not equipped with thrusters, simply hung on a tethered cable and maneuvered by up-down winch operations and surface ship's joy-stick dynamic positioning system.

A pendulum weight suspended by 250 cm thread (250 cm in the case of Stn 01 and 02, 230 cm in the other stations) served as a distance cue for winch operation and dimensioning of the objects. When the tip of the chain touched the bottom, rough estimation of the frame coverage was 2 by 2.5 m on the

bottom, as, in most cases, cameras were set perpendicular to the bottom and zooming was set as wide as possible. Strict stereo-photogrammetrical analysis and dimensioning and identification of photographed objects will be carried out in a laboratory on land.

Note that the depth figures superimposed on video monitor was fed from Seabeam *via* LAN, and the time in GMT. True vehicle depth was recorded continuously on CTD graphic and floppy data.

Tracks of the underwater vehicle together with the surface ship were fixed and guided by means of a SSBL (super-short-baseline) acoustic transponder subnavigation system (OKI Electronic Industry Co., Ltd.).

CTD measurements did not work well due to oscillation in some circuit board during this cruise.

The system was operated at 6 survey points (Stations 01, 02, 03, 04, 05 and 06) and the preliminary observations were briefly summarized in the following.

Brief Resume of the Video Observations

Station 01

Location; SW flank of Bosei (Mizunagidori) Seamount, E off Cape Shioya-saki 37°06.59'N: 145°16.87'E (3,040 m) ~ 37°05.79'N: 145°17.11'E (3,340 m)

Date and time of operation; June 28, 1990, 12:36-17:07 [JST]

Duration of bottom observations; 02:31-05:11, June 28, 1990 [GMT]

Depth range of bottom observations; 2,970 ~ 3,340 m [Seabeam]

Typical scenery: The top and SW flank of the Iwaki Seamount were fundamentally outcropping rocks covered only slightly with coarse sandy sediments. Most of the bare rock surface, angular cobbles and pebbles (most of them are cemented to very flat substratum) were darkly encrusted with probably Mn and iron hydro-oxides. Sometimes the texture of the rock surface resembles that of lapilli tuff. However, occasional white stones must be apatite. The scenery can be interpreted to be an ancient coral reef flat.

Biota: Large organisms observed frequently were red shrimps (*Nematocarcinus* sp.), *Antedon*-type sea-ferns, ophiuroids (*Ophiacantha normani* on the rocks and *Ophiura bathybia* on the sediment, *Asteronyx loveni* on slender biogenic sticks), cerianthid sea anemones, brotulid and macrourid fishes, deimatid (red and white ones) and paelopatid holothurians in the order of abundance. Other

organisms observed were squat lobsters (*Munidopsis* sp.), *Euplectella*-type hyaline sponges, zoroasterid and porcellanasterid asteroids, and antipathalian corals.

General remarks: The towing was the first full-scale operation of the DESMOS at the deep-sea, and was devoted mainly to master the operation. Bottom water movement must be rather strong, as was suggested by the erosive bottom feature and the dominance of filter-feeders. Biomass is not high, but not very poor.

Station 02

Location;Top of the Iwaki Seamount, E off Cape Shioya-saki
36°53.80'N: 144°51.39'E (1,735 m) ~ 36°51.33'N:144°48.59'E (1,788 m)
Date and and time of operation; June 28, 1990, 10:36-16:12 [JST]
Duration of bottom observations; 02:27-06:39, June 28, 1990 [GMT]
Depth range of bottom observations; 1,735 ~ 1,790 m [Seabeam]

Typical scenery : The top of the Iwaki Seamount was also covered only slightly with sandy sediments. The bottom was almost flat plane suggesting cementation of the original coral reef flat. Boulders reminiscent of coral blocks, microatoll and algal balls were encrusted with black coating of (probably) Mn-Fe hydro-oxides. Occasional pot holes suggest wave action in the shallow environment. The thin cover of sediments may consist of foraminiferan tests, and bioturbation has left whitish lebensspuren on the sediment surface.

Biota: Dominant organisms are long-legged shrimp *Nematocarcinus* sp., stone crab *Paralomis* sp., ophiacanthid ophiuroids, asteroid *Zoroaster* sp., echinothuriid echinoid *Hyglosoma hoplacantha* and deimatid holothurians such as *Ellipinion* sp. Large motile fishes like *Coryphaenoides acrolepis, Coryphaenoides longifilis, Aldrovandia affinis* were encountered frequently.

General remarks: To say nothing of the bottom characteristics, the composition of the fauna support that the water movement is rather strong and the bottom environment is erosive. Biomass is not high, but not very poor. The station (as in the preceding station) is located seaward of the Japan Trench. Nevertheless, the surface production seems to be rather rich owing to the neighborhood to the landmass and possible upwelling due to the bottom configuration.

Station 03

Location; Landward flank of the Japan Trench E off Kamaishi
39°19.98'N: 143°46.67'E (4,084 m) ~ 39°21.55'N: 143°47.22'E (4,058 m)
Date and time of operation; June 30, 1990; 13:03-19:28 [JST]
Duration of bottom observations;05:36-09:24, June 27, 1990 [GMT]
Depth range of bottom observations; 4,060 ~ 4,085 m [Seabeam]

Typical scenery: The bottom of this station consists fundamentally of flat sedimentary rock covered by relatively thin, say 10cm thick, coarse grayish brown silty sand smoothed by gentle bottom current. Many seemingly free-living sea anemones which must fasten themselves to hard substratum support this view. Sometimes slabs and boulders of sedimentary rocks are scattered on the sea floor. Sediment just beneath the surface is whitish. Occasional outcropping of small benches and cliffs from 10cm to 5m in altitude were trending NE-SW.

Biota: Biomass is rather high. Many suspension feeders such as simple corals, sea anemones (*Liponema multicornis, Actinoscyphia saginata, Branchiocerianthus imperator* and *cerianthid anemones*), sea pens (*Kophobelemnon stelliferum, Umbellula thomsoni* and *U. magniflora*), gorgonians (*Radicipes* sp. and *Bathypathes* sp.) predominated. Stalked tunicates *Culeolus* sp. and crinoid *Bathycrinus* are also included in this category. Organic detritus feeders are also abundant; most of them are holothurians (*Elpidia longicirrata, Peniagone spp., Pseudostichopus* sp., *Benthodytes typica, Scotoplanes globosa* and *Enypniastes* sp.). Other echinoderm members are spatangoids (probably Pourtalesiidae), asteroids (*Eremicaster crassus, Dytaster* sp.). Free living organisms are amphipods and isopods, shrimps (*Hepomadus glacialis, Sclerocrangon zenkevitchi), Munidopsis* sp. and large fishes such as *Coryphaenoides armatus, C. yaquinae, Histiobranchus bathybius* and slender brotulids. The occurrence of huge octopod *Vampyroteuthis* infernalis is noteworthy.

General remarks: The biomass and species richness of this station are one order of magnitude higher than the preceding stations which are located seaward of the Japan Trench. Rather thin coarse silty sediment of this station suggest the sediment movement along the slope toward the Japan Trench. The high

biomass and species richness are sustained by high surface productivity and the bottom-bound transport of nourishment. White granules around small benches and boulders suggest former seepage.

Station 04

Location; Mud diapir on the outer swell of the Japan Trench, E off Ofunato
38°46.22'N: 145°40.84'E (5,275 m) ~ 38°44.60'N: 145°42.13'E (5,275 m)
Date and time of operation; July 05, 1990, 11:51-19:53 [JST]
Duration of bottom observations; 04:35 - 09:15, July 5, 1990 [GMT]
Depth range of bottom observation; 5,275 ~ 5,275 m [Seabeam]

Typical scenery: General feature of the station was very flat bottom blanketed with grayish brown silt and, as can be expected, the silt was not sticky. Week bottom water movement from south to north was observed at the time of observations.

At the top of the mud diapir rocks, dark-colored boulders, cobbles and pebbles were scatted, and many gorgonians were sitting on the hard substratum.

Biota: Considering that the station is situated seaward of the Japan Trench and its depth is around 5,300 m, rather low biomass seems natural. In contrast to such an expectation the diversity of representative megabenthic organisms is very high. Animal frequently observed are listed below in taxonomic order.

Protozoa: Xenophyophores
Coelenterata: simple corals, *Kophobelemnon stelliferum, Umbellula* spp.
Macrura: *Plesiopenaeus* sp. and/or *Hepomadus glacialis*
Mollusca: *Neptunea*-type gastropod, *Vampyroteuthis infernalis*
Crinoidea: *Bathycrinus* sp.
Ophiuroidea: *Ophiura bathybia, Ophiacantha* sp. (clinging)
Asteroidea: *Styracaster* and/or *Dytaster* sp., 6-armed asteroids
Echinoidea: *Kamptosoma asterias,* tracks of spatangoids were observed frequently.
Holothurioidea: *Scotoplanes globosa, Psychropotes longicauda,*
Peniagone spp., *Benthodytes* sp., *Pseudostichopus* sp.,
Enypniastes sp.
Pisces: *Coryphaenoides yaquinae* and rarely *C. armatus*

General remarks: This station was planned to observe a mud diapir on the outer swell of the Japan Trench, which was realized at the end of the seismic reflection track (Chapt. 6 of this report). The present observation indicated that diapirism must be rather old.

Station 05

Location: Steep landward slope of the Japan Trench, E off Kinkasan
Date: July 07, 1990; 12:31-14:32 [JST]; depth range ca. 3,890 ~ 4,070 m

General remarks: Bottom observation was abandoned midway of the operation due to system trouble.

Station 06

Location; Landward flank of the Japan Trench, E off Kinkasan
38°05.04'N: 143°42.68'E (5,335 m) ~ 38°05.36'N: 143°43.75'E (5,486 m)
Date and time of operation; July 08, 1990; 10:27-16:53 [JST]
Bottom observations; 03:08-05:21, July 8, 1990 [GMT]
Depth range of bottom observations: 5,335 ~ 5,510 m [Seabeam]

Typical scenery: Almost flat bottom. Sediment is greenish-gray-brown in color, well oxidized and smoothed by bottom current. As a whole, the sedimentation environment is depositional and the bottom was studded with the fecal knots of many holothurians.

Biota: The observation track can be divided into two slightly different habitats from the biological point of view. The anterior half of the track was dominated by a slender but long echiuran worm *Jacobia birsteini*, and the posterior half was dominated by tubicolous polychaetes. The following biota were found common in both zones.

Coelenterata: simple corals and *Umbellula thomsoni*
anemones on the stalk of hyaline sponges
Isopoda: *Storthyngula* [facing windward: 270°]
Amphipoda: *Epimeria*-type
Anomura: *Munidopsis* sp.
Crinoidea: *Bathycrinus* sp.
Ophiuroidea: *Ophiura bathybia, Ophiacantha bathybia* [clinging],
Amphiophiura convexa, Amphiura patens

Asteroidea: *Styracaster* sp., *Dytaster* sp.
Echinoidea: *Kamptosoma asterias, Echinus* sp.
lebensspuren of spatangoids probably made by *Echinocrepis* sp.
Holothurioidea: *Peniagone azorica, Psychropotes longicauda, Peniagone* sp., *Benthodytes typica, Scotoplanes globosa, Hadalothuria* sp., *Elpidia longicirrata* and *Pseudostichopus* sp.
Pisces: *Coryphaenoides yaquinae*
Xenophyophore and lophenteropneusts were also observed leaving behind the characteristic meandering fecal coils.

General remarks: This station was established to see the land slide at the foot of the landward wall of the Japan Trench.

No positive evidence for recent land slide and frequent turbidity disturbance was observed. No indication of recent seepage was found along the observation track.

The biomass of this station is very high, roughly estimated to be in the order of $10g/m^2$. Surface organic production and downslope transport of food material to the spot must be high.

Data Storage and Inquiries

S. Ohta (ORI) is responsible for the storage of the original video and film records as well as the DESMOS-CTD data on graphic charts and floppy disks, event records and subnavigation records on floppy disks. The chief scientist of the cruise, K. Kobayashi is in charge of distribution and publicity of those data based on the full set of suboriginal copies at his hand.

12. Results of 3.5 kHz Subbottom Profiling

C. Igarashi

12. 1 3.5kHz Subbottom Profiling System on board the R. V. Hakuho Maru

The 3.5kHz Subbottom profiling system (SBP) on board the R. V. Hakuho Maru has a capability of surveying sedimentary characters and geological structure of the lithosphere from the bottom surface to a depth of nearly 120 m below the seafloor. The maximum survayable water depth range is 10,000m, and profiling survey is possible up to the normal cruising speeds of 15~17 knots.

The record of the 3.5kHz subbottom profiling system is clear with high resolution power compared to the normal seismic survey methods such as air-gun and water-gun systems, because of high frequency acoustic signal. So this system is fundamentally important not only for the surface layer structure study, but also for sampling procedure like piston coring and dredge hauls and for preliminary research before setting up the sea-floor stations as OBS.

The fundamental equipments of this system are composed of "LSR-1807M, CESP III, PTR-105B and Transceiver Units" of 3.5kHz SBP system produced by OCEAN DATA EQUIPMENT CORP.(USA). Onboard equipments such as main recording units and processing units are installed in the No.3 Laboratory. Sub-recording units are set at the stern control room. The transmitting and receiving units are installed in the bow acoustic dome of the ship.

Brief explanations concerning functions of principal components constituting this system are noted in the followings, and the block diagram of main onboard equipments is shown in Fig. 12-1.

(a) A Line Scan Recorder "LSR-1807M" is installed with processing and memory units and controls the signal interval and recording width.

(b) A Correlation Echo Sounder Processor "CESP III" improves S/N ratio 20dB by means of correlation processing of transmitting signals and receiving signals.

(c) A Solid State Sonar Transceiver "PTR-105B" amplifies the transmitting and receiving signals. The maximum transmitting signal power is 2,000 watts.

(d) The real time navigation data can be input to the LSR recorder through "on board LAN Systems" with an annotation generator by IMAGE AND MEASUREMENT INC. So LSR recorder is able to control the recording chart speed according to the ship's navigation speed. This system is controlled by personal computer, NEC PC9801-CV21. The annotation output record is shown in Fig. 12-2.

(e) The data recording-replaying units are constructed with RP-880 PCM Data Recorder and BR-6200 VTR Recorder. This system is equipped with "Record/ Replay Switch Panel" and is able to change recording-replaying mode by one-touch switch. These are designed by TOYO CORP.
(f) The transmitting-receiving equipment (Transceiver) of 3.5kHz SBP is "TR-109" installed in the bow acoustic dome, and constituted with 12 transceiver units arranged in 3*4.
(g) This 3.5kHz SBP system is also equipped with an inteference eliminating equipment between the Multi-narrow-beam echo sounder (Seabeam) by delaying of signal transmitting of 3.5kHz SBP System according to the transmission signal control trigger from Seabeam System.
Specification of the 3.5kHz Subbottom Profiler in the Hakuho Maru is as follows;

3.5kHz Subbottom Profiler
signal frequency : 3.5kHz
transmitting power : 2,000 watts, 0-30 dB (6dB step)
maximum survey depth: 10,000 m
research ability : 30~100 m under seafloor
resolution: about 30 cm

PCM Data Recorder
channels : 2ch
frequency width: DC-10kHz
VTR modes: standard

12. 2 Operation of 3.5kHz Subbottom Profiling in the Cruise KH-90-1

3.5kHz Subbottom Profiling was carried throughout the whole period of Leg 2 in the Cruise KH-90-1, except for a short interruption at the time of acoustic interference test between 3.5kHz SBP and side scan sonar "IZANAGI". Consequently surface layer profiling records of sea floor with excellent quality were obtained in the"Pacific-Izu-Bonin Trench Arc Transect Area " as shown in Ch. 19.

The 3.5kHz Profiling in the cruise was performed by recording condition shown below in the normal cruising speed and water depth deeper than 1,000 m.

LSR record width :1,000 m (1.33 sec/scan), record density : 120 lines/inch
PTR transducer output power : 0 or -6 dB

A recording width of 2,000 m (2.67 sec/scan) was selected in some particular cases such as drifting state at a station.

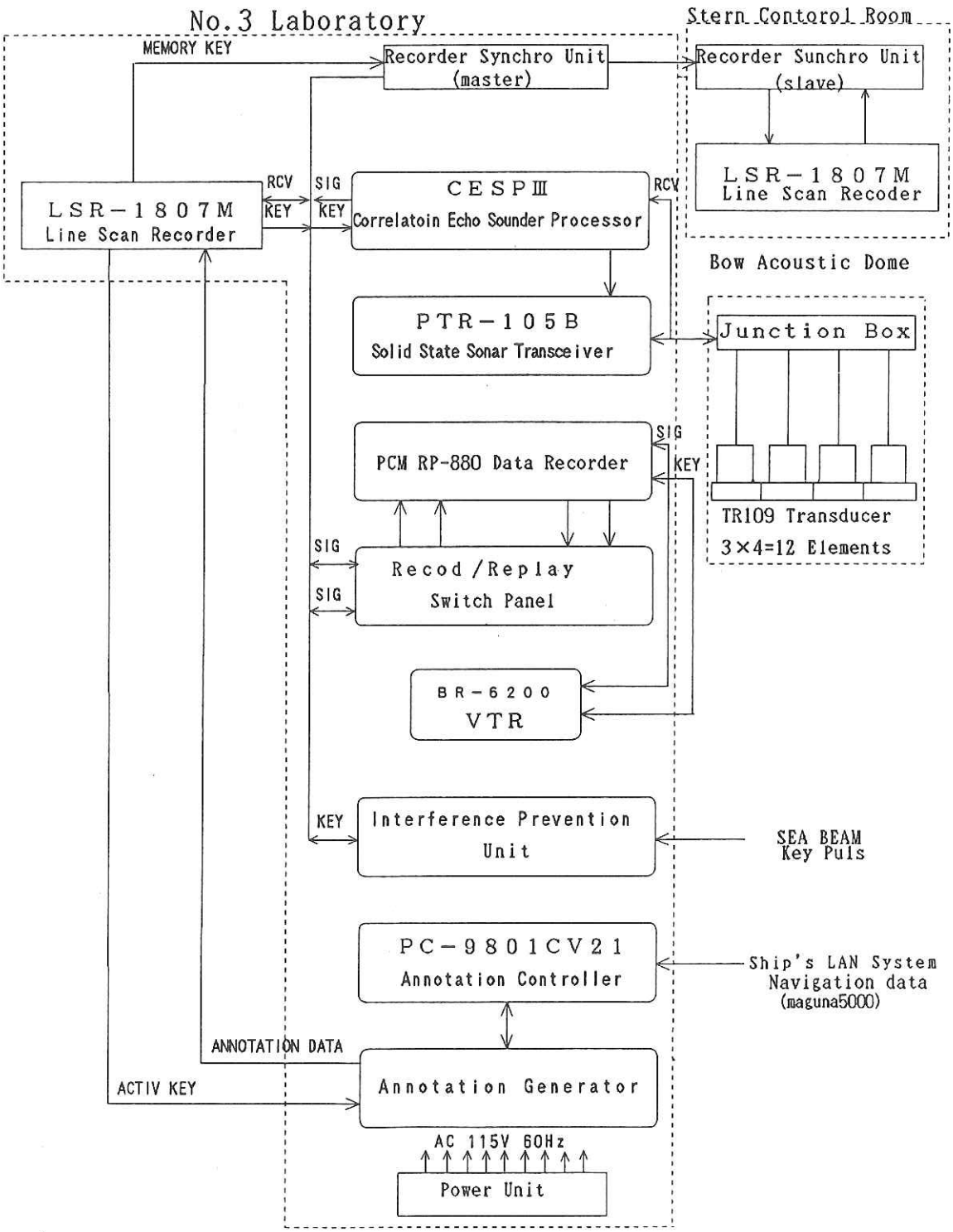

Fig. 12-1 Block diagram of onboard equipments for 3.5 kHz subbottom profiling.

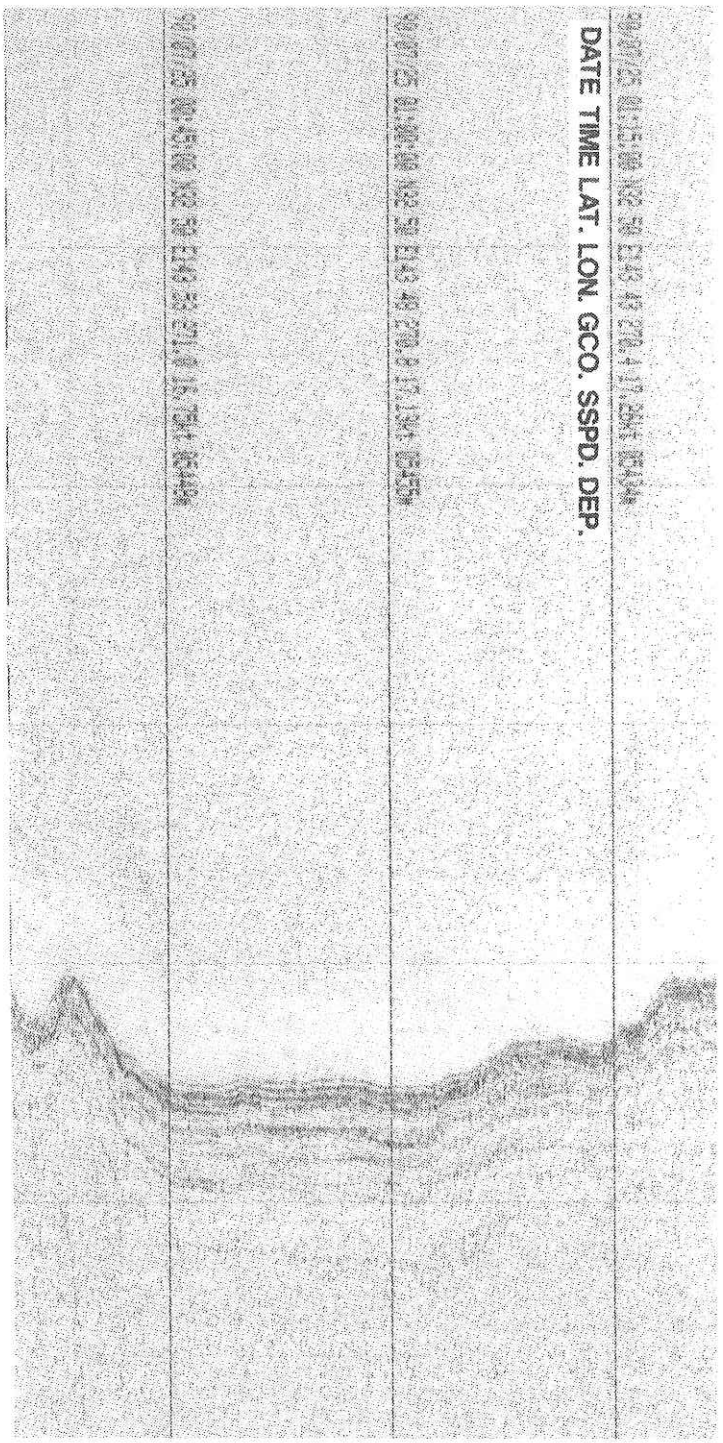

Fig. 12-2 An example of outputs from the 3.5 kHz recorder with annotation generator.

13. Seismic Refraction Experiment in the Fore-Arc Basin, Bonin Arc

S. Abe M. Shinohara, N.Takahashi, T.Amishiki, N.Hirata and K. Suyehiro

We carried out a seismic refraction study simultaneously with a seismic reflection profiling [1] during July 23-24, 1990 in the fore-arc basin of the Bonin Arc. The fore-arc basin shows a morphology similar to the northern extension of the Bonin Trough where a detailed refraction survey was made during the DELP cruise in 1987 [2].

Three ocean bottom seismographs (OBS's) were deployed every 15 n.m. along the same line as the multi-channel seismic reflection profile. Table 13-1 represents the positions of the deployed OBS's. The total length of the seismic reflection profile was about 360 n.m. The intended seismic refraction profile was about 70 n.m. long. The area of the seismic refraction survey is shown in Fig. 13-1.

Table 13-1 Detailed positions of the deployed OBS

	Location		
OBS	Latitude (N)	Longitude (E)	Depth (m)
OBS-1	32° 47.07'	140° 42.08'	2,009
OBS-2	32° 47.02'	141° 00.23'	2,490
OBS-3	32° 47.05'	141° 18.37'	2,918

An array of five waterguns was used as a controlled sound signal source. The guns were shot with an interval of 50 m. The shot was positioned and controlled by the R. V. Hakuho-Maru navigation system.

We used OBS's developed at Chiba University (Fig. 13-2). The OBS's are equipped with a vertical component and two horizontal component geophones. The characteristics of the instrument are described in Matsuda [3]. Two OBS's were recovered during the cruise after the experiment. Because of the acoustic releaser system trouble, we lost OBS-2.

All the analog data were converted into digital format. These data are processed for analysis. Shot times, necessary for producing seismic records, are obtained from log tapes of the navigation system together with navigation data for every shot. We will analyze the refraction data in both the time-distance and tau-p domains and a two-dimensional ray tracing forward modeling of the seismic wave field.

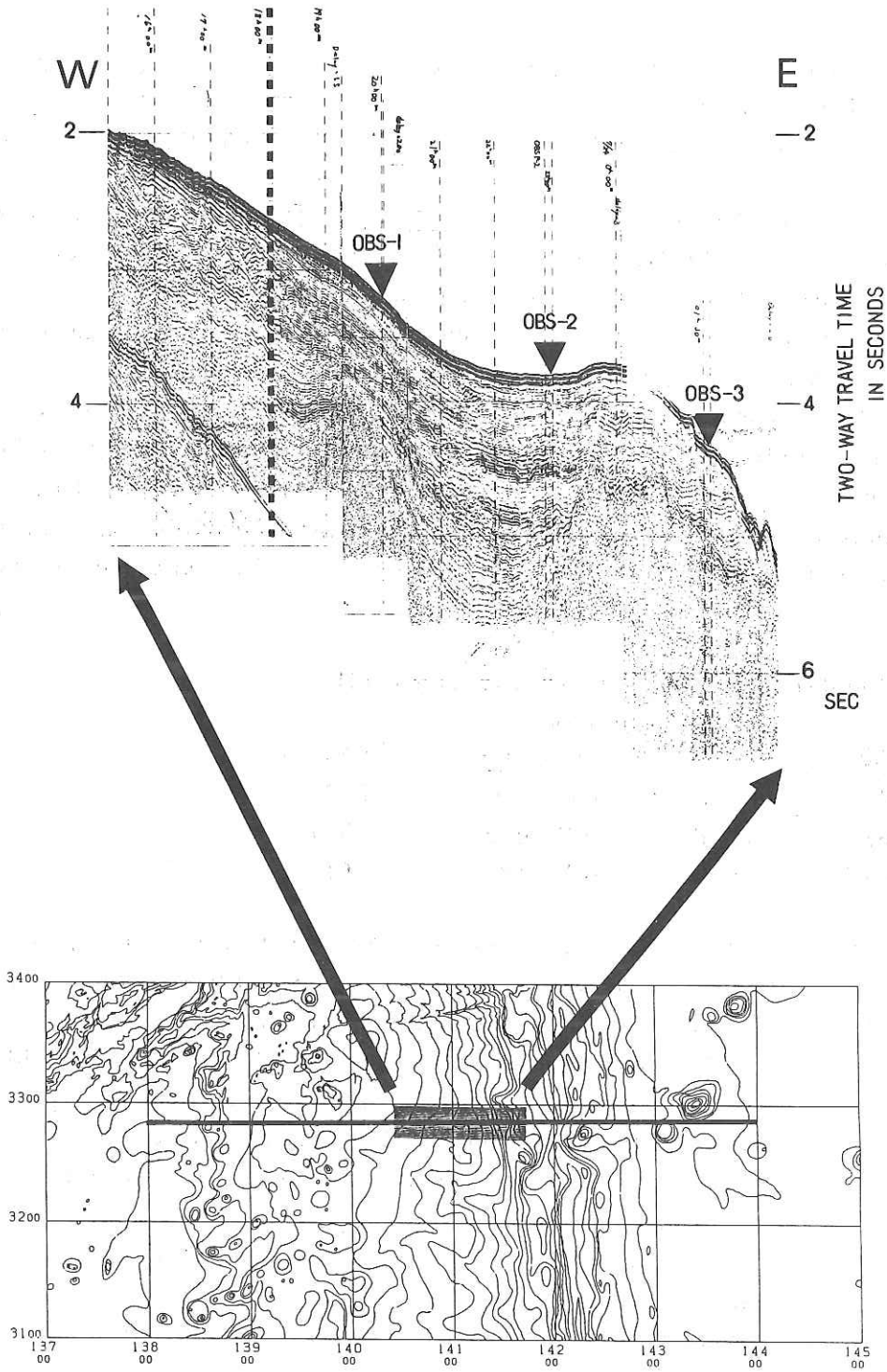

Fig.13-1 [above] Onboard near trace monitor record shown with OBS positions.
[below] Multichannel seismic reflection survey line (thick line) and refraction survey area (in a rectangular shaded zone).

References

[1] K. Suyehiro, C. Igarashi, Y. Jagadhiharja, M. Okada, and H. Nanbu, Multichannel seismic reflection profiling, 10-2 in this report, 1991

[2] S Abe, H. Tokuyama, S. Kuramoto, K. Suyehiro, A. Nishizawa and H. Kinoshita, Report on DELP 1987 cruises in the Ogasawara area Part II: Seismic reflection studies in the Ogasawara Trough, *Bull. Earthq. Res. Inst.*, **64**, 133-147.1989

[3] N. Matsuda, A pop-up type ocean bottom seismograph for the study of crustal structures, B. Sc. Thesis, Chiba Univ. (in Japanese).1986

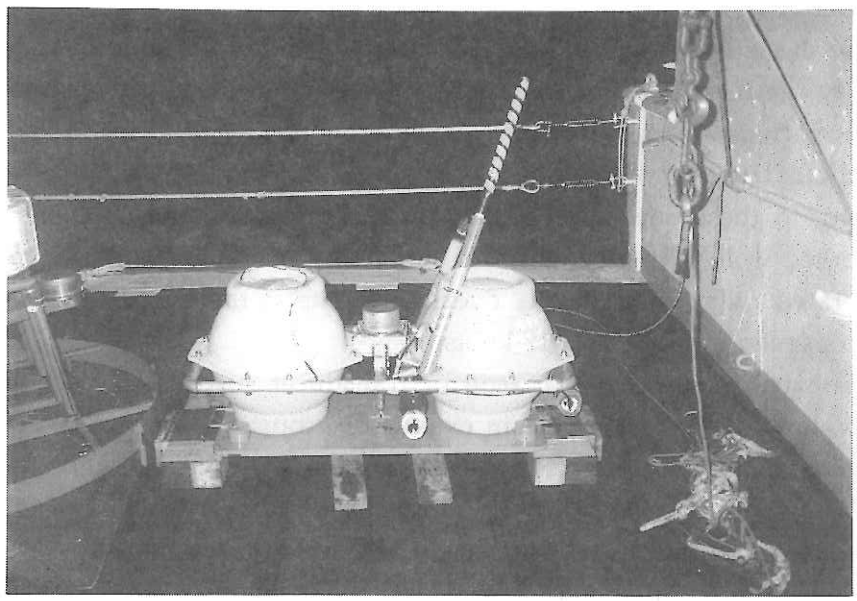

Fig. 13-2. Chiba University type OBS. The instruments are housed in the left side glass sphere. A flasher and a transmitter are attached on the right side glass sphere. Weight is an iron plate at the bottom. Acoustic releaser system is in the middle.

14. Measurement of Underwater Acoustic Noise Levels Around the Hakuho Maru

H. Fujimoto, M. Nakanishi, T. Fujiwara and T. Furuta

Ambient acoustic noise levels around the Hakuho Maru were measured in order to estimate the effect of countermeasures adopted for the ship to reduce acoustic noises emitted from the ship. The noise level was compared with that of the old Hakuho Maru, which was constructed in 1967 with all possible noise reduction techniques at that time.

The Hakuho Maru is equipped with several acoustic systems, such as Sea Beam system, SSBL acoustic transponder system, Acoustic Biomass Investigation System, PDR, 3.5 kHz sub-bottom profiler. Experiments of underwater acoustic data transmission have also been carried out. These instruments require quite low underwater acoustic noises around the ship. Therefore, reduction of the acoustic noises was one of principal items to design and build the ship. According to the results of computer simulation and several experiments, low noise diesel engines were adopted, and the beds of the engines were double resistently mounted on the frame. Bow thrusters were newly developed. In addition, various countermeasures to vibration and noise are installed around principal auxiliaries and pipings.

Owing to these countermeasures, all the under-hull acoustic instruments have worked well with sufficient S/N ratio. For example, the Sea Beam system was operated fully automatically over the nights at the water depth of 9200m and ship's speed of more than 17 knots.

Some experiments using an acoustic transducer suspended from the working deck, however, showed certain extents of acoustic noises. The noise level was nearly equal or a little bit higher than that of the old Hakuho Maru. The noise was estimated to be relatively narrow-banded, because the noise could be easily reduced by a porous acoustic absorber around the transducer.

Engineers from Mitsubishi Heavy Industries, shipbuilder of the Hakuho Maru, detected the source of the acoustic noise during the cruise KH-89-2. They found that the noise was caused by the motion of the oil which controlled the pitch angle of the propellers. When the blades of the propellers were mechanically latched, the oil did not move and the noise disappeared.

Underwater acoustic noise level around the Hakuho Maru were measured during the cruise KH-90-1. The measurement was carried out by using the onboard unit of the LBL (long baseline) acoustic transponder system, which have

been used these several years. Because many experiments were carried out on board the old Hakuho Maru by using the system, we can estimate the underwater acoustic noise level around the Hakuho Maru compared with that of the old Hakuho Maru.

Noise levels at frequencies around 9 kHz were measured by acoustic transducers suspended from the working deck at the starboard side of the after control room. Noise levels around 13 kHz were also measured by using the onboard unit of the new LBL system for the Hakuho Maru. The measurements were carried out in six conditions according to the state of the oil circuit for pitch angle control (active at the pitch angle 26.5° or inactive with pitch angle latched at 35°) and the state of rotation of the propellers in electric propulsive mode (-40, 0, or +35 rpm). Ship's heading was kept to be 240° by using the bow thrusters. Stern thruster remained stopped. Sea state was two to three.

Table 14-1 shows a part of the results measured at the check point of the LBL acoustic transponder system. Considering from the observed data, the underwater acoustic noise level around the Hakuho Maru is higher by a factor of 1.5 to 2 than that of the old Hakuho Maru when the pitch angle of the blades is actively controlled. When the blades are mechanically latched at the angle of 35°, however, the acoustic noises are reduced to one part of 10 to 30. Although the pitch angle of 35° was not planned for actual operation when the propeller was designed, there is no cavitation at the angle. Several experiments show that it has no problem to operate the ship in this condition at normal sea state. These experiments shows that it has become possible to perform quite sensitive acoustic experiments on board the Hakuho Maru with S/N ratio about ten times better than realized so far.

These measurements were carried out with co-operation of the officers and engineers of the Hakuho Maru. We owed much to advices both from the chief scientist Prof. K. Kobayashi and from the acting captain Y. Jinno. We wish to express our sincere thanks to them.

Table 14-1 Acoustic noise levels measured around the Hakuho Maru.
Voltage at the check point of the transponder systems is shown in unit of both Volt and dB. 1 Volt is assumed to be 0 dB and approximately equal to the threshold level of input signal. Frequencies of channel A, B, C, and D are 8.621, 9.091, 9.615, and 10.204 kHz, respectively. Frequencies of channel 1, 2, and 3 of the new LBL system are 12.295, 12.712, and 13.158 kHz. S and G show selection of the gain control of each system.

	Active (Pitch angle 26.5°)				Inactive (Pitch angle 35°)				
				0 rpm					
ch.	A	B	C	D	ch.	A	B	C	D
G=3	2.5 (+14dB)	3.0 (+15.5dB)	3.2 (+16.1dB)	2.0 (+12dB)	G=3	0.15 (-10.5dB)	0.2 (-8dB)	0.15 (-10.5dB)	<0.1 (-14dB以下)
G=4	4.0 (+15dB)	3.0 (+12.5dB)	3.5 (+13.9dB)	2.0 (+9dB)					
					G=5	0.4 (-8dB)	0.3 (-10.5dB)	0.4 (-8dB)	0.2 (-14dB)
				-40 rpm					
G=3	2.5 (+14dB)	3.5 (+16.9dB)	3.5 (+16.9dB)	3.0 (+15.5dB)	G=3	1.0 (+6dB)	0.8 (+4.1dB)	0.6 (+1.6dB)	0.4 (-2.0dB)
G=4	3.0 (+12.5dB)	4.0 (+15dB)	3.0 (+12.5dB)	2.0 (+9dB)					
G=5	3.5 (+10.9dB)	4.5 (+13.1dB)	4.5 (+13.1dB)	3.5 (+10.9dB)	G=5	2.0 (+6dB)	1.5 (+3.5dB)	1.0 (0dB)	1.0 (0dB)
				+35 rpm					
G=3	2.0 (+12dB)	3.0 (+15.5dB)	4.0 (+18dB)	2.0 (+12dB)	G=3	0.2 (-8dB)	0.1 (-14dB)	0.1 (-14dB)	<0.1 (-14dB以下)
G=4	3.5 (+13.9dB)	2.5 (+11dB)	2.0 (+9dB)	3.5 (+13.9dB)					
G=5	3.5 (+10.9dB)	3.5 (+10.9dB)	3.0 (+9.5dB)	4.0 (+12dB)	G=5	0.4 (-8dB)	0.3 (-10.5dB)	0.3 (-10.5dB)	0.2 (-14dB)

	14kHz hydrophone (New Type)						
				0 rpm			
ch.	1	2	3		1	2	3
S=2	3.0 (+18dB)	2.4 (+16.1dB)	1.6 (+12.6dB)	S=2	0.2 (-5.5dB)	0.4 (+0.5dB)	<0.1 (-11.5dB以下)
S=5	3.8 (+11.6dB)	3.7 (+11.4dB)	3.9 (+11.8dB)	S=5	2.0 (+6dB)	1.4 (+2.9dB)	0.5 (-6dB)
S=8	4.2 (+8.2dB)	4.0 (+7.8dB)	4.0 (+7.8dB)	S=8	3.0 (+5.3dB)	2.5 (+3.7dB)	0.8 (-6.2dB)

15. Bottom Observation by IZANAGI Oceanfloor Imaging Sonar System

F. Yamamoto, H. Tokuyama, T. Ueki, K. Yorimitsu, H. Shane, R. Ng,
H. Matsuoka, M. Murayama, M. Okada, N. Ohkouchi, Y. S. Djajadihardja,
K. Suyehiro and A. Taira

IZANAGI system

IZANAGI oceanfloor imaging sonar system which was introduced to Ocean Research Institute, the University of Tokyo in 1989, is an 11/12 kHz towed instrumentation package optimized for computer controlled compilation of acoustic images of broad swaths of oceanfloor. In addition, the system has an unique capability of being able to measure the direction to an oceanfloor reflector. When the range and direction to a reflector are accurately determined these data can be converted to position and depth, so that the bathymetry can be calculated for the ensonified swath of oceanfloor. Thus, the IZANAGI system generates synoptic acoustic back scattering images and hydrographic-quality swath bathymetry charts simultaneously in real time mode.

General specifications of the IZANAGI system are as follows.

Operating frequency	:	11kHz (port), 12kHz (starboard)
Ping rate	:	1 to 29 seconds per ping
Tow depth	:	5 to 500 meters
Effective water depth	:	50 to 10000 meters
Operating speed	:	1 to 10 knots
Real-time image format	:	slant-range and speed corrected
Pixel size	:	50 cm to 20 meters
Beam width (along track)	:	2.0 degrees
Real-time bathymetry format	:	color encoded depth plots
Swath width of bathymetry	:	3.4 times altitude

The hardware system is divided into three basic components such as the IZANAGI towfish, towfish handling system and on-board electronics system. The IZANAGI towfish employs a transducer array (64 transducer elements on one side) that is towed at a shallow depth, typically 100 m below the surface. The towfish handling system is composed of the Launch/Recovery System (LRS), towing winch and cable, depressor and towfish stabilizing system, and emergency recovery system. The LRS designed for use with IZANAGI system is an electro-procedure of towfish is shown in Fig. 15-1. The onboard electronics system offers towfish control instrumentation and data acquisition subsystem and data logging subsystem to optical disk and preliminary data processing (Fig. 15-2) .

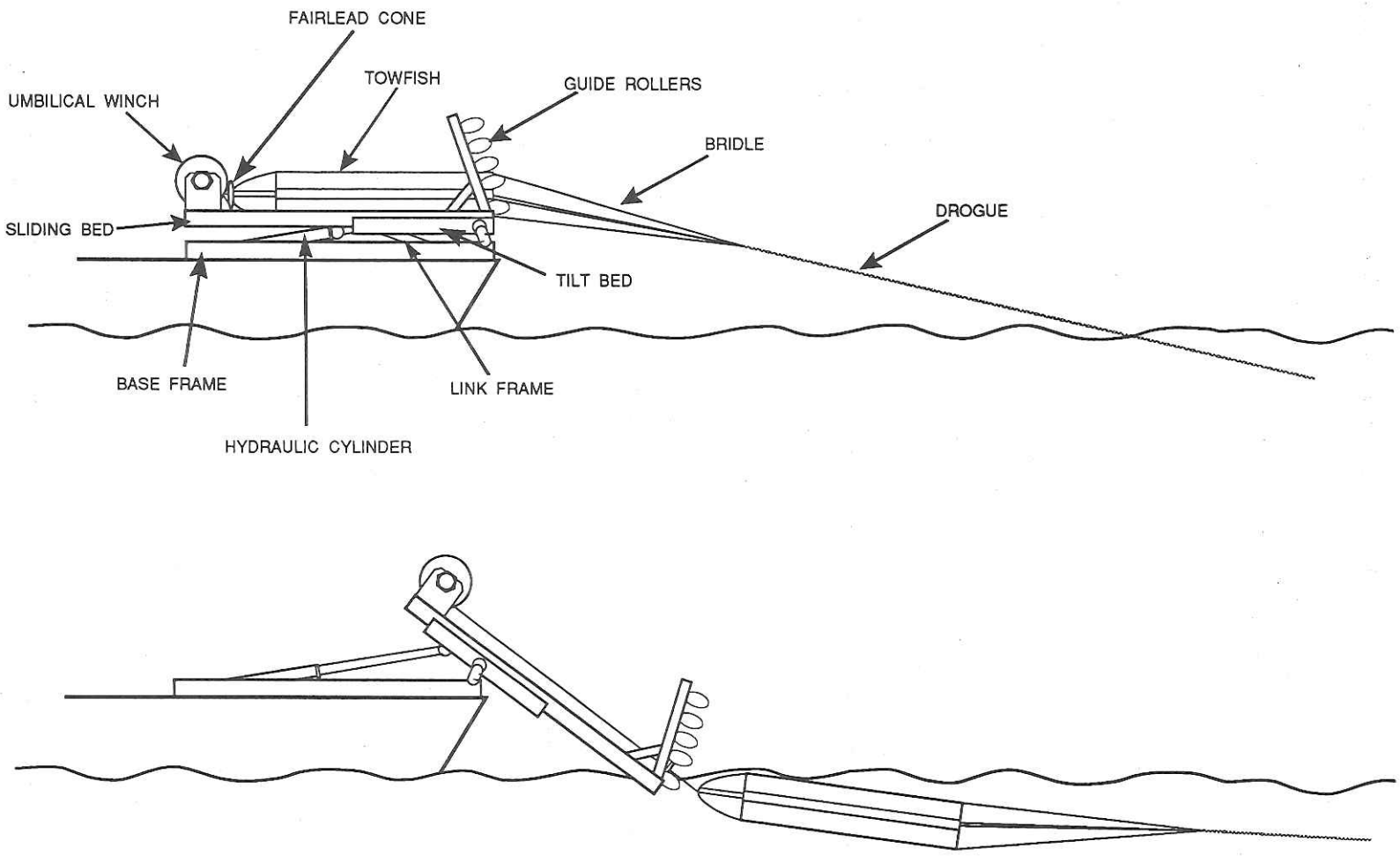

Fig. 15-1 IZANAGI towfish launching procedure.

The acoustic sensors are towed behind a depressor in a streamlined, passively stabilized, near neutrally buoyant vehicle. All side-scan data, fish attitude, depth, operator switch settings, and the echo angle vectors are recorded on optical disk for later processing on shore.

The IZANAGI back scattering images are composed of 1024 pixels on each side of the swath; thus for a 5-km swath each pixel represents the echo strength from a band at a constant width of 2.5 m. Monitor records of the side-scan data are produced on an EPC 8700 variable chart recorder, photographed, reduced in size, and assembled into a mosaic at sea. (IZANAGI plots strong reflectors as dark and shadows as light, so the images appear as negatives.)

Location of IZANAGI Survey

The expedition using the IZANAGI system during the KH-90-1 cruise Leg 2 was carried out at the Mikura Basin and Hachijo Depression south of Honshu, Japan (Fig. 15-3). Fig.15-4 shows the towing chart of IZANAGI system.

IZANAGI Back Scattering Image

Fig. 15-5 shows an onboard monitor record of IZANAGI back scattering image of 5 km swath width from the Mikura Basin. The data were acquired in less than 5 hours. The dimension of the Mikura Basin is approx. 60 km x 40 km. The basin is composed of flat floor and several seamounts such as Inanba Sima. Back scattering images' reveal that a flat floor is covered by soft sediments and slopes of seamounts expose igneous rocks such as lava flows (Fig. 15-5). A newly discovered structure is a lineament with a general trend of N30°~40°W recognized not only on the floor but also at a seamount. The seamount is split into two halves by the lineament. We interpret the lineament to be normal fault mainly because it is straight in spite of bottom morphology. The strike of normal faults is concordant with that of normal faults in the Sumisu Depression approx. 200 km south of the Mikura Basin [1]. Fig. 15-6 shows IZANAGI onboard image from the Hachijo depression. The depression located at west of the Hachijo-Shima represents N-S elongation. Many volcanic mounts and seamounts are recognized in the depression. The characteristic structure in the depression is a lineament which has similar trend as the Mikura Basin.

References

[1] G. Brown and B. Taylor, 1988, Sea-floor mapping of the Sumisu Rift, Izu-Ogasawara (Bonin) Island Arc, *Bull. Geol. Surv. Japan*, **39**, 23-38

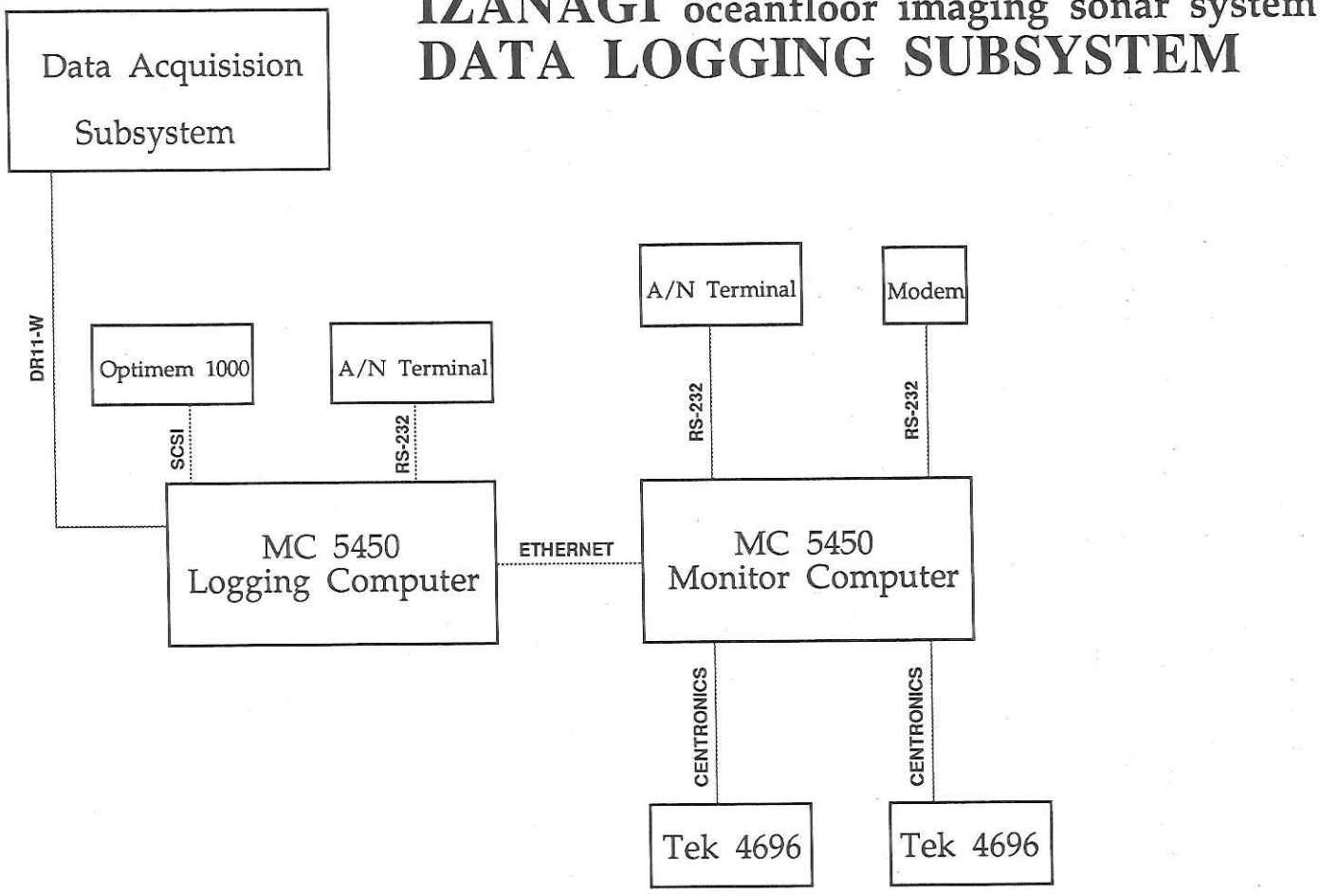

Fig. 15-2 Block diagram of the Data logging subsytem.

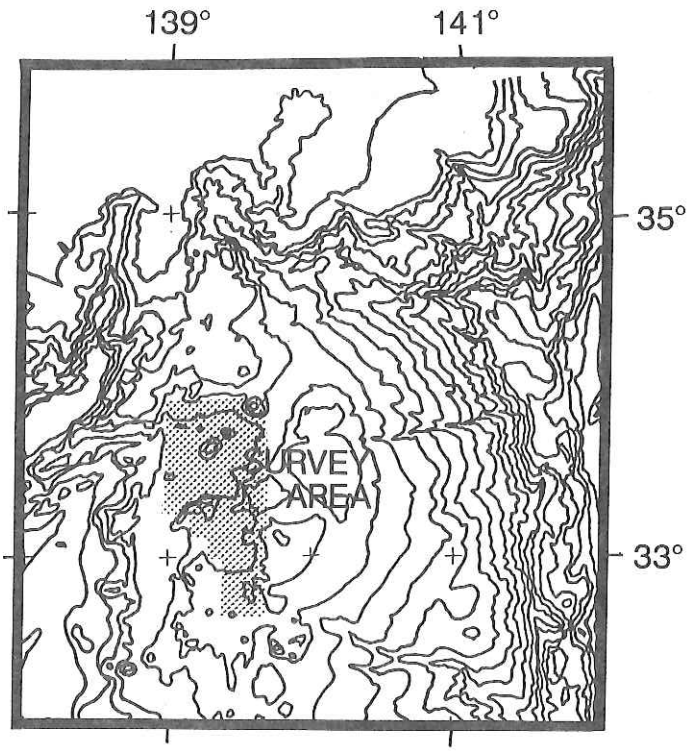

Fig. 15-3 Location of IZANAGI survey.

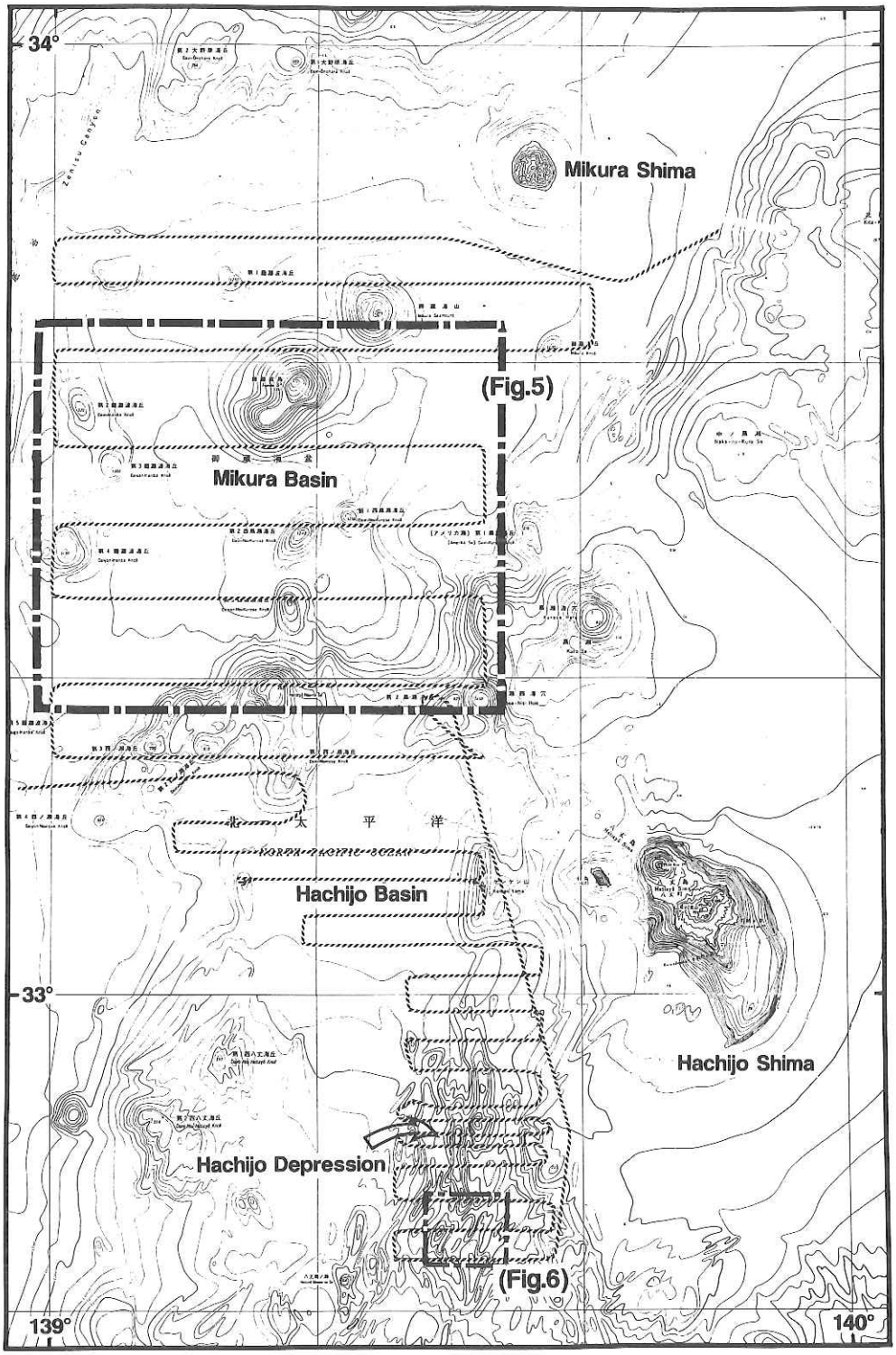

Fig. 15-4 Track chart of IZANAGI survey.

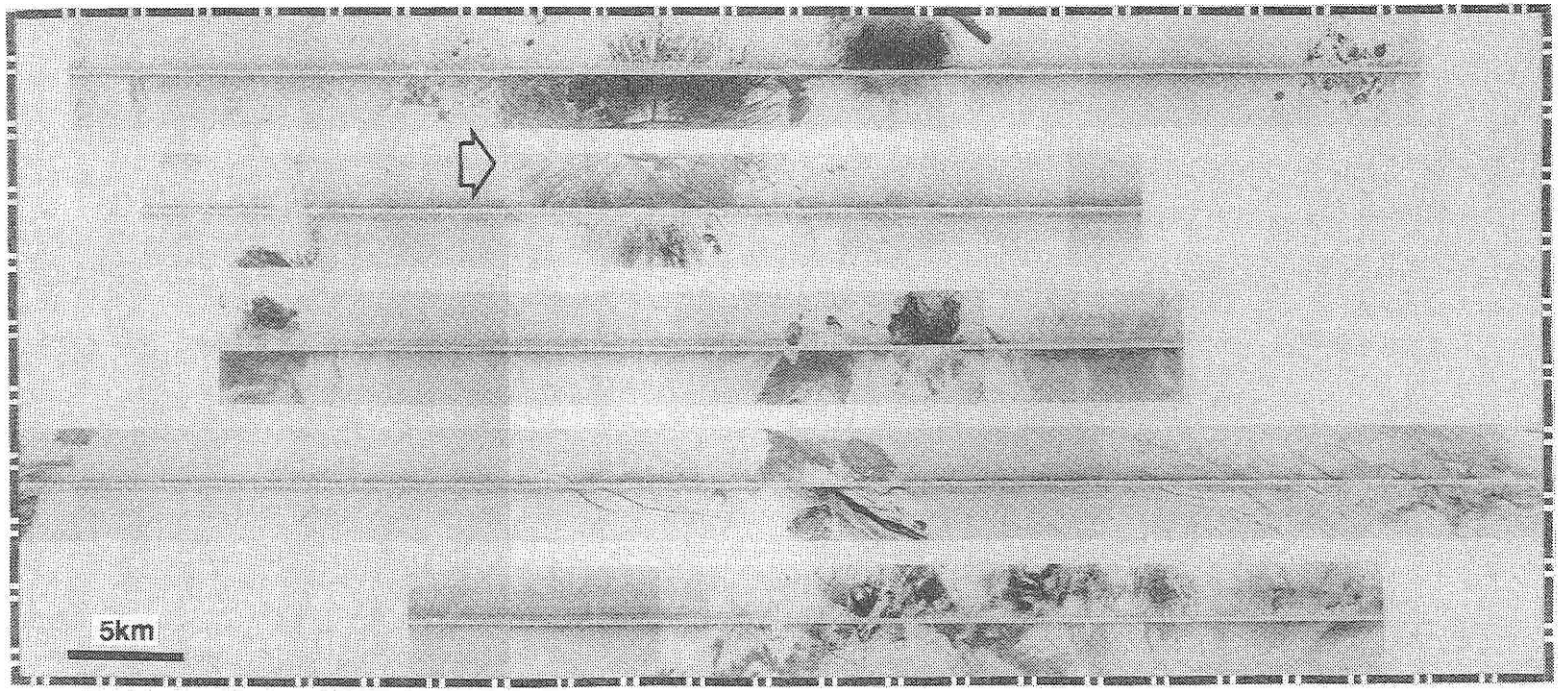

Fig. 15-5 Mikura Basin back scattering image.
Arrows shows exposure of igneous rocks.

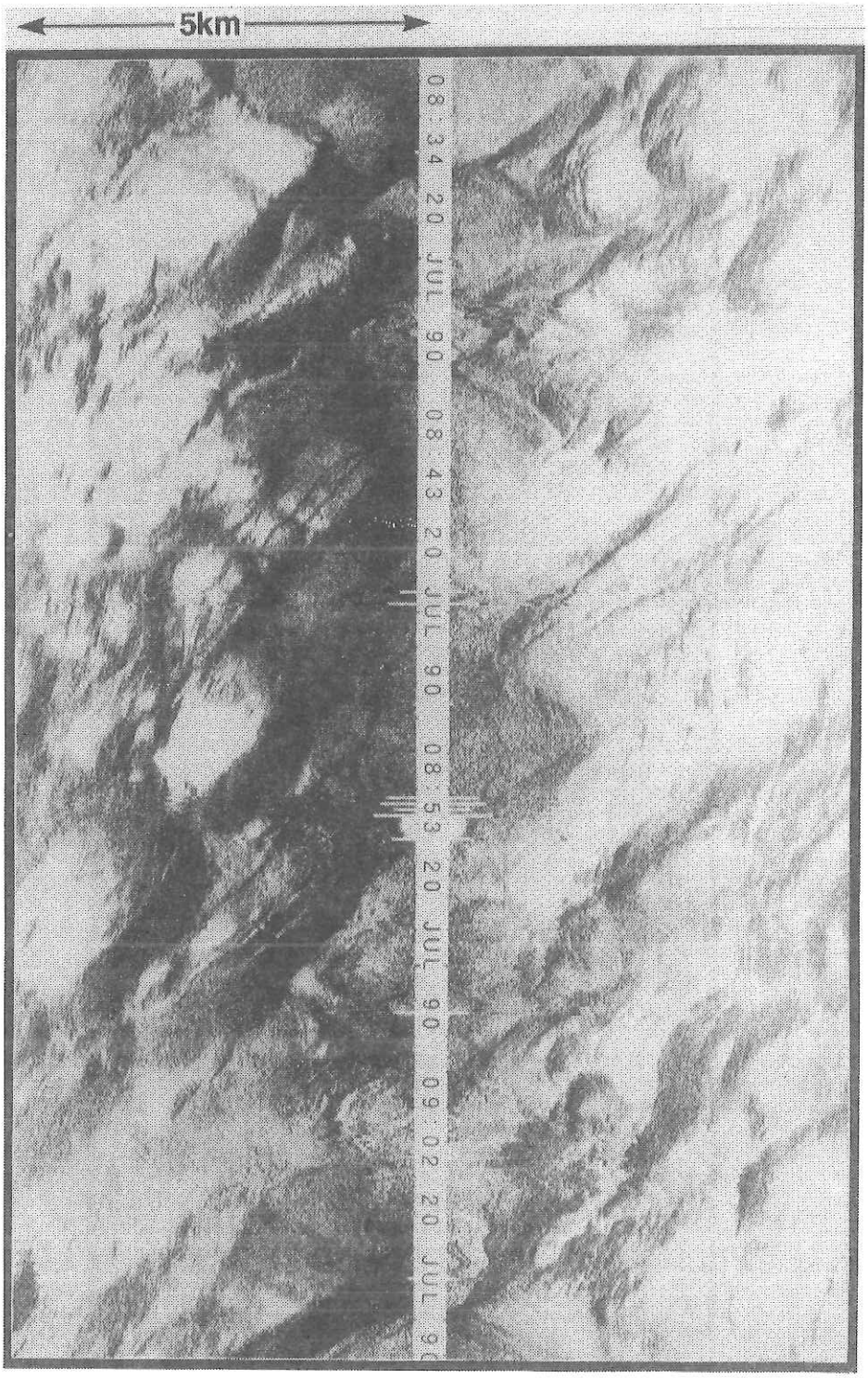

Fig. 15-6 Hachijo Depression back scattering image.

16. Precise Bathymetric Survey of the Mikura Basin Using the Seabeam System

A. Oshida, T. Tsukioka, H. Ikari, and T. Takeuchi

Outline of the survey

The Hakuho Maru cruise KH-90-1 was conducted from 25 June to 28 July 1990, consisting of two legs. The first leg of the cruise was between 25 June and 10 July and the second leg between 15 July and 27 July. Although the Seabeam survey was conducted throughout the whole cruise, I described here only Leg 2 results in this chapter, as the results in Leg 1 is presented in Ch. 4 ~ 5 of this report.

The overall view of ship's tracks in Leg 2 are shown in Fig. 16-1. In this leg, multi-channel seismic profiling, two kinds of the ocean-floor mappings using the Seabeam (multi-narrow beam echo sounder system) and the ocean-floor imaging sonar system IZANAGI (side-looking sonar system), geomagnetic measurement, gravity measurement, 3.5 kHz sub-bottom profiling and magnetotelluric study were carried out in the northern part of the Izu-Ogasawara Arc system.

Detailed Seabeam survey in Leg 2 was carried out at the southern part of the Mikura Basin on 17 July, while Seabeam survey mostly continued throughout the leg. Simultaneous operation of the Seabeam and the IZANAGI was attempted to check interference between the two acoustic instruments using nearly the same acoustic frequencies (12 kHz with Seabeam and 11/12 kHz (for port/stbd.) with IZANAGI). As interference was observed in this simultaneous operation, the Seabeam survey was interrupted during the IZANAGI survey.

Description of the operations

(1) Date and time logged in the digital files are in GMT. Note that there existed a time lag, which became large with the elapse time from a system reset because the Seabeam system does not have a self time adjustment function.

(2) The sound velocity profiles (SVP) used in Leg 2 of the cruise are follows;

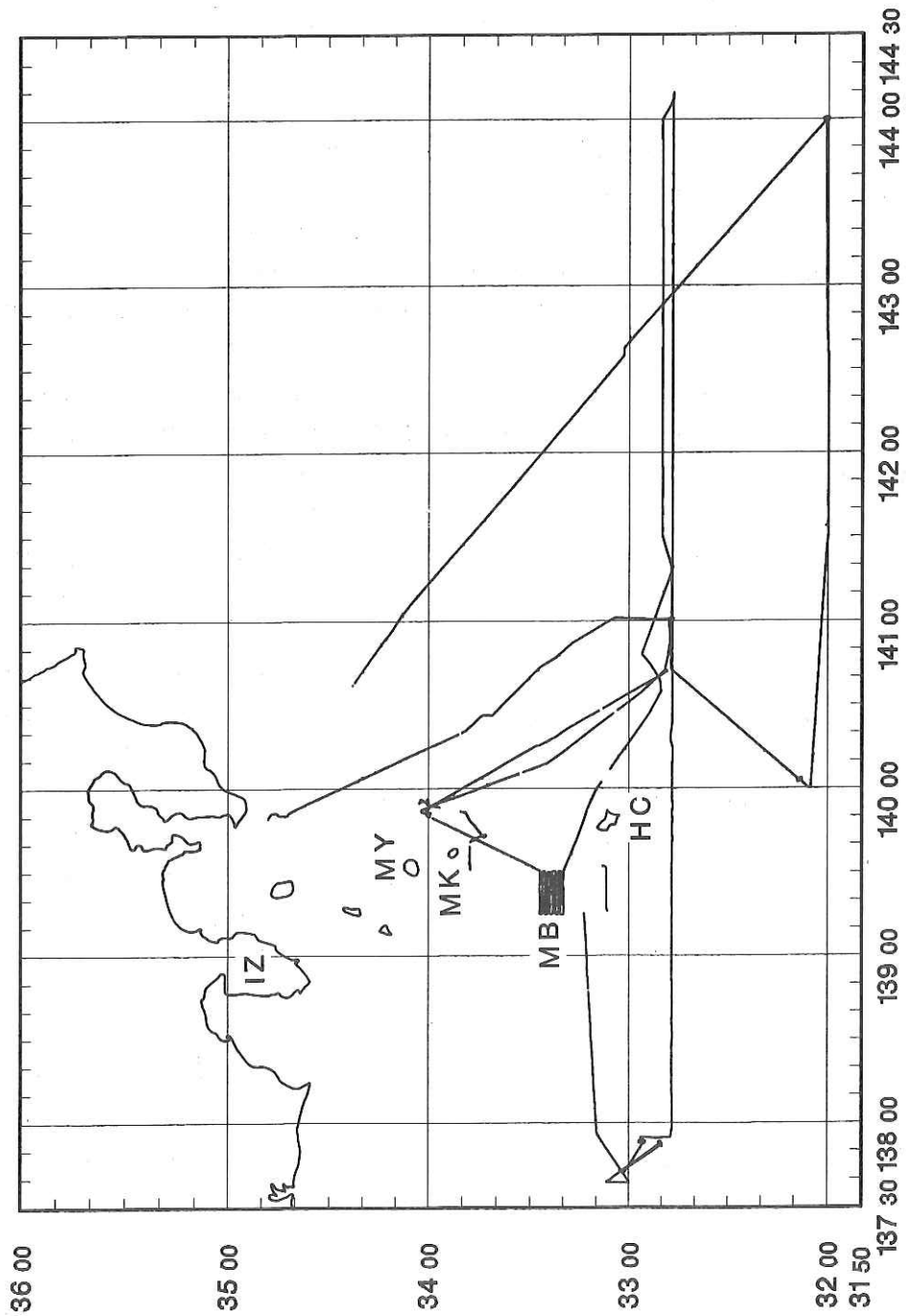

Fig. 16-1 Track chart of Seabeam survey in the KH-90-1 cruise Leg 2.
MB; study area of the Mikura Basin, MY; Miyakejima, MK; Mikurajima, HC; Hachijojima, IZ; Izu Peninsula.

July 15 (05:52) - July 18 (09:00)			July 21 (08:08) - July 26 (20:00)		
No.	Depth (m)	Velocity (m/s)	No.	Depth (m)	Velocity (m/s)
1	0	1500	1	1	1535
2	1000	1472	2	40	1540
		(default)	3	80	1528
			4	180	1517
			5	350	1511
			6	550	1491
			7	800	1480
			8	1000	1480

These sound velocity data were calculated from the result of XBT observation on July 21. See a chapter of the IES experiment (Chapt. 22) of this report.

(3) The data were logged in magnetic tapes of the Seabeam system (GIMT) at all times and in a hard disk of the real-time mapping system (as "G-file") only while the ship was running.

(4) System plotter of the Seabeam and an A0 size plotter of real-time mapping system were used only for detailed survey in the southern part of Mikura Basin.

Data handling

The GIMT data recorded in a density of 1,600 BPI were used for a backup of G-files, which are merged in a file and copyed on a magnet tape with EBCDIC code after fed to HP835 in No. 8 Lab. The data format of G-files is shown in Table 16-1.

Table 16-1 Final data format of the G-file.

Byte	Format	Description
001-006	I6	Date (yy:mm:dd)
007-012	I6	Block number (increment every ping)
013-018	I6	Hour in day (0 to 23)
019-024	I6	Second (unit=0.1 sec.; 0 to 35999)
025-030	I6	Heading (0 to 65535; 65536=360°)
031-036	I6	Average gate depth in meter
037-132	16I6	Sea Beam depth in meter (from Port to Starboard)
133-228	16I6	Cross-track distance in meter
229-324	32I3	Intensity of echo in 0.25 dB and its length in 3.3 ms
325	A1	Navigation data Header in EBCDIC 1 Character (=A)
326	A1	Position data status; V (valid) or I (invalid)
327	A1	Sign for latitude; N (North) or S (South)
328-329	I2	Degree of latitude
330-334	I5	Minute of latitude in 0.001 min
335	A1	Sign for longitude; E (East) or W (West)
336-338	I3	Degree of longitude
339-343	I5	Minute of longitude in 0.001 min
344-361	3A6	Terminators (=-00001)
362	A1	Blank

Mapping

Two application programs are available for mapping using G-files. Both were made by using a UNIRAS graphic software package and written by FORTRAN77.

(1) 'sbmap' and 'sbmapc'; these are for complete mapping supporting the Mercator conformable projection. The 'sbmap' makes a color shaded contour map or a color dot map and 'sbmapc' a contour map with contour level annotations or a dot map. The dot map (all data plot) and the contour map of the southern part of the Mikura Basin are shown in Figs. 16-2 and 16-3, respectively.

(2) 'quicksb'; this system was developed for a onboard quick graphic proceeding of the Seabeam data by Dr. Tamaki. Once the mesh data were generated from G-files, this system can draw five kinds of maps (*i.e.* dot map, color shaded contour map, 3D map and 3D solid model).

Both systems were supporting four output devices of a graphic display monitor, a YHP pen-plotter, a CALCOMP electrostatic plotter and a hard copy machine of the display monitor.

Mikura Basin

A map of the southern part of the Mikura Basin is shown in Fig. 16-3. This area is located in the western extension of the Shichito Ridge which is the volcanic arc in the Izu-Bonin Arc system.

The Hachijo-Nishinose knoll in the southwestern part is the shallowest of the surveyed area (about 600 m deep). The water depth gradually increases from the southeastern to northwestern parts (2,000 m), and an isolated knoll (720 m in height) is shown in the western part of the map. The most outstanding structure in the area is a set of the NW trending faults, which cut the knoll mentioned above as well as the southern and eastern walls of the Mikura Basin. Sediment in the basin has no evidence of faulting. A strike slip component of the faults can not be recognized from careful study of the shape of the knoll. The faults form a graben in the southeastern margin of the basin, indicating their normal fault origin.

The Mikura Basin is located north of the Hachijo Depression which is northernmost of the back-arc depressions of the Bonin Arc [1]. This situation infers that the most likely origin of these faults is a back-arc extension (rifting) behind the Isu-Bonin island arc.

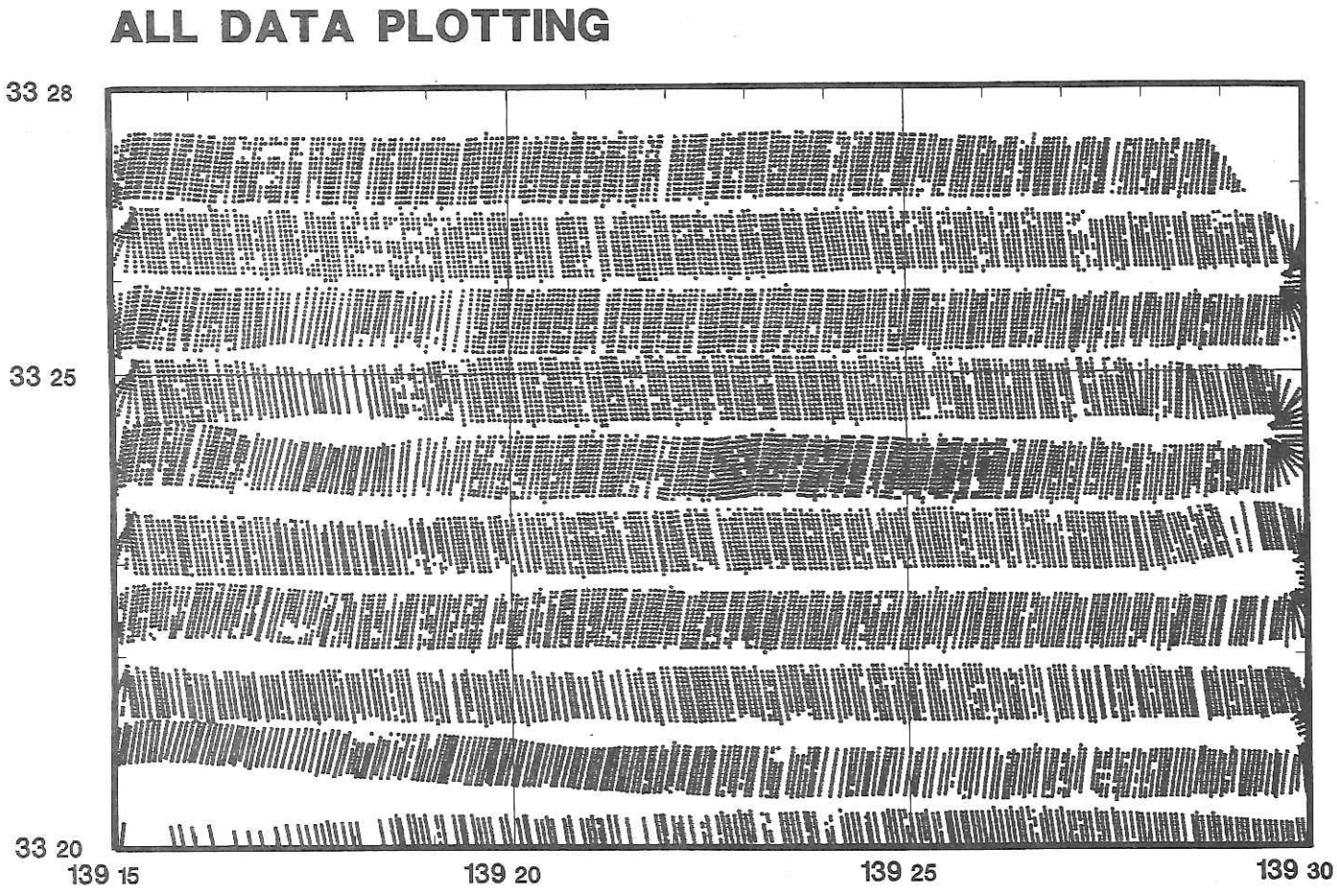

Fig. 16-2 All data utilized to make a Seabeam map of the southern Mikura Basin.

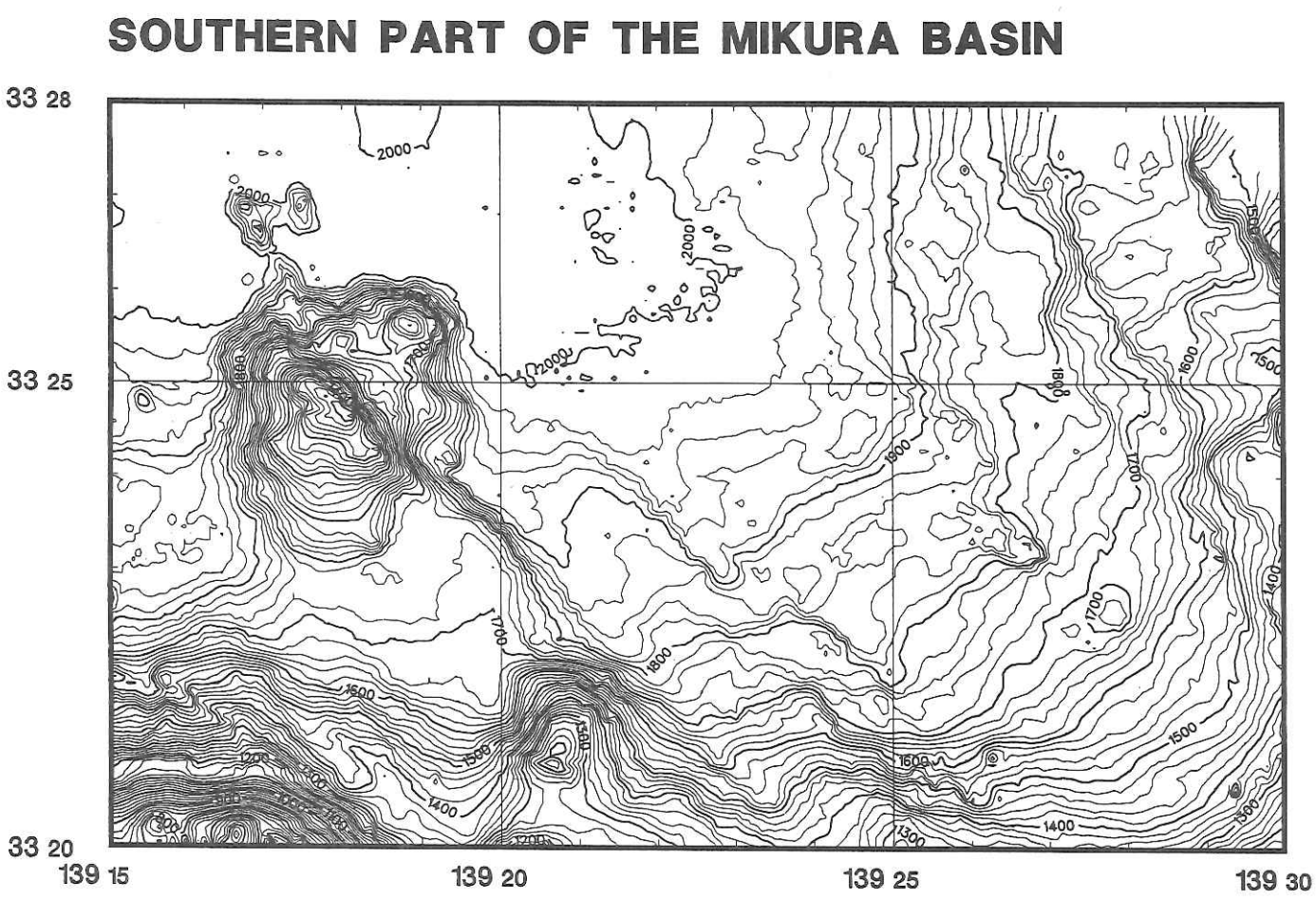

Fig. 16-3 Seabeam map of the southern Mikura Basin.

This area might also be affected by regional stress field of the northernmost part of the Philippine Sea Plate, probably caused by the collision between Izu peninsula and the Eurasia Plate, and by the subduction at both sides of boundaries (Sagami Trough and Suruga Trough) [2]. If these faults are young (less than 0.2 ~ 0.3 Ma) and dextral, their origin would be explained by the horizontal maximum tension with an E-W axis (Fig. 15 of Nakamura *et al.*, [2]), although no horizontal displacement of the faults is observed in this area.

Reference

[1] E. Honza and K.Tamaki: The Bonin Arc, in A.E.M. Nairn, S. Uyeda & F. Stehli (eds.), *The Ocean and Margins*, 7A, 459-502, Plenum Pub., 1985.

[2] K. Nakamura, K. Shimazaki and N. Yonekura, Subduction, bending and eduction. Present and Quaternary tectonics of the northern border of the Philippine Sea plate, *Bull. Soc. Geol. France* , **26**, 221-243, 1984.

17. Geomagnetic Total Force Measurement in the Northern Izu-Ogasawara Arc

A. Oshida

Geomagnetic Measurement

In the leg 2 of the Hakuho Maru cruise KH90-1 (Fig. 17-1), the measurement of the geomagnetic total force was carried out whenever the ship was running, although the measurement was interrupted during experiment of the ocean-floor imaging using the IZANAGI system in the Mikura Basin (Fig. 17-2). The geomagnetic measurement was done every 30 sec. Total number of the data obtained in leg 2 amounts to about 17,600 readings.

System of measurement

The system for measurement, originally designed by ORI, University of Tokyo, is composed of a proton sensor with towing cable (250 m), an onboard data processing unit, a capacitor box, a personal computer (NEC, model PC9801VM) system and MAGNAVOX SERIES 5,000 integrated navigation system (Fig. 17-3).

The proton sensor was towed 200 m behind the ship's stern by speeds faster than 15 knots against water. The towing distance between the ship's stern and the sensor is only twice the ship's length (100 m) so that a large magnetic effect biased the measured total force. This "head effect"might be approximately 10 to 20 nT.

The polarizing time is 5 sec and 110 msec after shut off of the polarizing power supply, a period counter starts to count wave number up to 1,000 cycles, calculating frequency from the counting period. Obtained frequency is fed to the micro-computer in the form of BCD code. The micro-computer converts the frequency to a total force of the geomagnetic field, saving it in a floppy disk together with the navigation data composed of date (day, hour, minute, second), latitude, longitude, heading, ship's speed against ground, direction of ship's motion and water depth transmitted through the optical fibre cable.

Onboard processing

The data logged in floppy disks were fed to the host computer (Hewlett Packard model 835 TurboSRX) by using NEC PC9801RA micro-computer linked with the optical Ethernet of the Hakuho Maru. The data format was changed to the MGD77 format and the magnetic anomalies were simultaneously calculated

based on IGRF 85 [1] . Track chart and magnetic anomaly map were drawn using the MAGBAT (modification being applied for Starbase) [2].

Results

One or two Mesozoic magnetic lineations (M10N ~ M11[3]) are observed in the region east of trench with a large positive anomaly. The Izu-Ogasawara (Bonin) Trench is characterized by negative magnetic anomalies with long wave-lengths. Relatively large amplitude of the anomaly is recognized in the place where a seamount exists near the trench axis. Positive anomalies are observed in Shinkuronose Bank, one of the fore-arc basement high, located east of the Hachijojima island of Izu Ogasawara Arc system. These anomalies are characterized by the short wave-length superimposed on those with relatively long wave-length. The anomalies with short to medium wave-length are dominant in the Shichito Ridge (volcanic island chain) and the back-arc region. This character suggests fresh volcanics are existent beneath the seafloor.

The magnetics and topography of a part of the Mikura Basin were precisely surveyed (Fig. 17-4). The magnetic anomalies are generally shifted to negative values. Relatively high anomalies are observed on the knoll in the west side of the area and the easternmost margin of the area. The former is elongated in the north direction. This distribution of anomaly implies existence of the buried volcanics in the N-S elongating direction. The peak of the magnetic anomaly is located south of the topographical summit of the knoll, whereas an eye of negative anomaly is lacking. This distribution of anomaly seems to indicate normal magnetization of this knoll, although it is not typical of the anomaly which seamount originates in a mid-latitude area. No magnetic anomaly is observed on the topographic high in the southwestern corner of the area.

References

[1] IAGA, Division I, Working Group 1, International Geomagnetic Reference Field Revision 1985, *J. Geomag. Geoelectr.*, **37**, 1157-1163, 1985.

[2] M. Nakanishi, C. H. Park, K. Sayanagi, K.Tamaki, Y. Nakasa, A. Oshida and N. Seama, Development of the basic processing of marine geophysical data (MAGBAT) (in Japanese with English abstract), *Geological Data Processing*, **12**, 217-226, 1987 .

[3] M. Nakanishi, K. Tamaki and K. Kobayashi, Mesozoic magnetic anomaly lineations and seafloor spreading history of the northwestern Pacific, *J. Geophys. Res.*, **94**, 15437-15462, 1989.

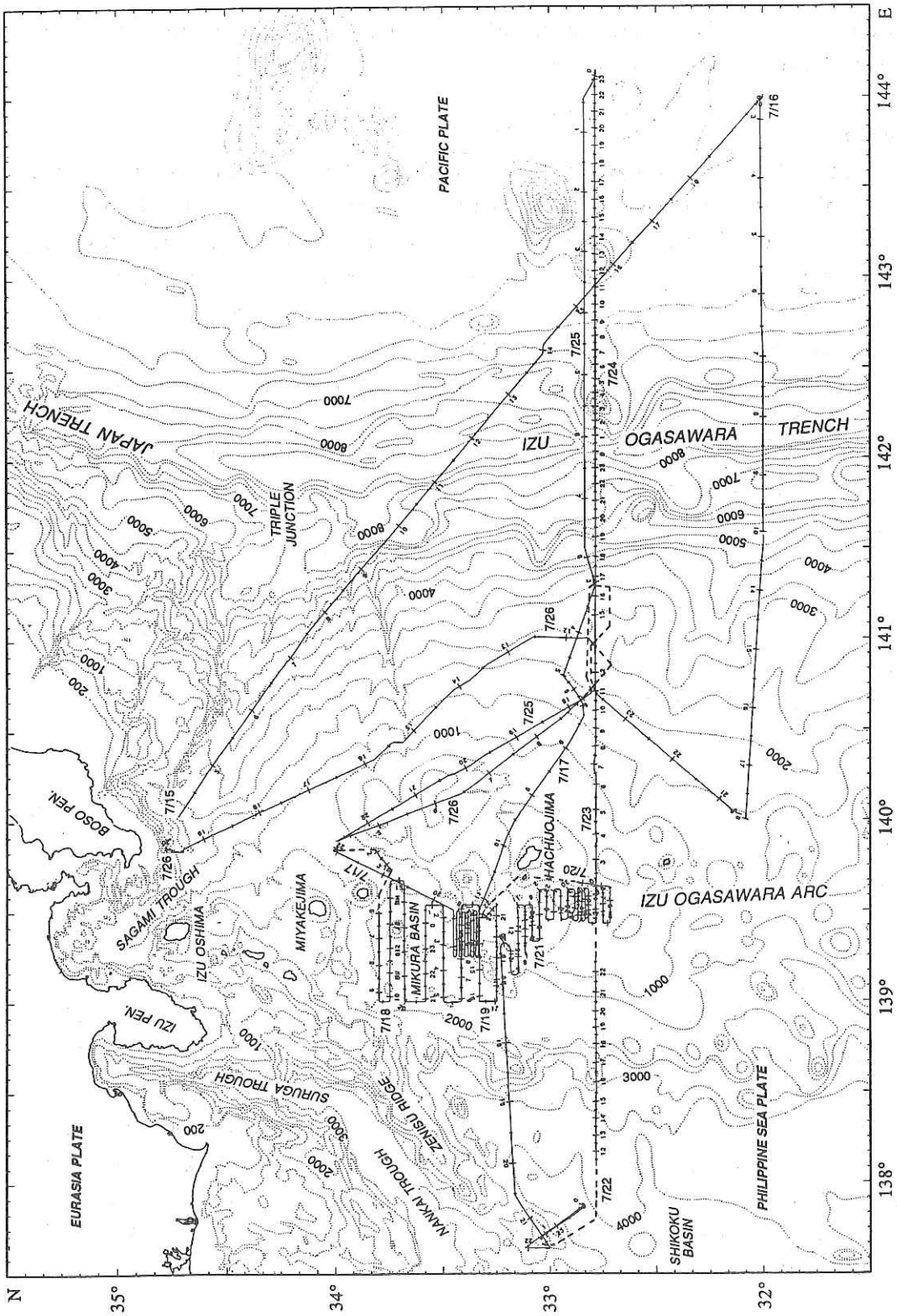

Fig. 17-1 Overall view of ship's tracks in leg 2 of KH90-1

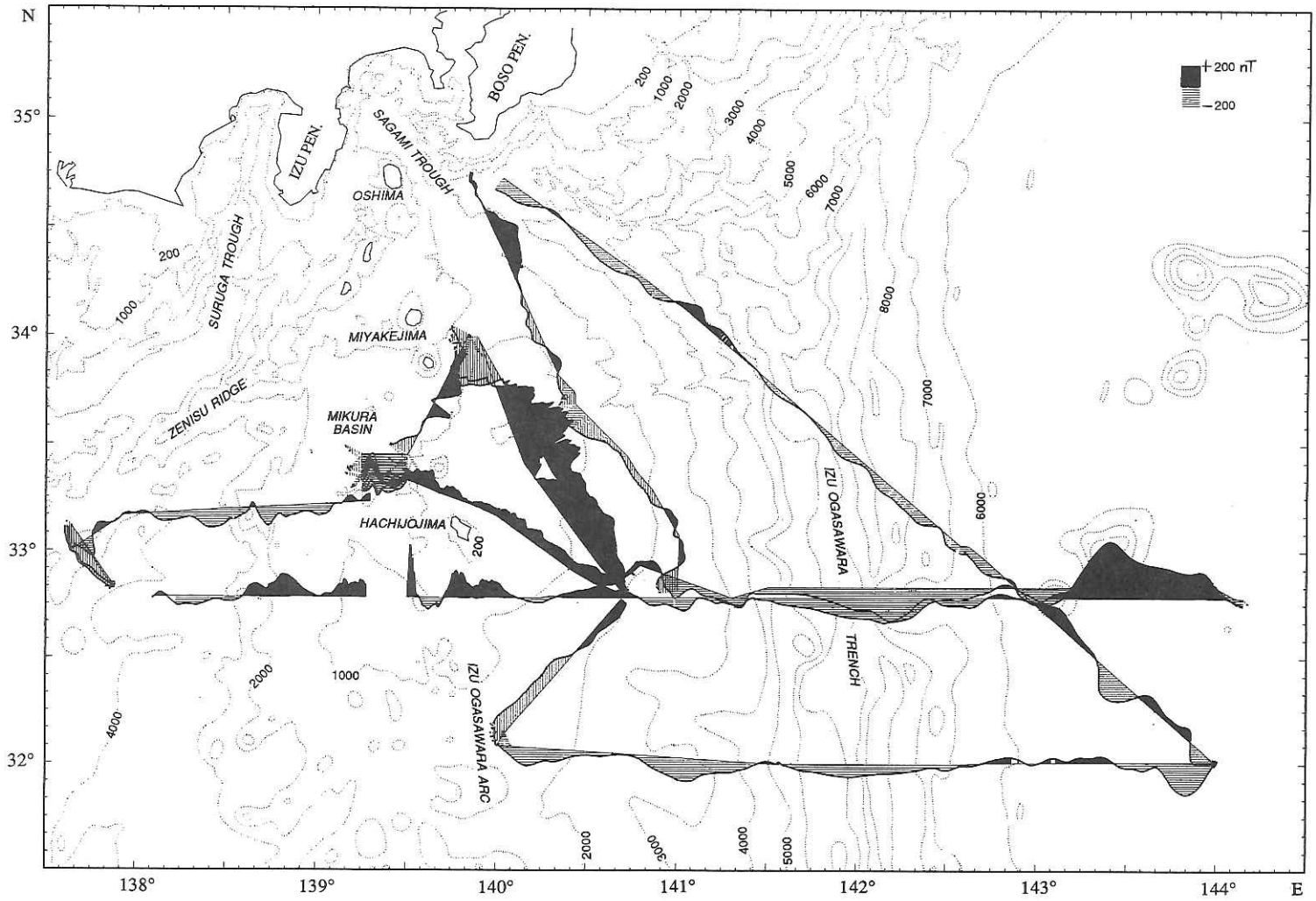

Fig. 17-2 Magnetic anomaly map along with ship's tracks.

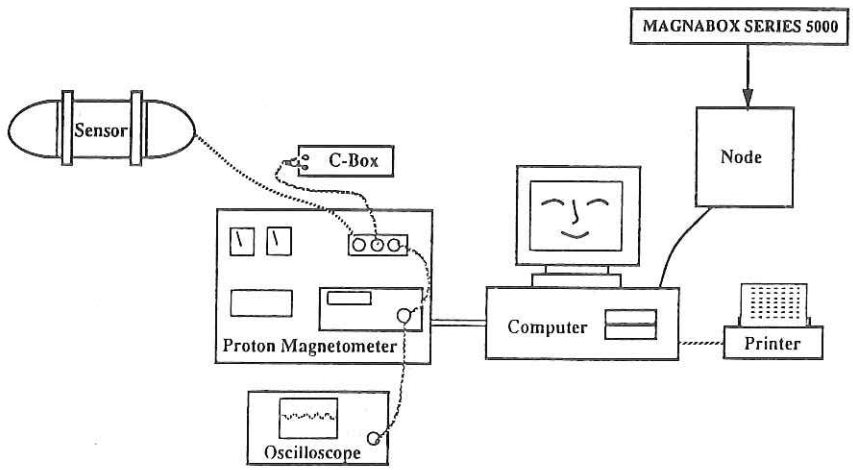

Fig. 17-3 Diagram of the system of magnetic measurement.

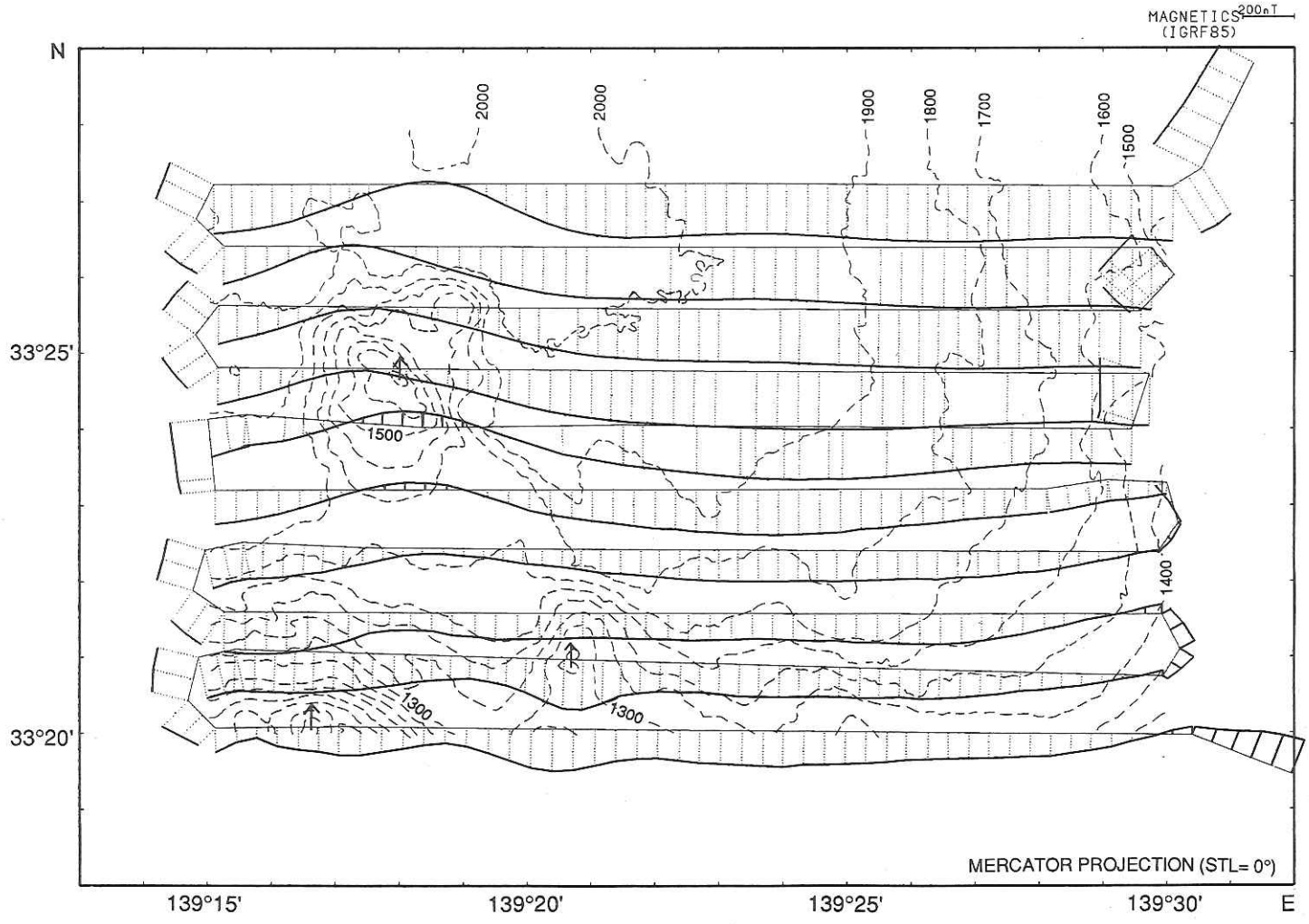

Fig. 17-4 Magnetic anomaly map of a part of Mikura Basin. Broken lines show bathymetric contour taken out from the Seabeam map with 100 m interval.

18. Geomagnetic Deep Sounding and Magnetotelluric Study of the Izu Bonin Arc

H. Toh, Y. Fukuda, C. S. Yang and I. Fujii

Introduction

We have been conducting sea floor geomagnetic and geoelectric observations around the Izu Bonin arc since 1986 [1, 2]. The target of these observations is set to construct a model of an electrical conductivity structure beneath the arc, which will lead to the whole understanding of the origin, evolution and present structure of a typical island arc system provided it is interpreted together with other geophysical investigations. The geomagnetic transfer functions obtained so far show a three-dimensional (3D) distribution rather than two-dimensional (2D), representing not only the effect of the Izu Bonin arc itself but also that of the Japan arc which is typically revealed by the induction vectors pointing toward south-southeast direction (Fig. 18-1). The effect of the Japan arc seems to be dominant especially along the northernmost profile (33°N) but the southernmost profile (31°N) shows, to some extent, 2 dimensionality compared with the other 2 profiles. This is the reason why our observations and model studies have been concentrated on the southernmost profile.

A 2D modelling of a conductivity structure requires boundary conditions at the lateral infinity, that is to say, we must know the one-dimensional (1D) conductivity structure below the oceanic plates on both sides of the arc where the structures can be, to first approximation, considered to be laterally homogeneous. Determination of the eastern boundary condition was the very purpose of our latest magnetotelluric (MT) observation conducted in 1989 [2]. Fig. 18-2 shows the MT result on the Pacific plate in which the 1D conductivity structure below the Pacific plate is found to be of the conductive, resistive and conductive configuration from top to bottom. The depth to the asthenospheric conductor is estimated as deep as 160 km. Fig. 18-3 shows the 2D conductivity model of the Izu Bonin arc obtained preliminarily, employing the 2D forward modelling technique based on the finite difference method originally evaluated by Jones and Pascoe in 1971 [3]. The 1D result of the conductivity structure described above was used as the eastern boundary condition in the modelling. As for the western boundary condition, the 1D conductivity structure followed Utada's model [4] which is similarly of the three layered conductivity configuration. The result of the model study is shown in Fig. 18-4 where calculated and ob-

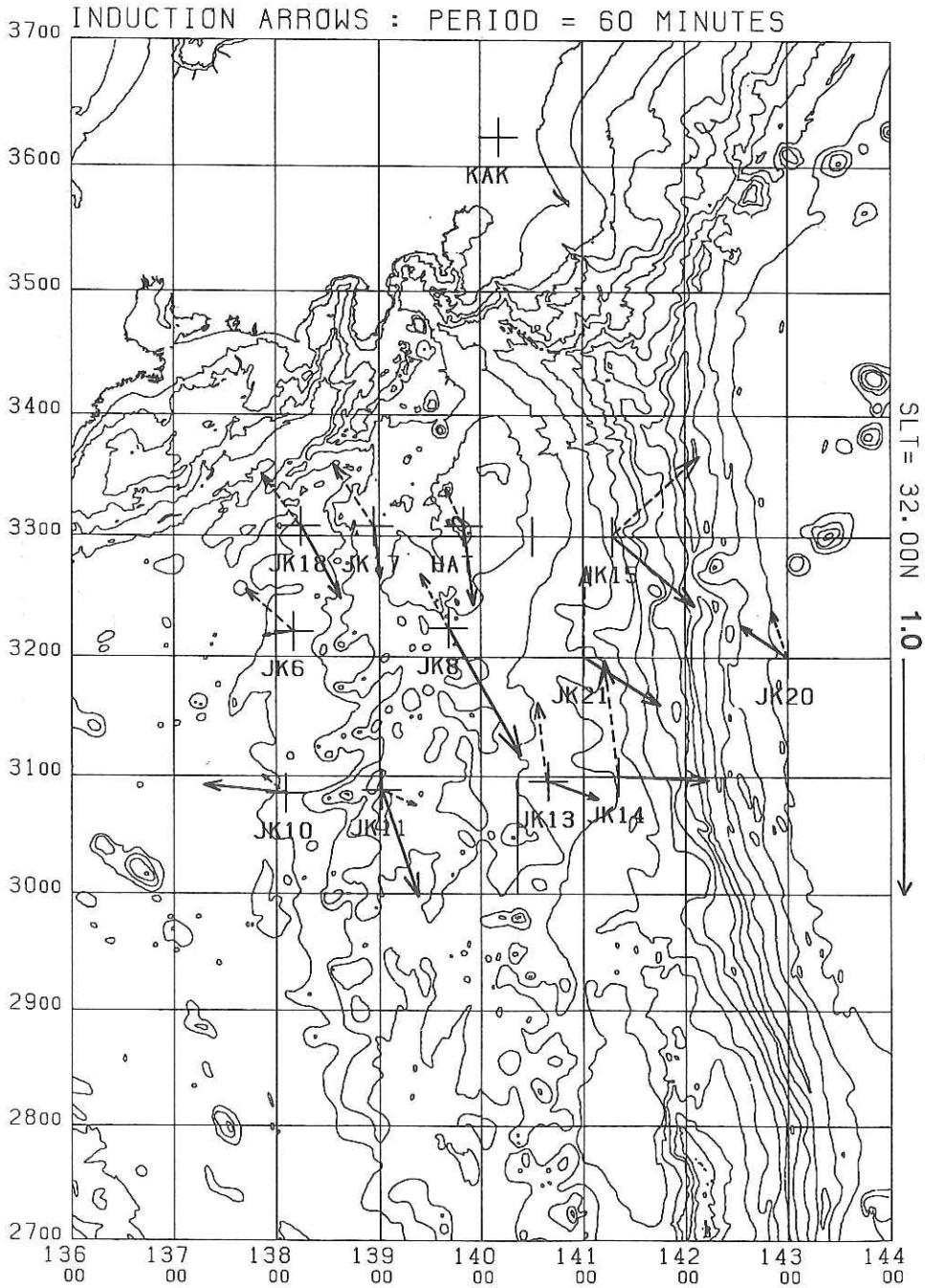

Fig. 18-1 Distribution of the observed induction vectors around the Izu-Bonin arc for the period of 60 minutes. The induction vectors were calculated from the data obtained during the previous four cruises; KT86-12, KH87-3, KT88-10 and KH89-1. Solid arrows indicate the real parts of the calculated transfer functions, while dashed arrows denote imaginary ones.

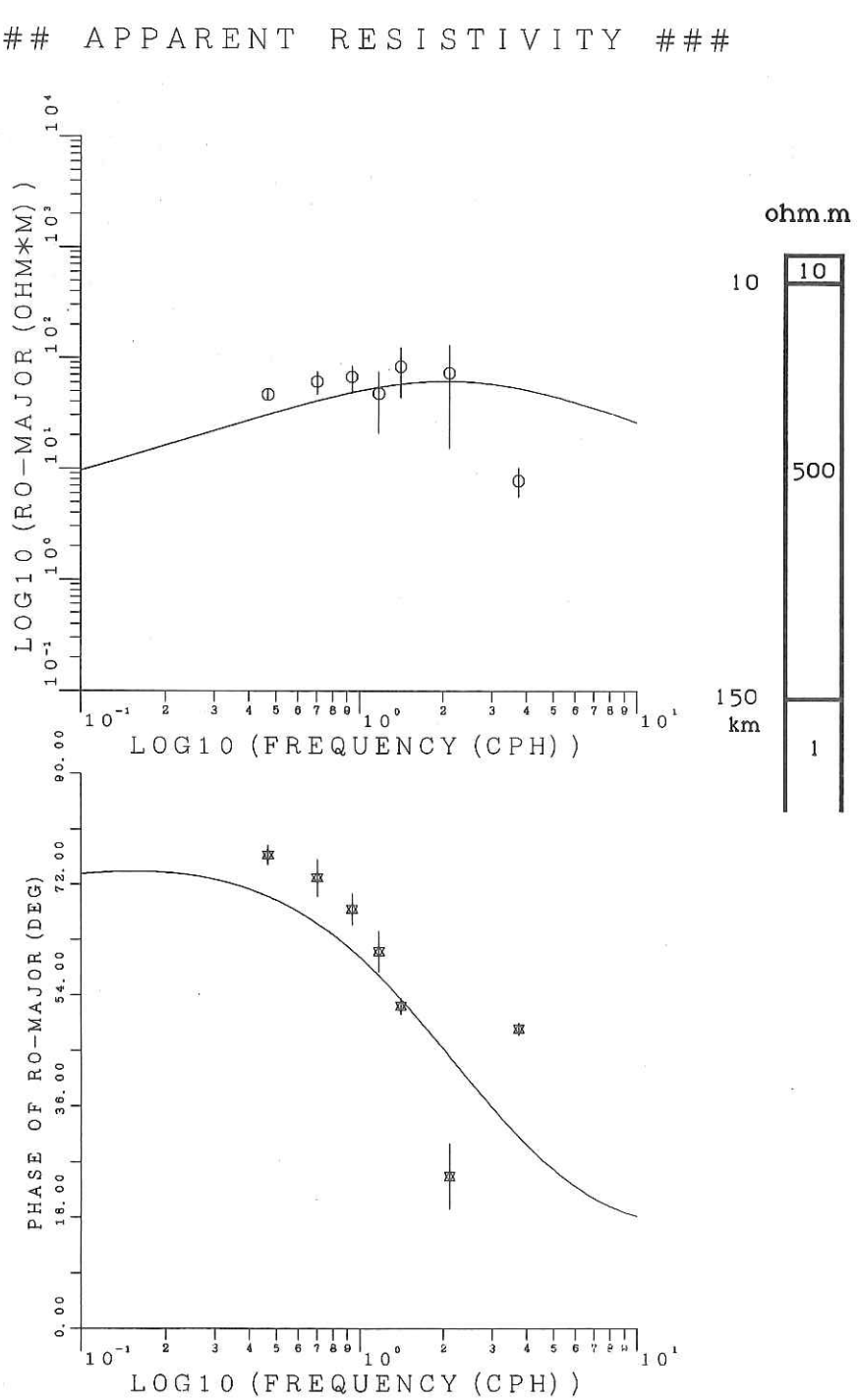

Fig. 18-2 Results of the MT observation in 1989. The upper and lower diagrams are amplitude and phase of apparent resistivity, respectively. Points with error bars are the observed EM responses and the solid lines are the calculated ones assuming the 1D structure drawn at right hand side.

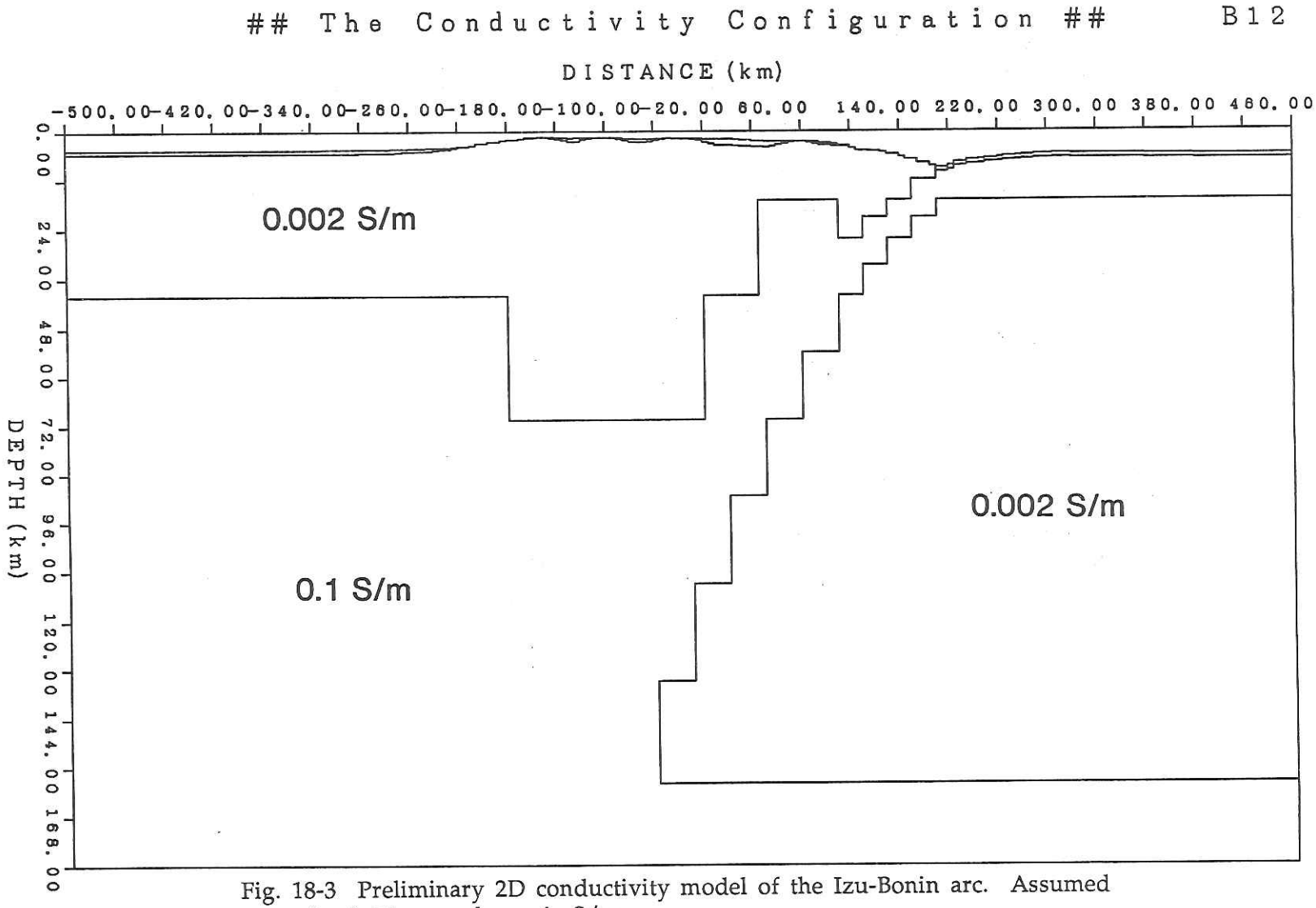

Fig. 18-3 Preliminary 2D conductivity model of the Izu-Bonin arc. Assumed conductivities are shown in S/m.

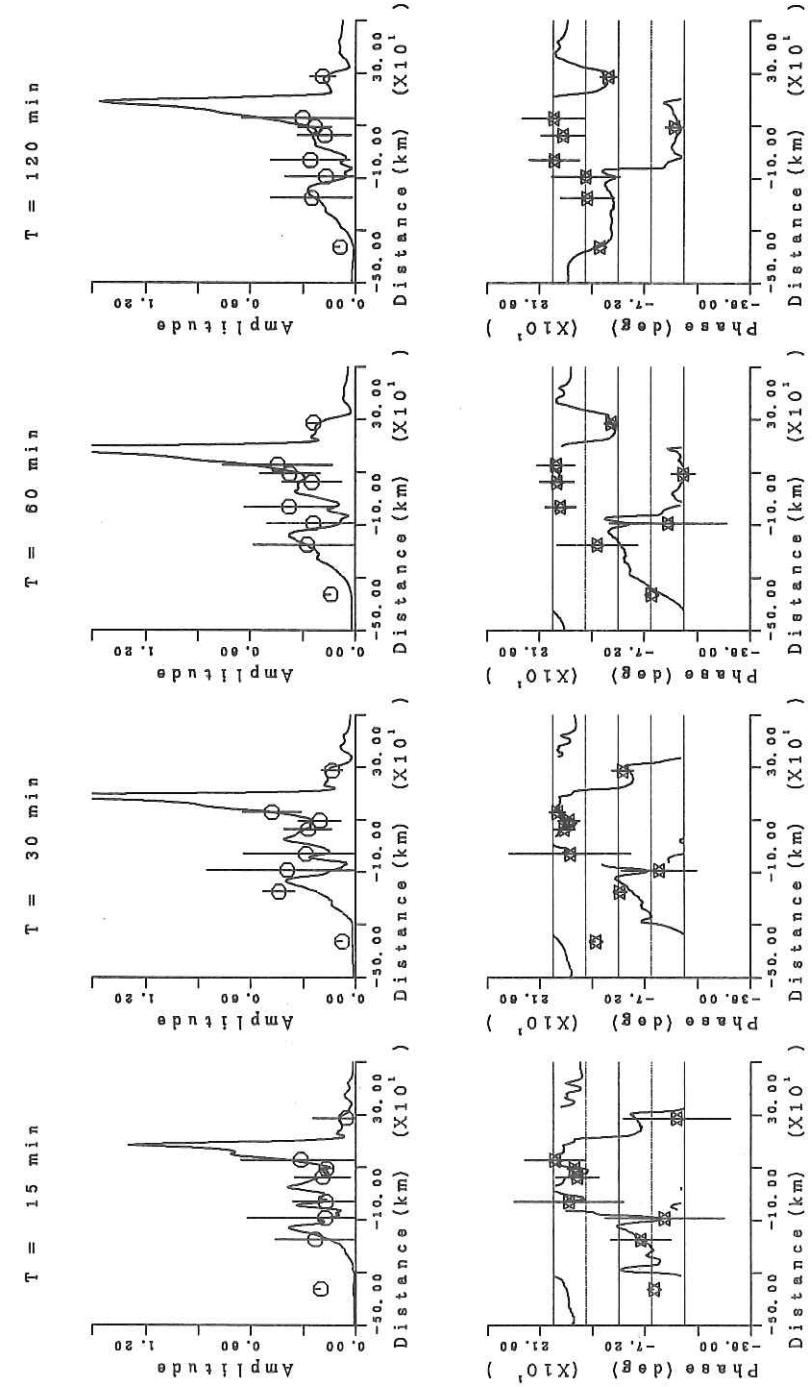

Fig. 18-4 Results of the 2D model calculation for the periods of 15 min to 2 hours from left to right. The upper and lower four diagrams are amplitude and phase of B-values of geomagnetic transfer function, respectively. Points with error bars are the observed EM responses and the solid lines are the calculated ones.

served electromagnetic (EM) responses are plotted at the same time. The characteristics of the model are summarized as follows:

1. The depth to the asthenospheric conductor is around 160 km below the Pacific plate while it is much shallower, around 40 km, below the Philippine Sea plate.
2. The resistive layer of the arc seems to be thick at the backarc side.
3. A thin, about 10 km or so, conductor at the top of the Pacific plate explains the observation on the plate well (see Fig. 18-2).
4. A forearc conductor was introduced in order to explain the small amplitudes of the induction vectors on the forearc region.

The first feature is directly derived from the lateral boundary conditions applied. The thickening of the lithosphere is necessarily inferred for accounting for the fact that the observed amplitudes on the backarc side of the arc are relatively large. The third and fourth features imply that a fraction of water is supplied from the subducting thin conductive layer and the first stage of dehydration occurs beneath the forearc region as has been pointed out by Tatsumi [5].

The characteristics of the conductivity structure of the Izu Bonin arc mentioned above are those obtained from our observations so far conducted. Our 2D model, however, still remains preliminary because of the poor horizontal resolution of the data. The variation of the calculated responses depends strongly on locations. This means that the improvement of the horizontal resolution and measurements at the critical points such as the forearc region is definitely necessary. This is the reason why we carried out again the seafloor EM observation in this cruise.

Instruments and Installation

Five total instruments were prepared for this observation, which consisted of two ocean bottom two-component electrometers (OBE's) and three fluxgate type three-component ocean bottom magnetometers (OBM's). Three sites were selected for this cruise, two of which were MT sites (JK25 and JK27) and the rest was a geomagnetic deep sounding (GDS) site (JK26). A set of OBE and OBM was installed at each MT site while only OBM was installed at the GDS site. The MT sites were configured on the Pacific plate and the ridge axis. The MT site on the Pacific plate has the role of the direst testing of the eastern boundary condition applied to our 2D model and the MT site on the ridge axis will make up for the particularly poor horizontal resolution around the ridge axis. The GDS site will

provide critical information about the existence of the forearc conductor because it locates closest to the trench among the sites including those of our previous observations.

Fig. 18-5 shows the outer view of OBM-S6 which was newly manufactured for this observation. Similar to the other OBM's, it has a 0.1 nT resolution sensor mounted on a free gimbal and is equipped with an acoustic release system. It contains, however, a different recording system. The data are stored in four static random access memory (SRAM) cards, each of which has 256 kbytes capacity in the case of OBM-S6 while, in the case of the other OBM's, the data are stored in three to five 128 kbytes read only memory (ROM) boards. It enables exactly 120-day observation with one minute interval in the case of OBM-S6.

The installation of the instruments was mainly made on the east-west transverse section of the Izu Bonin arc along the parallel of 32°N. Thanks to the calm weather, it took only about 42 hours to complete all the installations. Fig. 18-6 shows the location of the installation points on a bathymetric chart together with the previous observation points. As for the detailed information of the installation sites, refer to Table 18-1.

Table 18-1 Observation Log of KH-90-1 Cruise

Apparatus	Site	Position	Depth	Sampling Rate
OBE1	JK25	31°59.9'N 144°00.0'E	5614m	1 min
OBM-S4	JK25	32°00.0'N 143°59.3'E	5508m	2 min
OBM-C3	JK26	32°00.1'N 141°33.6'E	5146m	1 min
OBE2	JK27	32°05.7'N 140°00.0'E	1444m	1 min
OBM-S6	JK27	32°05.1'N 139°59.9'E	1446m	1 min

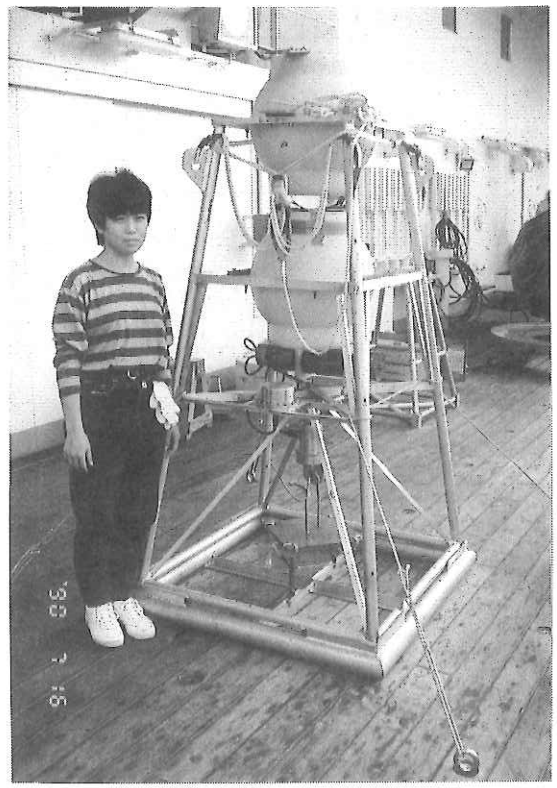

Fig. 18-5 A photograph of OBM-S6 and one of the authors (I.F.).

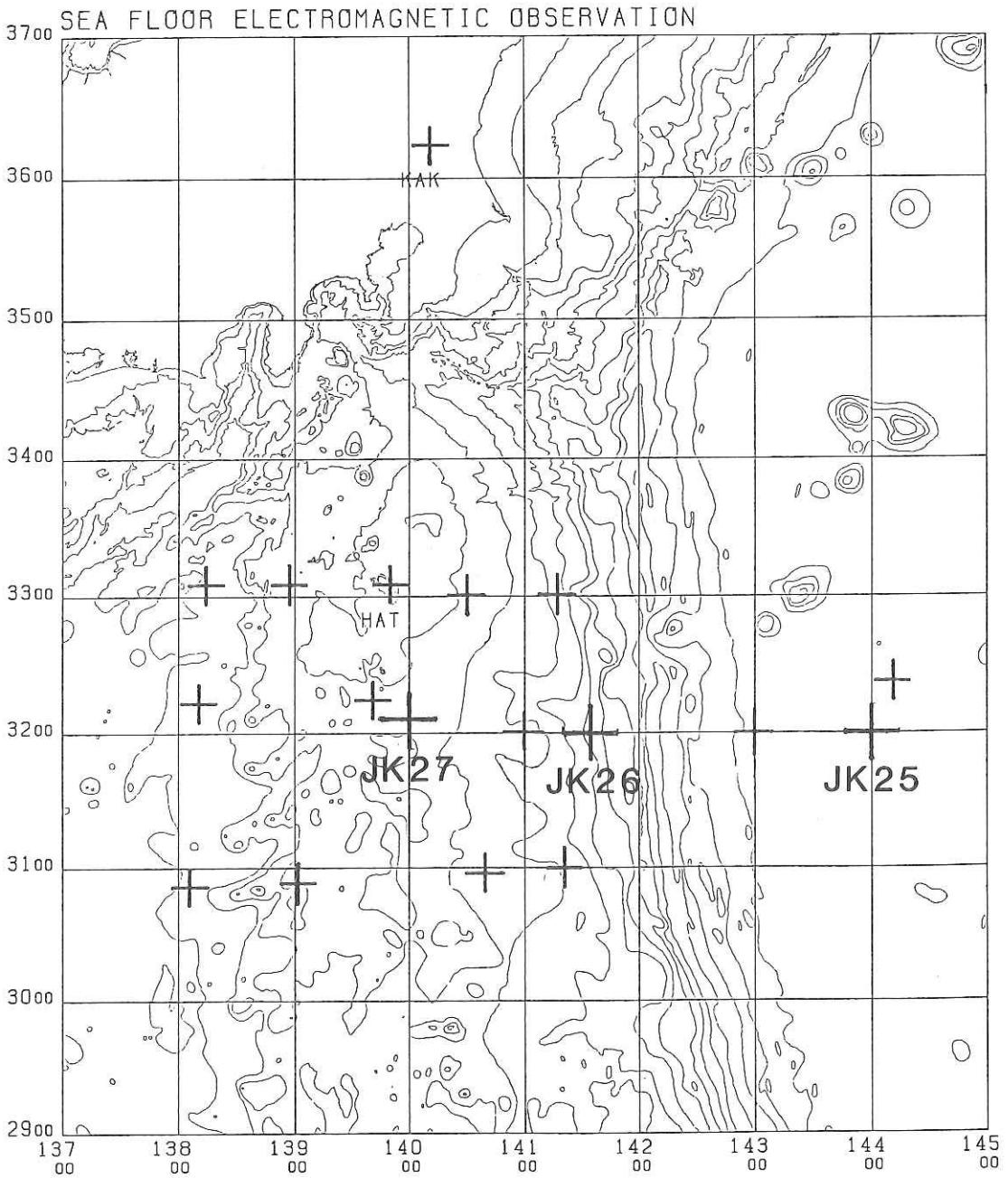

Fig. 18-6 The distribution of the observation points. JK25 through JK27 show the positions of the present observation points. Cross marks without site names denote the previous observation points in this area. It is also shown the locations of Kakioka (KAK) and Hachijo-jima (HAT) where permanent geomagnetic observatories are situated.

Summary

With respect to the data analysis and interpretation, we must wait until we get new data because the recovery of all the instruments will be made in case of the cruise KT90-16 in the next November. Hence, we would like to confine our discussion to giving some comments on our future work.

First, the shallower structure of our 2D model was determined by taking the seismic structure of the arc [6] as a priori information. This is because the seafloor EM data are always lacking in high frequency signals due to the existence of the conductive ocean. The most positive approach to improve this situation is the application of controlled source EM methods to marine regions. Although controlled source methods cannot explore crustal structures deeper than, say, 10 km, it would be possible to determine the distribution of sedimentary layers through some EM methods. Such efforts should be made in the future. It will be also important to introduce updated crustal structures around this region determined by seismological methods or direct ocean floor drilling because intensive seismic or drilling operations have recently got started around the Izu Bonin arc (*e.g.* ODP Leg 126 shipboard scientific party, [7]).

Second, the 3D distribution of the observed geomagnetic transfer functions has a notable frequency and spatial dependence. That is, the short-period induction vectors along the northernmost profile point to the north whereas the long-period induction vectors of all the three profiles point, in turn, to the south. The behavior of the short-period induction vectors could be qualitatively interpreted as showing the existence of current leakage from the Pacific ocean into the Philippine Sea (and *vice-versa*) *via* the north end of the arc while that of the long-period induction vectors might be considered to suggest a deep structure produced by the interaction of the Japan arc and the subducting oceanic plates. To reveal the deep structure observed in the long-period induction vectors, it is necessary to eliminate the conduction effect which appears in the short-period induction vectors. The conduction effect can be well estimated theoretically if a non-uniform thin sheet approximation is applied to describe the complicated land-sea distribution. We should make such a theoretical effort as well.

The 3D interpretation of the conductivity structure of the Izu Bonin arc seems to be very difficult when the poor horizontal resolution of our data is compared with the extraordinarily complicated bathymetry. However, a "2.5-dimensional" interpretation using both the traditional 2D modelling technique

and the non-uniform thin sheet approximation at the same time seems to be quite feasible now.

Acknowledgments

We are grateful to all the crew on the Hakuho-maru. We also wish to express our sincere thanks to Prof. K. Kobayashi, Prof. A. Taira and Dr. K. Suyehiro for their profound understanding of our work.

References

[1] J. Segawa , H. Fujimoto, K. Koizumi, C. S. Yang and H. Toh, Sea floor geomagnetic observation, in K. Kobayashi (ed.), *Preliminary Report of the Hakuho Maru Cruise KH-87-3*, 109-113, 1988

[2] H. Toh, J. Segawa, V. Bapat, Y. Nagaya and T. Ichikita, Magnetotelluric study of the sea floor, in J. Segawa (ed.), *Preliminary Report of the Hakuho Maru Cruise KH-89-1*, 80-87, 1990

[3] Jones, F. W. and L. J. Pascoe, A general computer program to determine the perturbation of alternating electric currents in a two-dimensional model of a region of uniform conductivity with an embedded inhomogeneity, *Geophys.J. R. astr. Soc.*, **24**, 3-30, 1971

[4] Utada, H., A direct inversion method for two-dimensional modeling in the geomagnetic induction problem, Ph. D. Thesis, Univ. Tokyo, 1987

[5] Tatsumi, Y., Migration of fluid phases and genesis of basalt magmas in subduction zones, *J. Geophys. Res.*, **94**, 4697-4707, 1989

[6] Honza, E. and K. Tamaki, The Bonin arc, in *The Ocean Basins and Margins*, A. E. M. Nairn, F. G. Stehli and S. Uyeda (eds.), 459-502, 1985

[7] ODP Leg 126 shipboard scientific party, Arc volcanism and rifting, *Nature*, **342**, 18-20, 1989

19. Results of 3.5 kHz Subbottom Profiling in KH-90-1, Leg 2 "Pacific-Izu-Bonin Transect Line IB90"

C. Igarashi, H. Iino, T. Kito and I. Fujii

KH-90-1 was the first cruise to accomplish composite survey by acoustic and seismic methods such as "Seabeam", "MCS (multi-channel seismic reflection system)", "SBP" and "IZANAGI". Comprehensive analysis of vertical section information obtained by SBP and MCS together with horizontal plane information taken by multi-narrow-beam echo sounder and side scan sonar, makes interpretation of three-dimension geological and topographical structure possible. Correlation of SBP and MCS sections enables us more accurate analysis of geological structures.

Results of 3.5kHz subbottom profiling of the Pacific-Izu-Bonin transect line "IB90" are briefly stated in the followings.

Outline of Izu-Bonin Transects "IB90"

Izu-Bonin Transect Line "IB90" runs along the latitude 32°48'N from 138°05'E to 144°00.5'E to get East-West section through Izu-Bonin Arc Trench system from the Philippine Sea back-arc region through the Izu-Bonin Arc Trench system to the Pacific Oceanic basin (Fig. 19-1). Observed 3.5kHz subbottom profiling records (Figs. 19-2~12) are very clear with a high power of resolution showing characteristic geological features of the active Izu-Bonin Arc-Trench system. Sedimentary and basement tectonics of the Pacific Ocean floor and seamounts can be revealed as well.

Back-Arc Region of Izu-Bonin Arc at Transect Line "IB90"

Records of 3.5kHz Subbottom Profiling show distinctly layered structure in the Philippine Sea Basin adjacent to the western back-arc margin of Izu-Bonin Arc. Surface of the basin floor is covered by bottom sub-parallel wavy layers. These structures indicate that the basin floor sedimentation pattern may be caused by re-sedimentation processes according to bottom water flow at the Philippine Sea Basin margin (Fig. 19-2).

The sediment facies in Philippine Sea Basin with layered structure change to gravity-induced mass sliding deposits at the western foot of the Izu-Bonin Arc. These sediment bodies formed by mass movement are clearly indicated by blocky and wavy reflection patterns there. Furthermore multiple onlapped

structure of layered sediments are recorded in the subbottom profiling record, showing active gravity collapse prevailing in this area (Fig. 19-3).

Back-Arc Side of the Crest of Izu-Bonin Arc

The area from back-arc region to the crest of Izu-Bonin Arc is generally characterized by moderately rugged topography lacking sediment cover. 3.5kHz SBP record of Nishi-Shichito Ridge is remarkable with a conspicuous hyperbolic reflection pattern because of very rugged topography in this ridge area. The plateau, southwestern extension of Mikura and Hachijo Basins, located at the western edge of Shichito-Iwojima Ridge is covered with thin layered sediment (Fig. 19-4). However, this layered structure has irregularity. The bottom surface seems to be erosive and the central submarine canyon is recognizable. These features may have originated from a mode of sediment transportation, as gravity- induced volcaniclastic sediment flow from Mikura and Hachijo Basins.

The crestal part of Shichito-Iwojima Ridge is characterized by topographic features of volcanoes. Very rugged topography of volcanic extrusive or collapsed bodies generated the very hyperbolic reflection patterns in this area. Especially, the top of the Shichito-Iwojima Ridge on this transect line "IB90" indicates typical caldera topography with parasitic volcanoes as lava domes on the rim (Fig. 19-5).

Fore-Arc region of Izu-Bonin Arc at "IB90"

Izu-Bonin Arc is noted as a typical arc system with sediment starved force arc region. The record of 3.5kHz SBP at transect line "IB90" clearly shows this characteristic nature of sediment lacking fore arc (Fig. 19-6). The pattern of the 3.5kHz SBP record is a distinct type surface reflection indicating distribution of coarse grained thin veneer of sediments or eroded surface exposure of indurated rocks in this area, except the limited region inner side of the trench slope break near water depth of 2,000 m. The record of wavy or notched surface reflection of short wave length is clearly recognized at the fore arc side of the crest of Sitito-Iwozima Ridge (Fig. 19-7). This is probably considered to be sand waves or sand dunes, caused by coarse sediment drift due to currents.

At the western limited, sediment sheet distribution with layered structure is recognized, as stated before. This is considered to be a poorly developed sediment body corresponding to fore arc basin sediments in other sediment rich arc trench system (Fig.19-8).

Trench Slope Break to the Floor of Izu-Bonin Trench

From the inner trench slope to the trench floor region of Izu-Bonin Arc along "IB90", its SBP profiler record is prevailed by very prominent hyperbolic echo throughout the area, reflecting the very rough and irregular topography in this area (Fig. 19-9). The little basin like depressions located in this slope area also displaying distinct to prolonged type echo suggesting the hard or indurated rocks exposed at the bottom surface of the slope basin like depressions.

These observations are also considered to be demonstration of a sediment starved fore arc trench system. The Trench floor area along the "IB90" transect line is also occupied by hyperbolic echo expressing the narrow trench floor lacking sediment layer (Fig. 19-9). This topographic roughness is probably caused by subduction of sea mounts into the trench floor one after another show in the index map (Fig. 19-1).

Pacific Ocean Floor along "IB90" Transect Line

The floor of Pacific Ocean adjacent to the Izu-Bonin Trench is also a region of remarkable hyperbolic echo type record on 3.5kHz SBP Profiling. This is originated from distribution of the seamount group in the last pre-subducting stage near the trench (Fig. 19-10).

Normal faults possibly originated from the bending of the Pacific Plate at the outer bulge are recognizable in the relatively flat part of the sea floor (Figs. 19-11, 19-12). Fig. 19-11 demonstrates an example of gravitational deformation affecting the surface sediment layer by a series of normal faults near the seamount moat. Under the surface sediments buried topography of sea mounts is noticed. So the deformation caused by the normal faulting is probably prevailing in this trench- neighboring region, although very rough and steep topography makes difficult to detect the tectonic deformation on the profiler record.

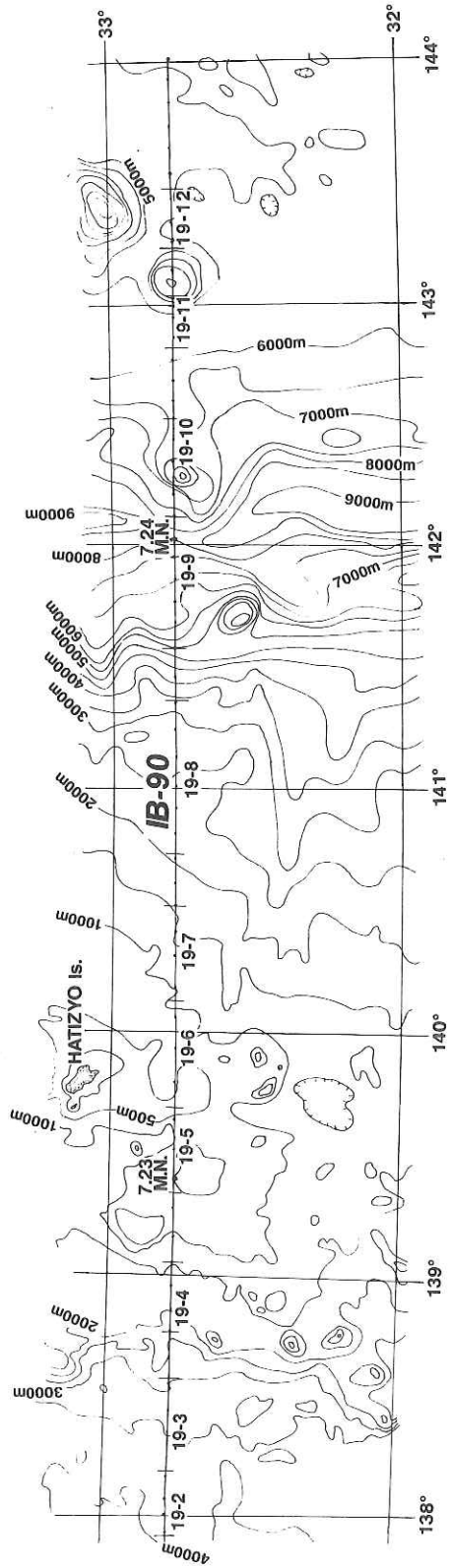

Fig. 19-1 Index map of a survey transect in Leg 2. Numerical figures shown below lines denotes position of each 3.5 kHz profile represented in the following (e.g., 19-2 = Fig. 19-2).

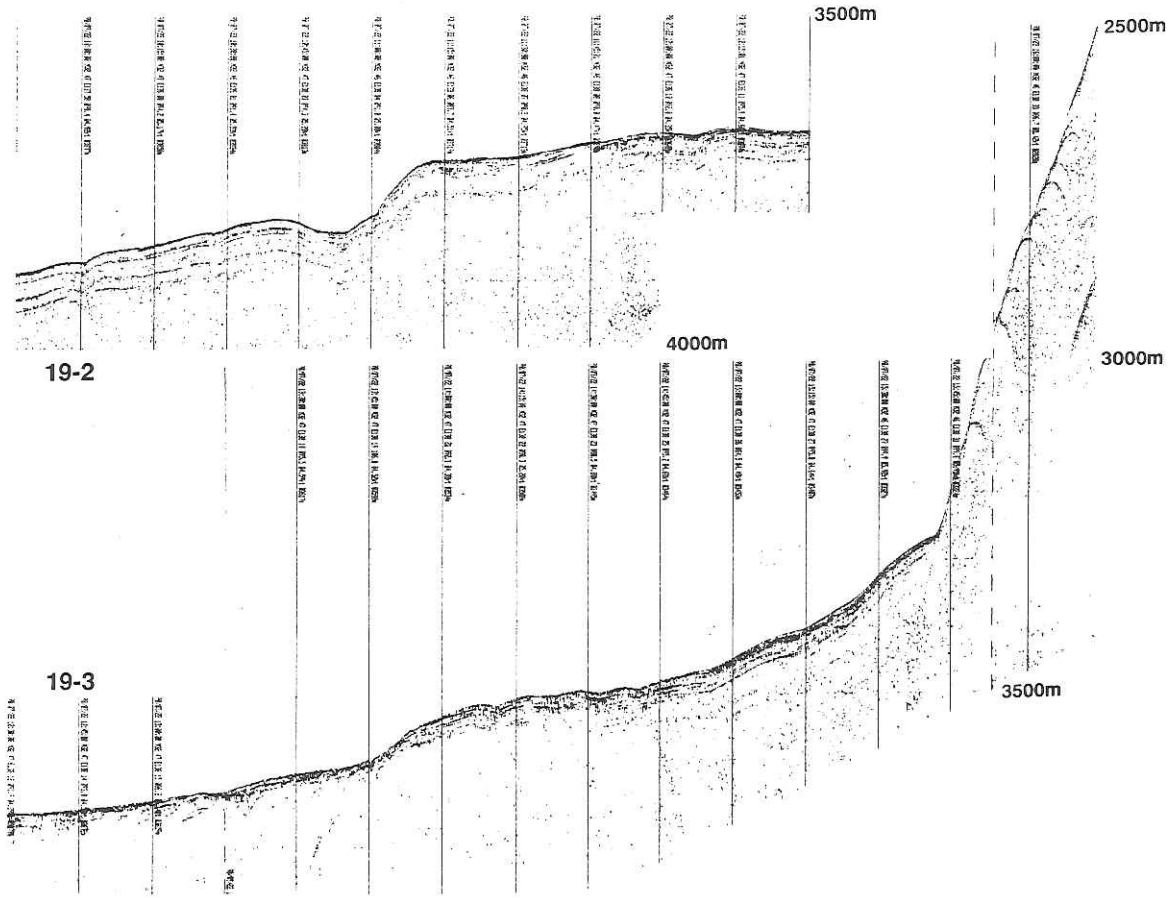

Fig. 19-2~3 Records of 3.5 kHz subbottom profiler in the back-arc region of Izu-Bonin Arc. Above (Fig. -2); the eastern zone of the northern Shikoku basin. Below (Fig.-3); the eastern margin of the northern Shikoku basin to the Arc.

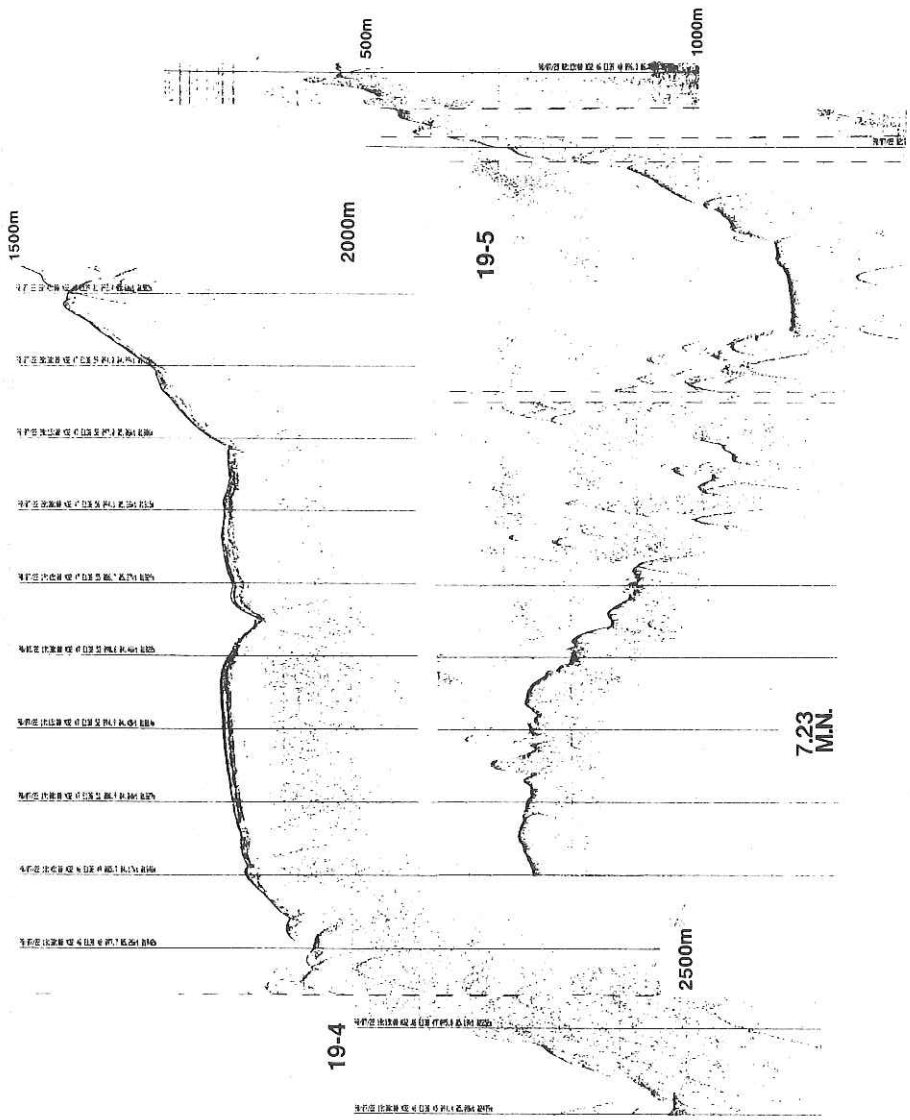

Fig. 19-4~5 Records of 3.5 kHz subbottom profiler. Above (Fig.-4); in the western edge of Shichito-Iwojima Ridge. Below (Fig.-5); Caldera topography in the crestal zone.

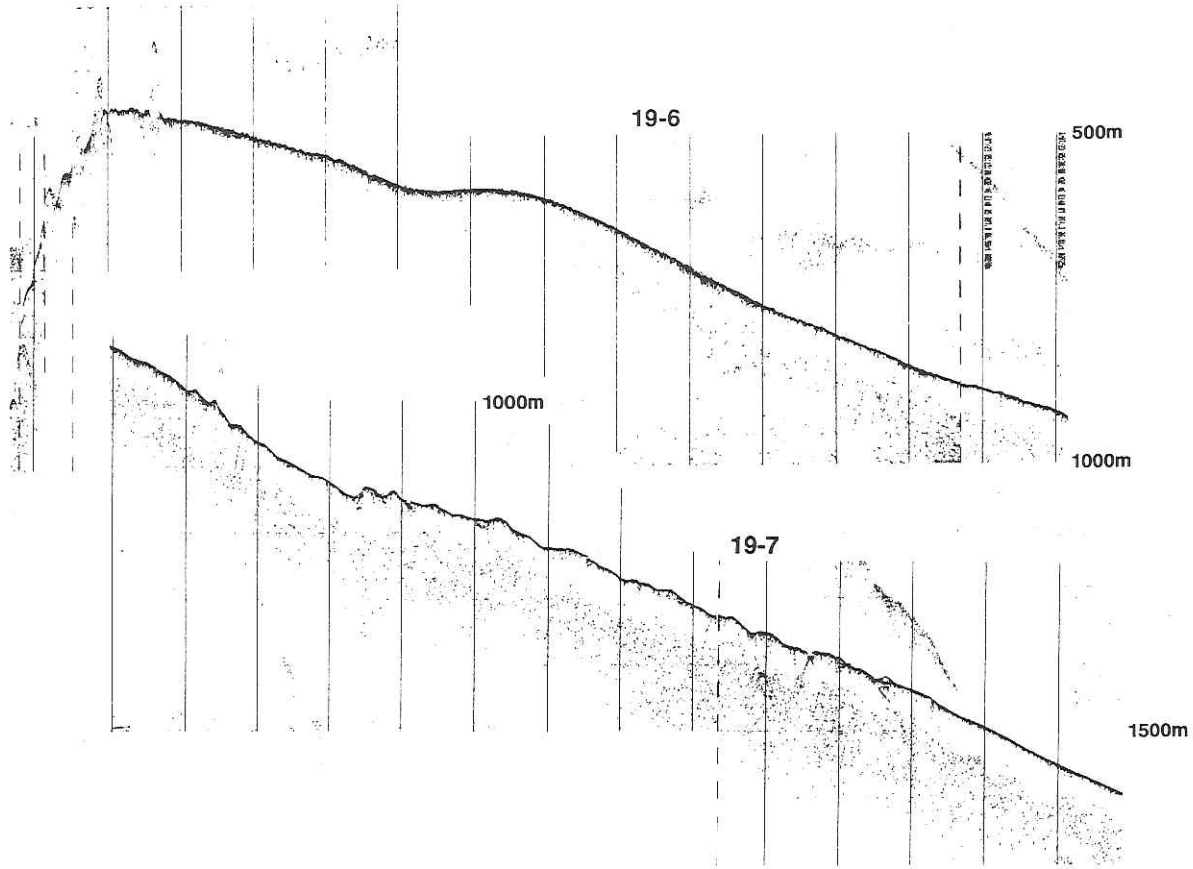

Fig. 19-6~7 Records of 3.5 kHz subbottom profiler in the sediment-starved fore-arc region of Izu-Bonin Arc. Above (Fig.-6); Bare frontal slope.
Below (Fig.-7); wavy or notched surface in the fore-arc slope.

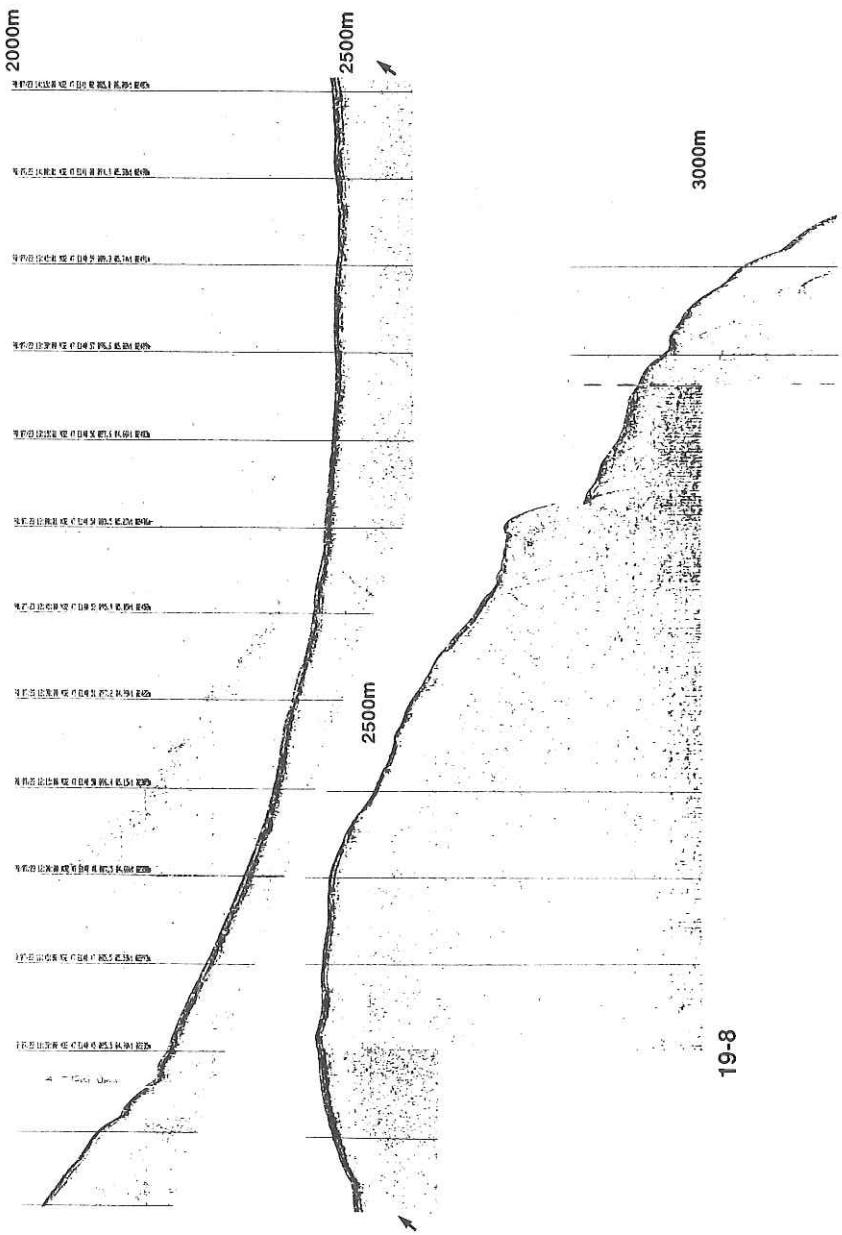

Fig. 19-8 Records of 3.5 kHz subbottom profiler in the middle trench slope of Izu Arc.

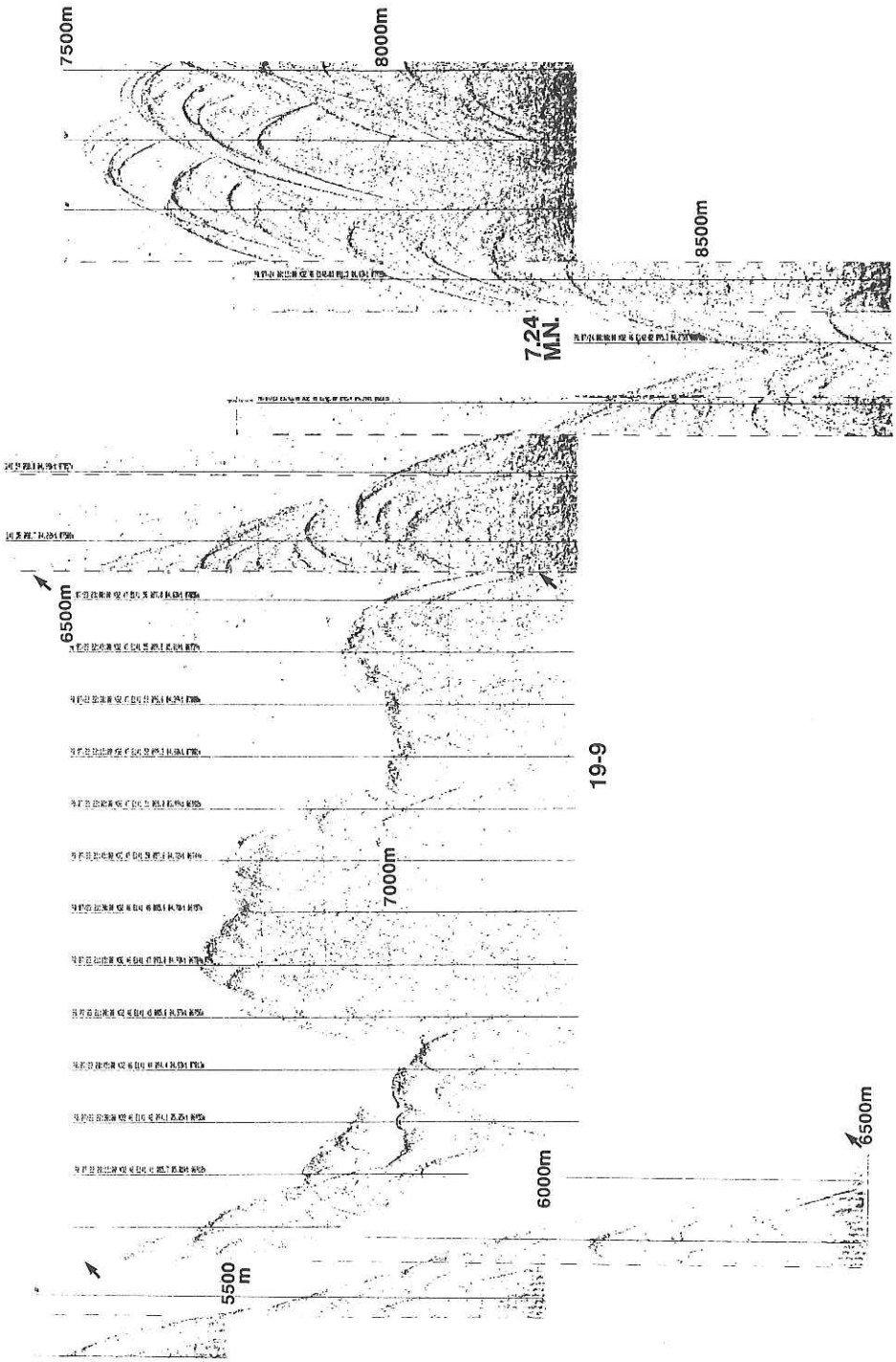

Fig. 19-9 Records of 3.5 kHz subbottom profiler in the lower toe of Izu-Bonin Trench

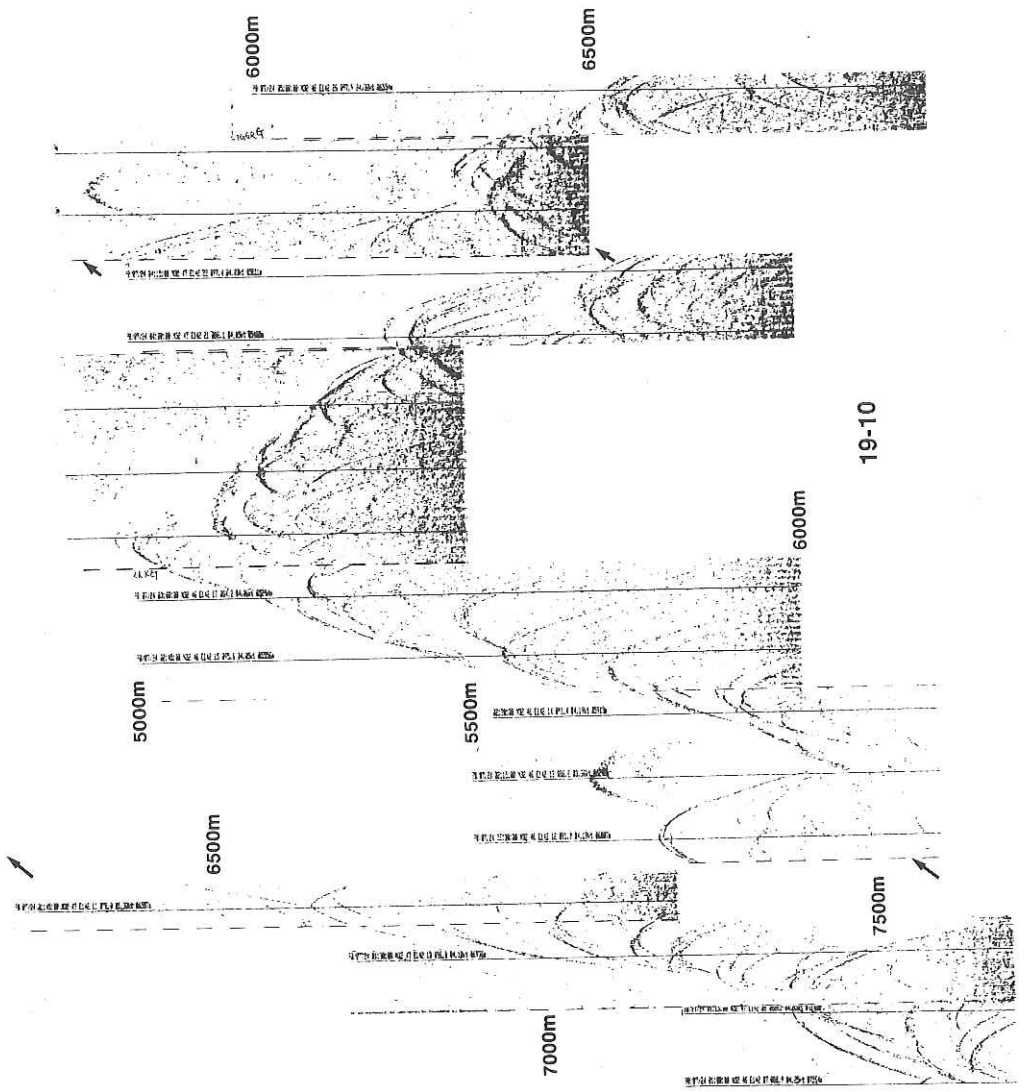

Fig. 19-10 Records of 3.5 kHz subbottom profiler in the lower seaward slope of the Izu-Bonin Trench. Note a number of hyperbolic reflections which may probably be generated by a group of small seamounts.

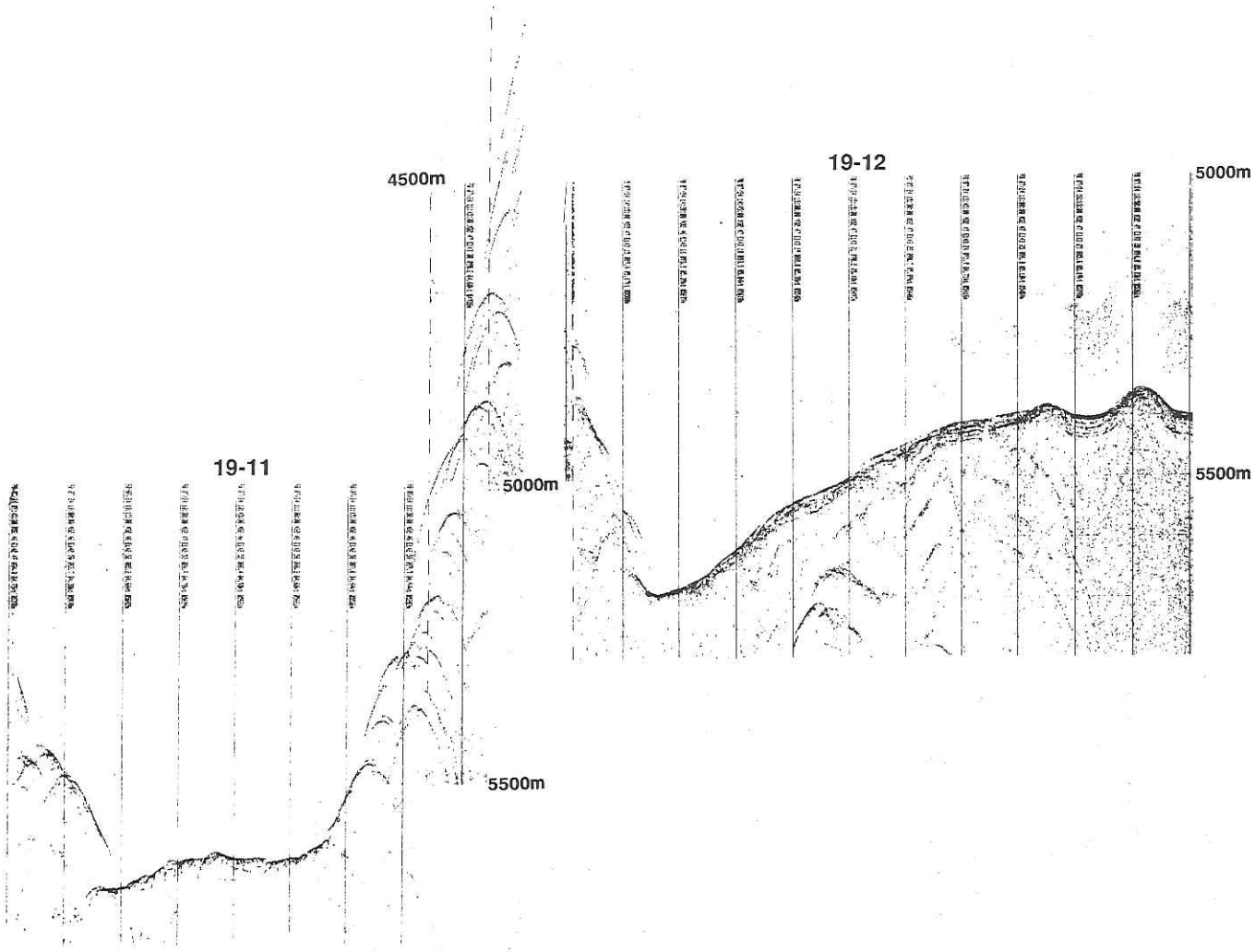

Fig. 19-11~12 Records of 3.5 kHz subbottom profiler in the seaward slope of the Izu-Bonin Trench.

20. Piston Coring

M. Murayama, M. Okada, N. Ohkouchi and H. Matsuoka

We carried out two Piston coring operations in order to test new system of our piston corer. We use connectable 7 m aluminium pipe with inner diameter of 80 mm, and with thickness of 6 mm attached to 900 kg head weight.

The coring operation was made on the starboard deck using the extension beam to pick up and set the corer into the sea.

The coring sites (P-1, P-2) and operation logs are shown in Tables 20-1 and 20-2. The sea bottom topography of these two sites are as follows; P-1: near the top of seamount, P-2: flat sea bottom with gentle slope.

Table 20-1 Summary of Coring Operation in KH90-1 Leg 2

No.	Latitude	Longitude	Water Depth	Wire out	Day and Time(GMT)	Recovery
P-1	33°02.20'N	137°42.30'E	2,716 m	2,690 m	22 JUL 90 02:42	0.3m
P-2	32°55.87'N	137°54.29'E	4,180 m	4,143 m	22 JUL 90 06:58	9.3 m

After the coring operation, the sediments in the pipe were pushed out by oil hydraulic cylinder mounted on the starboard deck and set on vinyl chloride half-cylinders of 1 m in length each with fixed relative orientation. Each sediment core set on the half cylinder was made measurements of magnetic susceptibility using Bartington pass through type magnetic susceptibility system. These cores were split into halves by a piano wire and set on the core array board in order to make core descriptions.

We represent the core description and the magnetic susceptibility data of P-2 in Fig. 20-1-a and -b, respectively.

Table 20-2 Coring operation log of KH90-1, P1 and P2

Date	July 22, 1990	Ship Hakuho-maru KH 90-1	Station P-1
Latitude	33° 02.2' N	Longitude 137° 42.3' E	
Location	northern Shikoku Basin, near a top of Smt west of the Zenisu Ridge		
Sea	smooth, moderate swell	Weather	
Bottom	slightly rough	Profiler	
Length of Core Pipe	7 x 2 m	Length Main Line	m
I.D. of Pipe	80 mm	Length Trigger Line	m
Wall Thickness	6 mm	Core Head Wt.	900 kg
Material	Al	Trigger Wt.	60 kg
Response at Hit		Response at Pull-out	
Time Lowered		Uncorrected Water Depth	m
Time Hit	11:42	Uncorrected Water Depth	2716 m
Wire Angle at Hit	1°	Wire-out at Hit	2690 m
Cored Length	30 cm	Trigger Cored Length	cm
Method of storage	1 m long tube	No. of Pipe Filled	
Length of Cores in Pipe	1. cm 2. cm 3. cm 4. cm 5. cm 6. cm		
No. of Cubic Sample for Paleomagnetism		(No. - No.)	

Date	July 22, 1990	Ship Hakuho-maru KH 90-1	Station P-2
Latitude	32° 55.9' N	Longitude 137° 54.3' E	
Location	northeasternern Shikoku Basinwest of the Zenisu Ridge		
Sea	smooth, moderate swell	Weather	
Bottom	flat with gentle slope	Profiler	
Length of Core Pipe	7 x 2 m	Length Main Line	m
I.D. of Pipe	80 mm	Length Trigger Line	m
Wall Thickness	6 mm	Core Head Wt.	900 kg
Material	Al	Trigger Wt.	60 kg
Response at Hit		Response at Pull-out	
Time Lowered		Uncorrected Water Depth	m
Time Hit	15:58	Uncorrected Water Depth	4180 m
Wire Angle at Hit	1°	Wire-out at Hit	4143 m
Cored Length	930 cm	Trigger Cored Length	cm
Method of storage		No. of Pipe Filled	
Length of Cores in Pipe	1. cm 2. cm 3. cm 4. cm 5. cm 6. cm		
No. of Cubic Sample for Paleomagnetism		(No. - No.)	

Fig.20-1-a KH90-1 P-2 0-5 m

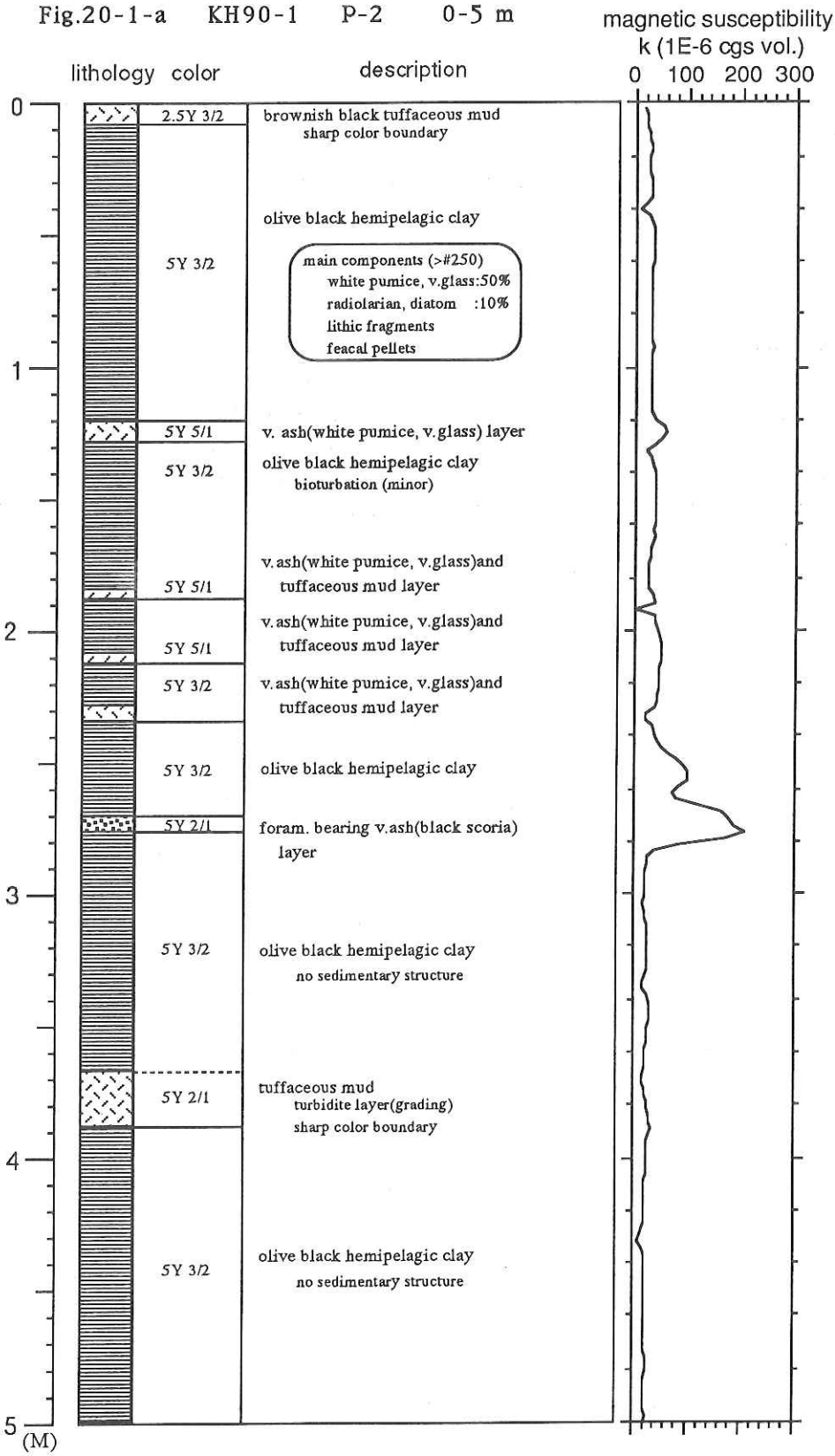

Fig.20-1-b KH90-1 P-2 5-10 m

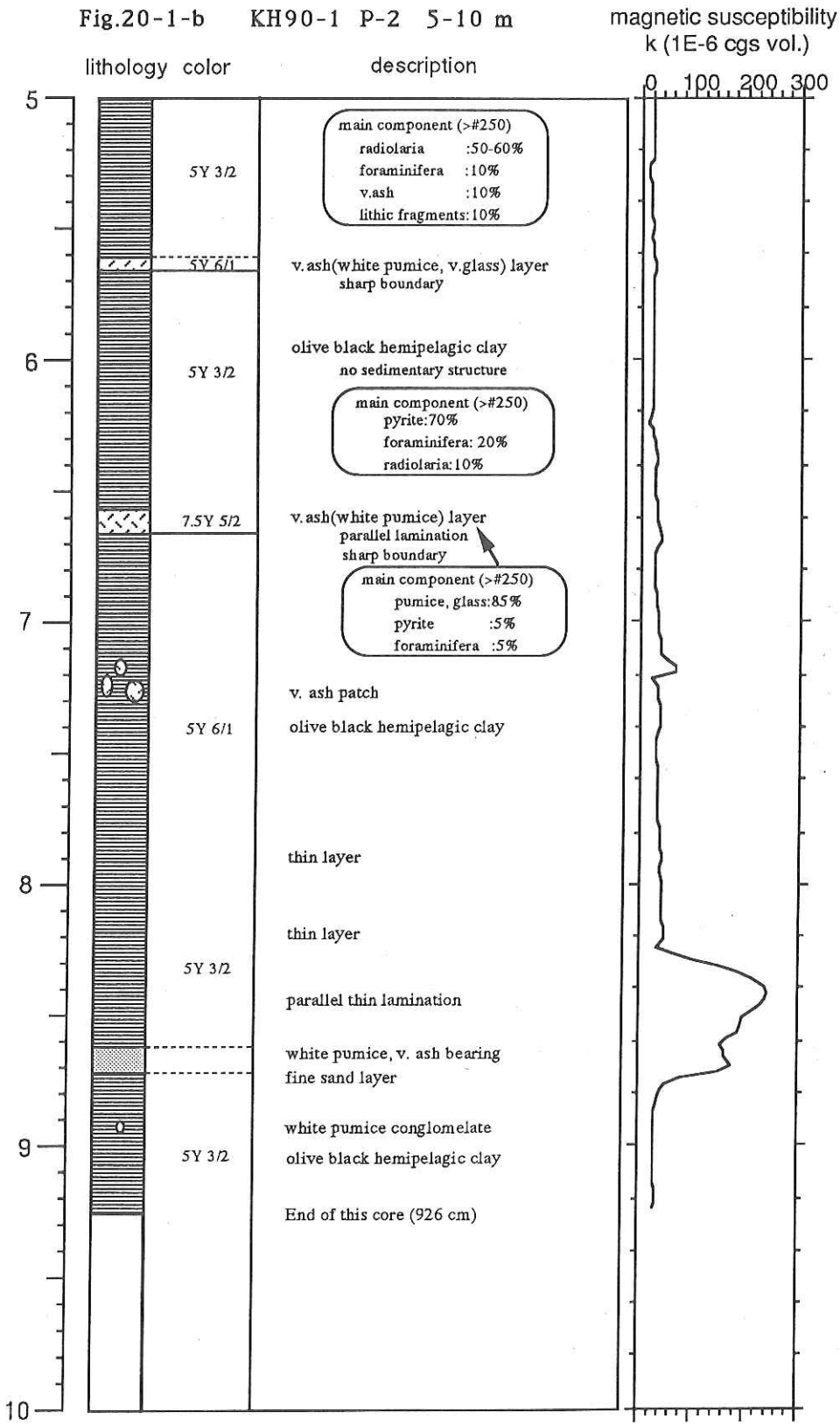

21. Surface Ship Gravity Measurement

C. S Yang, Y. Fukuda and I. Fujii

Throughout the whole cruise KH-90-1, sea surface gravity measurement was conducted with NIPR-ORI-2 gravimeter. Data processing procedure was the same as the previous Hakuho-maru cruise of KH-89-1 and KH-89-2. Main purpose of the gravity measurement was to obtain an accurate gravity profile across the Japan Trench. The observed gravity data was reduced to free-air anomlay after calibration of the scale factor of the gravimeter. Fig. 21-1 below shows a part of the processed free-air anomaly together with depth profile obtained in this cruise.

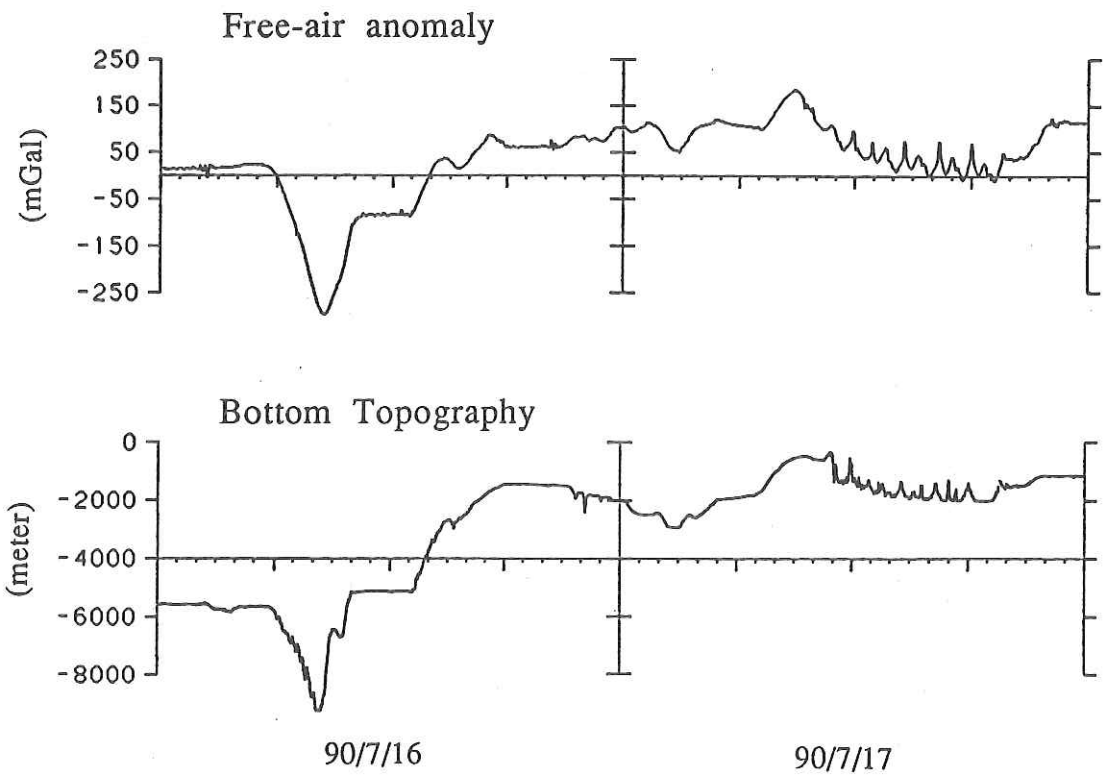

Fig. 21-1 Two days' profiles of free-air gravity anomaly (top) and bathymetry (bottom). The profiles crossed the Japan Trench along 32°N latitude on July 16, 1990.

22. Acoustic Travel Time Measurement between Two Moored IES's

T. Takeuchi and H. Ikari

Introduction

It is required to accurately track location of an underwater data-collecting platform acoustically in a long range. Historically, acoustic positioning systems can be classified into three types; the first is a long-base line system, which measures ranges from a platform hydrophone to two or more ocean bottom mounted transponders. The second is a short-base line system, which requires a single source or hydrophone on the platform and three or more receiving hydrophones (or sources) on the ocean bottom. The third is an ultra short-base line system, which requires a single source (or multi-element hydrophone) on the platform and a single multi-element hydrophone (or source) on the ocean bottom. The short-base line system measures range and calculates bearing by using time-difference of arrival measurements. The ultra short-base line system measures range and bearing. The bearing is obtained from phase difference at closely spaced hydrophones.

For long range tracking in the deep ocean, however, the bottom referenced range-range method used by a long-base line system may give the most accurate tracking results. The short-base line system which determines locations of the platform by time-difference of arrival measurements may also be used for tracking or remote monitoring [1], [2].

The acoustic system which has signal source phase-modulated by a maximal binary sequence and correlation processing unit gives accurate results in measuring acoustic signal travel time [3], [4]. That system for tracking is designed and preliminary tests are tried at sea.

Acoustic Transceiver

A source and receiver are integrated into a mechanical package to form transceiver shown in Fig. 22-1. Both are processed and controlled by a single CM05 V40 microprocessor. That operates on 1 MHz time base and possesses RS232C termination so that the transceiver and personal computer can be interconnected for data communication.

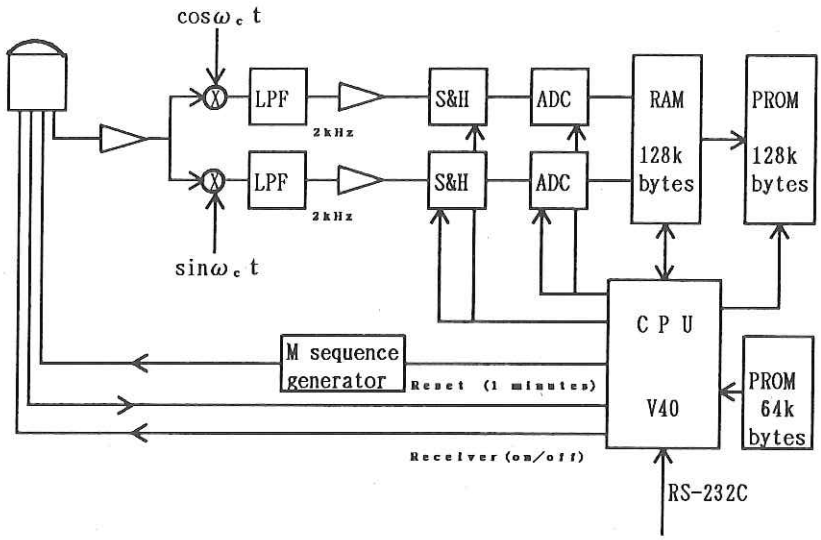

Fig.22-1 Block diagram of transmitter and receiver

The transmitted signal was chosen to have the following characteristics:

carrier frequency f_0=10 kHz
digit length=4 cycles of 10 kHz=0.4 msec
sequence length=127 digits=50.8 msec
transmission length=1 sequence period=50.8 msec

The transmitted signal is generated by reading out from PROM in which the phase-coded signal is stored as can be produced a square wave at frequency 10 kHz. The phase-coded digital signal is amplified by a constant power amplifier, filtered by a combination of broad band pass filter and impedance-matching network, and impressed on the ring ceramic drivers. Energy is supplied by Li-batteries.

The receiver is microprocessor-controlled units that digitize, process, and record on EPROM. The source transducer is used for acoustic signal reception also. A single CMOS V40 microprocessor performs both control and signal-processing functions in the receiver. Signal acquisition is initiated by the processor

at the source transmit time to preset time for the maximal range. The incoming signal is amplified and filtered using a broad band filter centered at 10 kHz. The filtered signal is then shifted to base band using a sinusoidal wave complex demodulator. The resulting quadrature components of the signal are degitized by followed A/D converters per component. Each sample is the result of a 0.5 msec integration. giving a frequency response closely matched to that of the transmitted signal. A 0.2 msec sample interval is achieved to give two sample Per digit. Since there are two quadratue components and 127 digits, a single period of the signal is 254 complex samples.

The processor squares each quadrature component and sums their results. The arrival time is obtained as the abscissa of resulting Peak value. The transceiver responds after preset interval from that arrival time. The arrival time in each peak value and the some adjacent amplitudes are stored on 1 Mbits EPROM for later analysis.

Preliminary Results

The transceiver described above was deployed during a week of 17 to 25 July of 1990 in the near sea of MIKURA island where is the depth of 1000 m Two moorings were deployed about 5 km apart in the ocean. The units were placed at approximately the depth of 900m on both moorings. The transceivers transmitted and received at every 20 minutes. Fig. 22-2 shows the correlation results with some different amplitudes which correspond some main paths respectively. The first is the direct path signal. The second is a reflected path signal to and off the surface.

Fig. 22-3 shows the zoom of the same correlation results as Fig. 22-2. The second peak may be the reflected path signal to and off the ocean bottom Only direct arrival time can be used for tracking, and other peaks are not used. The inferior band of variance of arrival time (Cramer-Rao bound) is 0.4 msec when SNR is o dB. The arrival peak locations, therefore, will be more accurately determined when SNR is higher than O dB. It is known that more accurate arrival peak locations are determined due to Gaussian interpolation [4]. Fig. 22-4 shows arrival peak amplitudes at every 20 minutes. The first peak locations are very stable and peak amplitudes are sufficiently high to detect. The arrival time was 3,561.6 msec.

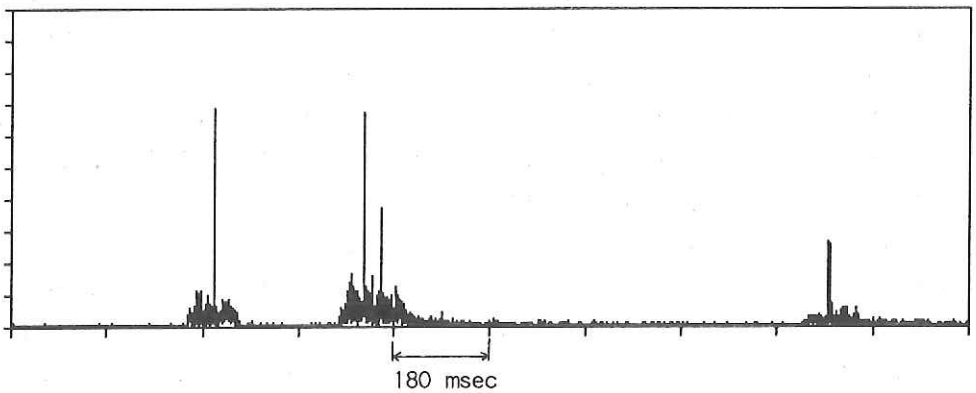

Fig.22-2 Correlation results

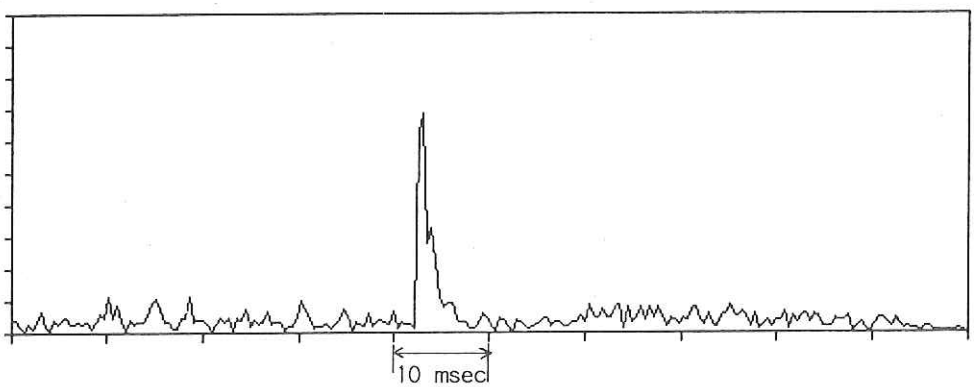

Fig.22-3 Zoom of the first peak arrival of Fig.22-2

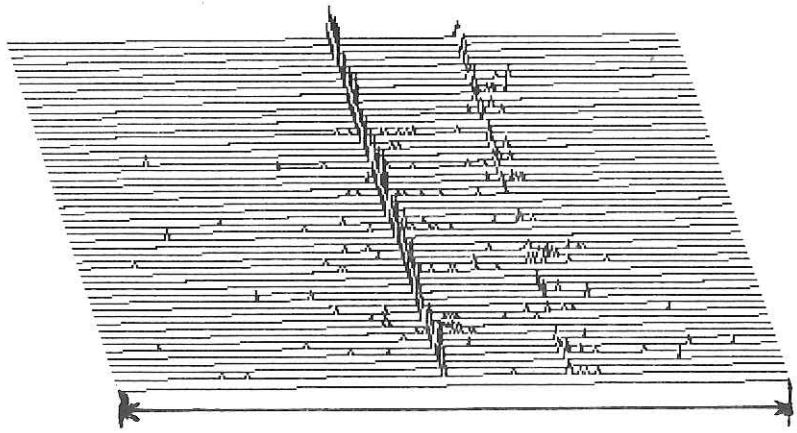

Fig.22-4 First arrival peak amplitudes at every 20 min.

The preliminary sea test results given above are promising us for accurate underwater acoustic locating system. An acoustic locating system which has the performance of resolution 1.4 msec in range 20 km will be capable by using a maximal length binary sequence and correlation units if the transceivers can be fixed.

References

[l] J. S, Abel and K. Lashkari, Track parameter estimation from multipath delay information. *IEEE Journal of Oceanic Engineering*, **OE-12**, No.l, 1987..

[2] G. A. Ransford, Locating and determining the orientation of underwater research equipment: Acoustic range and range rate data *IEEE Journal of Oceanic Engineering*, **OE-12**, No.3, 1987. .

[3] C.R. Spindel, An underwater acoustic pulse compression system, *IEEE Transaction on Acoustics, Speech, and Signal Processing*, **ASSP-27**, No.6. 1979.

[4] P.F.Worcester, Reciprocal acoustic transmissions: instrumentation for mesoscale monitoring of ocean currents. *IEEE Journal of Oceanic Engineering*, **OE-10**, No.2.1985.

23. STATION LOG IN THE R.V. HAKUHO MARU CRUISE KH 90-1

Leg 1

Day Time (GMT) HRMin	Position Latitude Longitude	Water Depth M	Head -ing Deg	Ship Speed Knot	Current Dir. Deg	Current Vel. Knot	Works
0625 0451	35°38.6N: 139°46.5E	n.d.	141	0.0	0	0	Lv. Harumi Pier(Tokyo)
0625 0515	35°36.5N: 139°46.3E	n.d.	148	7.7	092	0.8	Tokyo Bay West Passage
0625 0653	35°19.9N: 139°42.9E	n.d.	175	14.2	104	1.2	entering Uraga Passage
0625 0829	34°59.2N: 139°42.5E	62	182	16.4	101	1.4	Cape Sunosaki, a/c
0625 0908	34°51.4N: 139°50.6E	81	113	12.8	306	1.0	Start Tow Proton Mag.
0625 1729	35°38.3N: 142°52.2E	6,557	070	17.0	160	3.2	Crossing Japan Trench
0626 0327	37°17.5N: 145°36.8E	5,543	044	16.1	219	0.2	Bosei Seamount Survey
0627 0042	37°07.8N: 145°18.0E	2,192	312	1.3	n.d.		Start DESMOS [Stn-1]
0627 0231	37°06.6N: 145°16.9E	3,039	260	0.6	n.d.		DESMOS Near Bottom
0627 0511	37°05.8N: 145°17.1E	3,520	261	0.6	n.d.		DESMOS Lv. Bottom
0627 0640	37°04.3N: 145°16.5E	4,565	262	0.9	n.d.		Gear on Deck [end Stn-1]
0628 0136	36°54.1N: 144°51.9E	1,739	230	2.2	n.d.		Start DESMOS [Stn-2]
0628 0642	36°51.3N: 144°48.6E	1,789	211	0.7	n.d.		DESMOS Lv. Bottom
0628 0712	36°51.0N: 144°48.1E	1,828	221	1.1	n.d.		Gear on Deck [end Stn-2]
0628 1808	37°20.3N: 143°59.9E	6,502	020	7.1	076	1.8	Start Trench Traverse
0629 0247	39°38.7N: 144°30.6E	6,542	015	15.7	253	1.4	Start Trench Survey
0629 0350	39°39.3N: 144°14.8E	7,382	313	2.5	n.d.		Transponder Test
0630 0410	39°20.0N: 143°47.5E	5,483	218	3.5	n.d.		Start DESMOS [Stn-3]
0630 0536	39°20.0N: 143°46.7E	4,087	300	0.5	n.d.		DESMOS Near Bottom
0630 0928	39°21.6N: 143°47.3E	4,058	080	0.8	n.d.		DESMOS Lv. Bottom
0630 1028	39°21.8N: 143°46.1E	3,759	359	1.2	n.d.		Gear on Deck [end Stn-3]
0701 0644	38°45.0N: 145°52.5E	5,274	266	3.7	n.d.		Set Speed 5kt
0701 0653	38°45.0N: 145°51.7E	5,275	267	4.1	n.d.		Launch Water Gun
0701 0739	38°44.9N: 145°47.2E	5,264	271	4.6	n.d.		Launch Streamer Cable
0701 0753	38°44.9N: 145°45.8E	5,264	272	4.6	n.d.		Start Seismic Survey
0701 0810	38°44.9N: 145°44.0E	5,264	277	4.8	n.d.		Start Gradiometer
0703 0037	38°44.9N: 142°27.8E	1,165	257	3.8	n.d.		Retrieve Water Gun
0703 0046	38°44.8N: 142°27.0E	1,165	257	3.9	n.d.		End Gradiometer
0703 0235	38°44.5N: 142°20.6E	779	222	2.0	n.d.		Retrieve Streamer Cable
0704 0633	38°54.4N: 145°16.1E	5,295	155	0.5	n.d.		Start Deep-Tow Proton
0704 2353	38°11.4N: 145°43.2E	5,305	255	1.3	n.d.		End Deep-Tow Proton
0705 0253	38°46.3N: 145°40.7E	5,269	013	1.0	n.d.		Start DESMOS [Stn-4]
0705 0435	38°46.2N: 145°40.8E	5,278	332	0.6	n.d.		DESMOS Near Bottom
0705 0916	38°44.6N: 145°42.1E	5,275	010	0.6	n.d.		DESMOS Lv. Bottom
0705 1051	38°45.6N: 145°43.0E	5,262	048	0.8	n.d.		Gear on Deck [end Stn-4]
0707 0331	38°20.0N: 143°35.9E	3,893	185	2.8	n.d.		Start DESMOS [Stn-5]
0707 0532	38°19.4N: 143°37.9E	4,073	174	1.2	n.d.		Gear on Deck [end Stn-5]

Day Time (GMT) HRMin	Position Latitude Longitude	Water Depth M	Head -ing Deg	Ship Speed Knot	Current Dir. Deg	Current Vel. Knot	Works
0708 0117	38°05.1N: 143°41.3E	5,182	213	2.3	n.d.		Start DESMOS [Stn-6]
0708 0310	38°05.1N: 143°42.7E	5,344	218	0.9	n.d.		DESMOS Near Bottom
0708 0519	38°05.4N: 143°43.8E	5,486	178	0.3	n.d.		DESMOS Lv. Bottom
0708 0529	38°05.3N: 143°43.8E	5,488	243	0.3	n.d.		Start Acoustic Measure.
0708 0627	38°04.6N: 143°44.1E	5,528	273	0.7	n.d.		End Acoustic Measure.
0708 0753	38°04.8N: 143°44.1E	5,512	020	0.7	n.d.		Gear on Deck [end Stn-6]
0709 2100	34°50.6N: 139°47.6E	93	291	11.5	234	0.2	End Proton Survey
0709 2314	35°12.6N: 139°46.8E	6	359	10.7	270	0.5	Pass Uraga Suido
0710 0056	35°16.8N: 139°40.9E	6	018	0.1	n.d.		Arr. Shinko Pier Yokosuka

Leg 2

Day Time (GMT) HRMin	Position Latitude Longitude	Water Depth M	Head -ing Deg	Ship Speed Knot	Current Dir. Deg	Current Vel. Knot	Works
0715 0101	35°17.7N: 139°42.3E	6	073	6.0	216	0.5	Lv. Yokosuka Shinko
0715 0110	35°18.4N: 139°43.5E	6	065	8.0	040	0.4	entering Uraga Trafic
0715 0329	34°48.2N: 139°52.9E	6	131	16.8	025	1.6	Start Proton Survey
0715 2056	31°59.9N: 143°60.0E	5,614	202	0.9	n.d.		Launch OBE-1 JK-23
0715 2145	31°60.0N: 143°59.3E	5,516	205	2.4	n.d.		Launch OBM-S4 JK-23
0716 1030	32°00.1N: 141°33.6E	5,144	203	2.8	n.d.		Launch OBM-C3 JK-24
0716 1832	32°05.1N: 139°59.9E	1,445	219	1.2	n.d.		Launch OBM-S6 JK-25
0716 1856	32°05.7N: 140°00.0E	1,445	220	1.1	n.d.		Launch OBE-2 JK-25
0716 2359	32°47.1N: 140°42.1E	2,010	352	2.8	n.d.		Launch OBS-1
0717 0121	32°47.0N: 141°00.2E	2,492	085	6.5	275	1.6	Launch OBS-2
0717 0237	32°47.1N: 141°18.4E	2,911	063	6.3	284	1.3	Launch OBS-3
0717 1113	33°20.0N: 139°30.0E	1,120	265	16.6	335	1.5	Seabeam Survey
0717 2320	34°00.0N: 139°50.2E	1,140	259	0.6	n.d.		Launch IES-A
0717 2354	34°02.3N: 139°51.8E	1,154	232	3.3	n.d.		Launch IES-B
0718 0024	33°59.9N: 139°53.0E	1,189	223	5.0	075	1.7	Launch IES-C
0718 0342	33°43.9N: 139°42.5E	1,425	191	6.0	145	0.5	Start IZANAGI
0719 2243	33°18.9N: 139°27.9E	1,699	257	3.0	n.d.		Finish IZANAGI
0720 0118	33°07.7N: 139°49.4E	239	072	0.5	n.d.		Off Hachijo Jima
0720 0441	32°52.3N: 139°39.6E	519	265	5.6	015	1.4	Start IZANAGI
0721 1501	33°11.1N: 139°16.9E	444	113	5.8	353	2.3	Finish IZANAGI
0722 0242	33°02.1N: 137°42.2E	2,719	024	0.4	n.d.		Piston Coring [P-1]
0722 0704	32°55.9N: 137°54.3E	4,180	197	0.1	n.d.		Piston Coring [P-2]
0722 0921	32°47.3N: 137°55.0E	3,927	094	7.0	037	1.8	Launch Water Gun
0722 1058	32°47.0N: 138°04.6E	3,810	093	5.1	325	0.2	Launch Streamer Cable
0722 1059	32°47.0N: 138°04.6E	3,809	093	5.1	306	0.1	Start MC Seismic
0724 2200	32°47.0N: 144°00.7E	5,889	094	4.8	n.d.		End MC Seismic
0724 2321	32°46.9N: 144°07.3E	5,749	094	3.2	n.d.		Retrieve Streamer Cable
0724 2344	32°46.9N: 144°08.8E	5,716	108	3.5	n.d.		Retrieve Water Gun
0725 0847	32°47.1N: 141°18.2E	2,918	084	2.0	n.d.		Release OBS-3
0725 0959	32°47.2N: 141°18.5E	2,924	011	0.5	n.d.		Retrieve OBS-3
0725 1504	32°47.2N: 140°42.2E	2,011	075	2.4	n.d.		Release OBS-1
0725 2254	34°00.0N: 139°53.6E	1,169	106	2.9	n.d.		Release IES-C, not found
0726 0029	34°00.1N: 139°54.9E	1,150	130	2.4	n.d.		Retrieve IES-A
0726 0118	34°02.5N: 139°55.3E	1,182	171	1.5	n.d.		Retrieve IES-B
0726 0923	32°49.1N: 140°41.9E	1,995	070	4.3	n.d.		Retrieve OBS-1
0726 2253	35°19.5N: 139°43.5E	n.d.	350	11.3	137	0.2	Pass Uraga Suido
0726 2348	35°25.0N: 139°41.1E	n.d.	032	2.3	n.d.		ArrYokohama Dockyard
0728 0024	35°25.0N: 139°41.0E	n.d.	031	0.0	n.d.		Lv Yokohama Dockyard
0728 0255	35°38.6N: 139°46.5E	34	142	0.4	n.d.		Arr. Harimi Pier (Tokyo)